Twin screw extrusion pre-treatment of wheat straw for biofuel and lignin biorefinery applications

A thesis submitted to Brunel University London for the degree of

Doctor of Philosophy

in the Wolfson Centre of Material Processing

2013

Thian Hong, Ng

Wolfson Centre of Material Processing

Brunel University London

Abstract

Pre-treatment of wheat straw (lignocellulosic) biomass is a crucial step as it has direct impact on the subsequent yield of enzymatic saccharification and alcohol fermentation processes in the production of biofuel. Twin screw extrusion is a highly feasible pre-treatment method and has been received great interest in the recent year pre-treatment studies. Twin screw extrusion is a continuous process, where the biomass feedstock can be subjected to a combination of simultaneous physical, thermal and chemical treatments. Steam explosion is a batch process and is the most commonly used method for lignocellulosic pre-treatment. In the initial stage of this study, the yield of glucose obtained from enzymatic saccharification for both methods (extrusion and steam explosion) were compared to identify the most effective pre-treatment approach. Effectiveness of the conventional steam explosion pre-treatment was used as benchmark for the directions of development of effective extrusion fractionation for wheat straw. In subsequent study, the impact of physical operating parameters (moisture, barrel temperature, compaction, screw speed and size reduction before extrusion) over twin screw extrusion with and without NaOH were studied. Low temperature (50°C) and increased moisture extrusion were preferred extrusion conditions. Yield of glucose can be improved by addition of NaOH (0.04g / g straw) and barrel temperature profile optimisation. Post extrusion washing was recommended. Findings from FTIR and TGA help to understand the chemical and structural changes took place in the pre-treatment and can be correlated with the glucose yield at the end of enzymatic hydrolysis. Characterisation analysis was extended to FT-NIR, morphology, crystallinity and specific surface area analysis to analyse the structural changes of lignocellulose biomass in extrusion pre-treatment and correlation with glucose yield. Chemometric analysis was used to statistically process large amounts of spectral data. The PCA scores plots showed good cluster segregation of the samples and were thus able to distinguish the effects of different pre-treatment conditions. The PLS regression models for both FTIR and FT-NIR showed good statistical regression and predictive ability correlated to the glucose yield. For the lignin ultilisation study, crude lignin was recovered from black liquor and fractionated with solvents. Lignin and the fractions were characterised with

solvent solubility, SEC, UV, FTIR, ^{1}H and ^{13}C NMR and evaluated for the antioxidant activity with AAI ranged from 0.3 to 2.4. Reason for the low performance was proposed and experiment was extended to the intended application performance screening. Lignin application study was further extended to assess the feasibility of using lignin as an antioxidant in carboxylated acrilonitrile-butadiene rubber, XNBR glove. Evaluation involved physical observation, mechanical properties and thermal analysis – DSC-OIT after incorporation of lignin into XNBR glove. Lignin antioxidant performance was compared with current chemical antioxidant in used in industry. A part from antioxidant behaviour, lignin was also found can enhance the softness of XNBR film after accelerated heat aging.

Keywords : Pre-treatment; extrusion; steam explosion; wheat straw; biofuel; characterization; lignin; antioxidant

List of Content

List of Figures

List of Tables

Acknowledgements

I want to acknowledge my supervisor Prof. Jim Song for his unconditional support and contribution to all my ideas. With his knowledge, guidance, kindness and patience I could develop the research assembled in this dissertation. I would also like to express my appreciation to my co-supervisor Dr Karnik Taverdi who provided valuable guidance and support to my research.

I also would like to express my appreciation for Ministry of Science, Technology and Innovation, Malaysia for the financial support through my Ph.D program. I want to thank HOOCH project partner especially team at IFR, Norwich, team at Innventia AB. Sweden and team at Synthomer Sdn. Bhd., Malaysia for their interest in collaboration and providing valuable suggestions and contributions.

I want to recognize the scientific support from Dr Afandi Ahmad for his advice contributed to research methodology. I want to extend my gratitude to Brunel Library team, Brunel International team and Brunel Graduate School team for their support throughout my Ph.D study.

I want to express gratitude to team at Wolfson Centre for Material Processing, Experimental Techniques Centre and School of Engineering and Design for their cooperation in all the administrative and academic activities related to this research.

I also would like to thank all my friends from Brunel University, my House 5 members, my friends in Sweden and my friends in Malaysia and everywhere for all the support and companion during my research time in UK, Sweden and Malaysia.

I want to thank my parents and my family for all their encouragement, love and support.

Finally, thanks to life for love, friends, chemistry, tea and everything…

Abbreviations and acronyms

AFEX = Ammonia Fibre Explosion

Ara = Arabinose

ARP = Ammonia Recycle Percolation

ASTM = American Society for Testing and Materials

ATR = Attenuated Total Reflectance

BET = Brunauer, Emmett and Teller

BP = British Petroleum

BSG = Brewers' grain

$Ca(OH)_2$ = Calcium Hydroxide

CO_2 = Carbon Dioxide

DAP = Diluted Acid Pre-treatment

DEFRA = Department for Environmental Food and Rural Affairs

DME = Dimethyl ether

DP = Degree of Polymerization

DPPH = 2,2-diphenyl-1-picrylhydrazyl radical

DSC – OIT = Differential Scanning Calorimetry - Oxidation Induction Times

DTG = Derivative Thermogravimetry

DVS = Dynamic Vapour Sorption

EA = Ethyl Acetate

EJ = Exajoule

ETBE = Ethyl *tert*-butyl ether

EU = European Union

FAME = Fatty acid methyl esters

FTIR = Fourier transform infrared (Mid-infrared)

FT-NIR	**=** Fourier transform near infrared
G lignin	= Guaiacyl lignin
GA	= Gallic acid
GAE	= Gallic acid equivalents
Gal	= Galactose
GHG	= Green house gases
Glc	= Glucose
GWS	= Ground wheat straw
HGCA	= Home-grown cereals authority
HOOCH	= Project name : Production of Bioalco**h**ols From Lignocellulosic Waste Materials Produced in the Agri-F**oo**d **Ch**ain
HPLC	= High-performance liquid chromatography
IEA	= International Energy Agency
IFR	**=** Institute Food Research
KBr	= Potassium bromide
KOH	= Potassium Hydroxide
LCA	= Life cycle assessment
LVs	= Latent Variables
M	= Molar
Man	= Mannose
MBDOE	= millions of barrels per day of oil equivalent
MeOH	= Methanol
mM	= milimolar
Mn	= number average molecular weights

Mp = molecular weight of the highest peak

MSC = Multiplicative Signal Correction

MTBE = Methyl tertiary butyl ether

Mw = Weight average molecular weights

MWD = Molecular weight distribution

N = Normality

N_2O = Nitrous Oxide

NaOH = Sodium Hydroxide

NH_3 = Ammonia

NMR = ^{13}C and ^{1}H Nuclear Magnetic Resonance

NNFCC = National Non-Food Crops Centre

NRP = Norwich Research Park

OECD = Organisation for Economic Co-operation and Development

PCA = Principal Component Analysis

phr = Part Per Hundred Rubber

PLS = Partial Least-Squares

ppm = Part per million

PRESS = Predicted Residual Error Sum of Squared

PTFE = Polytetrafluoroethylene

PWS = Powdered wheat straw

R^2C = Correlation Coefficient

R^2p = Correlation Coefficient of Determination for Prediction

RMSEC = Root Mean Square Error of Calibration

RMSECV = Root Mean Square Error of Cross Validation

RMSEP = Root-Mean-Square Error of Prediction

rpm = Rotation per minute

RWS = raw wheat straw

S lignin = Syringyl lignin

S = Sulphur

S:W = Straw : Water ratio

SCAN Standard = Scandinavian standard

SEC = Size Exclusion Chromatography

SEM = Scanning Electron Microscope

SEP = Standard error of prediction

SNV = Standard Normal Variate

TAPPI = Technical Association of the Pulp and Paper Industry

TFEC = Total Final Energy Consumption

TGA = Thermogravimetric analysis

THF = Tetrahydrofuran

Toe = Tonnes of oil equivalent

UEA **=** University of East Anglia

UV = Ultra-violet

WL = Wingstay L

XNBR = Carboxylated Nitrile Rubber

XRD = X-ray diffraction

Xyl = Xylose

ZDEC = Zinc Diethyldthiocarbamate

ZnO = Zinc Oxide

Chapter 1

Introduction

1.1 Background of the research

There is a growing demand for sustainable energy to address the future limitations in oil, and to address climate change. It is accepted that green house gas emissions must be reduced. The World Energy Outlook 2009, 450 Scenario analyses how future energy demand could evolve up to 2030, if countries take co-ordinated action to restrict the global temperature increase to 2°C (Eisentraut, Brown and Fulton, 2011). Under such CO_2-constrained conditions, biofuels provide 9% (11.7 EJ) of total transport fuel demand (126 EJ) in 2030, with roughly 7 EJ if this being second-generation biofuels. Based on this IEA projection, biofuel in particular second generation biofuel is one of the most important technologies to decorbonise the future transport sector. This is on top of the concern on first generation biofuel with competition over food supply.

The development of "2nd Generation" biofuels from non-food energy crops may suffice temporarily whilst land is available, or where land is unsuitable for growing food crops. An alternative and highly attractive approach is to develop green technologies to produce second generation bioalcohol from the large quantities of lignocellulose waste materials that are created during food production. Sources of lignocellulose include field straw (cereals, rape) and waste food residues (wheat bran, brewers' grain (BSG); approximately 600,000 tonnes BSG and 15.5 million tonnes of straw are produced in the UK annually (DEFRA, 2013).

Lignocellulosic bioalcohol production is being developed in worldwide. It is mainly in bioethanol form. Iogen has been producing cellulosic ethanol at its Ottawa demonstration plant since 2004 (Iogen Corporation, 2013). Currently, several R&D projects as well as pilot and demonstration plants on cellulosic bioethanol are being implemented in Europe such as Sweden, Denmark, Germany, France and Spain, which

details listed in Table 1.1 (Gnansounou, 2010). However, there is, and remains relatively little activity in the UK.

Table 1.1 : Second generation bioethanol, pilot, demonstration and projected commercial plants in Europe (Gnansounou, 2010).

Operator	Location	Ethanol capacity	Scale	Status
Abengoa Bioenergy	Salamanca, Spain	4000 t/yr	Demo	Under construction, start-up 2009
BioGasol	Bornholm, Denmark	4000 t/yr	Demo	Planned start-up 2009
DTU, BioGasol	Copenhagen, Denmark	10 t/yr	Pilot	Operational, start-up 2006
SEKAB	Örnsköldsvik, Sweden	100 t/yr	Pilot	Operational, start-up 2004
	Örnsköldsvik, Sweden	4500 t/yr	Demo	Planned, start-up 2011
	Örnsköldsvik, Sweden	50,000 t/yr	Demo	Planned, start-up 2014
	Örnsköldsvik, Sweden	120,000 t/yr	Comm.	Planned, start-up 2016
Inbicon, DONG Energy	Fredericia, Denmark	110 t/yr	Pilot	Operational, start-up 2003
	Fredericia, Denmark	1100 t/yr	Pilot	Operational, start-up 2004
	Kalundborg, Denmark	4000 t/yr	Demo	Under construction, start-up 2009
Procethol 2G, Futurol	Pomacle, France	140 t/yr	Pilot	Under construction, start-up 2010
	Pomacle, France	2840 t/yr	Demo	Planned
Süd-Chemie	Münich, Germany	2 t/yr	Pilot	Operational, start-up 2009

There are a number of scientific challenges to be addressed in bioethanol production via biochemical conversion. It is recognised that improvements are required in three of the major steps in the conversion process, namely pre-treatment, enzymatic hydrolysis and fermentation (Virkajärvi *et al.*, 2009). In particular of pre-treatment, few R&D issues still need to be addressed (Eisentraut, Brown and Fulton, 2011; Taherzadeh and Karimi, 2008; Mosier *et al.*, 2005),

- development of advanced pre-treatment technologies that control mechanisms, are tuned to unique characteristics of different types of biomass and minimize cost;
- efficient fractionation of lignocellulose into multiple streams that contain value-added compounds in concentrations that make purification, utilization, and/or recovery economically feasible e.g. biorefinery of C5 sugars and lignin into bio-based chemical to reduce cost of bioethanol production;
- fundamental understanding of the chemical and physical mechanisms that occur during pre-treatment along with an improved understanding of the relationship between the chemical composition and physico-chemical structure of lignocellulose on the enzymatic digestibility of cellulose and hemicelluloses;

- development of predictive pre-treatment models will enable the selection, design, optimization, and process control pre-treatment technologies.

1.2 Overview of the project

This PhD is part of the DEFRA sponsored project. The project was named as HOOCH Project which is the short form for full project title "Production of Bioalco**h**ols From Lignocellulosic Waste Materials Produced in the Agri-F**oo**d **Ch**ain".

1.2.1 Background of HOOCH Project

The British Bioalcohol Group, in conjunction with industrial collaborators from throughout the supply chain, has created a unique UK consortium to develop an East-of England Pilot Plant system on the Norwich Research Park (NRP). This will be used to develop, evaluate and eventually commercialise tailored approaches for converting different sources of food-chain waste lignocellulose into bioalcohols for the automotive and related industries. The pilot plant system will enable the Group to target their multidisciplinary expertise on the creation of sustainable, second generation biofuels.

The 4-year research programme will involve the development of a tailored and unique physical (continuous steam explosion) pre-treatment with Brunel University, and enzyme-based combination processes for the saccharification of selected, large tonnage lignocellulosic wastes from cereals (straw, bran, brewer's grain) and brassicas (rape straw). The research will also involve the exploitation of unique microbiological expertise for fermenting the sugars released (e.g. specialised pentose-fermenting yeasts from the National Collection of Yeast Cultures at IFR and bacterial-based fermentation at UEA) and the optimisation of bioalcohol exploitation in combustion.

Figure 1.1 highlights the key steps required to convert waste biomass to bioalcohol. The HOOCH partners provide complementary research and industrial expertise throughout this process chain.

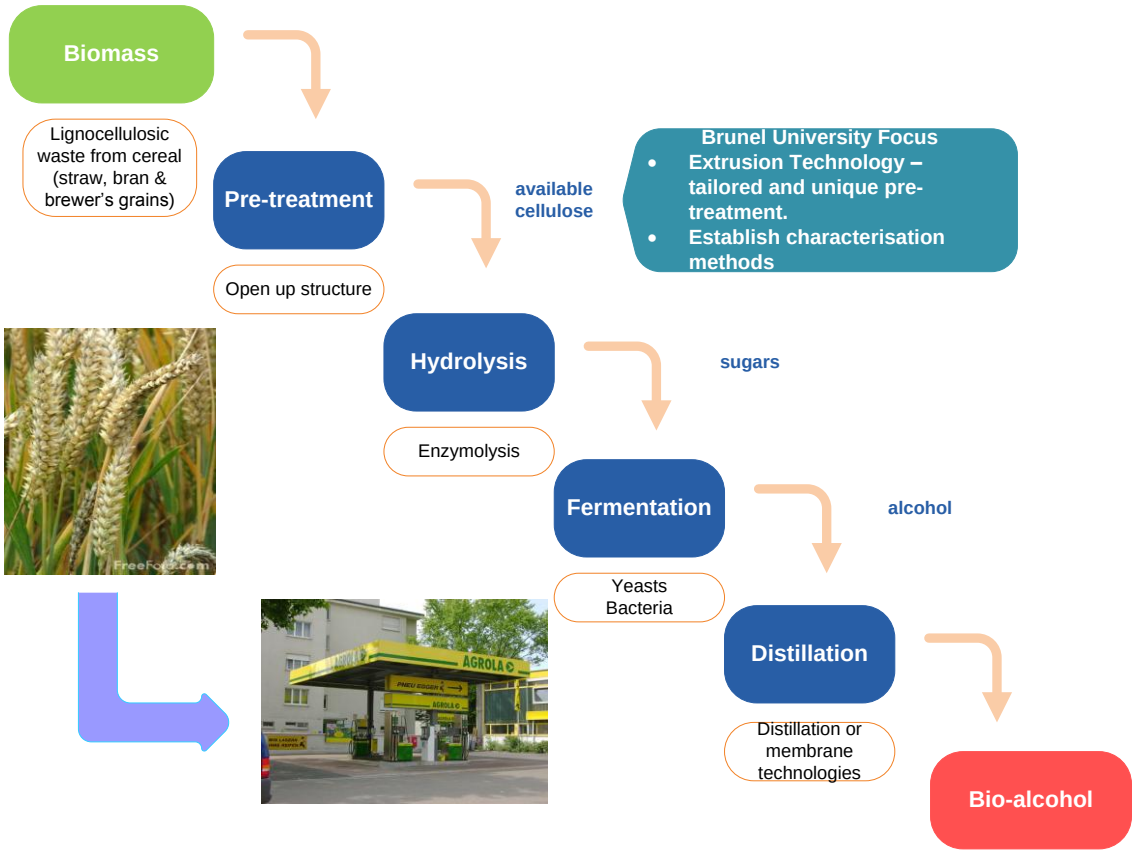

Figure 1.1 : Simplified scheme diagram for production of bioalcohol from biomass

1.2.2 HOOCH Project partners

The consortium members from both research and industrial contribute their expertise in research and development, consultant, supply of materials, experimental tests and industry trials. The participants include:

- Institute Food Research, IFR – IFR focuses on research and development relevant to the exploitation of agri-food chain residues and co-products with special reference to the production of bioalcohol.
- University of East Anglia, UEA – UEA focuses on fermentation study.
- John Innes Centre – research centre in plant and microbial science.
- Wolfson Centre for Material Processing, Brunel University – specialise in research for utilisation and renewable materials.
- Thermo Fisher Scientific – extruder supplier
- Adnams Soutwold - Brewers of the carbon neutral East Green beer.

- Achor - international scientific research, technology development and commercialisation company.
- HGCA – HGCA's mission is to continuously improve the production, wholesomeness and marketing of UK cereals and oilseeds so as to increase their competitiveness in UK and overseas markets in a sustainable manner.
- Biocatalyst Ltd – Biocatalyst speciality enzyme company based in the UK, offering a unique customer based and quality orientated approach to the manufacture of enzymes.
- Lotus Engineering
- Renewables East
- Vireol
- GR Wright & Sons Ltd

1.3 Aims and Objectives

1.3.1 Aims of the project HOOCH

An East-of England multidisciplinary research team consisting of the British Bioalcohols Group from the Norwich Research Park (BBG 2007) and eight industrial collaborators will bring together their multidisciplinary expertise to create bioalcohols from food chain lignocellulose waste streams. This will involve integrating their substantial expertise on all parts of the bioalcohol production process in order to develop a pilot plant suitable for economic and environmental evaluation, further development and commercial exploitation. The research will involve the development of tailored and unique physical (pre-treatment) and enzyme-based combination processes for the saccharification of selected, large tonnage lignocellulosic wastes from cereals (straw, bran, brewer's grain) and brassicas (rape straw). Yield optimisation will be achieved through the evaluation of limiting interpolymeric interactions within the lignocellulose. The research will also involve the exploitation of unique microbiological expertise for fermenting the sugars released (e.g. specialised pentose-fermenting yeasts from the National Collection of Yeast Cultures at IFR and bacterial fermenters at UEA) and the optimisation of bioalcohol exploitation in combustion.

1.3.2 Objectives

The topic of this PhD research is "Twin screw extrusion pre-treatment of wheat straw for bio-fuel and lignin bio-refinery applications". This PhD work focuses on pre-treatment development with Betol twin screw extruder, which including actual extrusion pre-treatment experiments, material characterisation analysis and experimental work involved with various collaborators. This form a base to address the research objectives that defined during early of the PhD work.

Objective 1,

Develop and optimise the twin screw extrusion technology for pre-treatment processing of lignocellulosic biomass (wheat straw) for biofuel application.

Objective 2,

To investigate the mechanism of change of biomass before and after pre-treatment.

Objective 3,

To correlate the mechanism of change with downstream processing output.

Objective 4,

To investigate the potential utilisation for by-product obtained from pre-treatment.

1.4 The general approaches

The PhD work was planed within a time frame of three years duration. Research activities were conducted in few key location to ensure sufficient coverage on research facility, those location were namely at

- Wolfson Centre of Material Processing, located campus of Brunel University, West London.

- Institute Food Research, Norwich Research Centre, Norwich
- Innventia AB, Sweden
- Synthomer Sdn Bhd, Malaysia

For the 1st and 2nd Year of PhD study, the work was mainly covering the experimental trials for wheat straw pre-treatment. Various key factors were selected to understand and further improve the effectiveness of extrusion pre-treatment. Characterisation of raw and pre-treated wheat straw were also conducted with the analytical facility at Brunel University e.g. FTIR, TGA, SEM, XRD and UV Spectrophotometer. In order to enhance the material characterisation capability, external collaborator partners were introduced. They are

- Institute Food Research, who provides glucose yield analysis;
- Surface Measurement System Ltd, who provides surface area analysis by using Dynamic Vapour Analysis;
- Bangor University, who provides surface area analysis by BET analyser
- Thermo Fisher Scientific, who provides facility of FT-NIR

In the 3rd Year of PhD, external collaboration was conducted. This involved of a 3 months placement at Innventia AB, Stockholm, Sweden. Study of lignin recovery, characterisation and antioxidant screening were mainly conducted at Innventia AB. When the study extended to lignin application evaluation, collaboration with an emulsion polymerisation manufacturer – Synthomer Sdn Bhd was initiated. This involved a 1 ½ months placement at the mentioned company to conduct the lignin antioxidant application study in glove application.

Literature review and attendance to conference and project meeting were ongoing activities throughout the PhD study duration.

1.5 Structure of the thesis

Chapter 2 gives a general overview of relevant areas associated with this work, including review of energy supply, lignocellulosic biomass, biorefinery, biomass transform as energy, pre-treatments and extrusion as potential pre-treatment were discussed.

Chapter 3 describes experimental details including pre-treatment trial of extrusion and steam explosion (conducted by IFR), sample identity, ID and description, glucose yield analysis, lignin recovery method and various analytical technique and setting.

In Chapter 4, findings for representative extrusion pre-treatment were compared to conventional steam explosion pre-treatment. The characteristic of pre-treated material was also compared. This serves as good benchmark comparison information in between extrusion and conventional pre-treatment method.

Extensive extrusion trial outcome was summarised in Chapter 5 which consist of extrusion with and without chemical additive. Impact of various operating parameters was discussed.

Chapter 6 outlined the characterisation work on FTIR and FT-NIR. Output of chemometric analysis and glucose yield prediction model were also summarised in this chapter.

Wheat straw characterisation analysis on specific surface area was captured in Chapter 7. It consists of comparison of specific surface area information determined by three different techniques.

Chapter 8 summaries the lignin recovery work from wash black liquor and lignin characterisation analysis. Kraft lignin was included for this study and recovered lignin was screened for antioxidant properties performance.

Extension application work from Chapter 8 was continued in Chapter 9. Selected lignin samples were studied as an antioxidant source in rubber glove with comprehensive application testing.

Chapter 10 outlines the key conclusion of the study and suggests further work which this project was unable to address.

1.6 References

1. DEFRA *ARCHIVE: Defra, UK - Farming - Crops* . Available at: http://archive.defra.gov.uk/foodfarm/growing/crops/index.htm (Accessed: 2/16/2013 2013).
2. Eisentraut, A., Brown, A. and Fulton, L. (2011) *Technology Roadmap - Biofuels for Transport*, IEA, France.
3. Gnansounou, E. (2010) "Production and use of lignocellulosic bioethanol in Europe: Current situation and perspectives", *Bioresource technology*, vol. 101, no. 13, pp. 4842-4850.
4. Iogen Corporation *Iogen Corporation* . Available at: http://www.iogen.ca/index.html (Accessed: 2/16/2013 2013).
5. Mosier, N., Wyman, C., Dale, B., Elander, R., Lee, Y.Y., Holtzapple, M. and Ladisch, M. (2005) "Features of promising technologies for pretreatment of lignocellulosic biomass", *Bioresource technology*, vol. 96, no. 6, pp. 673-686.
6. Taherzadeh, M. and Karimi, K. (2008) "Pretreatment of lignocellulosic wastes to improve ethanol and biogas production: a review", *Int J Mol Sci*, vol. 9, no. 9, pp. 1621-1651.
7. Virkajärvi, I., Niemelä, M.V., Hasanen, A. and Teirb, A. (2009) "Cellulosic ethanol via biochemical processing poses a challenge for developers and implementors", *BioResources*, vol. 4, no. 4, pp. 1718-1735.

Chapter 2

Literature Review

2.1 Energy demand and supply

2.1.1 Energy demand present and future

Energy is one of the most fundamental parts of universe. Everything we do is connected to energy in one form or another. Between 1990 and 2005, global energy consumption increased by 23%. Energy consumption grew most quickly in the service and transport sectors, both sectors showing an increase of 37% (OECD, 2008b). **Figure 2.1**, shows that in 2005, manufacturing industry globally was the single biggest user and consumed a 33% share. It was followed by households (29%) and transport (26%) (OECD, 2008b).

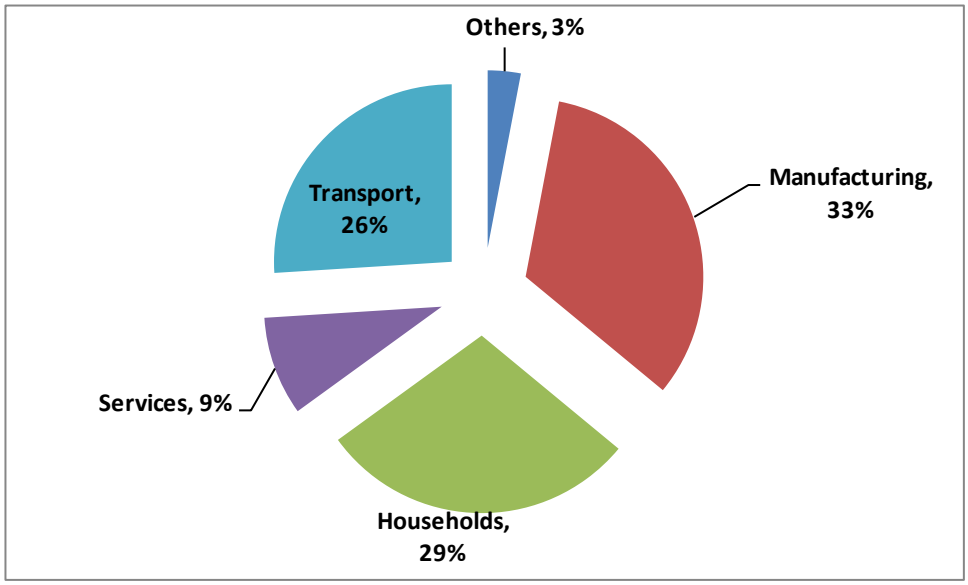

Figure 2.1: Shared of global final energy consumption by sector, 2005

Fossil fuel remains the dominant sources of primary energy worldwide in the Reference Scenario, accounting for 77% of the overall increased in energy demand between 2007

– 2030. In absolute terms, coal sees by far the biggest increase in demand over the projected period, followed by gas and oil (**Figure 2.2**).

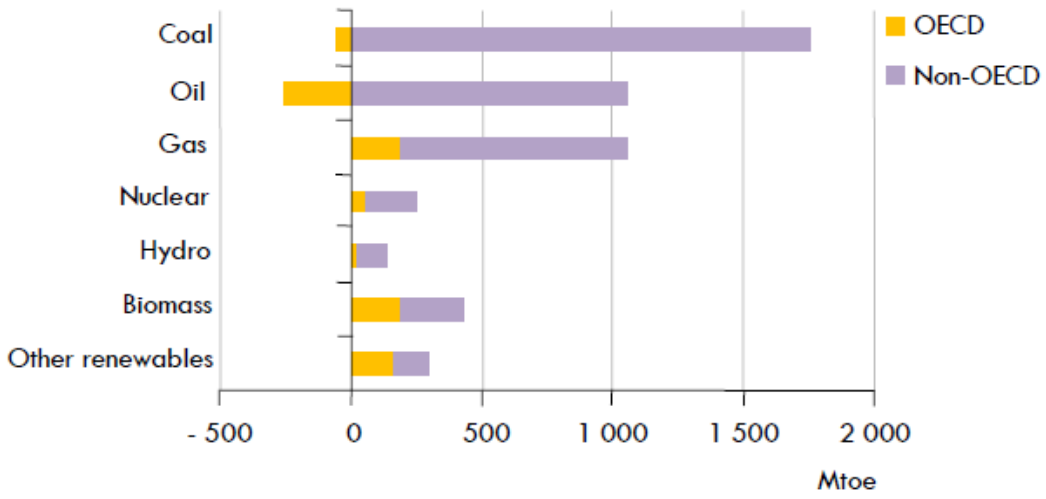

Figure 2.2: Change in primary energy demand in Reference Scenario, 2007 – 2030 (OECD, 2009)

Energy resources can be classed into 2 main categories, there are renewable and non-renewable energy. In this thesis, the renewable energy resources in particular biofuel are the key focus. Non-renewable energy is covered for literature introduction purpose.

2.1.2 Non-renewable energies

2.1.2.1 Fossil fuels and the world resources

Fossil fuels (coal, oil and gas) are burned to provide energy. They are in simple terms oxidised to generate heat emitting carbon dioxide (CO_2), water and some other toxic pollutants such as methane (CH_4) and nitrous oxide (N_xO) during the fuel combustion process. Of fossil fuels, coal combustion in thermal power stations result in greater amounts of CO_2 emissions per unit of electricity generated (2249 lbs/MWh) while oil produces less (1672 lb/MWh) and natural gas produces the least 1135 lb/MWh) (US EPA,2 010). Carbon dioxide is the major green house gases which contributed about 70% of the enhanced greenhouse effect, CH_4 about 24% and N_xO about 6% (Houghton, 2005).

Fossil fuels are non-renewable resources because they take millions of years to form, and the reserves are being depleted much faster than new ones are being formed. The estimation of the remaining fossil fuels on the planet depends on a detailed understanding of the Earth crust. Significant uncertainty exists to estimate the remaining reserves of fossil fuels. The estimation of the remaining fossil fuels on the planet depends on a detailed understanding of the Earth crust. To date, the understanding is still less than perfect. Nevertheless, most of the early estimates of the reserves of the fossil fuels are conservative and tend to grow with time. According to findings from European Commission in the Second Strategic Energy Review (Commission of the European Communities, 2008), the estimated years based on current production are summarised in **Table 2.1**. for oil, gas and coal. With the continuous increase of world energy demand dominated by fossil fuels, the production will increase and the depletion time of the resources is expected to shorten considerably.

Table 2.1: Estimated years of production oil, gas and coal by British Petroleum p.l.c (BP) (Commission of the European Communities, 2008)

Feul	Estimated years on current production
Oil	41.6
Gas	60.3
Coal	133

On the other hand, as world populations grow at a rate of greater than 2% on average the need for more energy is exacerbated (see **Figure 2.3**) (Omer, 2009). Therefore, energy security, economic growth and environment protection are the key energy policy drivers for all countries around the world.

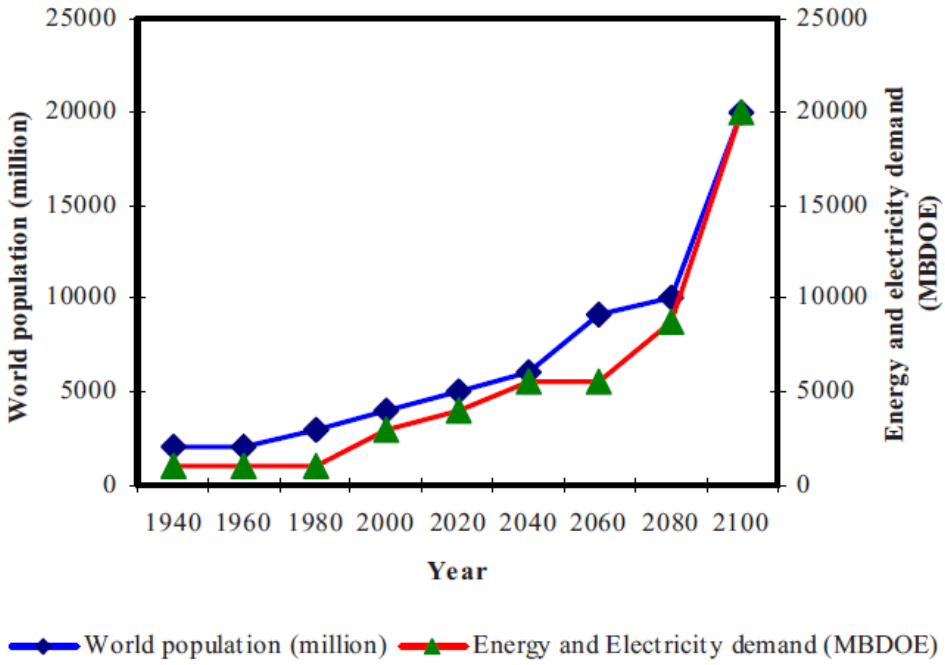

Figure 2.3: Annual and estimated world population and energy demand as oil equivalent in (in MBDOE - millions of barrels per day of oil equivalent) (Omer, 2009).

2.1.2.2 Nuclear energy

Nuclear power is produced by controlled (i.e., non-explosive) nuclear reactions. Commercial plants currently use nuclear fission to heat water to generate steam which is then used to generate electricity. Identified world resources of uranium are around 5.5 million tonnes and at current rate of consumption, these resources correspond to about 100 years of use (Commission of the European Communities, 2008). Nuclear fuel is low carbon source but able to provides significant amount of energy. Existing nuclear power generation save CO_2 emissions of about 2.9 billion tonnes/annum compared with coal-fired power generation, or about 24% CO_2 annual emissions by the power sector (IEA, 2010). A stringent regulatory environment for further development of nuclear power is necessary to address the concern on potential treat to environment and human safety.

2.1.3 Renewable energy

Renewable energy is energy that is derived from resources that are naturally replenished constantly. There are various forms of renewable energies derived directly or indirectly from:

- The sun- solar energy;
- Heat generated deep within the earth-geothermal energy;
- Kinetic/potential energy of air-wind energy, and of water- hydro or tidal energy;
- Biomass- biofuels.

According to EU primary energy consumption statistic in 2008, share of renewables is currently low, as shown in **Figure 2.4** and shares of renewable energy from different sources is shown in **Figure 2.5**.

In recent years however, the worldwide consensus in the development of renewable energy has spurred and accelerated Governmental actions, in research and industrial projects in renewable energies to counter the global challenges in rising energy requirements, rapid growth in world population and global environmental problems including climate change and global warming. Therefore, options for a long-term and environmental friendly energy supply have to be developed leading to the use of renewable sources (Omer, 2009). In 2007, European commission, propose the '20-20-20' target initiative which including,

- Reducing greenhouse gas emissions by at least 20 % (compared with 1990 levels) by 2020;
- Improving energy efficiency by 20 % by 2020;
- Raising the share of renewable energy to 20 % by 2020;
- Increase use of biofuels in transport fuel sector to 10 % by 2020).

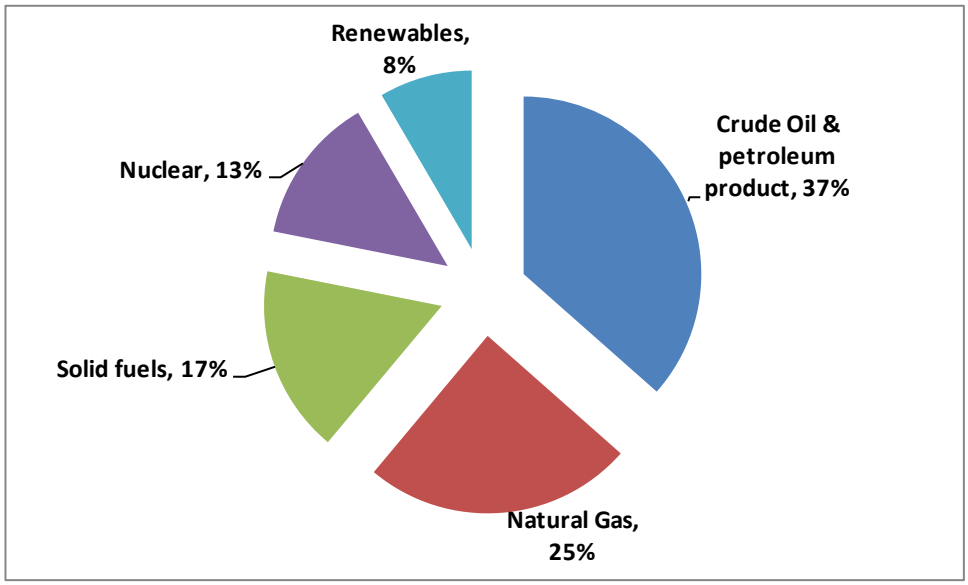

Figure 2.4 Comparison of promary production of energy from different fuels in EU27, Gross Inland Consumption (in 1000 toe,%) 2008 (Eurostat, 2010)

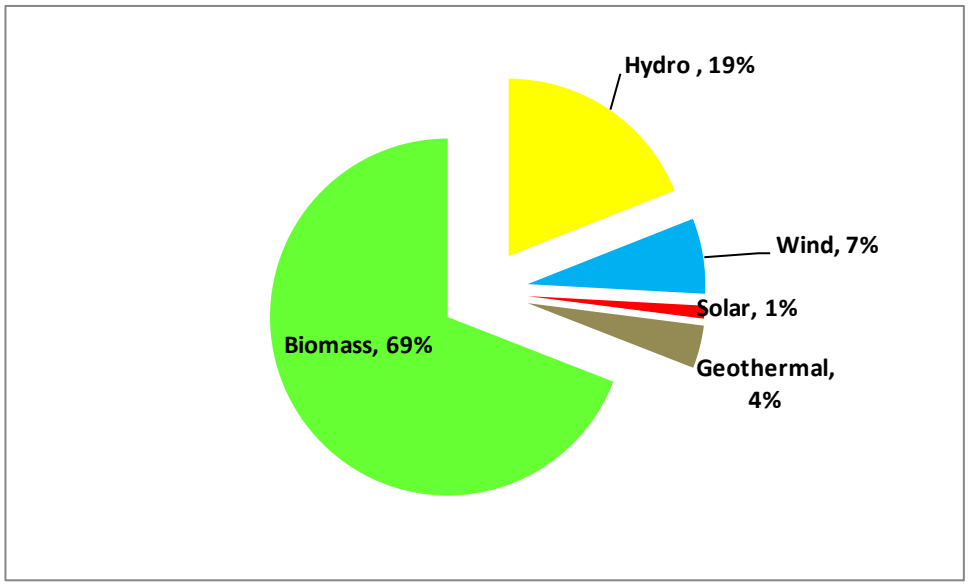

Figure 2.5 Share of primary production of renewable energy in EU27, Primary production of renewable energy from different sources (in 1000 toe), 2008 (Eurostat, 2010)

2.1.3.1 Solar energy

Solar energy, radiant light and heat from the sun, has been harnessed by a range of ever-evolving technologies. Solar energy is vital to support life on earth in producing food,

light and heat. Solar radiation from the sun, can also been harnessed by a range of ever-evolving technologies to generate/store electricity and heat. Solar technologies are broadly characterized as either passive or active solar depending on the way they capture, convert and distribute solar energy.

2.1.3.2 Hydroprower

Hydropower is energy harnessed from kinetic/ potential energy of water which can be harnessed for useful purpose. The fall and movement of water is part of a continuous natural cycle known as water cycle. Hydropower is a renewable energy source because the water on the earth is continuously replenished naturally by water cycle (**Figure 2.6**).

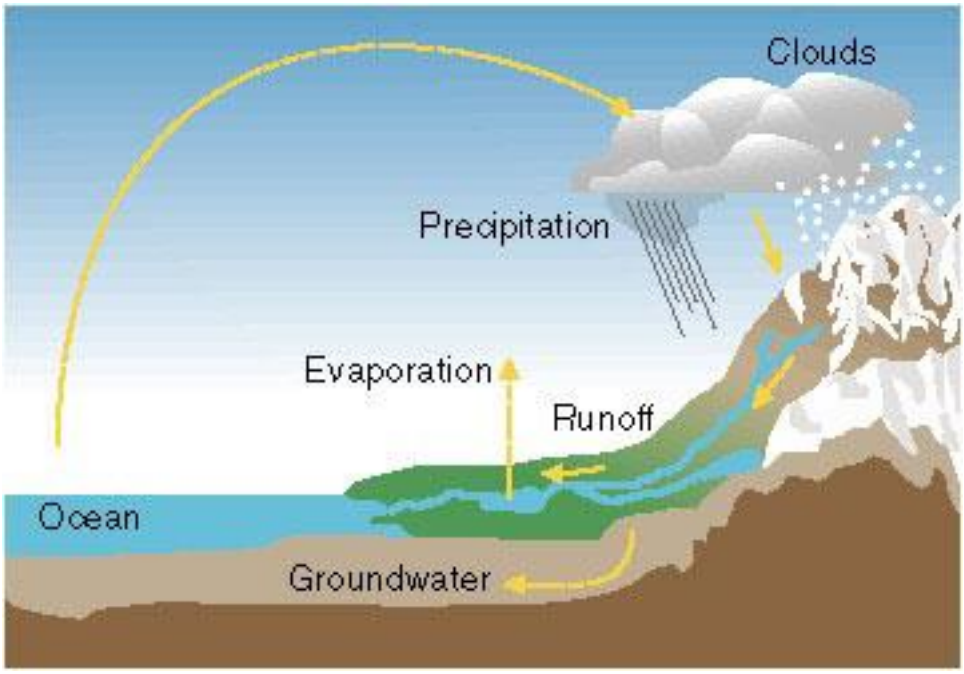

Figure 2.6: The natural water cycle (U.S. Department Energy, 2013)

Depending on the way of harnessing the hydropower, there are several forms in use or development :

a) Waterwheels
b) Hydroelectricity
c) Damless hydro
d) Vortex power
e) Tidal power

f) Tidal stream power
g) Wave power
h) Osmotic power
i) Marine current power
j) Ocean thermal energy conversion

2.1.3.3 Wind

Wind energy system harness the kinetic energy of the wind using wind turbines to generate electricity, wind mills to drive machines, wind pumps to pump water or drainage, or wind sails to propel ships. A wind turbine operates like a fan in reverse for electricity generation. The wind turns the blades, which spin a shaft connected to a generator that makes electricity (New Jersey Board of Public Utilities, 2010). **Figure 2.7** showed the schematic diagram of a typical wind turbine system. Wind energy is plentiful, renewable and widely available geographically, clean and produces no greenhouse gas emissions during harness and use. However, the construction of wind farms is not universally welcomed because of e.g. visual and acoustic impacts on the environment.

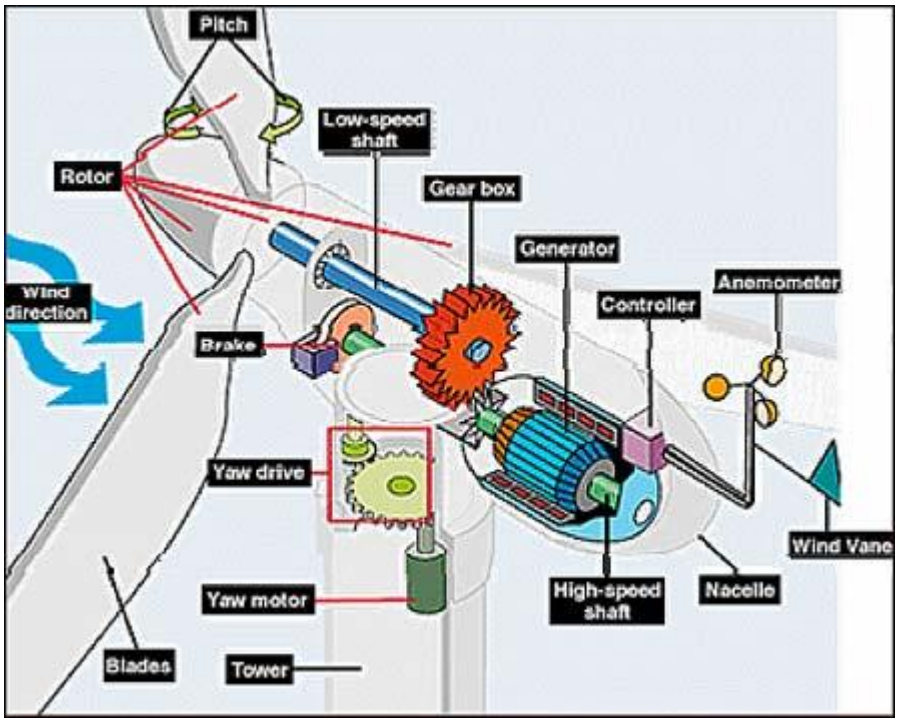

Figure 2.7: A schematic diagram of wind turbine system (New Jersey Board of Public Utilities, 2010)

2.1.3.4 Geothermal

Geothermal energy is power that extracted from heat stored in the earth originated from the formation of the planet, from radioactive decay of minerals or from solar energy absorbed by the earth's surface. **Figure 2.8** is a simplified representation of an ideal geothermal system. Geothermal does not generate pollution and the green house effect (Darvill, 2012). However, not every location is suitable for geothermal power station.

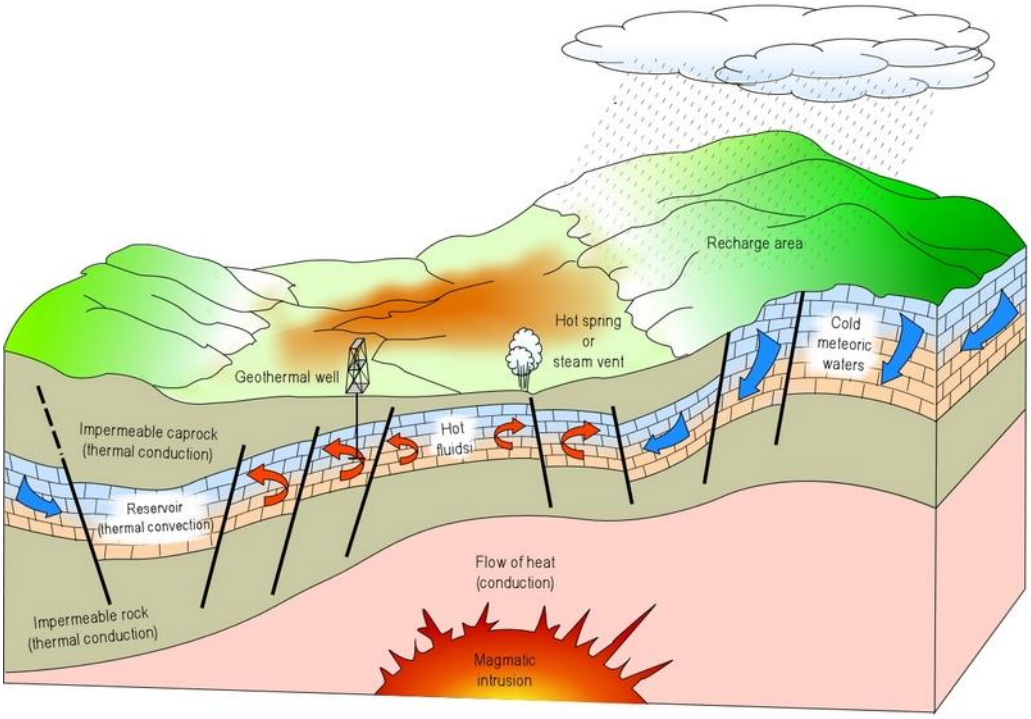

Figure 2.8: Schematic representation of an ideal simplified geothermal energy and flow system (Dickson and Fanelli, 2010; New Jersey Board of Public Utilities, 2010).

2.1.3.5 Biofuels

Biofuels harness energy from direct or indirect use of energy stored in biomass. Biomass is any renewable organic matter that can be used as an energy source. There are many different types of sources of biomass energy that can be used such as wood and forestry residues, plants, by products or residues from horticultural/ agricultural/ animal farming or forestry industries, and such organic components ended up in municipal and industrial waste streams. **Figure 2.9** summaries typical biomass resources.

Direct combustion is a still the most conventional way of harnessing on how heat from biomass and is used. However, burning renewable biomass is a more sustainable practice than burning the non-renewable fossil fuels. In addition, burning fossil fuel leading to a net emission of carbon into the atmosphere that has been locked underground for millions of years while for biomass, in particular plant-based materials, it is virtually "carbon-neutral" as the release CO_2 is that sequestered during photosynthesis of the plants. As shown by the

schematic diagram of the carbon cycle in **Figure 2.10**.

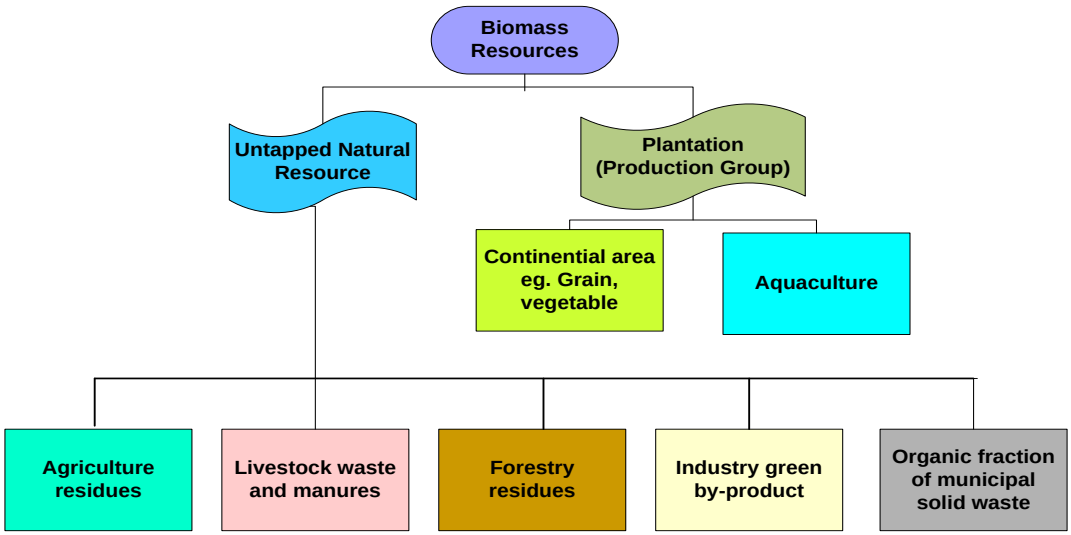

Figure 2.9: Summary of biomass resources

Alternative technologies utilising biomass as energy resource are relatively new and have only find limited applications at industrial scales. Combined heat and power technology, biogas generation by gasification and aerobic digestion and biofuels are among the technologies that can be used to recover energy from biomass.

Several processes exist to convert feedstocks and raw materials into biofuels.

i. 1st generation biofuel - refer to the fuels that are produced through processes such as cold pressing/extraction, transesterification, hydrolysis and fermentation, and chemical synthesis and mainly derive the fuels from sources such as starch, sugar, animal fats, and vegetable oil.
ii. 2nd generation biofuel – produces biofuel based on lignocellulosic biomass through advanced processes.

Lignocellulose is the most abundant renewable biomass; its annual production has been estimated in 1 x 10^{10} MT worldwide (Alvira *et al.*, 2010; Sánchez and Cardona, 2008). Among them, agricultural residuals are the most abundant and cheapest feedstock potentially usable for production of industrial chemicals, materials and fuel. With increasing concerns over first generation biofuel based on starch or sugar in competition with food or feed uses,

second generation biofuel, based on conversion of lignocellulosic biomass as feedstock, has attracted increasing attention in the production of biofuels.

Figure 2.10: Carbon cycle of plant-based biomass (Canadian Biofuel, 2010)

2.2 Lignocellulosic biomass

Lignocellulosic biomass referred to plant biomass which is a compound of cellulose (and hemicelluloses) with lignin in fibrous plants to strengthen the plant cell walls. It consist mainly primary and secondary cell wall. **Figure 2.11** illustrates lignocellulosic macro-fibrils (or plant fibre) embedded in plant cell walls and the main components within it. In general, lignocellulosic biomasses comprise cellulose (20 – 50%), hemicelluloses (20 – 35%), polyphenolic lignin (10 – 35%) and other components (Kumar *et al.*, 2009b; NNFCC, 2009).

Primary cell wall contain crystalline cellulose and amorphous matrix namely pectins and hemicelluloses. Secondary cell wall contain also above matrix but with another critical component – lignin. **Figure 2.12** illustrated the structure of lignocelluloses and the relation to its key components.

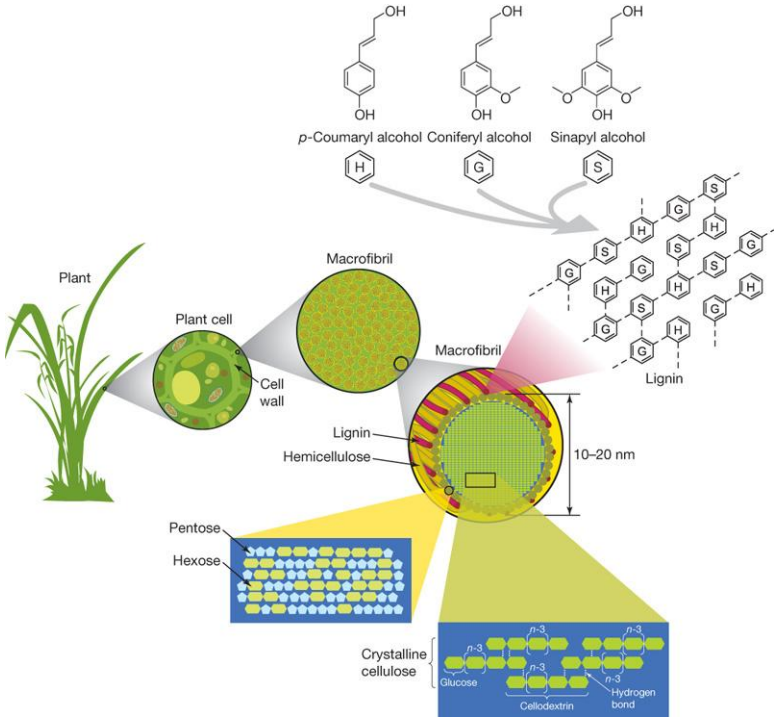

Figure 2.11: Structure of lignocelluloses biomass: plant fibre as macrofibrils embedded in cell walls and microfibrils in a fiber and the key components (cellulose, hemicelluloses and lignin) (Potters, Van Goethem and Schutte, 2010).

Figure 2.12, gives a schematic three-dimensional view (top) and transverse view (bottom) of the cell wall structure of plant fibre or macrofibril in some further details. It consist primary and secondary cell walls. Adjacent fibres are separated by thin middle lamella (6). The primary cell wall (5) contains crystalline cellulose or microfibrils in an amorphous matrix of pectins and hemicelluloses. The secondary cell wall (1 – 3) surrounding the dead lumen (4) contain also the above matrix but with another critical component – lignin. (Bowes, 1996). Epidermis, the outer layer containing waxy chemical for water regulating in plant cell.

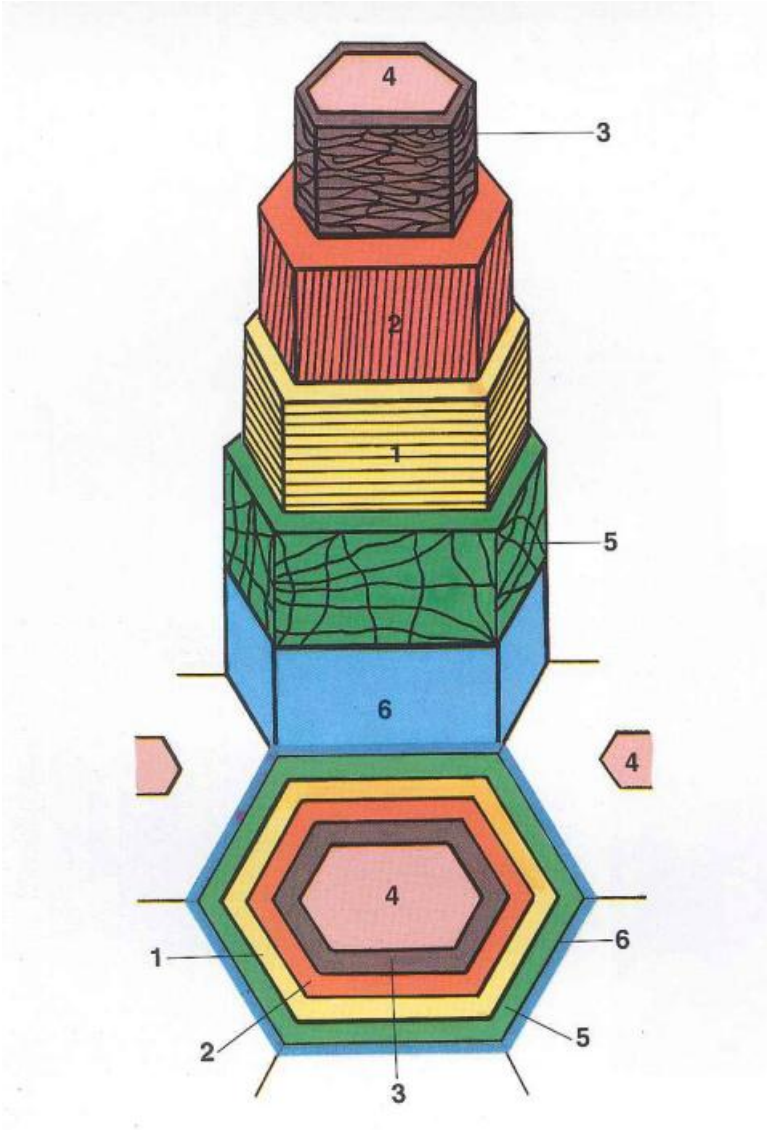

Figure 2.12: Schematic diagram of the cell wall structure of a plant fibre seen in transverse view (bottom) and three dimensional view (top), where 1 – 3 are secondary wall, 4 is lumen, 5 is primary wall and 6 is middle lamella (Bowes, 1996).

2.2.1 Cellulose

Cellulose is a precisely defined polymer composed purely of 8000 – 15000 C6 glucose monomers linked to each other by β-1,4 bonds (Mauseth, 1988) . As shown in **Figure 2.13**, the basic repeating unit of cellulose is cellobiose. The specific structure of cellulose favours the ordering of the polymer chains into tightly packed, highly crystalline structures that are water insoluble and resistant to depolymerisation (Mosier *et al.*, 2005). The crystalline structure is

stabilised by internal hydrogen bonds between molecules. Those molecules can lie parallel to each other and form more hydrogen bonds between themselves, crystallizing and producing aggregates called microfibrils (Mauseth, 1988). These fibrils are attached to each other by hemicelluloses, an amorphous polymer of different sugars as well as other polymers such as pectin, and covered by lignin (Taherzadeh and Karimi, 2008). With this unique orientation in the structuring, it makes cellulose a difficult polymer to break. Cellulose can be hydrolytically broken down to glucose either enzymatically by cellulases or chemically by sulphuric acid or other acids (Mosier *et al.*, 2005). Two form of crystalline cellulose are known: cellulose I and cellulose II, which in its native state cellulose always exists in the cellulose I form unless being processed (physical or chemical treatments e.g.by mercerization) (Dey and Harborne, 1997).

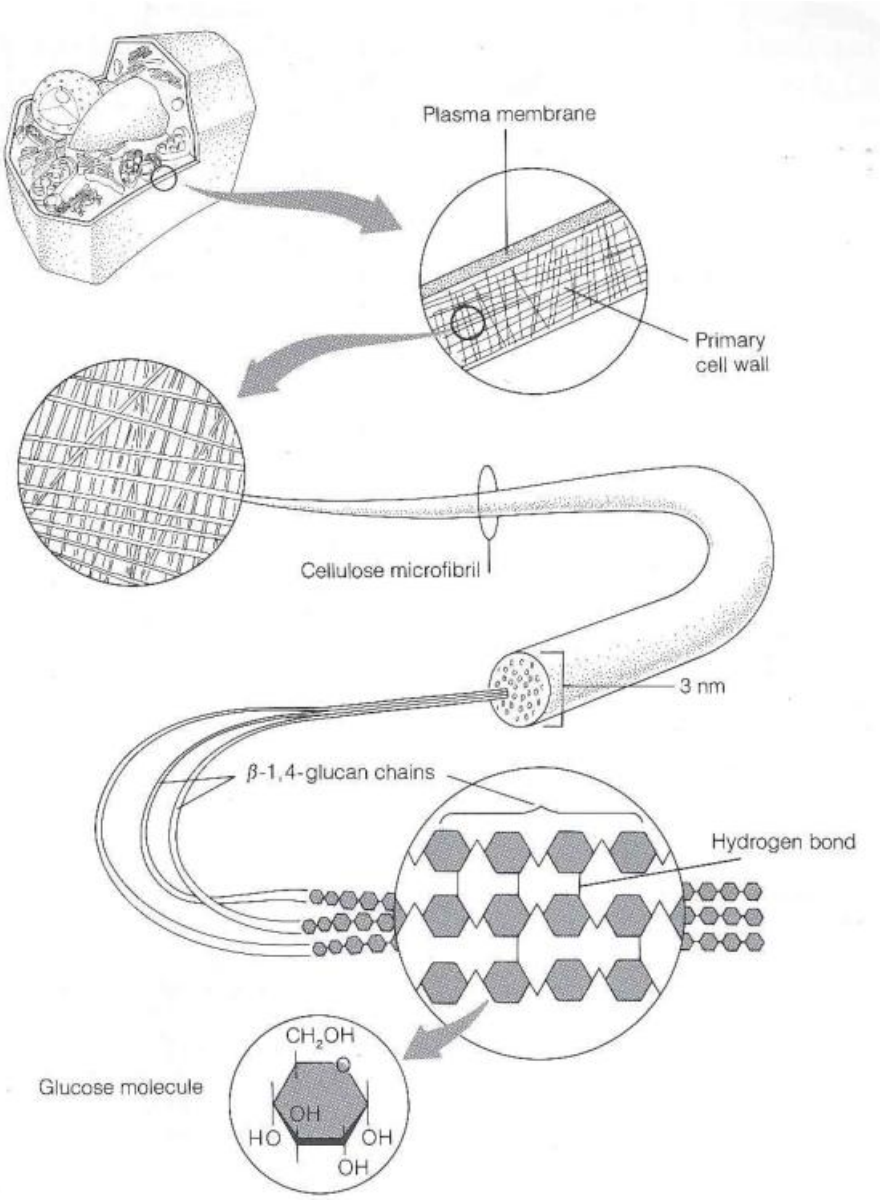

Figure 2.13: Schematic diagram of microfibril in a primary plant cell wall (and held together by hemicelluloses and lignin but not shown here) , the glucose molecule as repeating units in the *β*-1,4-glucan chains and the crystallisation of the chains bonded by hydrogen bonding within a microfibril and cellulose in cell wall (Taiz and Zeiger, 1991).

2.2.2 Hemicellulose

Hemicelluloses are a group of heterogeneous polysaccharides which are formed through biosynthetic routes different from that of cellulose (Corredor, 2008). Hemicelluloses are polysaccharides in plant cell walls that have *β*-1,4-linked backbones with an equatorial

configuration with the function to strengthening the cell wall by interaction with cellulose and, in some walls, with lignin (Scheller and Ulvskov, 2010). Unlike cellulose, hemicellulose is composed of combinations of C5 and C6 sugars such as pentoses (xylose, Xyl and arabinose, Ara) and/or hexoses (mannose, Man, galactose, Gal), and glucose, Glc), and it is frequently acetylated and has side chain groups such as uronic acid and the 4-O-methyl ester (Hu and Ragauskas, 2012). In general, the dominant component of hemicellulose from hardwoods and agricultural plants, such as grasses and straws, is xylan, while glucomannan is prevalent for softwoods (Hu and Ragauskas, 2012; Pu *et al.*, 2008). Diagram of xylan and glucomannan structures are showed in **Figure 2.14**. In contrast to cellulose, which is crystalline and strong, hemicelluloses have a random, amorphous, and branched structure with little resistance to hydrolysis, and they are more easily hydrolysed by acids to their monomer components (Taherzadeh and Karimi, 2008).

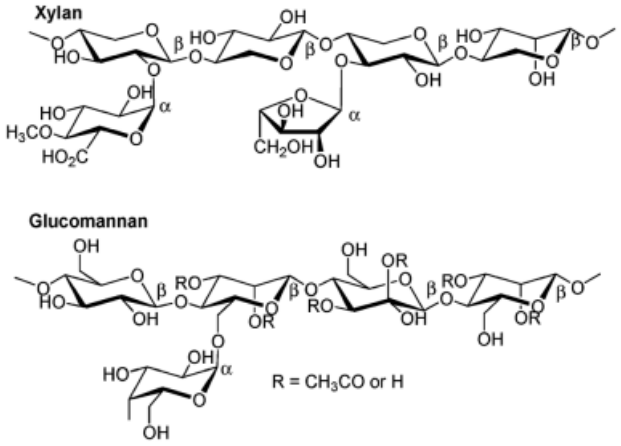

Figure 2.14: Example of xylan and glucomannan structures (Dutta *et al.*, 2012).

2.2.3 Lignin

Lignin is an amorphous, heterogeneous, long chain mostly linked by ether bonds within three dimensional phenolic polymer structures. It consists of three phenylpropane units called *guaiacyl*, G, syringyl, S, and *p*-hydroxyphenyl, H units, and their respective precursors three aromatic alcohols (monolignols), namely, coniferyl, sinapyl, and *p*-coumaryl alcohols as shown in Figure 2.15. The hardwood consist G and S lignin, whereas softwood consist mainly G lignin with small proportion of H lignin. (Brodin *et al.*, 2012; Hu and Ragauskas, 2012; Corredor, 2008). Grass and herbaceous consist all the three forms with *p*-hydroxycinamic acids (*p*-

coumaric acid, ferulic acid and sinapic acid (Hu and Ragauskas, 2012).

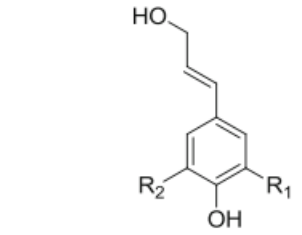

Coniferyl alcohol/guaiacyl: $R_1 = OCH_3$, $R_2 = H$
Sinapyl alcohol/syringyl: $R_1 = R_2 = OCH_3$
p-Coumaryl alcohol/p-hydrophenyl: $R_1 = R_2 = H$

Figure 2.15 Three building blocks of lignin (Hu and Ragauskas, 2012).

The phenolic groups and methoxyl groups are functional groups in lignin, which are importance for the reactivity of lignin (Brodin *et al.*, 2012). Lignin is the most recalcitrant component of the plant cell wall, and the higher the proportion of lignin, the higher the resistance to chemical and enzymatic degradation (Taherzadeh and Karimi, 2008). It bonded together with cellulose and hemicelluloses and contributes to strength of plant cell wall. Lignin effectively protects the plant against microbial attack and only a few organisms, including rot-fungi and some bacteria, can degrade it (Corredor, 2008). A tentative wheat straw lignin example was showed in **Figure 2.16**. Kraft pulping is the most used chemical pulping process in paper pulp industry (Faustino *et al.*, 2010). Following the Kraft pulping process for cellulose extraction, lignin is the main component left in the black liquor and was traditionally viewed as waste material or a low value by-product (Wang, Xu and Sun, 2010; Zhang and Chuang, 2001; Mohan and Karthikeyan, 1997). Approximately 2% of the available lignins from the paper pulp industry were used commercially for specialty products (Ropponen *et al.*, 2011; Faustino *et al.*, 2010) while most lignin and hemicelluloses are thus wasted when the black liquor is simply burnt at mill site for energy recovery (Faustino *et al.*, 2010; Wallberg, Linde and Jönsson, 2006). With a new extraction technology developed in Sweden, more Kraft lignin can be generated at the mill site as either an thermal energy source for heat or electricity generation for external uses or for the production of value-added chemicals (de Jong *et al.*, 2012; Ohman *et al.*, 2010).

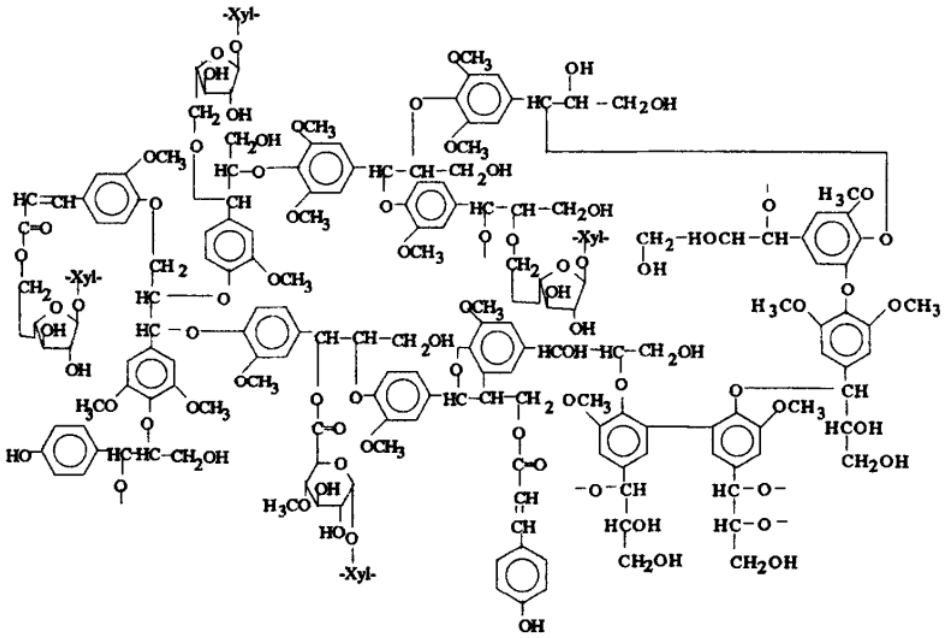

Figure 2.16: A tentative chemical structure for wheat straw lignin (Sun, Lawther and Banks, 1997).

2.3 Bio-refinery

According to IEA Bioenergy Task 42 (de Jong *et al.*, 2012), bio-refinery is defined as the sustainable processing of biomass into as spectrum of marketable products (food/feed, materials /chemicals and energy as fuels for power/heat). The principal goal in the development of biorefineries is defined by the following:

(biomass) feedstock-mix + process-mix → product-mix

and in particularly, the combination between biotechnological and chemical conversion of biomass feedstock to intermediates and final products will play an important role (Kamm and Kamm, 2004).

2.3.1 Biomass for fuel applications

Apart from direct combustion, there is few more way to convert biomass for energy recovery. Conversion technologies may release the energy directly, in the form of heat or electricity, or may convert biomass into liquid biofuels or combustible biogas. A summary of pathways for biomass conversion technologies for energy is given showed in **Figure 2.17**.

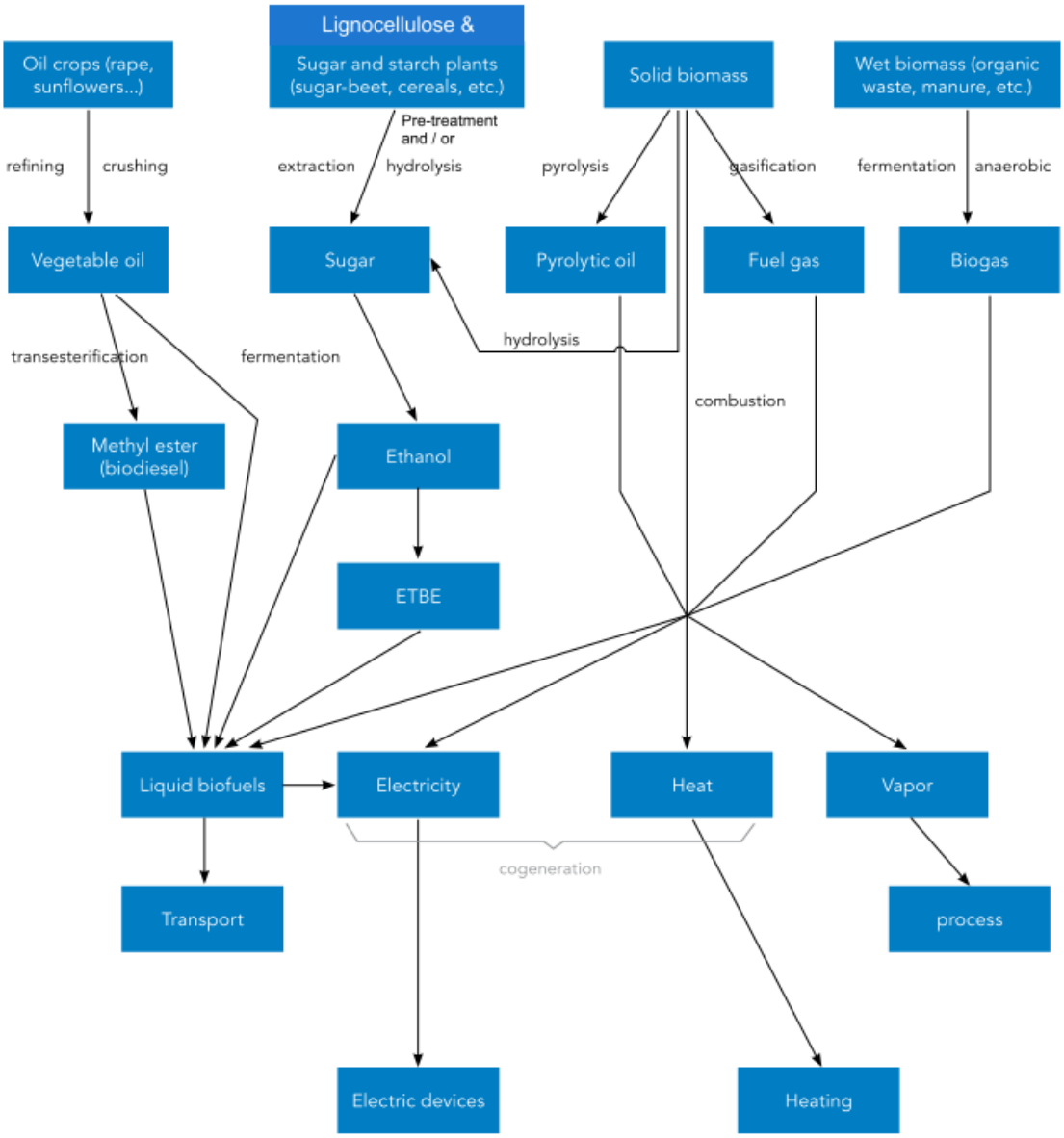

Figure 2.17: Pathways for conversion of biomass for energy conversion overview (UEMOA, 2013).

2.3.2 Development of biofuels

History of biofuels can be traced back to the first few decades in 1800s but has only received new interests since the mid-1990s when growing concerns over energy security and sustainability and climate change has raised worldwide interest in bio-based liquid transport fuels or biofuels as alternative to fossil liquid fuels. However, the development of biofuel has not happened only since then but in fact the development history of biofuel can be traced back since first few decades of 1800s. **Figure 2.18** gives a brief overview of biofuel development from historic perspectives correlated to their growth from 1900s and sharp increase in recent years.

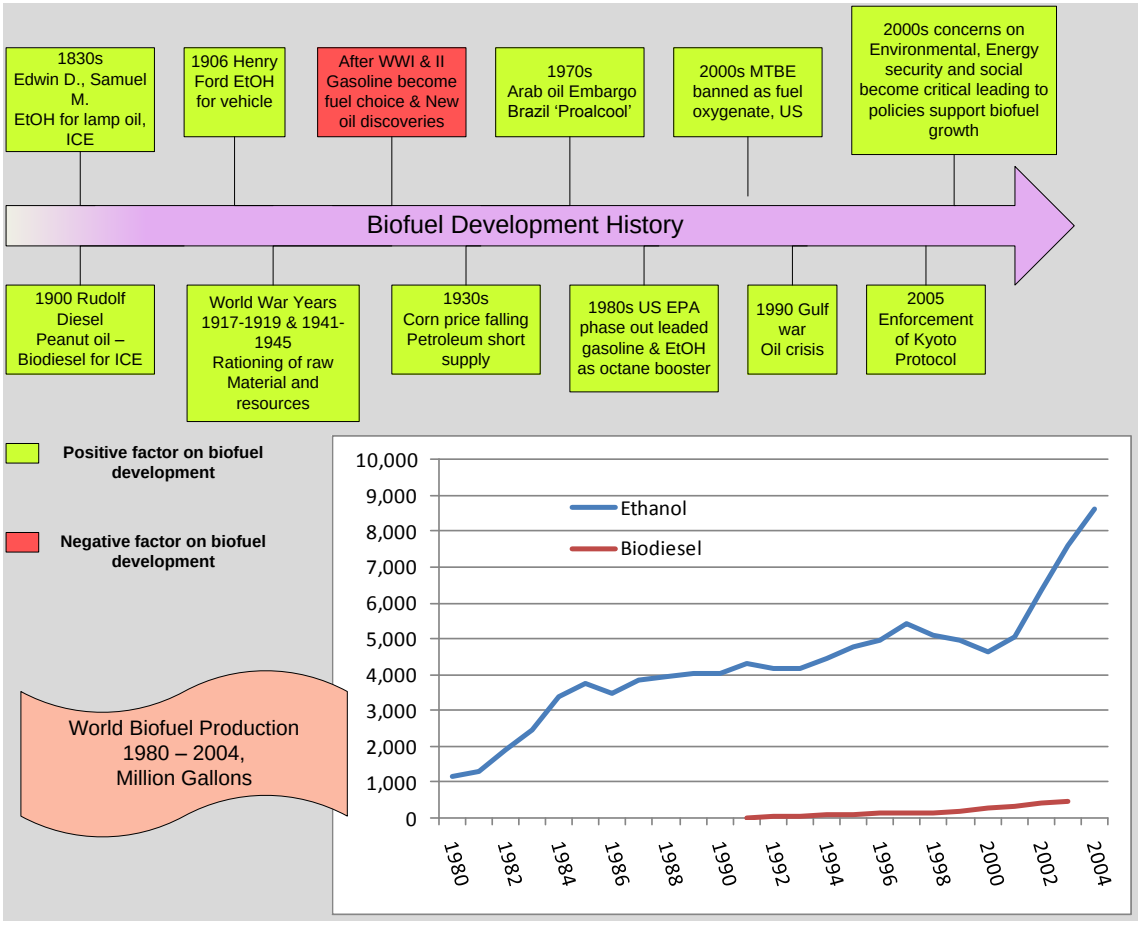

Figure 2.18: World Historical Development of Biofuel (Songstad *et al.*, 2009; Pousa, Santos and Suarez, 2007; Solomon, Barnes and Halvorsen, 2007; Rosillo-Calle and Walter, 2006; EPI, 2005; IEA, 2005; Körbitz, 1999)

As a result of the considerable efforts devoted to legislations, financial assistance or /subsidisation in development of infrastructure for production and supply, the EU has achieved a significant fraction of its energy (as heat and electricity) from the combustion of residues and wastes (European Commission, 2000). With the enforcement of European directives, there is a reduction of waste and increased recycling of materials thus waste is a limited and declining resource. To meet the proposed targets on bioenergy, it will require greater use of agricultural and forest residues as well as the introduction of energy crops and adoption of cost-effective, environmentally friendly processes, attractive to investors and acceptable to planning authorities and the public in general (European Commission, 2000).

With the global concern on fossil fuel depletion and climate change, biofuel has become more and more important as a sustainable fuel which is able to provide energy while significant reduce net carbon emissions. The energy fuelling terrestrial life processes is initially captured from sunlight by photosynthesis, fixed into carbon based molecules, and gradually released again through the metabolism of these energy-rich molecules (Gomez, Steele-King and McQueen-Mason, 2008) in, for instance, plant biomass. This is an ecosystem where bonds formed and broken between carbon, hydrogen and oxygen act as vectors for energy transfer (Gomez, Steele-King and McQueen-Mason, 2008). Conversion of biomass into biofuels falls into this concept in line with the basis of global carbon cycle.

Liquid fuels (or "oil" such as petrol and diesel) are currently the predominant energy sources in the transport sector. The percentage of oil in the total final energy consumption (TFEC) of road transport was about 97% and road transport accounted for 92% of the transport sector TFEC (Gnansounou, 2010). Currently the whole transportation sector produces about 25% of global energy-related CO_2 emissions and accounts for roughly 50% of global oil consumption (OECD, 2010). Biofuels are seen as one of the most feasible options for reducing carbon emissions in the transport sector. In 2008, global biofuel production reached about 83 billion litres, a more than fourfold increase compared to that in 2000 (OECD, 2010). United States, Brazil and the European Union are amongst the largest producers of biofuels. This amount currently contributes about 1.5% of global transport fuel consumption, with demand projected to rise steadily over the coming decades (OECD, 2009)(OECD, 2010)(OECD, 2008a). United States, Brazil and the European Union are amongst the largest producers of

biofuel.

Biofuels have the advantage that they can be employed in the currently existing vehicles without significant adaptations and with improvements in fuel efficiency and electrification in light vehicle fleet. For heavy-duty vehicles, marine vessels and airplanes in particular, biofuels will play an increasing role to reduce CO_2 emissions since electric vehicles and fuel cells are not feasible for these transport modes (OECD, 2010).

Biofuels can be classed into liquid biofuels and gaseous biofuels. Liquid biofuels include:

i. Bioalcohol – used as gasoline substitute mainly as blends in spark ignition and petrol engine.
ii. Biodiesel – used as a mineral diesel fuel substitute in compression ignition engines. Untreated raw vegetables oil is used in old diesel engine with direct injection system.

Gaseous biofuels or biogas are used in internal combustion engines designed or modified for gas combustion. They are less popular than liquid biofuels due to lacking of compatibility with existing vehicles and infrastructure. Focus from hereon will be given to liquid biofuels. **Figure 2.19** shows a summary of current and future biofuel products and applications.

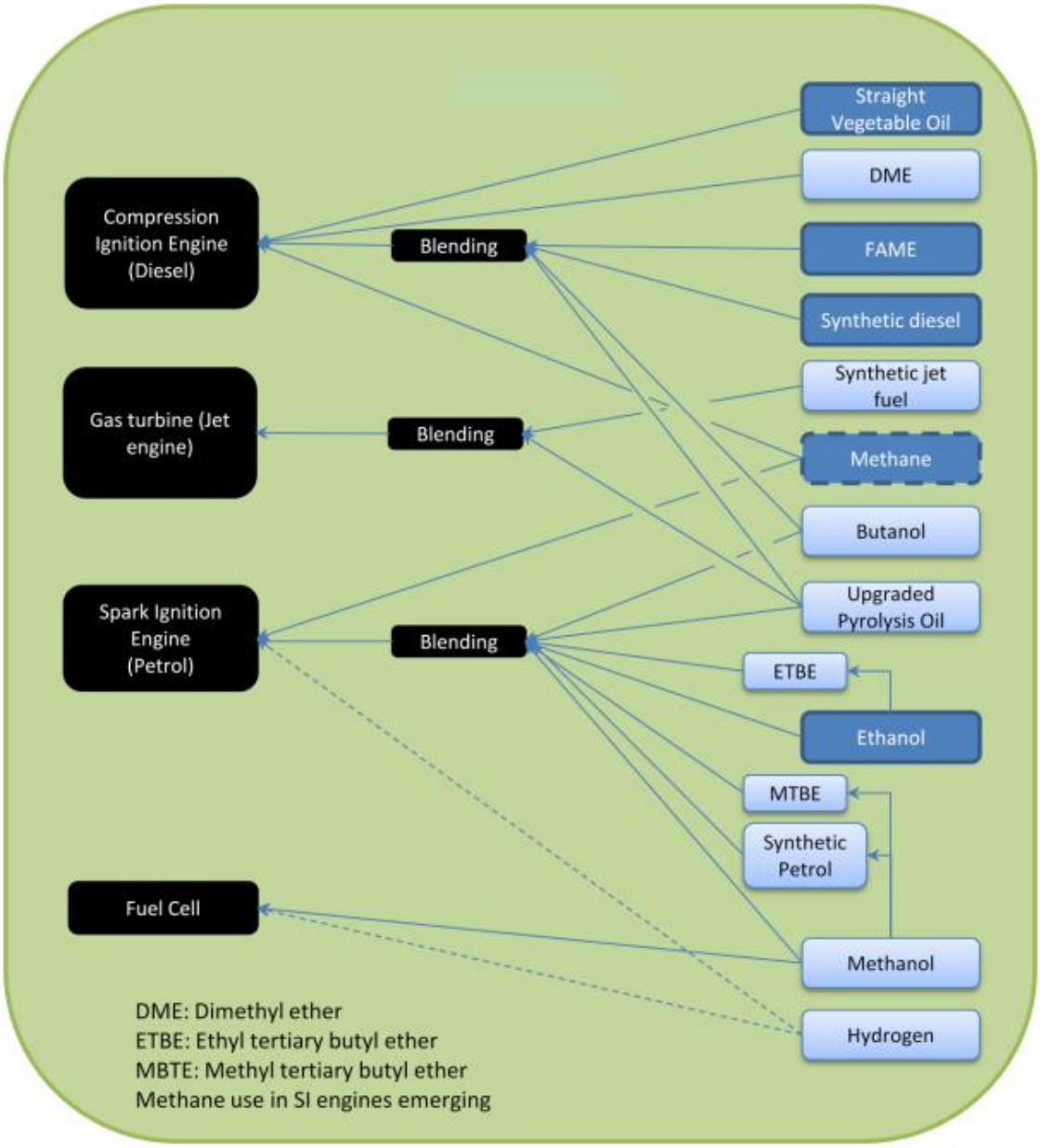

Figure 2.19: Biofuel products and its application (NNFCC, 2010).

2.3.3 The 1st generation biofuels

The first generation biofuels refer to the fuels that have been derived from sources like starch, sugar, animal fats and vegetable oil which are all also food sources as shown in **Figure 2.20**. In general, biodiesel is made from the same oil crops used in the food industry, and bioethanol is produced by fermentation of sugars from sugar cane (*Saccharum officinarum*) or sugar beet (*Beta vulgaris*), or derived from hydrolysis of starch (see the route from starch in **Figure 2.20**)

(Gomez, Steele-King and McQueen-Mason, 2008).

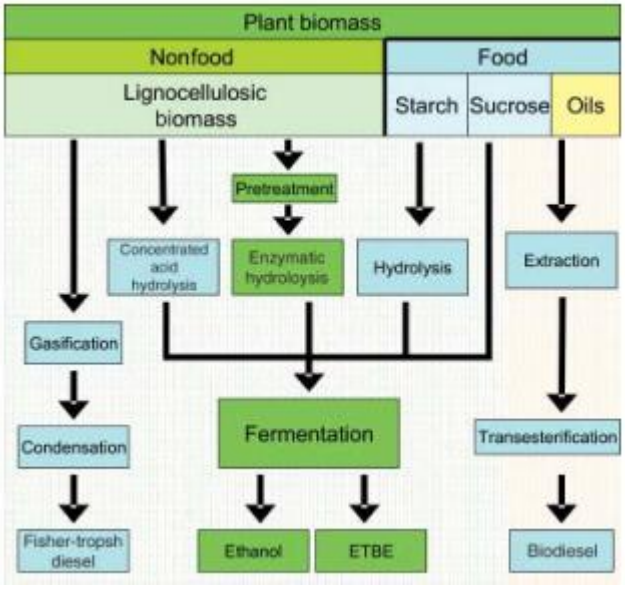

Figure 2.20: Liquid biofuel production from biomass (Gomez, Steele-King and McQueen-Mason, 2008).

1st generation biofuel has been commercially produced to meet the demand of bioenergy. The United States has become as largest producer, followed by Brazil and then Europe. However, the 1st generation biofuels have attracted criticisms due to the constrains and concerns on 1st generation biofuels as they:

- contribute to higher food prices due to competition in use of land or food crops;
- are an more expensive option for long term energy security in terms of total production cost excluding government grants and subsidies;
- provide only limited GHG reduction benefits (with the exception of sugarcane ethanol) and at relatively high costs in terms of $ / tonne of carbon dioxide ($/t CO_2) avoided;
- do not always lead to environmental benefits as claimed because the biomass feedstock may not always be produced sustainably. For instance, sugar and starch crops require very substantial inputs of fertilizers and pesticides which is source of N_2O emission, among others;
- are potentially accelerating deforestation and over-exploitation of land and water resources in some environmentally vulnerable regions (OECD, 2008a);

- Compete for scarce water resources in some regions (OECD, 2008a).

These have stimulated development in the 2nd generation biofuel to avoid the impacts mentioned.

2.3.4 The 2nd generation biofuels

Second generation biofuels are produced from the non-food biomass (**Figure 2.20**) in a more sustainable fashion, which can be truly carbon-neutral or even carbon-negative in terms of its impact on CO_2 emissions(Gomez, Steele-King and McQueen-Mason, 2008). Plant biomass is often referred to lignocellulosic material which is cheap and abundant non-food materials available from forestry or agriculture crop residues and energy crops. These biomass can be converted thermochemically or biochemically into biofuels (see **Figure 2.20**). The 2nd generation biofuels are expected to be superior than the 1st generation in terms of energy balances, green house gases emission reductions, land use requirements and competition for land, food and water. The 2nd generation biofuels are mostly in earlier stage of development but a considerable number of pilot and demonstration plants have been announced or set up in recent years in North America, Europe, Brazil and a few emerging countries. In 2007, the 2nd generation biofuels have remained around 0.1% of total ethanol biofuel production (OECD, 2008a). This is largely because that the necessary technologies are not yet efficient or cost effective or technically proven at commercial scale (OECD, 2008a).

Most of the published LCA studies for biofuels focus on the overall GHG mitigation potential in comparison with fossil fuels (OECD, 2010). Consolidated results of selected international studies for greenhouse gas emissions per energy content are shown in **Figure 2.21** for the 1st as well as 2nd generation biofuels (OECD, 2010).

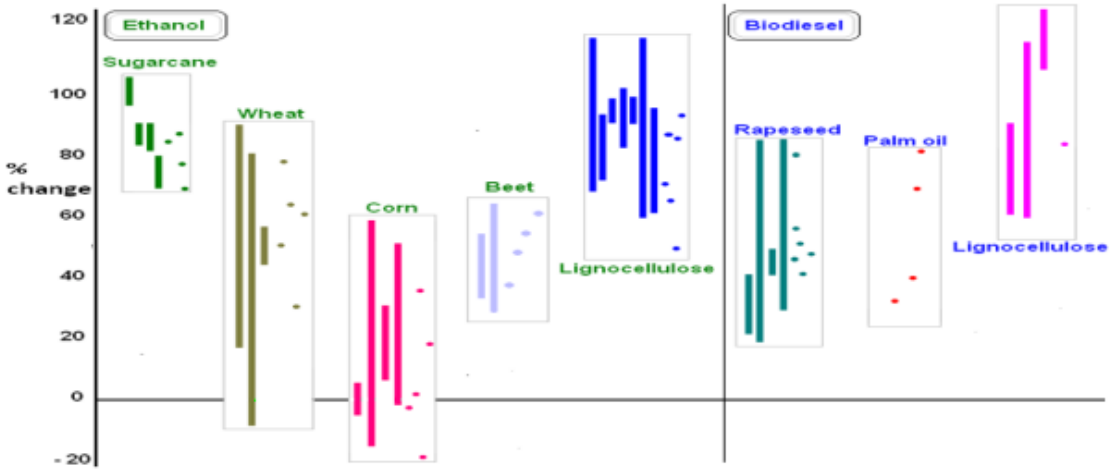

Source: IEA, 2008c based on IEA and UNEP analysis of 60 published life-cycle analysis studies giving either ranges (shown by the bars) or specific data (shown by the dots).

Figure 2.21 Comparison of well-to-wheel emission changes of for different biofuels (the 1st generation from food crops and the 2nd generation from lignocelluloses) compared with "well-to-wheel" for fossil fuels (OECD, 2010).

The majority of the 1st generation biofuels do not produce high GHG mitigation except some data on sugarcane based bioethanol where the bagasse co-product has also been used for generating heat and power for the processing plant. The lignocellulosic biofuels tend to produce higher GHG mitigation due to extra technologies used in the up-stream processing (**Figure 2.20**). However, owning to lack of data on commercial scale, these LCA data are theoretical and based only on that as the pilot/demonstration stage and thus further research is required to provide more accurate and complete assessment.

The 2nd generation biodiesel and bioethanol are the most studied options. Both fuels were used on their own or as blends with fossil fuels. The 2nd generation biodiesel has received attention with growing attention of diesel engine vehicles in the transportation fleets while bio-ethanol is expected to more competitive in having more potential of fuel cost reduction (Gnansounou, 2010).

It should be noted that bio-SNG, synthetic gas similar to natural gas, can also be produced from a wider variety of biomass feedstocks (e.g. waste streams with mixture of bio- and nonbio-residues). It can be further compressed or liquefied for use as transport fuel in modified vehicles

(OECD, 2010) or the gas can be converted biologically to liquid fuels. The biofuel yields in terms of fuel equivalent are higher in this conversion route compared to bioethanol and biodiesel mentioned earlier.

With the need of further improvement for 2nd generation biofuel, the following sections will focus on the conversion technology development.

2.3.5 Conversion technology for 2nd generation biofuel – bioethanol

The 2nd generation bioethanol can be produced using two main routes, namely thermochemical and biochemical route. Both processes can potentially convert 1 dry tonne of biomass (~ 20GJ/t) to around 6.5 GJ/t of energy carrier in the form of biofuels, thereby giving averall biomass to biofuel conversion efficiency of around 35% (Mabee and Saddler, 2010). The key different between biochemical and thermochemical route is lignin component is a residue for the formal and a part of synthetic gas in the later.

2.3.5.1 Thermochemical conversion route

Thermochemical conversion technologies rely on heat and / or physical catalysts to convert biomass to an intermediate gas ($CO + H_2$) or liquid, followed by a conversion step (Fischer-Tropsch) to convert that intermediate to a biofuel, such as synthetic diesel, aviation fuel or ethanol (Sims *et al.*, 2010; Foust *et al.*, 2009). This route also known as biomass-to-liquids process. An example process diagram of thermochemical conversion was shown in **Figure 2.22**.

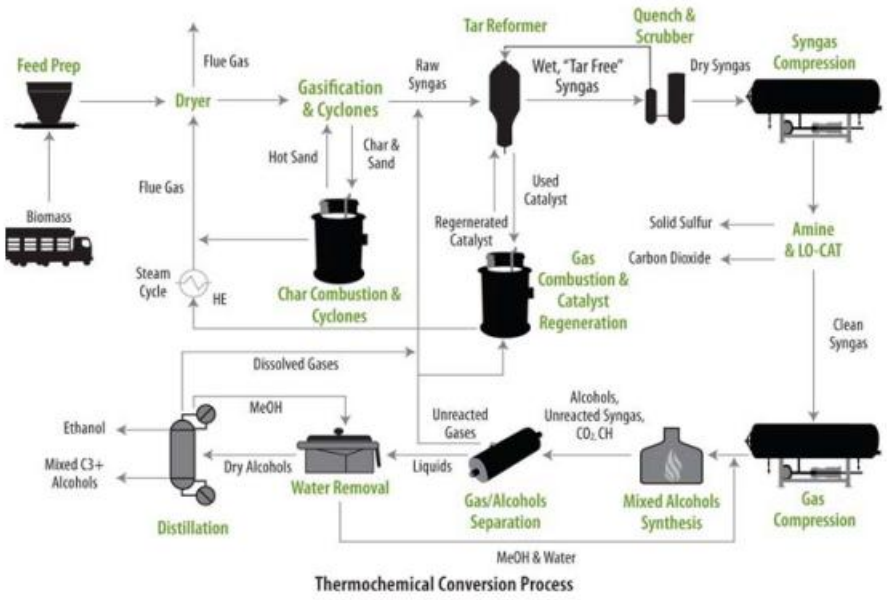

Figure 2.22 Schematic diagram of thermochemical conversion of biomass (Foust *et al.*, 2009).

2.3.5.2 Biochemical conversion route

Biochemical conversion route featuring enzymatic hydrolysis involves few key steps : pre-treatment, enzymatic hydrolysis and fermentation (see **Figure 2.23** an example biochemical route process flow diagram).

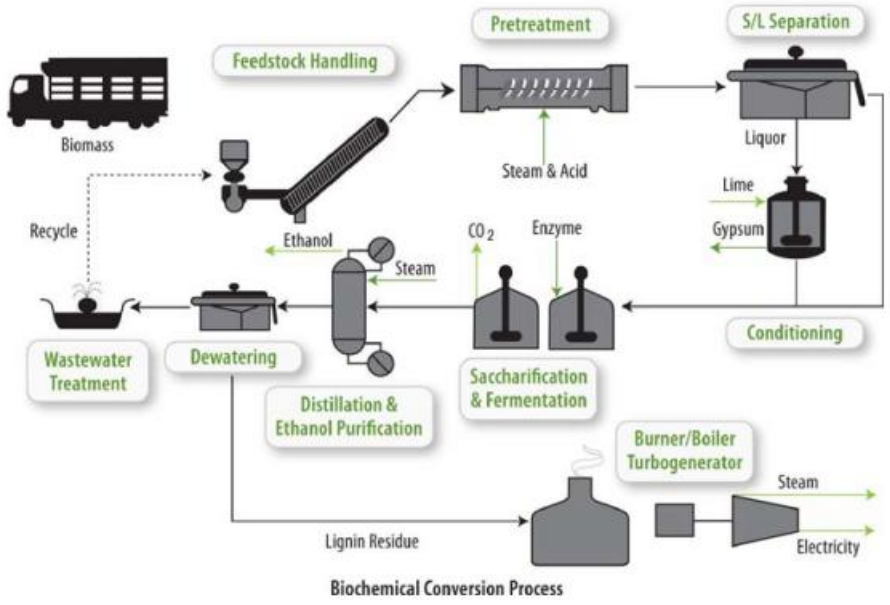

Figure 2.23 Biochemical conversion process (Foust *et al.*, 2009).

The main challenges of bio-chemical route are in the integration of the system which requires a coordinated effort to improve efficiency in each step in order to achieve an overall higher yield and thus lower cost of bioethanol (Gnansounou, 2010).

i. Pre-treatment

See session 2.4.3.2

ii. Enzymatic hydrolysis

Enzymatic hydrolysis is the second key step in the biochemical conversion route and it involves cleaving the polymer cellulose and hemicellulose into the monomeric sugars by using enzymes. Cellulose conversion involves cellulose degradation enzymatically to glucose by the synergistic action of three distinct classes of enzymes: the "endo-1,4-β - glucanases" (EC 3.2.1.4), which act randomly on soluble and insoluble 1, 4-β- glucan substrates; the "exo-1,4-β-D- glucanases" (EC 3.2.1.91), which release D-glucose from 1, 4-β-D-glucans and hydrolyze D-cellobiose slowly and liberate D-cellobiose from 1, 4-β-glucan; and the "β-D-glucosidases" (EC 3.2.1.21), which release D-glucose units from cellobiose and soluble cellodextrins as well as a

group of glycosides (Himmel, M.E., Adney, W.S., Baker, J.O., Elander, R., McMillan, J.D., Nieves, R.A., Sheehan, J.J., Thomas, S.R., Vinzant, T.B. and Zhang, M., (1997) Advanced bioethanol production technologies: a perspective. ACS Symp. Ser. 666 2-45. && Corredor D thesis). **Figure 2.24** outlined the proposed reaction path.

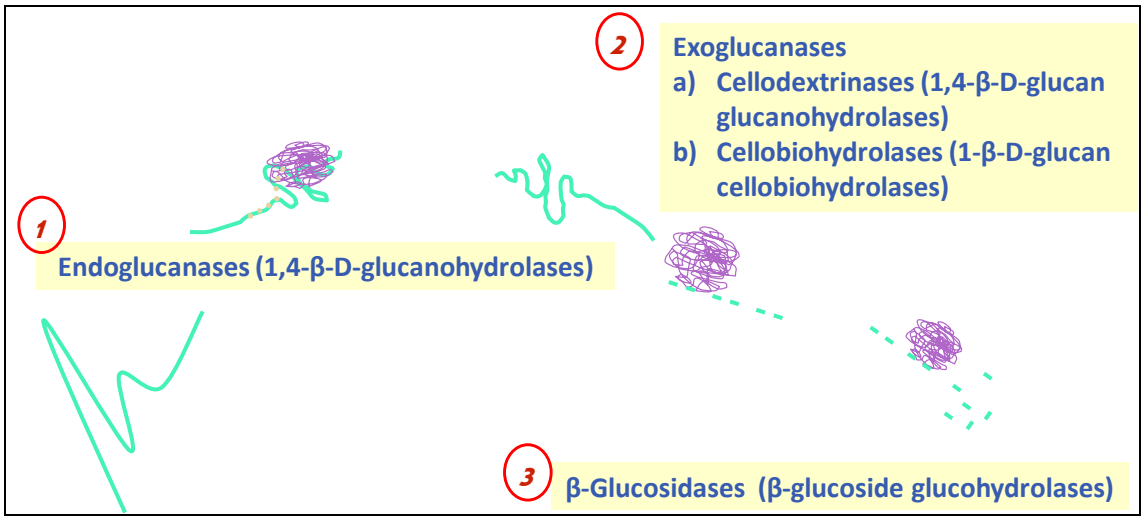

Figure 2.24: Diagram of cellulose conversion reaction catalysted by various cellulase.

iii. Fermentation

Fermentation of hydrolysates from lignocellulosic substrate is more difficult than the well-established processes of ethanol production e.g., from molasses and starch. Hydrolysates contain a broader range of inhibitory compounds, where the composition and concentration of these compounds depend on the type of lignocellulosic biomass, the chemical used and nature of the pretreatment, and the hydrolysis process (Corredor, 2008).

2.4 Pre-treatment of lignocellulose biomass for biofuel production

2.4.1. The role of pre-treatment

Cellulose in lignocellulosic biomass is harder to be accessed and enzymatically hydrolysed to glucose than the polysaccharide in starch, and hence it is generally more expensive to produce ethanol from cellulose than starch (or sugar cane) ethanol (Virkajärvi *et al.*, 2009). Pre-treatment of lignocellulosic biomass is therefore necessary to open up the plant cell structure enabling enzymes to access the cellulose.

Pre-treatment refers to a number of technologies which physically (and chemically in some cases) alter plant biomass so as either to alter the physical/chemical characterisatics of the biomass to assist the biomass breakdown during down-stream processes or to increase the cellulose content in the treated feedstock (by e.g. extraction and removal of the non-cellulose) (NNFCC, 2009). A schematic diagram of pre-treatment of biomass for bio-alcohol application is given in **Figure 2.24**. It is with two scenarios to outline the yield output for the comparison of path with and without pre-treatment.

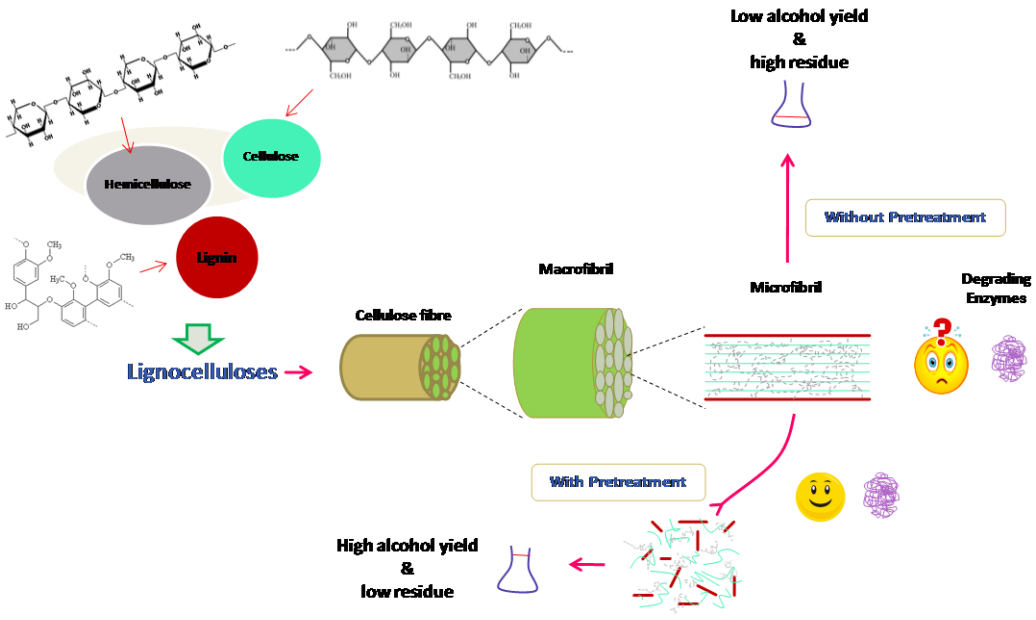

Figure 2.24 Schematic diagram of general concept of biomass pre-treatment for bioalcohol production.

An effective pre-treatment technology should: (Kumar *et al.*, 2009a; Taherzadeh and Karimi, 2008; Mosier *et al.*, 2005),

i) Be economic such as reducing cost of feedstock size reduction and material for construction of pre-treatment reactors.
ii) maximise the yield and quality of fermentable sugars
iii) avoiding formation of possible inhibitors to hydrolytic enzymes and fermenting microorganisms.
iv) maximise the potential for co-product production or bio-refinery
v) be suitable for range of biomass types.
vi) be easily adapted and suitable for commercial scale operation.

A range of pre-treatment methods have been studied and introduced for pre-treatment of lignocellulose biomass. These include physical, physico-chemical, chemical, biological or a combination of them. Among various pre-treatment technologies developed during the past two decades, diluted acid pre-treatment (DAP), hydrothermal pre-treatment, steam explosion and alkaline pre-treatment are among the various pre-treatment technologies developed (Hu and Ragauskas, 2012) and are close to commercial applications.

2.4.2 Factors contributing lignocellulosic recalcitrance

There are several factors which are believed to contribute to the recalcitrant lignocellulose to pre-treatment and subsequent hydrolysis (Sierra *et al.*, 2008):

i) Structure and content of lignin

Lignin is tightly bonded with cellulose and hemicelluloses and acts as a barrier to prevent enzyme access to the polysaccharides fraction of lignocelluloses. G lignin was reported to restrict fibre swelling and enzyme accessibility more than S lignin (Ramos, Breuil and Saddler, 1992). Softwood has more G lignin compared with hardwood and hence was believed to be more recalcitrant than hardwood (Taherzadeh and Karimi, 2008). In addition, enzymes tend to irreversibly bond to lignin through hydrophobic interactions during enzymatic hydrolysis leading to a loss in their activities (Hu and

Ragauskas, 2012; Balan *et al.*, 2009).

ii) Acetylated hemicelluloses and lignin-carbohydrate complexes, LCCs

Hemicelluloses sheath cellulose microfibrils and the acetyl groups of hemicelluloses are believed to sterically hinder enzyme attack (Hu and Ragauskas, 2012; Sierra *et al.*, 2008). Apart from bonding with cellulose, hemicellulose and the side chains of branched hemicelluloses (e.g. uronic acid and arabinose) may be covalently bonded to lignin to create enzyme-impenetrable cross-links known as lignin-carbohydrate complexes or LCCs (Chundawat *et al.*, 2011).

iii) Cellulose crystallinity and degree of polymerisation, DP

The cellulose microfibrils have both crystalline and amorphous regions, and the crystallinity is given by the relative amounts of these two regions (Taherzadeh and Karimi, 2008). By common understanding, higher crystallinity and thus tighter structure would limit the accessibility of enzyme. However, the correlation between crystallility of pre-treated biomass and sugar yield from enzymatic hydrolysis was found to vary considerably in the literature (Zhang, Xu and Hanna, 2012; Zhang *et al.*, 2012; Sannigrahi, Miller and Ragauskas, 2010; Zhang and Lynd, 2004). Further study is thus needed to gain more insight into of the role of crystallinity in enzymatic hydrolysis. During the enzymatic hydrolysis, endo-cellulases are involved in cleaving the internal β-1,4 linkages of cellulose chains, decreasing degree of polymerisation (DP) of cellulose ends leading to attack by exo-cellulases (Hu and Ragauskas, 2012; Srisodsuk *et al.*, 1998). Reduction in DP is expected to have better enzymatic accessibility as exo-cellulases are known to have preference for lower DP substrates (Hu and Ragauskas, 2012; Zhang and Lynd, 2004).

iv) Pore volume and specific surface area of cellulose

Degree of fractionation measures the physical disintegration of the native biomass structure and is related to size reduction and openness of the treated feedstock. Effective fractionation creates higher specific surface area and more porous structure enabling cellulose to be more available for enzymatic activities(Zhang, Xu and Hanna, 2012;

Zhang *et al.*, 2012).;

Pre-treatment should thus be targeted to address the above mentioned factors.

2.4.3 Pretreatment technologies

Few key pre-treatment technologies will be discussed here in term of the definition of technology, advantages, disadvantages and realisation.

2.4.3.1. Physical pre-treatment

Physical pretreatment are physical methods to change physical state of the feedstck. Different types of physical processes such as milling (e.g. ball milling, two-roll milling, hammer milling, colloid milling and vibro energy milling) and irradiation (e.g. by gamma rays, electron beam or microwaves) can be used to improve the enzymatic hydrolysis or biodegradability of lignocellulosic materials (Taherzadeh and Karimi, 2008). This method is commonly in used in combination with the rest of pre-treatment technique to make the pre-treatment process more efficient.

2.4.3.2 Physico-chemical pre-treatment

These methods combines some physical (including mechanical and thermal treatments) and chemical treatments of biomass. Most of the current key pre-treatment technology falls under this category. A number of key pre-treatment technologies are described here in term of the processes pros and cons and applications.

2.4.3.2.1 Steam Explosion

Steam explosion pre-treatment is a process where the lignocellulosic biomass is treated in batch with high pressure steam in a pressure vessel for a given time followed by a sudden release of pressure leading to an explosive decompression and opening up of the biomass structure. This pre-treatment releases most of the hemicellulose. Typically, temperature between 160 - 260°C are used together with pressure of 6 – 34 bars for a period ranging from a few seconds to minutes in the pressure vessel. It can become catalytic by addition of sulfuric acid or sulfur dioxide, typically at 0.3 – 3 wt% prior to the pre-treatment (Jørgensen, Kristensen and Felby,

2007). Removal of the acetyl groups from the hemicellulose during the process (at high temperature) can result in the formation of acetic and other acids which catalyse the breakdown of hemicelluloses to mono and oligosaccharides (NNFCC, 2009). Lignin is to some extent removed from the biomass structure and redistributed(Mosier *et al.*, 2005). Addition of acid catalyst can be beneficial, especially for softwood, since the hemicellulose in softwood contains less acetylated groups, and therefore autohydrolysis cannot occur to the same extent as in hardwood (Virkajärvi *et al.*, 2009).

Steam explosion offers several advantages including significantly lower environmental impacts, enabling use of less hazardous process chemicals and greater potential for energy efficiency (Alvira *et al.*, 2010). The addition of catalyst can helps to improve the yields, reduce time and temperature while reduce risks of formation of inhibitors to subsequent processes. The process however also has some limitations. These include risk of partial destruction of xylan, incomplete disruption of lignin-carbohydrate matrix, limited lignin release and lignin redistribution on the cellulose surfaces (Chen and Qiu, 2010; Hongzhang and Liying, 2007). Steam explosion has advanced to the demonstration scale in Iogen (Canada) and to the pilot scale at the Iotech Pilot Plant (Canada), the Souston pilot plant (France) and in Örnsköldsvik (Sweden) (Virkajärvi *et al.*, 2009).

2.4.3.5.2 Liquid hot water

Liquid hot water pre-treatment is also named as hydrothermolysis process, which the biomass was incubated in high pressure liquid under superheated condition (e.g. 180 - 230°C for around 15 – 24mins) (NNFCC, 2009). Water under high pressure can penetrate into biomass, hydrate cellulose, and remove hemicelluloses and part of lignin (Taherzadeh and Karimi, 2008). The autohydrolysis occurred with addition of water at high temperatures and pressures in a batch or co-current flow mode, with the release of acetic acid postulated to catalyze the removal of hemicelluloses and enhance cellulose digestibility (Yang and Wyman, 2008). The major advantage of liquid hot water pre-treatment is it requires less demand on size reduction for biomass feedstock as the biomass breaks apart on cooking (NNFCC, 2009). However, acidic pre-treatment condition can lead to degradation of hemicelluloses further and generate toxic by-products such as furfural and hydroxymethylfurfural. This prompted to have liquid hot water pre-treatment with pH controlled. The pH is controlled to maintain at range of 4 – 7 to minimise

the acid-catalysed degradation of sugars by addition of base (Pienkos and Zhang, 2009; Laser *et al.*, 2002). Although very tempting cost-wise (no chemicals, no extreme pH, therefore chemical and equipment material costs are low) then very dilute conditions may lead to costly production of ethanol (Virkajärvi *et al.*, 2009). It also reported less suitable for high lignin feedstock (NNFCC, 2009).

2.4.3.5.3 Dilute acid

Dilute acid hydrolysis makes use of lower concentrations of acid (typically 0.5 – 5% sulphuric acid) at elevated temperatures and pressures in a batch vessel, plug flow or flow through bed, and typically achieves hydrolysis of hemicelluloses and yields enzymatically accessible cellulose (Pienkos and Zhang, 2009). Sulphuric acid is the most commonly in used acid but other acid such as nitric acid, hydrochloric acid were also reported (Mohammad J. Taherzadeh, Keikhosro Karimi, 2007). It named as diluted acid pre-treatment when high temperature and low acid concentration in used; and as concentrated acid pre-treatment when low temperature and high acid concentration in used. At elevated temperature (e.g. 140 - 190°C) and low concentration of acid (e.g. 0.1 – 1% sulphuric acid), the dilute acid pre-treatment can achieve high reaction rates and significant improve cellulose hydrolysis (Pienkos and Zhang, 2009; Mohammad J. Taherzadeh, Keikhosro Karimi, 2007). Need for the expensive construction material (due to corrosive nature of acid), formation of by-product gypsum are formation of toxic degradation products are among the disadvantages of dilute acid pre-treatment (NNFCC, 2009; Virkajärvi *et al.*, 2009). This pre-treatment method is being used by Royal Nedalco in the Netherlands for lignocellulosic ethanol technologies whilst Dong Energy in Denmark are operating a 100 – 1000 kg per hour pilot plant and SEKAB in Sweden are using this method for wood residues and as a pre-treatment prior to enzymatic breakdown of biomass (Gnansounou, 2010; NNFCC, 2009; Virkajärvi *et al.*, 2009).

2.4.3.5.4 Alkaline pre-treatment

Alkaline pre-treatment refers to the application of alkaline solution such as sodium hydroxide, NaOH, Calcium hydroxide, $Ca(OH)_2$ or ammonia to remove lignin and a part of the hemicelluloses and efficiently increase the accessibility of enzyme to cellulose (Taherzadeh and Karimi, 2008). Compared with acid or oxidative reagents, alkali treatment appears to be the

most effective method in breaking the ester bonds between lignin, hemicelluloses and cellulose and avoiding fragmentation of the hemicelluloses polymers (Taherzadeh and Karimi, 2008; Gáspár, Kálmán and Réczey, 2007).

$Ca(OH)_2$ is one of the alkaline agent used to depolymerise lignin. The long reaction time and low biomass concentration are among disadvantages for this method, whilst the benefit is, it can proceeds at atmospheric pressure and at low temperature (Virkajärvi *et al.*, 2009).

In Ammonia Fibre Explosion, AFEX pre-treatment, lignocellulosic biomass is being exposed to liquid ammonia (typically 1-2kg per kg of dry biomass) at high pressure (17 – 20 bar) for a set amount of time (around 30 minutes), with moisture content of 20 – 80% and finally a sudden release of pressure like in steam explosion process (NNFCC, 2009). AFEX pre-treatment has led to very good yields: nearly 95% (Virkajärvi *et al.*, 2009). Less inhibitory by-product formation and operating at high solid concentration are also advantages of AFEX. The key drawback of this technology is the cost of recycling the used ammonia.

The Ammonia Recycle Percolation (ARP) method uses aqueous ammonia (10 – 15% w/w), percolated through a packed bed of biomass at elevated temperatures (150 - 170°C) to solubilise hemicelluloses and lignin and the ammonia is recovered and recycled to the reactor (NNFCC, 2009; Pienkos and Zhang, 2009). AFEX and ARP is not clearly distinguished but these processes differ in having different ammonia concentration and ARP does not require a compressive explosion step (NNFCC, 2009).

2.4.3.5.5 Organosolv

In brief, the organosolv process refers to the cooking of lignocellulosic biomass in an organic solvent such as methanol, ethanol or acetone and water at 150 – 200 °C for 30 – 60 minutes under pressure (NNFCC, 2009). Dilute acid e.g. sulphuric acid can be used as catalyst. The fermentablility of sugars after ethanol pre-treatment is reported to be very high copared to steam explosion (Virkajärvi *et al.*, 2009; Berlin *et al.*, 2006). The Lignol process (Lignol Energy Corporation,) in used in pulping industry is one of the example of organosolv pre-treatment. Organosolv id generally thought to be too expensive, because it relies on recovery and recycle of solvents (Pienkos and Zhang, 2009).

2.4.3.6 Biological pre-treatment

Microorganisms can also be used to treat the lignocellulosic biomass by degrade lignin and hemicelluloses to enhance the enzymatic hydrolysis (Taherzadeh and Karimi, 2008). Among the several fungi in used, white-rot fungi is among the most effective microorganisms for lignocelluloses pre-treatment (Sun and Cheng, 2002). A part from suffering from the rate of pre-treatment, biological pre-treatment having benefits of low energy, no chemical required and mild environmental conditions (Sun and Cheng, 2002).

2.4.4 Wheat straw as lignocellulosic feedstock

Lignocellulosic biomass such as wheat straw is the feedstock for second generation bioethanol. Biomass is comprised mostly of plant cell walls, of which typically 75% of this material is composed of polysaccharides and is a valuable pool of potential sugars for bioethanol production (Gomez, Steele-King and McQueen-Mason, 2008). In the UK, wheat is the most widely grown arable crop covering around 2 million hectares and producing about 15.5 million tonnes each year (DEFRA, 2012). There is an abundant supply of cereal straw in UK. Approximately 5-7 million tonnes of wheat straw are produced in the UK annually but only 1% is currently traded (Kang *et al.*, 2009). Wheat straw is also the most plentiful in Europe and the second most abundant worldwide after rice straw (Salvachúa *et al.*, 2011; Kim and Dale, 2004). Therefore, wheat straw is one of the most popular renewable sources of lignocellulose feedstock for materials, chemicals and energy applications. Typically, wheat straw contains 29 - 42 wt% cellulose, 25 – 32 wt% hemicelluloses and 16-23 wt% lignin (Mckean and Jacobs, 1997).

2.5 Potential of extrusion as effective pre-treatment method

As discussed in Section 2.4.3.4, 2.4.3.5 & 2.4.3.6, several physical, chemical, physio-chemical and enzymatic pre-treatments have been developed to improve the digestibility of biomass, but the need to reduce the energy inputs, and the costs of the procedure in general, has generated consensus around the use of simple thermochemical pre-treatments (Gomez, Steele-King and McQueen-Mason, 2008). Conventional batch steam explosion process (Inbicon, 2012)was reported with limitation of carbohydrate degradation and oxidation of lignin, which would

result in potential fermentation inhibitors (Chen and Qiu, 2010; Pienkos and Zhang, 2009). Selig et al. reported corn stover pre-treated at acidic condition and higher temperature deposited droplets on the surface, which mainly was composed of lignin and lignin-carbohydrate complexes and might have negative effect on enzymatic hydrolysis (Zhang *et al.*, 2012; Selig *et al.*, 2007). Continuous steam explosion type of pre-treatment was reported in used in the recent big demonstration bio-ethanol production plants in Italy and Denmark (Inbicon, 2012; Janssen, 2013). Continuous process will be in preference in pre-treatment comparing to batch process. An effective pre-treatment method must be able to expose the fibre, preserve fractionated hemicellulose, avoid inhibitor or by-product formation, while use only simple equipment and cost effective chemical during the pre-treatment process. Extrusion pre-treatment was found with high potential as a good candidate for effective pre-treatment method (Choi and Oh, 2012; Zhang, Xu and Hanna, 2012; Zhang *et al.*, 2012; Lamsal *et al.*, 2010; Lee, Teramoto and Endo, 2010; Lee *et al.*, 2010b; Lee *et al.*, 2010a; de Vrije *et al.*, 2002; Karunanithy and Muthukumarappan, In press).

Screw extruder represents the major processing part in extrusion. Extrusion had been extensively in used in food and polymer industry (Guy, 2001; Rauwendaal, 1994; Kokini, Ho and Karwe, 1992). It can be a single screw, twin or multi-screw extruder depending on the application needs. In particular in biofuel application, single screw extruder has been used for study the pre-treatment of switch grass, prairie cord grass and corn stover by Karunanithy et al. in his research (Karunanithy and Muthukumarappan, 2011a; Karunanithy and Muthukumarappan, 2011b; Karunanithy and Muthukumarappan, 2010a; Karunanithy and Muthukumarappan, 2010b; Karunanithy and Muthukumarappan, 2009); twin screw extruder has been used for pre-treatment study for DF flour, Douglas-fir, corn stover, soy hull, wheat bran and rape straw pre-treatment by Lee et al., Zhang et al., Lamsal et al. and Choi et al., respectively (Choi and Oh, 2012; Zhang, Xu and Hanna, 2012; Zhang *et al.*, 2012; Lamsal *et al.*, 2010; Lee, Teramoto and Endo, 2010; Lee *et al.*, 2010b; Lee, Teramoto and Endo, 2009). Extrusion is a continuous cost effective, fast, and simple process hence practical and useful for large-scale operation with high throughput and adaptability for many different process in combination (steam explosion, high pressure, chemical addition and reactive extrusion) (Karunanithy and Muthukumarappan, In press).

References :

1. Alvira, P., Tomás-Pejó, E., Ballesteros, M. and Negro, M.J. (2010) "Pretreatment technologies for an efficient bioethanol production process based on enzymatic hydrolysis: A review", *Bioresource technology*, vol. 101, no. 13, pp. 4851-4861.
2. Balan, V., Sousa, L.d.C., Chundawat, S.P.S., Marshall, D., Sharma, L.N., Chambliss, C.K. and Dale, B.E. (2009) "Enzymatic digestibility and pretreatment degradation products of AFEX-treated hardwoods (Populus nigra)", *Biotechnology progress*, vol. 25, no. 2, pp. 365-375.
3. Berlin, A., Gilkes, N., Kilburn, D., Maximenko, V., Bura, R., Markov, A., Skomarovsky, A., Gusakov, A., Sinitsyn, A., Okunev, O., Solovieva, I. and Saddler, J. (2006) "Evaluation of cellulase preparations for hydrolysis of hardwood substrates", *Applied Biochemistry and Biotechnology*, vol. 130, no. 1-3, pp. 528-545.
4. Bowes, B.G. (1996) *A colour atlas of plant structure*, Manson Publishing, London.
5. Brodin, I., Ernstsson, M., Gellerstedt, G. and Sjöholm, E. (2012) "Oxidative stabilisation of kraft lignin for carbon fibre production", *Holzforschung: International Journal of the Biology, Chemistry, Physics, & Technology of Wood*, vol. 66, no. 2, pp. 141-147.
6. Canadian Biofuel *Canadian Biofuel - Densified Biomass Fuel* . Available at: http://www.canadianbiofuel.ca/biomassfuel.html (Accessed: 7/16/2010 2010).
7. Chen, H. and Qiu, W. (2010) "Key technologies for bioethanol production from lignocellulose", *Biotechnology Advances*, vol. 28, no. 5, pp. 556-562.
8. Choi, C.H. and Oh, K.K. (2012) "Application of a continuous twin screw-driven process for dilute acid pretreatment of rape straw", *Bioresource technology*, vol. 110, no. 0, pp. 349-354.
9. Chundawat, S.P.S., Beckham, G.T., Himmel, M.E. and Dale, B.E. (2011) "Deconstruction of lignocellulosic biomass to fuels and chemicals", *Annual Review of Chemical and Biomolecular Engineering*, vol. 2, pp. 121-145.

10. Commission of the European Communities (2008) *Second Stractegic Energy Review - Europe's Current and future energy position : Demand - Resources - Investments*, European Comission, Europe.
11. Corredor, D.Y. (2008) *Pretreatment and exzymatic hydrolysis of lignocellulosic biomass*, Kansas State University.
12. Darvill, A. (2012) *Energy Resources: Geothermal power* . Available at: http://www.darvill.clara.net/altenerg/geothermal.htm (Accessed: 2/28/2013 2013).
13. de Jong, E., Higson, A., Walsh, P. and Wellish, M. (2012) *Bio-based Chemicals : Value Added Products from Biorefineries*, IEA Bioenergy, Task 42 Biorefinery.
14. de Vrije, T., de Haas, G.G., Tan, G.B., Keijsers, E.R.P. and Claassen, P.A.M. (2002) "Pretreatment of Miscanthus for hydrogen production by Thermotoga elfii", *International Journal of Hydrogen Energy*, vol. 27, no. 11–12, pp. 1381-1390.
15. DEFRA *ARCHIVE: Defra, UK - Farming - Crops* . Available at: http://archive.defra.gov.uk/foodfarm/growing/crops/index.htm (Accessed: 2/16/2013 2013).
16. Dey, P.M. and Harborne, J.B. (1997) *Plant biochemistry*, Academic Press, San Diego, Cal. ; London.
17. Dickson, M.H. and Fanelli, M. *What is Geothermal Energy? - IGA International Geothermal Association* . Available at: http://www.geothermal-energy.org/314,what_is_geothermal_energy.html (Accessed: 7/15/2010 2010).
18. Dutta, S., De, S., Saha, B. and Alam, M.I. (2012) "Advances in conversion of hemicellulosic biomass to furfural and upgrading to biofuels", *Catalysis Science & Technology*, vol. 2, no. 10, pp. 2025-2036.
19. EPI (2005) *Plan B Updates - 49: Ethanol's Potential - Looking Beyond Corn | EPI*. Available at: http://www.earth-policy.org/index.php?/plan_b_updates/2005/update49 (Accessed: 8/5/2010 2010).
20. European Commission (2000) *Biomass An Energy Resource for the European Union*, European Communities, Luxembourg.
21. Eurostat, E.C. (2010) *Energy Yearly Statistics 2008*, Eurostat, Luxembourg.

22. Faustino, H., Gil, N., Baptista, C. and Duarte, A.P. (2010) "Antioxidant Activity of Lignin Phenolic Compounds Extracted from Kraft and Sulphite Black Liquors", *Molecules*, vol. 15, no. 12, pp. 9308-9322.
23. Foust, T.D., Aden, A., Dutta, A. and Phillips, S. (2009) "An economic and environmental comparison of a biochemical and a thermochemical lignocellulosic ethanol conversion processes", *Cellulose*, vol. 16, no. 4, pp. 547-565.
24. Gáspár, M., Kálmán, G. and Réczey, K. (2007) "Corn fiber as a raw material for hemicellulose and ethanol production", *Process Biochemistry*, vol. 42, no. 7, pp. 1135-1139.
25. Gnansounou, E. (2010) "Production and use of lignocellulosic bioethanol in Europe: Current situation and perspectives", *Bioresource technology*, vol. 101, no. 13, pp. 4842-4850.
26. Gomez, L.D., Steele-King, C. and McQueen-Mason, S. (2008) "Sustainable liquid biofuels from biomass: the writing's on the walls", *New Phytologist*, vol. 178, no. 3, pp. 473-485.
27. Guy, R.C.E. (2001) *Extrusion cooking: technologies and applications*, CRC Press; Woodhead, Boca Raton, Fla.; Cambridge, England.
28. Hongzhang, C. and Liying, L. (2007) "Unpolluted fractionation of wheat straw by steam explosion and ethanol extraction", *Bioresource technology*, vol. 98, no. 3, pp. 666-676.
29. Houghton, J. (2005) *Global warming*.
30. Hu, F. and Ragauskas, A. (2012) "Pretreatment and Lignocellulosic Chemistry", *BioEnergy Research*, vol. 5, no. 4, pp. 1043-1066.
31. IEA, M.A. (2005) *Biofuel Use Growing Rapidly, Vital Signs 2005*, International Energy Agency, Washington.
32. IEA, N. (2010) *Technology Roadmap - Nuclear Energy*, International Energy Agency, Paris.
33. Inbicon *Hydrothermal pretreatment*. Available at: http://www.inbicon.com/Technologies/Hydrothermal_pretreatment/Pages/Hydrothermal pretreatment.aspx (Accessed: 1/3/2013 2013).

34. Janssen, R. *The BIOLYFE Proejct : feedstock pretreatment*. Available at: http://www.biolyfe.eu/index.php?option=com_content&view=article&id=58&Itemid=71&lang=en (Accessed: 1/3/2013 2013).
35. Jørgensen, H., Kristensen, J.B. and Felby, C. (2007) "Enzymatic conversion of lignocellulose into fermentable sugars: challenges and opportunities", *Biofuels, Bioproducts and Biorefining*, vol. 1, no. 2, pp. 119-134.
36. Kamm, B. and Kamm, M. (2004) "Principles of biorefineries", *Applied Microbiology and Biotechnology*, vol. 64, no. 2, pp. 137-145.
37. Kang, Y.G., Xia, W., Song, J. and Tarverdi, K. (2009) " Extrusion fractionation of wheat straw for biocomposites utilising the entire straw constituents", *INTERNATIONAL JOURNAL OF MATERIALS & PRODUCT TECHNOLOGY*, vol. 36, no. 1-4, pp. 334-347.
38. Karunanithy, C., and Muthukumarappan, K. (In press) "Thermo-Mechanical Pretreatment of Feedstocks" in *Green biomass pretreatment for biofuels production*, 1st edn, SpringerLink, .
39. Karunanithy, C. and Muthukumarappan, K. (2011a) "Optimization of alkali soaking and extrusion pretreatment of prairie cord grass for maximum sugar recovery by enzymatic hydrolysis", *Biochemical engineering journal*, vol. 54, no. 2, pp. 71-82.
40. Karunanithy, C. and Muthukumarappan, K. (2011b) "Optimization of switchgrass and extruder parameters for enzymatic hydrolysis using response surface methodology", *Industrial Crops and Products*, vol. 33, no. 1, pp. 188-199.
41. Karunanithy, C. and Muthukumarappan, K. (2010a) *Effect of Extruder Parameters and Moisture Content of Switchgrass, Prairie Cord Grass on Sugar Recovery from Enzymatic Hydrolysis*.
42. Karunanithy, C. and Muthukumarappan, K. (2010b) *Influence of extruder temperature and screw speed on pretreatment of corn stover while varying enzymes and their ratios*.
43. Karunanithy, C. and Muthukumarappan, K. (2009) "Combined effect of alkali soaking and extrusion conditions on fermentable sugar yields from switchgrass and prairie cord grass", , pp. 5165.

44. Kim, S. and Dale, B.E. (2004) "Global potential bioethanol production from wasted crops and crop residues", *Biomass and Bioenergy,* vol. 26, no. 4, pp. 361-375.
45. Kokini, J.L., Ho, C. and Karwe, M.V. (1992) *Food extrusion science and technology,* M. Dekker, New York.
46. Körbitz, W. (1999) "Biodiesel production in Europe and North America, an encouraging prospect", *Renewable Energy,* vol. 16, no. 1-4, pp. 1078-1083.
47. Kumar, P., Barrett, D.M., Delwiche, M.J. and Stroeve, P. (2009a) "Methods for Pretreatment of Lignocellulosic Biomass for Efficient Hydrolysis and Biofuel Production", *Industrial & Engineering Chemistry Research,* vol. 48, no. 8, pp. 3713-3729.
48. Kumar, S., Singh, S.P., Mishra, I.M. and Adhikari, D.K. (2009b) "Recent advances in production of bioethanol from lignocellulosic biomass", *Chemical Engineering and Technology,* vol. 32, no. 4, pp. 517-526.
49. Lamsal, B., Yoo, J., Brijwani, K. and Alavi, S. (2010) "Extrusion as a thermo-mechanical pre-treatment for lignocellulosic ethanol", *Biomass and Bioenergy,* vol. 34, no. 12, pp. 1703-1710.
50. Laser, M., Schulman, D., Allen, S.G., Lichwa, J., Antal Jr., M.J. and Lynd, L.R. (2002) "A comparison of liquid hot water and steam pretreatments of sugar cane bagasse for bioconversion to ethanol", *Bioresource technology,* vol. 81, no. 1, pp. 33-44.
51. Lee, S.H., Chang, F., Inoue, S. and Endo, T. (2010a) "Increase in enzyme accessibility by generation of nanospace in cell wall supramolecular structure.", *Bioresource technology,* vol. 101, no. 19, pp. 7218-7223.
52. Lee, S.-., Inoue, S., Teramoto, Y. and Endo, T. (2010b) "Enzymatic saccharification of woody biomass micro/nanofibrillated by continuous extrusion process II: Effect of hot-compressed water treatment", *Bioresource technology,* vol. 101, no. 24, pp. 9645-9649.
53. Lee, S.-., Teramoto, Y. and Endo, T. (2010) "Enhancement of enzymatic accessibility by fibrillation of woody biomass using batch-type kneader with twin-screw elements", *Bioresource technology,* vol. 101, no. 2, pp. 769-774.

54. Lee, S.-., Teramoto, Y. and Endo, T. (2009) "Enzymatic saccharification of woody biomass micro/nanofibrillated by continuous extrusion process I - Effect of additives with cellulose affinity", *Bioresource technology*, vol. 100, no. 1, pp. 275-279.
55. Lignol Energy Corporation *Lignol - The Future of Fuel* . Available at: http://www.lignol.ca/ (Accessed: 2/16/2013 2013).
56. Mabee, W.E. and Saddler, J.N. (2010) "Bioethanol from lignocellulosics: Status and perspectives in Canada", *Bioresource technology*, vol. 101, no. 13, pp. 4806-4813.
57. Mauseth, J.D. (1988) *Plant anatomy*, Benjamin/Cummings Pub. Co, Menlo Park, Calif.
58. Mckean, W.T. and Jacobs, R.S. (1997) *Wheat Straw as a Paper Fiber Source*, Clean Washington Center, Washington.
59. Mohammad J. Taherzadeh, Keikhosro Karimi (2007) "Acid-Based Hydrolysis Processes for Ethanol From Lignocellulosic Materials : A Review", vol. 2, no. 3, pp. 472-499.
60. Mohan, S.V. and Karthikeyan, J. (1997) "Removal of lignin and tannin colour from aqueous solution by adsorption onto activated charcoal", *Environmental Pollution*, vol. 97, no. 1–2, pp. 183-187.
61. Mosier, N., Wyman, C., Dale, B., Elander, R., Lee, Y.Y., Holtzapple, M. and Ladisch, M. (2005) "Features of promising technologies for pretreatment of lignocellulosic biomass", *Bioresource technology*, vol. 96, no. 6, pp. 673-686.
62. New Jersey Board of Public Utilities *FAQs | NJ OCE Web Site* . Available at: http://www.njcleanenergy.com/renewable-energy/technologies/wind/faqs (Accessed: 7/15/2010 2010).
63. NNFCC (2009) *Marketing study for biomass treatment technology: Technical Appendix 2 - Biomass processing review*, NNFCC, United Kingdom.
64. NNFCC, L.C. (2010) *Pathways to UK Biofuels : A Guide to Existing and Future Options for Transport*, National Non-Food Crops Centre & Low Carbon Vehicle Partnership, United Kingdom.

65. OECD, I. (2010) *Sustainable production of Second-Generation biofuels : Potential and perspectives in major economies and developing countries*, International Energy Agency, Paris.
66. OECD, I. (2009) *World Energy Outlook*, International Energy Agency, Paris.
67. OECD, I. (2008a) *From 1st to 2nd Generation Biofuel Technologies : An overview of current industry and RD&D activities*, International Energy Agency, Paris.
68. OECD, I. (2008b) *Worldwide Trends in Energy Use and Efficiency*, International Energy Agency, Paris.
69. Ohman, F., Theliander, H., Tomani, P. and Axegard, P. (2010) *Method for separating lignin from black liquor, a lignin product, and use of a lignin product for the production of fuels and materials*, 20100325947 A1, US.
70. Omer, A.M. (2009) "Energy use and environmental impacts: A general review", *Journal of Renewable and Sustainable Energy*, vol. 1, no. 5, pp. 053101.
71. Pienkos, P.T. and Zhang, M. (2009) "Role of pretreatment and conditioning processes on toxicity of lignocellulosic biomass hydrolysates", *Cellulose*, vol. 16, no. 4, pp. 743-762.
72. Potters, G., Van Goethem, D. and Schutte, F. (2010) "Promising Biofuel Resources: Lignocellulose and Algae.", *Nature Education*, vol. 3, no. 9, pp. 14.
73. Pousa, G.P.A.G., Santos, A.L.F. and Suarez, P.A.Z. (2007) "History and policy of biodiesel in Brazil", *Energy Policy*, vol. 35, no. 11, pp. 5393-5398.
74. Pu, Y., Zhang, D., Singh, P.M. and Ragauskas, A.J. (2008) "The new forestry biofuels sector", *Biofuels, Bioproducts and Biorefining*, vol. 2, no. 1, pp. 58-73.
75. Ramos, L.P., Breuil, C. and Saddler, J.N. (1992) "Comparison of steam pretreatment of eucalyptus, aspen, and spruce wood chips and their enzymatic hydrolysis", *Applied Biochemistry and Biotechnology*, vol. 34-35, no. 1, pp. 37-48.
76. Rauwendaal, C. (1994) *Polymer extrusion*, 3rd edn, Hanser, Munich.
77. Ropponen, J., Räsänen, L., Rovio, S., Ohra-aho, T., Liitiä, T., Mikkonen, H., van, d.P. and Tamminen, T. (2011) "Solvent extraction as a means of preparing homogeneous lignin fractions", *Holzforschung: International Journal of the Biology, Chemistry, Physics, & Technology of Wood*, vol. 65, no. 4, pp. 543-549.

78. Rosillo-Calle, F. and Walter, A. (2006) "Global market for bioethanol: historical trends and future prospects", *Energy for Sustainable Development*, vol. 10, no. 1, pp. 20-32.
79. Salvachúa, D., Prieto, A., López-Abelairas, M., Lu-Chau, T., Martínez, Á.T. and Martínez, M.J. (2011) "Fungal pretreatment: An alternative in second-generation ethanol from wheat straw", *Bioresource technology*, vol. 102, no. 16, pp. 7500-7506.
80. Sánchez, O.J. and Cardona, C.A. (2008) "Trends in biotechnological production of fuel ethanol from different feedstocks", *Bioresource technology*, vol. 99, no. 13, pp. 5270-5295.
81. Sannigrahi, P., Miller, S.J. and Ragauskas, A.J. (2010) "Effects of organosolv pretreatment and enzymatic hydrolysis on cellulose structure and crystallinity in Loblolly pine", *Carbohydrate research*, vol. 345, no. 7, pp. 965-970.
82. Scheller, H. and Ulvskov, P. (2010) "Hemicelluloses", *ANNUAL REVIEWS, PALO ALTO*, , pp. 263-289.
83. Selig, M.J., Viamajala, S., Decker, S.R., Tucker, M.P., Himmel, M.E. and Vinzant, T.B. (2007) "Deposition of lignin droplets produced during dilute acid pretreatment of maize stems retards enzymatic hydrolysis of cellulose", *Biotechnology progress*, vol. 23, no. 6, pp. 1333-1339.
84. Sierra, R., Smith, A., Granda, C. and Holtzapple, M.T. (2008) "Producing fuels and chemicals from lignocellulosic biomass", *Chemical Engineering Progress*, vol. 104, no. 8, pp. 10.
85. Sims, R.E.H., Mabee, W., Saddler, J.N. and Taylor, M. (2010) "An overview of second generation biofuel technologies", *Bioresource technology*, vol. 101, no. 6, pp. 1570-1580.
86. Solomon, B.D., Barnes, J.R. and Halvorsen, K.E. (2007) "Grain and cellulosic ethanol: History, economics, and energy policy", *Biomass and Bioenergy*, vol. 31, no. 6, pp. 416-425.
87. Songstad, D.D., Lakshmanan, P., Chen, J., Gibbons, W., Hughes, S. and Nelson, R. (2009) "Historical perspective of biofuels: Learning from the past to rediscover the future", *In Vitro Cellular and Developmental Biology - Plant*, vol. 45, no. 3, pp. 189-192.

88. Srisodsuk, M., Kleman-Leyer, K., Keränen, S., Kirk, T.K. and Teeri, T.T. (1998) "Modes of action on cotton and bacterial cellulose of a homologous endoglucanase-exoglucanase pair from Trichoderma reesei", *European Journal of Biochemistry*, vol. 251, no. 3, pp. 885-892.
89. Sun, R., Lawther, J.M. and Banks, W.B. (1997) "A tentative chemical structure of wheat straw lignin", *Industrial Crops and Products*, vol. 6, no. 1, pp. 1-8.
90. Sun, Y. and Cheng, J. (2002) "Hydrolysis of lignocellulosic materials for ethanol production: a review", *Bioresource technology*, vol. 83, no. 1, pp. 1-11.
91. Taherzadeh, M. and Karimi, K. (2008) "Pretreatment of lignocellulosic wastes to improve ethanol and biogas production: a review", *Int J Mol Sci*, vol. 9, no. 9, pp. 1621-1651.
92. Taiz, L. and Zeiger, E. (1991) *Plant physiology*, Benjamin/Cummings Pub. Co, Redwood City, Calif. ; Wokingham.
93. U.S. Department Energy (2013) *Tribal Energy Program: How Hydropower Works* . Available at: http://www1.eere.energy.gov/tribalenergy/guide/hydropower_works.html (Accessed: 2/28/2013 2013).
94. UEMOA (2013) *Sustainable Bioenergy Development in UEMOA Member Countries*. Available at: http://www.globalproblems-globalsolutions-files.org/gpgs_files/pdf/UNF_Bioenergy/UNF_Bioenergy_5.pdf (Accessed: February, 13 2013).
95. US EPA (a) *Coal | Clean Energy*. Available at: http://www.epa.gov/cleanrgy/energy-and-you/affect/coal.html (Accessed: 7/13/2010 2010).
96. US EPA (b) *Natural Gas | Clean Energy | US EPA* . Available at: http://www.epa.gov/cleanrgy/energy-and-you/affect/natural-gas.html (Accessed: 7/13/2010 2010).
97. US EPA (c) *Oil | Clean Energy | US EPA* . Available at: http://www.epa.gov/cleanrgy/energy-and-you/affect/oil.html (Accessed: 7/13/2010 2010).

98. Virkajärvi, I., Niemelä, M.V., Hasanen, A. and Teirb, A. (2009) "Cellulosic ethanol via biochemical processing poses a challenge for developers and implementors", *BioResources,* vol. 4, no. 4, pp. 1718-1735.
99. Wallberg, O., Linde, M. and Jönsson, A. (2006) "Extraction of lignin and hemicelluloses from kraft black liquor", *Desalination,* vol. 199, no. 1–3, pp. 413-414.
100. Wang, K., Xu, F. and Sun, R. (2010) "Molecular Characteristics of Kraft-AQ Pulping Lignin Fractionated by Sequential Organic Solvent Extraction", *International Journal of Molecular Sciences,* vol. 11, no. 8, pp. 2988-3001.
101. Yang, B. and Wyman, C.E. (2008) "Characterization of the degree of polymerization of xylooligomers produced by flowthrough hydrolysis of pure xylan and corn stover with water", *Bioresource technology,* vol. 99, no. 13, pp. 5756-5762.
102. Zhang, Q. and Chuang, K.T. (2001) "Adsorption of organic pollutants from effluents of a Kraft pulp mill on activated carbon and polymer resin", *Advances in Environmental Research,* vol. 5, no. 3, pp. 251-258.
103. Zhang, S., Keshwani, D.R., Xu, Y. and Hanna, M.A. (2012) "Alkali combined extrusion pretreatment of corn stover to enhance enzyme saccharification", *Industrial Crops and Products,* vol. 37, no. 1, pp. 352-357.
104. Zhang, S., Xu, Y. and Hanna, M. (2012) "Pretreatment of Corn Stover with Twin-Screw Extrusion Followed by Enzymatic Saccharification", *Applied Biochemistry and Biotechnology,* vol. 166, no. 2, pp. 458-469.
105. Zhang, Y.P. and Lynd, L.R. (2004) "Toward an aggregated understanding of enzymatic hydrolysis of cellulose: Noncomplexed cellulase systems", *Biotechnology and bioengineering,* vol. 88, no. 7, pp. 797-824.

Chapter 3

Experimental Detail

3.1 Materials

3.1.1 Wheat Straw

A winter wheat straw was selected for this study. The raw wheat straw (RWS) was supplied by Dixon Brothers (Norfolk, UK). It was chopped to an average length of 10mm and dust extracted. The moisture content was around 10% as received as determined by HR73 Halogen Moisture analyser (Mettler Toledo, USA).

For the size reduction trial, RWS was grinded with a cutting mill machine (SM100 RETSCH, Germany) with 4mm sieve. The grinded straw was named as ground straw (GWS) and used for size reduction trial. GWS was further reduced the size with a lab grinder (Krups, UK) and sieve through a 1mm sieve. This further grinded straw was named as powdered straw (PWS).

3.1.2 Chemicals

Sodium hydroxide, NaOH (general purpose grade) was from Fisher Scientific. Laboratory grade of calcium hydroxide, ethylene glycol, maleic acid, cellulose and birchwood xylan were from Sigma-Aldrich. HPLC grade of tetrahydrofuran (THF) and dioxane, analytical grades of methanol, ethyl acetate, pyridine and acetic anhydrate were from Merck Millipore. Wingstay L, **WL** (Butylated reaction product of p-cresol and dicyclopentadiene) was from Eliokem (via Revertex (M) Sdn. Bhd., Malaysia). XNBR emulsion latex, Synthomer 6311 were supplied by Synthomer Sdn. Bhd., Malaysia. Compounding ingredients – zinc oxide, ZnO, sulphur, S, vulcanizing accelerator zinc diethyldthiocarbamate, ZDEC, titanium dioxide, TiO_2 and dispersing agent for dispersion preparation were from Revertex (M) Sdn Bhd, Malaysia.

Laboratory grade of neutraliser potassium hydroxide, KOH and ammonia and NH_3 were supplied by Merck Millipore.

3.2 Extrusion pre-treatment of straws

A five-barrel Betol twin screw (40 mm diameter) co-rotating extruder with screw length-to-diameter ratio of L/D=21:1 was used for the pre-treatment trial as shown in **Figure 3.1a** showing the extruder and details of the screw profile. At the discharge point of last barrel (end of screw), a 28mm die cap was fitted for all the extrusion trials unless mentioned otherwise (i.e. as trial without die). For the trial with die end modification, an additional temperature chamber was added after die and with temperature set at 150°C (as shown in **Figure 3.1b**).

Tables 3.1 - 3.4 summarise samples pre-treatment details, where applicable. They are used for further analysis in coming chapters:

Table 3.1 provides summary condition for wheat straw samples either RWS, extrusion pre-treatment or steam explosion pre-treatment for the analysis in Chapter 4. It is supplied with sample label which able to trace back to actual trial sample ID (given in blanket).

Table 3.2 summaries the samples and extrusion conditions without chemical conditioning of straw which will be referred in Chapter 4, 5, and 7 (tracable with sample ID). RWS or ground straw (GWS) was pre-soaked in water (at a straw:water ratio as specified) at ambient temperature for overnight and then fed into the extruder. For extrusion trial with dry straw, RWS as-received was used with no additional water added. Barrel temperature for the first barrel was always set at 30°C while the temperature for the rest of four barrels were set as per listed.

Table 3.3 summaries the samples and extrusion conditions with different chemical conditioning of straw which will be referred in Chapter 4, 5, 7 and 8 (traceable with sample ID). Prior to extrusion of straw with NaOH conditioning, RWS or ground straw, GWS were treated with NaOH solution at 4% w/w based on dry mass of RWS or GWS

(0.04g NaOH/g dried straw). NaOH was pre-dissolved in water at a defined straw:water ratio and mixed with straw manually and left overnight before extrusion. Procedures for the extrusion with other conditioning additives (calcium hydroxide, maleic acid and ethylene glycol) were identical with that of the NaOH conditioning except in dosage of the individual chemical (as shown in **Table 3.3**). Barrel temperature for the first barrel was always set at 30°C while the temperatures for the rest of four barrels were set as per listed.

Post-extrusion washing was conducted by mixing the extruded straw into water at straw:water ratio of 1:10 (w/w) for an hour at ambient temperature. The mixture was filtered with a 100 mesh sieve to separate the solid and filtrate. The solid portion was used for enzymatic hydrolysis trial and the liquid filtrate was treated as black liquor.

Due to a huge sampling amount involved in Chapter 6, a summary table – **Table 3.4** was created to capture the sampling categories for chemometric analysis purpose.

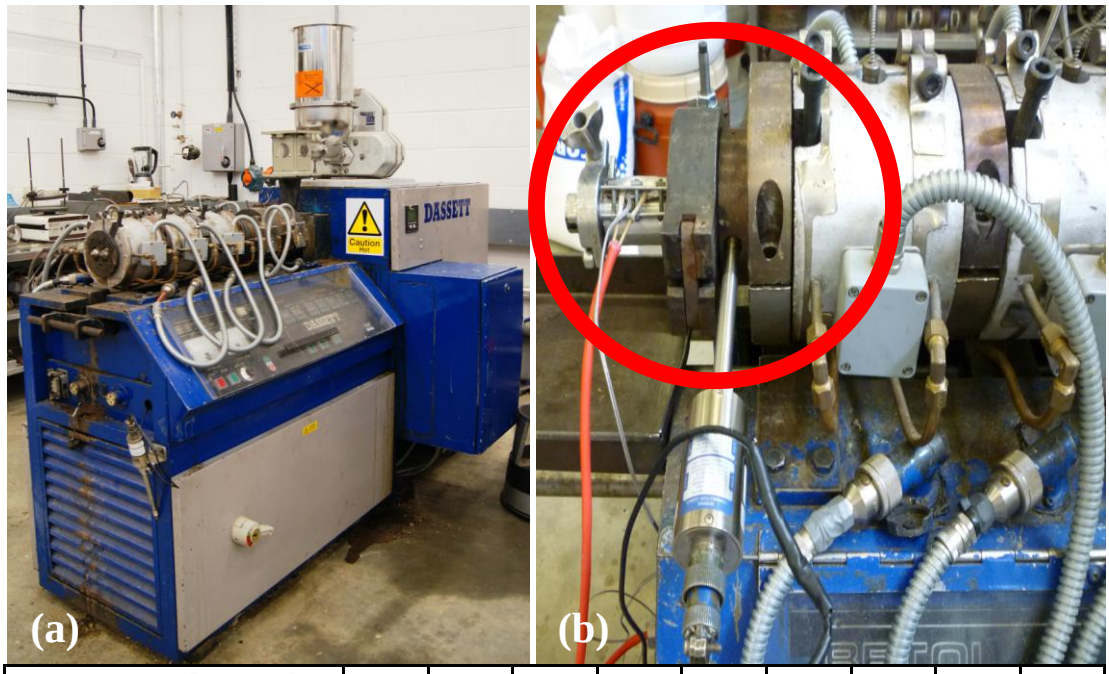

Screw Length mm (l)	120	150	120	15*	120	80	160	25*	80
Pitch mm (t)	24	24	24		16	16	12	16	8
Flight width (mm) (b)	4	8	8		4	4	4	4	2

*** 3 trilobals of 5mm each and 25mm reverse screw with 3 slots of 8mm width were used**

Figure 3.1 : Pictures of the Betol Twin Screw Extruder (and the screw profile shown in the table insert) : a) Front view of extruder without the die. b) Close shot of extrusder fitted with an extension die of additional temperature chamber heater and a pressure sensor.

Table 3.1 Summary of sample IDs and the straw pre-treatment details.

Sample label (Sample ID traceable to trial detail)	Pre-treatment Condition
RWS	Wheat straw as received without pre-treatment
EX01 (WCB10008)	Extruded straw pre-soaked in water (at straw: water 1:2) at screw speed of 100 rpm and barrel temperature of 50°C for barrel 2 – 5.
EX02 (WCB10009)	Extruded straw pre-soaked in NaOH solution (at straw: solution =1:2 resulting in 4% NaOH on dry mass of straw) at screw speed of 100 rpm and

	barrel temperature of 50°C for barrel 2 – 5.
SE01 (W02)	Steam exploded RWS with holding at 190^0C and 11.6 bar for 10 mins and straw:water at 1:0.7
SE02 (W11)	Steam exploded RWS with holding at 220^0C and 22.2 bar for 10 mins and straw:water at 1:0.7

Table 3.2 : Straw sample IDs and details of extrusion pre-treatments without chemical additive

Sample IDs	Processing parameters
RWS	Raw wheat straw without extrusion
Ground straw (GWS)	RWS grinded with cutting mill SM100 RETSCH , and through a 4mm sieve
Powered straw (PWS)	Ground straw mill with a lab grinder (Krups) and through a 1mm sieve
WCB10003	RWS, 50°C (barrel 2 – 5), 100 rpm screw speed, dry extrusion, without die
WCB10004	RWS, 50°C (barrel 2 – 5), 100 rpm screw speed, dry extrusion
WCB10005	RWS, 100°C (barrel 2 – 5), 100 rpm screw speed, dry extrusion without die
WCB10006	RWS, 100°C (barrel 2 – 5), 100 rpm screw speed, dry extrusion
WCB10007	RWS, 50°C (barrel 2 – 5), 100 rpm screw speed, dry extrusion, double extrusion
WCB10008	RWS, 50°C (barrel 2 – 5), 100 rpm screw speed, straw:water 1:2 w/w
WCB09007	RWS, 60°C (barrel 2 – 5), 100 rpm screw speed, dry extrusion
WCB09008	RWS, 120°C (barrel 2 – 5), 100 rpm screw speed, straw:water 1:2 w/w
WCB09031	RWS, 240°C (barrel 2 – 5), 100 rpm screw speed, straw:water 1:4 w/w
WCB09033	RWS, 240°C (barrel 2 – 5), 150 rpm screw speed, straw:water 1:4 w/w
WCB09032	RWS, 240°C (barrel 2 – 5), 200 rpm screw speed, straw:water 1:4 w/w
WCB11002	Ground straw, 50°C (barrel 2 – 5), 100 rpm screw speed, straw:water 1:2 w/w
WCB11003	Ground straw, 150°C (barrel 2 – 5), 100 rpm screw

	speed, straw:water 1:2 w/w
WCB11004	Ground straw, 250°C (barrel 2 – 5), 100 rpm screw speed, straw:water 1:2, w/w
WCB11008	Ground straw, temperature profile 30, 50, 70, 150, 150 and 150°C, 100 rpm screw speed, straw:water 1:2 w/w
WCB11009	Ground straw, barrel temperature profile 30, 50, 70, 160, 180 and 150°C (at extension heating chamber), 100 rpm screw speed, straw:water 1:3 w/w
WCB11017	RWS, barrel temperature profile 30, 50, 70, 200, 200 and 150°C (at extension heating chamber), 100 rpm screw speed, straw:water 1:2 w/w

Table 3.3 : Straw sample IDs and details of extrusion pre-treatments with chemical additive conditioning.

Sample IDs	Processing parameters
WCB10009	RWS, 50°C (barrel 2 – 5), 100 rpm screw speed, straw:water 1:2 w/w, with 4% w/w NaOH
WCB10010	RWS, 50°C (barrel 2 – 5), 100 rpm screw speed, straw:water 1:2, with 1% w/w $Ca(OH)_2$
WCB10011	RWS, 50°C (barrel 2 – 5), 100 rpm screw speed, straw:water 1:2, with 4.8% w/w Maleic acid
WCB10012	RWS, 50°C (barrel 2 – 5), 100 rpm screw speed, straw:etylene glycol:water 1:1:1
WCB09035	RWS, 140°C (barrel 2 – 5), 100 rpm screw speed, straw:water 1:4, with 4% w/w NaOH
WCB09036	RWS, 180°C (barrel 2 – 5), 100 rpm screw speed, straw:water 1:4, with 4% w/w NaOH
WCB09034	RWS, 200°C (barrel 2 – 5), 100 rpm screw speed, straw:water 1:4, with 4% w/w NaOH
WCB09037	RWS, 220°C (barrel 2 – 5), 100 rpm screw speed, straw:water 1:4, with 4% w/w NaOH
$Control_{NaOH}$	RWS, without extrusion, straw:water 1:2, only 10% w/w NaOH, as Control
WCB10024	RWS, ambient temperature (all barrels), 100 rpm screw speed, straw:water 1:2, with 10% w/w NaOH
WCB10023	RWS, 50°C (barrel 2 – 5), 50 rpm screw speed, straw:water 1:2, with 10% w/w NaOH
WCB10013	RWS, 50°C (barrel 2 – 5), 100 rpm screw speed, straw:water 1:2, with 10% w/w NaOH
WCB10022	RWS, 50°C (barrel 2 – 5), 200 rpm screw speed, straw:water 1:2, with 10% w/w NaOH

WCB10014	RWS, 50°C (barrel 2 – 5), 100 rpm screw speed, straw:water 1:2, with 10% w/w NaOH, double extruded
WCB10017	RWS, 50°C (barrel 2 – 5), 100 rpm screw speed, straw:water 1:2, with 10% w/w NaOH, double extruded, washed
WCB10015	RWS, 150°C (barrel 2 – 5), 100 rpm screw speed, straw:water 1:2, with 10% w/w NaOH
WCB10019	RWS, 250°C (barrel 2 – 5), 100 rpm screw speed, straw:water 1:2, with 10% w/w NaOH,
WCB10020	RWS, 250°C (barrel 2 – 5), 100 rpm screw speed, straw:water 1:2, with 10% w/w NaOH, double extruded
WCB10021	RWS, 250°C (barrel 2 – 5), 100 rpm screw speed, straw:water 1:2, with 10% w/w NaOH, double extruded, washed
WCB11005	Ground straw, 50°C (barrel 2 – 5), 100 rpm screw speed, straw:water 1:2, with 4% w/w NaOH
WCB11006	Ground straw, 150°C (barrel 2 – 5), 100 rpm screw speed, straw:water 1:2, with 4% w/w NaOH
WCB11007	Ground straw, 250°C (barrel 2 – 5), 100 rpm screw speed, straw:water 1:2, with 4% w/w NaOH
WCB12001	RWS, barrel temperature profile 30, 30, 50, 200, 200 and 150°C (at extension heating chamber), 100 rpm screw speed, straw:water 1:2, with 4% w/w NaOH
WCB12003	Repeat of WCB12001 with bigger amount for study in Chapter 8.
WCB10009W	RWS, 50°C (barrel 2 – 5), 100 rpm screw speed, straw:water 1:2, with 4% w/w NaOH, washed.

Table 3.4 : Summary of sample IDs and details of pre-treatment conditions for chemometric analysis.

Sample ID	Pre-treatment Conditions
RWS	1 wheat straw sample as received without pre-treatment and
PWS	1 GWS , powdered and through 1mm sieve.
EX	Total of 18 samples of extrusion treated RWS without NaOH including:
	i. 6 RWS dry extruded without water, barrel temperatures range between 50 – 100 °C, with and without die, screw speed of 100 rpm.
	ii. 2 RWS pre-soaked in water (at straw: water =1:2) at ambient temperature for overnight and extruded at screw speed of 100 rpm at temperature 50 and 120°C respectively.
	iii. 3 RWS pre-soaked in water (at straw:water =1:4 w/w) at ambient temperature for overnight and extruded at screw speed ranging 100 - 200 rpm at 240°C.
	iv. 3 GWS samples pre-soaked in water (at straw: water =1:2) at ambient temperature for overnight and then extruded at temperature ranging 50 - 150°C at screw speed of 100 rpm.
	v. 2 GWS pre-soaked in water (at straw: water =1:3 w/w) at ambient temperature overnight and extruded, with the extension die fitted, at maximum temperature 180°C (temperature profile as per WCB11008 and WCB11009, **Table 3.2**), at screw speed 100 rpm.
	vi. 1 RWS was extruded, with the extension die fitted, water pumped in during extrusion at

straw: water =1:3 w/w, with temperature profile as WCB11017 (**Table 3.2**) and screw speed 100 rpm.

vii. 1 RWS extruded, with the extension die fitted, water pumped in during extrusion (at straw:water = 1:1), with temperature profile as WCB11017 (**Table 3.2**) and screw speed 100 rpm.

EXC 21 samples extrusion treated RWS with NaOH :

i. 2 RWS extruded at temperature 50 and 120°C. RWS was pre-soaked in NaOH solution (straw:water =1:2 resulting in 4% w/w NaOH on dry mass of straw) at ambient temperature for overnight and extruded at screw speed 100 rpm.

ii. 2 RWS extruded at temperature 140 and 200°C. NaOH solution pumped in during extrusion (straw:solution =1:4 resulting in 4% w/w NaOH on dry mass of straw) and extruded at screw speed 100 rpm.

iii. 13 RWS extruded at temperature range of ambient to 250°C. RWS was pre-soaked in NaOH solution (straw:water =1:2 resulting in 10% w/w NaOH on dry mass of straw) at ambient temperature for overnight and extruded single or double round at screw speed range from 50 to 200 rpm.

iv. 3 GWS extruded at temperature range of 50 to 250°C. GWS was pre-soaked in NaOH solution (straw:water = 1:2 resulting in 4% w/w NaOH on dry mass of straw) at ambient temperature for overnight and extruded at screw speed 100 rpm.

	v. 1 GWS was extruded at temperature of 180°C with extension die fitted. GWS was pre-soaked in NaOH solution (at straw:water = 1:2 resulting in 4% w/w NaOH on dry mass of straw) at ambient temperature for overnight and extruded at screw speed 100 rpm.
EXCW	1 NaOH extruded straw was washed as per detailed in WCB11021 (**Table 3.3**)
SE	3 steam exploded RWS with 10 minutes holding time, straw: water = 1:0.7 W02 - 10 min at 190°C and 11.6 bar W11 -10 min at 220°C and 22.2 bar D01 - 10 min at 200°C and 14.5 bar (exploded into water and then spin dried in a nylon mesh bag 100 μm).

3.3 Steam Explosion Pre-treatment

Steam explosion samples were provided by a project partner – Institute of Food Research.

3.3.1 Steam explosion pre-treatment for sample SE with sample ID SE01 (W02) and SE02 (W11) in used in Chapter 4, 6 and 7

RWS as described in sub-section 3.1.1 was steam-exploded in batches of 250g fresh weight (containing ~10% moisture) in a steam explosion unit (Cambi AS, Asker, Norway) within a 20 L pressure vessel at the Norwegian University of Life Sciences. Before each pre-treatment the pressure vessel was preheated for 10 min to the desired temperature. The pre-treated materials was the stored frozen (see **Table 3.1** under SE01 and SE02 for details,).

3.3.2 Steam explosion pre-treatment for sample SE with sample ID D01 (sample in used in Chapter 6) and D21 (Sample in used in Chapter 8 for lignin recovery)

In addition, a 35 L pressure vessel (Cambi AS, Asker, Norway)was used to prepare the samples in used in Chapter 6 and 8. The vessel was preheated for 10 minutes to designated temperature and the condensed steam was released. 1500 g of wheat straw was fed into the chamber and the straw was steam treated at the designated temperature for 10 minutes. The straw was exploded into 10 Litres of warm water (50°C) and the slurry was filtered using a 100 µm nylon mesh bag and spin dried using a centrifuge unit . The solid portion was used for enzymatic hydrolysis trial and the liquid filtrate was treated at black liquor.

i. D01 - 10 min at 200°C and 14.5 bar (sample in used in Chapter 6)
ii. D21 - 10 min at 190°C and 11.5 bar (Sample in used in Chapter 8 for lignin recovery)

3.4 Enzymatic Hydrolysis

Enzymatic hydrolysis was conducted by a project partner – Institute of Food Research. Details of preparation were given below.

The digestibility of the pre-treated straws in enzymatic hydrolysis was assessed at 1% and at 10% substrate concentrations. The frozen extrudate of straws was thawed. An amount of straw containing 0.25 g or 2.5 g dry weight was placed in a 60 mL polypropylene container and dispersed in a total volume of 24.4 mL in NaOAc buffer (adjusted to pH 4.7) and then 0.625 mL of Accellerase 1500 (Genencor) was added. This was incubated at 50°C for 16 h with rotary stirring at 200 rpm. The minimum acetate salt concentration was 50 mM but with the alkali-treated samples a much higher acetate concentration (up to 0.54 M) was required to obtain pH 4.7. The liquor was filtered off (Whatman Paper No. 4). The undigested residue and the filter were dried at 45 °C.

Glucose was measured using the GOPOD assay (Megazyme.com) in which glucose oxidase converts glucose to gluconate and H_2O_2, which reacts to form a coloured dye

(absorbance 510 nm). The assay was performed by measuring the slope of the absorbance against volume using 0.6 mL of reagent and 6, 13 and 20 µL of hydrolysate diluted as necessary. Reducing sugar concentrations were measured, in a similar way, by reduction of 3,5-dinitrosalicylic acid.

Biomass samples to be analysed for polysaccharides were dried at 45 °C and freeze milled for 3 min. Triplicate samples (up to 18 mg) were dispersed in 200 µL 72% w/w H_2SO_4 at 20 °C for 2.75 h, then 2.2 ml water was added and the samples were hydrolysed at 100 °C for 2.5 h. The hydrolysate was neutralised with 32% NH_3, the solution was diluted to 10 mL and centrifuged for 2 min at 5000 rpm. The glucose in the supernatant was analysed using the GOPOD reagent. Chemically treated samples will contain additional ash but this has not been measured.

3.5 Recovery of crude lignin

3.5.1. Crude straw lignin

Black liquor with initial pH 9.5 and 3.9 from the washing process of post extrusion (described in sub-section 3.2) or steam explosion (described in sub-section 3.3.2), respectively, were adjusted to pH below 2.0 with 6M of sulphuric acid (Merck Millipore, analytical grade) at temperature 60°C under mild stirring. The precipitated black liquor was left to cool to room temperature before being centrifuged to recover the solid precipitate at 20°C and 11000 rpm for 20 minutes with a Sorvall RC SC Plus centrifuge machine (rotor 30 / SLA 3000).

As the yield of crude straw lignin was low in such laboratory operation (approximately ~ 2% over dried straw weight), no further purification or washing process was conducted to remove impurities, such as carbohydrates and inorganic salt, from the solid precipitate. Hence, the presence of impurities such as carbohydrates and inorganic salt are expected. The crude lignin was freeze dried and kept in desiccators before further analysis. Details of the samples and descriptions are summarised in **Table 3.5**.

3.5.2. Crude Kraft lignin

Softwood Kraft lignin was obtained from Innventia AB, Sweden. The Kraft lignin was recovered from black liquor with a patented Lignoboost process (Ohman *et al.*, 2010). Sample was dried at ambient temperature and kept in desiccators before analysis. Samples and descriptions are also summarised in **Table 3.5**.

Table 3.5 : Sample labelling lignin sample in used in Chapter 8

Sample	Detail
RH	Crude Kraft lignin H from Lignoboost process, Innventia AB
RF	Crude Kraft lignin F from Lignoboost process, Innventia AB
REX	Crude wheat straw lignin from black liquor generated from extrusion pre-treatment (WCB12003, **Table 3.3**).
RSE	Crude wheat straw lignin from black liquor generated from steam explosion (D21, sub-section 3.3.2).
EH	Fraction from ethyl acetate extraction of the crude Kraft lignin H (RH)
EF	Fraction from ethyl acetate extraction of crude Kraft lignin F (RF)
EEX	Fraction from ethyl acetate extraction of crude wheat straw lignin – REX (extrusion process)
ESE	Fraction from ethyl acetate extraction of crude wheat straw lignin - RSE (steam explosion process)
MH	Fraction from methanol extraction of RH.
MF	Fraction from methanol extraction of RF.
MEX	Fraction from methanol extraction of REX.

MSE	Fraction from methanol extraction of RSE.

3.6 Solvent fractionation of the crude lignins

The sequential solvent fractionation of the crude lignin (RH, RF, REX and RSE) was performed according to the scheme illustrated in **Figure 3.2**. Selection of the solvent was based on Hildebrand solubility index with the rationale to have polar fraction (methanol, MeOH), and non-polar / medium polar fraction (ethyl acetate, EA) as adopted elsewhere (Wang, Xu and Sun, 2010; Burke, 2008; Grulke, 1999; Mörck, Yoshida and Kringstad, 1986; Wang *et al.*, 2009). Dioxane was placed last in the sequence owning to its complete solubilisation of lignin, even though its Hildebrand solubility index is less than that of methanol (Wang, Xu and Sun, 2010). All the solvents used were analytical grade supplied by Merck Millipore except dioxane which was from Alfa Aesar as a HPLC grade. This is because a non-stabilized dioxane was used to prevent error in antioxidant activity measurement for dioxane fraction. The solvent fractionation initially conducted with a Soxtec unit (2050 Soxtec Auto Extractor unit FOSS TECATOR) with cellulose thimble. However, there is some problem for cellulose thimble (chipped at the bottom part) in used to withstand multiple extractions. The extraction was then conducted with a Soxhlet extraction unit for a total 4 hours extraction time with at least 4 cycles per hour to replace Soxtec extraction. At the end of the extraction, the supernatant liquid has evaporated in a fume cupboard at ambient temperature for at least 48 hours and stored in desiccators prior to for further characterisation analysis e.g. FTIR, UV, SEC, NMR and etc. No elevated temperature was used in drying in order to prevent deterioration of phenolic structure in the crude lignins and extracted fractions. Estimated yield for each extraction was recorded based on gravimetric calculation.

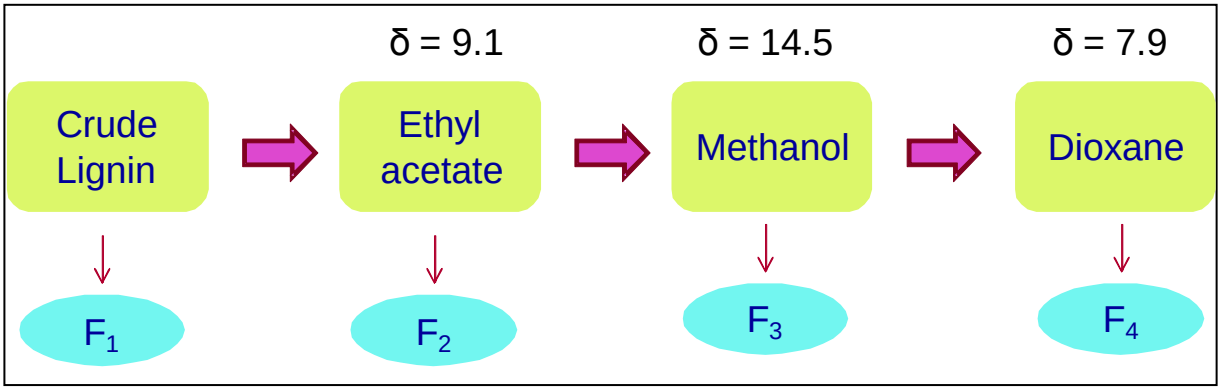

Figure 3.2 : Scheme for obtaining fractions (F1-F4) from sequential solvent fractionation of the crude lignins using solevents with different Hildebrand solubility index (δ).

MEX fraction from methanol extraction of wheat straw was used for assessment of antioxidant application (in Chapter 9). MEX was selected because the DPPH evaluation on REX is too low and MEX was the best for wheat straw lignin under extrusion pre-treatment.

RH crude Kraft lignin H from Lignoboost process, Innventia AB was selected for assessment of antioxidant application (in Chapter 9). This was because that Chapter 8 showed only marginal difference between crude Kraft lignin and the fractions from ethyl acetate and methanol extraction. Furthermore, avoiding the lignin purification steps would a cost-saving measure benefiting the competiveness of the bio-based chemical.

3.7 Lignin as an antioxidant in rubber glove manufacturing

3.7.1 Preparation of lignin dispersion

Both RH and MEX lignin samples (Table 3.5) were prepared into dispersion according to the standard in-house dispersion preparation procedures for the existing counterpart antioxidant, Wingstay L at Revertex (M) Sdn. Bhd, Malaysia using a high speed glass bead ball mill. The pH for the dispersion was adjusted to alkaline (pH 9 - 13). Total solid content for dispersion of MEX, RH and WL (Control Wingstay L) were 4.6%, 17.1% and 50%. This variation in solid content was mainly resulted from the available

amount of MEX and RH for smallest scale dispersion preparation. But the solid content variation shall not be a concern as dosage of lignin/fraction in the subsequent latex compounding stage was based on the total dry matter used. Upon the pH adjustment, the MEX dispersion was fully dissolved in the dispersed water medium and formed as a solution. Particle size for RH and WL were tested as 2.6 and 4 μm, respectively using Mastersizer 2000, Malvern Instruments.

3.7.2 Latex compounding and glove dipping

A virgin XNBR latex (Synthomer 6311) was supplied by Syntomer Sdn. Bhd. Malaysia and 0.6 parts per hundred rubbers (phr) of dispersion WL, RH or MEX was dosed into the latex as shown in **Table 3.6** where a blank control (the pure latex) was also included for comparison. Antioxidant / lignin dosed latex was then subjected for dipping compounding process. The other ingredients added to the latex for dipping compounding are listed in **Table 3.7** with pH adjusted to pH 10.0. A total of 16 gloves were then dipped from each of the compound according to Synthomer's standard dipping regime with glove palm thickness at 0.10 – 0.11mm. Due to limited amount of Compound EL0.6 (latex dosed with MEX lignin), ceramic dip space was used to produce a dip film instead of ceramic glove former for dipped glove. Gloves / films were then cured at 120°C for 20 minutes.

Table 3.6 : Antioxidant and lignin dosages in the virgin XNBR latex

Compound ID	Antioxidant / Lignin	Dosage of antioxidant, Parts per hundred rubber, phr
Blank	**-**	**0**
Control WL (antioxidant in used in industry)	**WL**	**0.6**
KL 0.6	**RH**	**0.6**
EL 0.6	**MEX**	**0.6**
KL 1.2	**RH**	**1.2**

Table 3.7 : Compounding formulation of the latex for glove / films dipping

Component	Parts per hundred rubber, phr
6311	**100**
KOH	**1.5**
ZnO	**1**
S	**0.8**
ZDEC	**0.5**
TiO_2	**1.5**

3.7.3 Tensile and stress relaxation testing

The dumbbell cutters used in specimen preparation (from films of ~ 0.10 – 0.11mm in thickness) was an ASTM type C (D412 -6mm test width) cutter. A total of 13 pieces of specimens (for each sample) were obtained and conditioned, prior to testing, by storing the specimens at a temperature of 23 °C and a relative humidity of 50 % for 16 hours.

Tensile strength, elongation at break and modulus at 100 %, 300 % and 500 % strains were determined following ASTM D412 (ASTM, 2007) using a Hounsfield H10KS Tensiometer fitted with a H500LC Laser extensometer.

Heat accelerated aging on the dipped films was performed by heating the specimens in an air ventilated oven at 100 °C for 22 hours and 48 hours. Tensile strength, elongation at break and modulus at 100 %, 300 % and 500 % strains were determined for specimens after heat accelerated aging process.

3.8 Analytical analysis and characterisation

3.8.1 Attenuated total reflectance fourier transform infra-red (ATR-FTIR)

ATR-FTIR spectra (4000 – 600cm^{-1}) were obtained using a Perkin Elmer (Spectrum One) FTIR spectrometer equipped with a Specac Golden Gate^{TM} ATR MKII with diamond crystal. Spectra were obtained with 4cm^{-1} resolution and 32 scans for both background and the samples. Dried RWS and pre-treated straws were ground into powder with a Krups twin blade grinder. Powdered samples were pressed against the diamond surface using a pressure tower to ensure a constant pressure was applied. Spectra were recorded from five different specimens per sample type and all spectra were baseline corrected. The averaged spectrum of the five corrected spectra was used for each sample type.

3.8.2 Fourier Transform Near Infrared (FT-NIR)

Dried RWS and pre-treated straw samples were analysed on an Antaris II NIR spectrometer (Thermo Fisher Scientific, UK) equipped with an integrating sphere module designed for diffuse reflectance measurements. A 5 cm diameter spinning cup module was used for sample presentation. The samples were placed in the cup and mounted onto the spinner. Spectra were collected over the range of 10,000-4,000 cm^{-1} at a resolution of 8 cm^{-1} using the RESULT software. Each sample reading taken was an average of 64 scans, taking approximately 32 seconds per sample. Each sample was re-packed to take triplicate readings and the averaged spectrum from the 3 spectra was used for each sample type.

3.8.3 Chemometric Analysis

All multivariate analysis of the FTIR and FT-NIR spectra for glucose yield prediction was performed using TQ Analyst version 8 (Thermo Fisher Scientific, UK). The background and applications of Partial least-squares (PLS) regression and chemometrics can be found in a publication by Wold *et al.* (2001).

Principal component analysis (PCA) was conducted using the FTIR and FT-NIR spectra of straw from different pre-treatments. Key chemical information due to structural changes were extracted from the spectra and correlated to changes in the processing by identifying clusters in the principal component scores plot.

Partial least-squares (PLS) regression was then used to generate calibration models which correlate changes in the FTIR and FT-NIR spectra to sugar yield. The models were then developed for both FTIR and FT-NIR spectra. Approximately 80% of samples (37 in total, **see Table 3.4**) were used to develop the calibration models, and the other 20% (8 in total) were used for validation. The sample selection for calibration and validation was carried out randomly by the software and same set of samples were used for validation of models from both FT-NIR and FTIR spectra. Various spectral pre-treatments were investigated prior to generating the calibration. The accuracy of the regression model was tested by varying a) the spectral format (raw absorption spectra, their first derivative, or second derivative); b) path length correction, standard normal variate (SNV) and multiplicative signal correction (MSC). The first and second derivative spectra were smoothed using a Norris derivative filter (with segment length =7 and gap between segments =7). The calibration models for FTIR were screened for three wave number regions: 4000 – 650 cm^{-1}, 1800 – 700 cm^{-1}, or both 3700 – 2700 and 1800 – 700 cm^{-1} in order to optimise a meaningful signal for extraction. Calibration models for FT-NIR were narrowed down to wavenumber region 7500 – 4000 cm^{-1} as there was no absorption peaks outside this region. The TQ Analyst software suggested the optimum number of PLS factors based on the predicted residual error sum of squared (PRESS) value to avoid under- or over fitting of the model. The number of factors recommended was adjusted if necessary taking into account the chemical knowledge about the samples. The root mean square error of calibration (RMSEC) and the correlation coefficient (R^2_C) were then calculated. The predictive performance of the models was evaluated using validation samples to calculate root-mean-square error of prediction (RMSEP) and correlation coefficient of determination for prediction (R^2_P). Definitions and significance of R^2, SEP and RMSEP are explained in a previous publication (Daviesa and Fearnb, 2006).

3.8.4 Thermal Gravimetric Analysis (TGA)

Thermal analysis of the straw samples was performed using TGA Q500 Series (TA Instrument, USA). The apparatus was continuously flushed with nitrogen at a flow rate of 100ml/min. Each sample weighed between 3 – 5 mg and was heated from room temperature to 700°C at a rate of 10°C/min.

3.8.5 Scanning Electron Microscope (SEM)

The straw samples were sputter coated with gold and the morphology of them was assessed using a Scanning Electron Microscope (SEM) Zeiss Supra 35VP, operated at 20kV.

3.8.6 Colorimetric Measurement

The straw samples were ground into fine powder (1mm sieve) and compacted in a UV sample holder. The colour of the sample was measured using a ChromaMagic, Minolta CR-300 Chromameter. Average reading was presented based on 3 measurements.

3.8.7 X-ray Diffraction (XRD)

The crystallinity of the RWS and pre-treated wheat straw was examined using a Bruker D8 ADVANCE diffractometer. The samples were grinded into powder form (1mm sieve). The radiation was Cu Kα (λ = 0.1542nm) with 40kV voltage and 40 mA intensity. The samples were scanned from 2θ = 5° to 45°. The crystallinity (%C) was calculated from the diffraction intensity data:

$$\%C = \frac{100 \times Icr}{Icr + Iam} \qquad (1)$$

Where I_{am} is the total intensity arising from the amorphous component and I_{cr} is the total intensity arising from the crystalline component of the straw.

3.8.8 Determination of specific surface area of pre-treated straws

The straw samples was dried in vacuum oven at 40°C for overnight and stored in sealed plastic bag before being assessed for properties related specific surface using three different methods.

3.8.8.1 B.E.T. from absorption of nitrogen

Surface area of the samples was determined using nitrogen adsorption and the Brunauer, Emmett and Teller (B.E.T) theory. This analysis was done by collaborator partner at Bangor University. Analysis was carried out on the dried and degassed samples using a Micromeritecs Gemini surface area analyser with nitrogen as the adsorbate, and liquid nitrogen as coolant for maintaining the sample temperature at -198°C for stability. The machine was calibrated using a Kaolinite calibration standard. Surface area was calculated by the Micromeritecs Stardriver software using the B.E.T. theory, based on volume of nitrogen adsorbed at different partial pressures (zeroed for background pressure). The results are given as mean values of three different replicates.

3.8.8.2 Water vapour sorption

All water sorption measurements on the samples were performed using a dynamic vapour sorption analyser (DVS Advantage 1, SMS, UK). The actual testing was done by collaborator Surface Measurement Systems Ltd. UK. During the measurements, the instrument was run in dm/dt mode (mass variation over time variation) to decide when the equilibrium of vapour humidity is reached. A fixed dm/dt value was selected at each relative humidity (RH) segment. This criterion permits the DVS software to automatically determine when equilibrium has been reached and complete a step. When the rate of change of mass falls below this threshold over a determined period of time, the relative humidity set point will proceed to the next programmed level. All analyses were carried out using the SMS DVS Analysis Suite version 6.1.1.2 and SMS DVS Analysis Suite version 6.1.1.2 (Advanced) macros.

3.8.8.3 Organic dye - Congo red (CR) adsorption

The CR adsorption method has been used to determine specific surface area of pre-treated biomass (Lee, Teramoto and Endo, 2010; Ougiya *et al.*, 1998). The method was modified slightly where a 0.3% w/v straw substrate was incubated in the mixture of 10ml CR solution (29mg/L) and 10ml 100mM sodium phosphate buffer (pH ~ 6.5). The straw mixture was swirled with Flask Shaker SF-01 at 300 OSC/min for 90 minutes. After incubation for 24 hours at 30°C, the mixture was centrifuged and the amount of CR in the supernatant was determined by Perkin Elmer UV/Vis spectrophotometer at 492nm. By using the Langmuir Equation 2 described below, the amount of dye adsorbed is calculated from a plot of $1/q_e$ versus $1/C_e$ (Lee, Teramoto and Endo, 2010; Annadurai, Chellapandian and Krishnan, 1999).

$$\frac{1}{q_e} = \left(\frac{1}{q_{mon}}\right) + \left(\frac{1}{k_L q_{mon}}\right)\left(\frac{1}{C_e}\right) \qquad (2)$$

where $1/q_e$ is the amount of CR adsorbed (mg/g), C_e is the amount of dye not being adsorbed (mg/ml), k_L is the Langmuir constant, and q_{mon} is the amount of dye adsorbed at saturation which can be calculated from a plot of $1/q_e$ versus $1/C_e$ (Lee, Teramoto and Endo, 2010; Annadurai, Chellapandian and Krishnan, 1999). The specific surface area (SSA) of straw can then be calculated from the Equation 3,

$$SSA = q_{mon} \times N_A \times SA_{CR}/MW \qquad (3)$$

Where N_A is the Avogadro constant, SA_{CR} is the surface area of a molecule of CR ($1.73nm^2$), and MW is the molecular weight of CR (696.7g/mol) (Lee, Teramoto and Endo, 2010).

3.8.9 Size exclusion chromatography, SEC

Acetylation was conducted on all the SEC analysis samples (lignin fraction samples from ethyl acetate and methanol extraction as listed in Table 3.5) to ensure that the samples can dissolve well in tetrahydrofuran solvent (THF). A weighted amount of lignin is acetylated overnight at room temperature with a mixture of purified pyridine-acetic anhydride (1:1, v/v). Excess acetic anhydride is decomposed by the addition of

methanol in iced bath for about 2 hours. Excessive pyridine was removed by azeotropic distillation with the addition of toluene and evaporation to dryness (repeated for 5 -6 times). The toluene can then be removed by addition of methanol and evaporation (repeated twice). Finally, 5 mg of dried acetylated lignin was dissolved in 1ml of THF ready for high performance liquid chromatography, HPLC analysis. SEC was then performed in a Waters HPLC system with the solution pumped at a flow rate 0.8ml/min under 381psi. The HPLC unit was fitted with a Waters 2414 Refractive Index Detector. A Styragel HR column was used. The molecular weight distribution (MWD) and the number average and weight average molecular weights (Mn and Mw) of lignin were calculated against monodisperse polystyrene standards (Mp 580 – 34500).

3.8.10 UV spectrophotometer

UV spectra were obtained using a Hewlett Packard 8453 UV-Vis Spectrophotometer (Agilent Technologies, USA). A lignin sample (0.01g) was dissolved in ~ 9.99ml of methanol in 10ml volumetric flask to produce a base to be referred to as methanolic lignin solution hereafter. The solution (0.5ml) was then diluted further with 14.5ml methanol and the homogenised solution was then used for UV scanning across 200 – 600 nm.

3.8.11 Total phenolic content, TPC

Total phenolic content was determined using modified Folin-Ciocalteu colorimetric method (Faustino *et al.*, 2010) with gallic acid, GA as a standard phenolic compound. A linear calibration curve of GA was prepared based on a series standard solution ranging from 52.5 to 200ppm (r^2 = 0.9993). The diluted methanolic lignin solution (0.5ml, twice dilution) was oxidized with 2.5 ml Folin-Ciocalteu reagent (0.2N, Sigma-Aldrich) and the reaction was neutralised with 2 ml sodium carbonate (7.5% w/w Merck) for 90 minutes. The solution was then filtered with syringe filter (PTFE 0.20 µm) before UV absorbance taken at 765nm. The total phenolic content was expressed as mg of gallic acid equivalents (GAE) / L of methanolic lignin.

3.8.12 Total lignin content, TLC

The total lignin content was estimated as summation of total acid-insoluble content (Klason lignin) and total acid-soluble content. The TLC was determined according to modified method outlined by Aldaeus (Aldaeus *et al.*, 2011; Aldaeus, 2010) with reference to the relevant standards (TAPPI, 1991 Useful Methods; ASTM, 2007; TAPPI, test methods 2004–2005; TMCD-04, 2004.). The sample amount was scaled down with factor of 3 to improve the filtration time. After hydrolysis, the suspensions were filtered while hot, and the retentates were measured gravimetrically for Klason lignin while for acid-soluble lignin contents in the filtrate were determined by UV absorption at 205 nm (Hewlett Packard 8453 UV-Vis Spectrophotometer, Agilent Technologies, USA).

3.8.13 Total carbohydrate content, TCC

The filtrate obtained from sub-section 3.8.12 was also used for total carbohydrate content determination. The TCC was determined by high-performance anion exchange chromatography equipped with a pulsed ampero-metric detector (Dionex Sweden, Va¨stra Fro¨lunda, Sweden) based on relevant standards (SCAN standard, 2009; ASTM, 2007).

3.8.14 Fourier transform infrared, FTIR (for work in Chapter 8)

ATR-FTIR spectra (4000 – 600cm^{-1}) were obtained using a Varian 680-IR FTIR spectrometer equipped with a MIRacle ATR (Pike Technologies) with a zinc selenide crystal. Spectra were obtained with 4cm^{-1} resolution, using 32 scans for both background and the sample. Dried lignin and extracts were pressed against the crystal surface using a pressure tower to ensure that a constant pressure was applied.

3.8.15 ^{13}C and ^{1}H Nuclear Magnetic Resonance, NMR

The NMR spectra of the crude lignins / fractions were obtained using a Bruker Ultrashield 400 plus spectrometer (74.5 Hz) at room temperature. Approximately 100 mg of sample was mixed with 0.5 mg of Chromium (III) acetylacetonate (from Sigma-

Aldrich) and dissolved in 600 µl Dimethyl sulfoxide (from Sigma-Aldrich). Sample was then placed in 5mm i.d. NMR tube for testing.

For ^{13}C-spectra 100000 or 360000 scans were recorded with 70° pulses, for MEX and EH (see sub-section 3.5) respectively. For ^{1}H-spectra 128 scans were recorded with 30° pulses, for both samples.

3.8.16 Antioxidant activity

The antioxidant activities of the lignin, lignin fractions and the WL control were determined based on the radical scavenging activity method using 2,2-diphenyl-1-picrylhydrazyl radical (DPPH) as explained elsewhere (Faustino *et al.*, 2010; Scherer and Godoy, 2009). A linear calibration curve for 4 DPPH standard solutions in methanol (0 – 78 ppm) was plotted (r^2 = 0.995). UV absorbance was taken at 517nm using a Hewlett Packard 8453 UV-Vis Spectrophotometer (Agilent Technologies, USA). The methanolic lignin solution of sample (0.1 ml) was mixed with DPPH standard solution 78ppm (3.9 ml) and then kept from light for an incubation period of 90 minutes before measuring the absorbance under UV. The antioxidant activity was reported at percentage of inhibition (I%) and Antioxidant activity index (AAI). I% and AAI was calculated based on Equation 4 and Equation 5 (Faustino *et al.*, 2010; Scherer and Godoy, 2009),

$$I\% = \left[\frac{Abs_0 - Abs_1}{Abs_0}\right] \times 100 \qquad (4)$$

where Abs_0 was the absorbance of the blank and Abs_1 was the absorbance in the presence of the test compound at different concentrations and

$$AAI = \left[\frac{Final\ concentration\ of\ DPPH\ in\ blank\ (ppm)}{IC_{50}(ppm)}\right] \times 100 \qquad (5)$$

where IC_{50} (concentration providing 50% inhibition) was calculated graphically using a calibration curve in the linear range by plotting the sample concentration versus the corresponding I%.

3.8.17 Differential scanning calorimetry for the oxidation induction time, DSC-OIT

DSC-OIT tests on the rubber glove samples were performed using DSC Q2000 Series (TA Instrument, USA). The sample weighed between 10 – 15mg and placed in Tzero aluminium crucibles without cover was heated from 30°C to 175°C at a heating rate of 10°C /minute with continuously flushed with nitrogen at 100ml/min. When reached 175°C, 5 mins equilibrium time was allowed before the purge gas was switched to pure oxygen. Isothermal condition was maintained until a significant oxidative exothermic response is observed. The DSC-OIT value is defined as the onset time of oxidation obtained using the "onset" option in the TA Universal Analysis software.

3.9 References

1. Aldaeus, F. (2010) *COST FP0901 - Protocol for round robin test of lignin content in lignin samples - version 3.doc* . Available at: http://web.abo.fi/fak/tkf/spk/costfp0901/Round_robin/COST_FP0901-Protocol_for_round_robin_test_of_lignin_content-version_3.pdf (Accessed: 12/10/2012 2012).
2. Aldaeus, F., Schweinebarth, H., Törngren, P. and Jacobs, A. (2011) "Simplified determination of total lignin content in kraft lignin samples and black liquors", *Holzforschung: International Journal of the Biology, Chemistry, Physics, & Technology of Wood,* vol. 65, no. 4, pp. 601-604.
3. Annadurai, G., Chellapandian, M. and Krishnan, M.R.V. (1999) "Adsorption of Reactive Dye on Chitin", vol. 59, no. 1.
4. ASTM (2007) *D412 - 06a Test methods for vulcanized rubber and thermoplastic elastomers - tension,* ASTM.
5. Burke, J. (2008) *Solubility Parameters*-- . Available at: http://cool.conservation-us.org/byauth/burke/solpar/solpar2.html (Accessed: 12/5/2012 2012).
6. Daviesa, A. and Fearnb, T. (2006) "Back to basics: calibration statistics", *Spectroscopy Europe,* vol. 18, pp. 31.
7. Faustino, H., Gil, N., Baptista, C. and Duarte, A.P. (2010) "Antioxidant Activity of Lignin Phenolic Compounds Extracted from Kraft and Sulphite Black Liquors", *Molecules,* vol. 15, no. 12, pp. 9308-9322.
8. Grulke, E.A. (1999) "Solubility Parameter Values" in *Polymer handbook,* eds. J. Brandrup, E.H. Immergut and E.A. Grulke, 4th edn, Wiley, New York ; Chichester, pp. 675 - 714.
9. Lee, S.-., Teramoto, Y. and Endo, T. (2010) "Enhancement of enzymatic accessibility by fibrillation of woody biomass using batch-type kneader with twin-screw elements", *Bioresource technology,* vol. 101, no. 2, pp. 769-774.
10. Mörck, R., Yoshida, H. and Kringstad, K. (1986) "Fractionation of Kraft Lignin by Successive Extraction with Organic Solvents I : Functional Groups, 13C-NMR-Spectra and Molecular Weight Distributions", *Supplement,* vol. 40, pp. 51-60.

11. Ohman, F., Theliander, H., Tomani, P. and Axegard, P. (2010) *Method for separating lignin from black liquor, a lignin product, and use of a lignin product for the production of fuels and materials*, 20100325947 A1, US.
12. Ougiya, H., Hioki, N., Watanabe, K., Morinaga, Y., Yoshinaga, F. and Samejima, M. (1998) "Relationship between the physical properties and surface area of cellulose derived from adsorbates of various molecular sizes.", *Bioscience Biotechnology and Biochemistry*, vol. 62, no. 10, pp. 1880-1884.
13. SCAN standard (2009) *CM 71:09, Pulps – Carbohydrate composition*, Scandinavian Pulp, Paper and Board testing Committee, Stockholm, Sweden.
14. Scherer, R. and Godoy, H.T. (2009) "Antioxidant activity index (AAI) by the 2,2-diphenyl-1-picrylhydrazyl method", *Food Chemistry*, vol. 112, no. 3, pp. 654-658.
15. TAPPI (test methods 2004–2005; TMCD-04, 2004.) *T 222 om-02; Acid-insoluble lignin in wood and pulp.*, TAPPI.
16. TAPPI (1991 Useful Methods) *UM 250. Acid soluble lignin in wood and pulp.*, TAPPI.
17. Wang, K., Jiang, J.X., Xu, F. and Sun, R.C. (2009) "Influence of steaming pressure on steam explosion pretreatment of Lespedeza stalks (Lespedeza crytobotrya): Part 1. Characteristics of degraded cellulose", *Polymer Degradation and Stability,* vol. 94, no. 9, pp. 1379-1388.
18. Wang, K., Xu, F. and Sun, R. (2010) "Molecular Characteristics of Kraft-AQ Pulping Lignin Fractionated by Sequential Organic Solvent Extraction", *International Journal of Molecular Sciences,* vol. 11, no. 8, pp. 2988-3001.
19. Wold, S., Sjöström, M. and Eriksson, L. (2001) "PLS-regression: a basic tool of chemometrics", *Chemometrics and Intelligent Laboratory Systems,* vol. 58, no. 2, pp. 109-130.

Chapter 4

Comparison between Pre-treatment of wheat straw using Extrusion and Conventional Steam Explosion

4.1 Introduction

Global bio-fuel production has increased rapidly over the last decade. Concerns about the long-term sustainability of liquid bio-fuels such as bio-alcohol/ bio-diesel industry and competition with supply of foods have also been raised, particularly with regard to first-generation bio-fuels, which are produced primarily from food crops such as grain, sugar cane and vegetable oils. This has driven the development of second-generation bio-alcohol mainly derived from lignocellulosic feedstock agricultural residues such as wheat straw.

Lignocellulosic biomass is the most abundant organic material on earth and it is also a promising raw material for bioenergy production; its annual production has been estimated to be about 10^{10} MT worldwide (Alvira *et al.*, 2010; Sánchez and Cardona, 2008). It contains cellulose and hemicellulose that are bound together by lignin. Cellulose and hemicellulose are both polymers of built up by long-chain sugar monomers, which after pre-treatment and hydrolysis to sugars can be converted into ethanol by microbial fermentation (Lu, Zhang and Angelidaki, 2009). There is an abundant supply of cereal straws in UK. Approximately 5-7 million tonnes of wheat straw are produced in the UK annually but only 1% is currently traded (Kang *et al.*, 2009). Pre-treatment of wheat straw (lignocellulosic) biomass is a crucial step as it has direct impact on the subsequent yield of enzymatic saccharification and alcohol fermentation processes in the production of bio-fuels. Pre-treatment process is a major cost component of the overall biochemical route for bio-fuel production and no 'best' option yet exists and R&D continues to improve cost and performance goals (Sims *et al.*, 2010). Several physical (Mosier *et al.*, 2005;Karunanithy and Muthukumarappan, 2010a; Karunanithy and Muthukumarappan, 2010b; Lee, Teramoto and Endo, 2010), chemical (Kootstra *et al.*, 2009; Sun and Chen, 2008; Li *et al.*, 2009) and biological pre-

treatments (Bak *et al.*, 2010; Ma *et al.*, 2010) have been developed, as described in more details in Chapter 2, to improve the digestibility of biomass, but the need to reduce the energy inputs, and the costs of the procedure in general, has generated consensus around the use of simple thermochemical pre-treatments (Gomez, Steele-King and McQueen-Mason, 2008). A batch process, such as steam explosion is the most commonly used method for lignocellulosic pre-treatment. However, steam explosion process has been reported to have limitation of carbohydrate degradation and oxidation of lignin, which would result in potential fermentation inhibitors (Karunanithy and Muthukumarappan, 2011b; Chen and Qiu, 2010; Pienkos and Zhang, 2009). Issues of inhibitor formation will have direct impact on final yield of bio-alcohol. Other than steam explosion pre-treatment, dilute acid pre-treatment is also commonly applied (Gomez, Steele-King and McQueen-Mason, 2008; Mohammad J. Taherzadeh, Keikhosro Karimi, 2007). Costly equipment maintenance due to corrosion and post treatment neutralisation would be the consideration of using acid pre-treatment.

Extrusion technology was recently reported with good potential for pre-treatment of lignocelluloses biomass. Lamsal et al. (2009) and Lee et al. (2010) used a twin screw extruder to pre-treat wheat bran and woody biomass (Douglas fir and Eucalyptus) (Lamsal *et al.*, 2010; Lee, Teramoto and Endo, 2010; Lee, Teramoto and Endo, 2009). Karunanithy et al. used a single screw extruder to pre-treat corn stover (Karunanithy and Muthukumarappan, 2010b), switchgrass and prairie cord grass (Karunanithy and Muthukumarappan, 2011b; Karunanithy and Muthukumarappan, 2010a). Other extrusion pre-treatments have been combined with hot-compressed water treatment (Lee *et al.*, 2010) and chemical soaking pre-treatment methods (Karunanithy and Muthukumarappan, 2011a). An extruder has the ability to provide high shear, rapid heat transfer, effective and rapid mixing and is easily combined with chemicals or additives pre-treatments in a single continuous process. Extrusion at low barrel temperatures has the potential to minimise energy consumption and generation of inhibitors. Detailed analytical characteristics of extruded straw in direct comparison to steam exploded straw has not been reported in the literature. Hence, this chapter aims to obtain a good understanding of low temperature twin-screw extrusion pre-treatment of wheat straw by systematic comparison between extrusion and conventional steam explosion. Pre-treated

straw was characterised with a portfolio of analytical techniques and correlated to the yield of glucose after enzymatic hydrolysis in order to identify the effectiveness of the pre-treatment process.

The experimental details are described in sub-section 3.2 and **Table 3.1** and the results are discussed in rest of the chapter.

4.2 Results and Discussion

4.2.1 Physical Observation

The pre-treated straw changed colour from light to dark shades of brown. The trend of darkness followed the sequence:

$$RWS < EX01 < SE01 < EX02 < SE02$$

and sample SE02 was the most brown darkest in colour (**Figure 4.1**).

Figure 4.1: Picture of sample RWS, SE01, SE02, EX01 and EX02 (from left to right)

The phenomenon of colour change is believed to be related to the chemical breakdown of lignin and extractives and the condensation reactions which could activate tannins and flavonoids towards condensation by lysing of protection group (sugars) which react with furfural and hydroxymethylfurfural (Wang *et al.*, 2009; Sun *et al.*, 2005)**.** The colour of the sample was evaluated according to the L*, a*, b* measurement system

(see sub-section 3.8.6) and results are tabulated in **Table 4.1**. Index of L* is an indication of lightness while a* and b* are colour opponent indices of red/green and yellow/blue, respectively. As brightness of the straw samples decreases in the sequence mentioned above, they become less reflective to light. It indicates the removal of extractives and waxes embedded at the surface of straw. Under the severe pre-treatment condition (SE02), the redness index, a*, increased, which serve as an indication of more polysaccharides (hemicellulosic sugar) and lignin fractionated and lead to the chemical reaction that darkens the colour. Alkaline extrusion pre-treated straw has highest yellowness index, b*, and could probably due to catalytic effect of NaOH or reaction between ferulate and phenolate anion. With less severe treatment such as EX01 more hemicellulosic sugar remained unhydrolysed and hence, there was less colour change in comparison with the RWS.

Table 4.1 : Colorimetric measurement for various sample straw

Sample	L	a*	b*
RWS	**59.05**	**3.38**	**16.90**
EX01	**52.61**	**2.97**	**14.34**
EX02	**52.60**	**2.21**	**20.98**
SE01	**54.50**	**4.90**	**16.47**
SE02	**46.08**	**5.15**	**13.59**

SEM images for individual straw sample are shown in **Figure 4.2**. Without pre-treatment, the anatomy of the harvested and chopped RWS was observed. More intact structures and partial exposure of parenchyma cells can be seen (**Figure 4.2a**). Each pre-treatment showed further degree of fractionation of the straw and fibre bundles compared to RWS. Among the pre-treated straw, SE02 which is steam pre-treated at a temperature over 200°C was found to have most remarkable break down of fibrous structures (**Figure 4.2e in comparison with 4.2a-4.2d**).

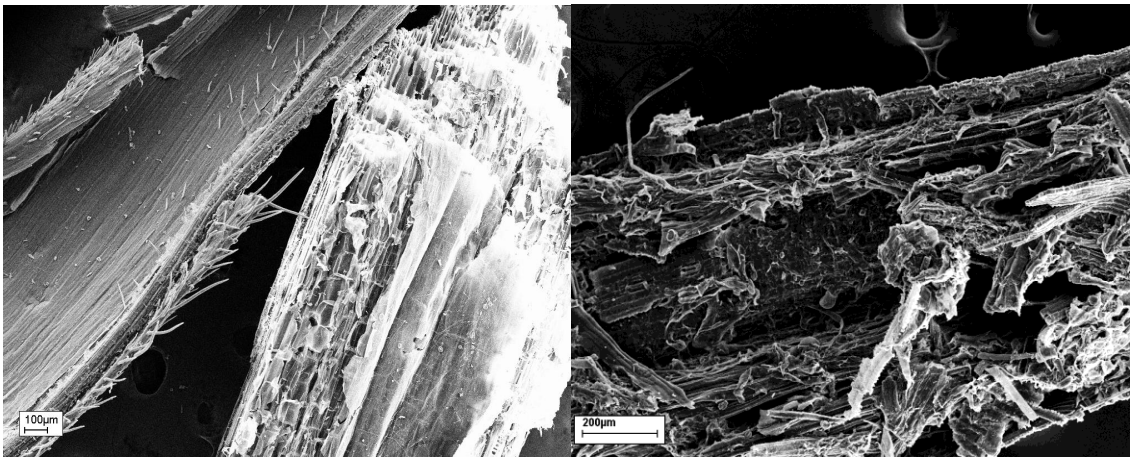

(a) (b)

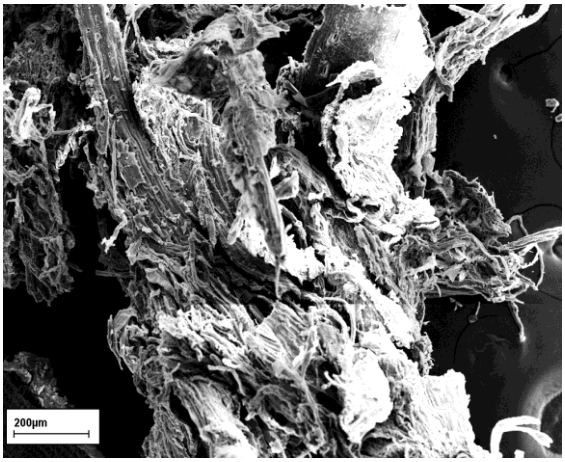

(c)

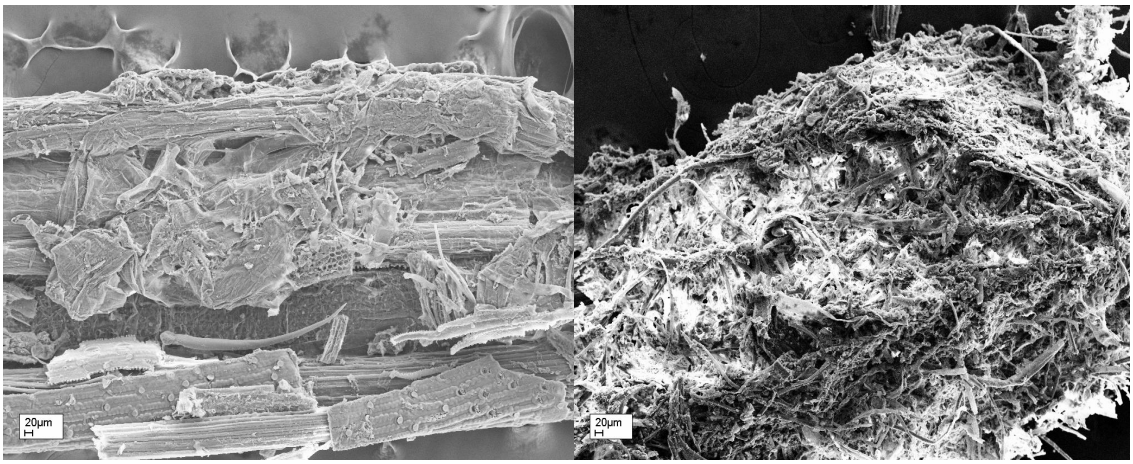

(d) (e)

Figure 4.2 : SEM microscopy images for various straw sample: a) RWS; b) EX1; c) EX02; d) SE01; e) SE02

4.2.2 ATR-FTIR spectroscopic analysis

FTIR is widely used as an analytical tool for investigations of physicochemical properties of lignocellulosic biomass for the comparison before and after pre-treatment by chemical identification of numerous functional groups. The sampling method commonly used in previous lignocellulosic studies uses KBr discs embedded with particulate biomass under transmittance mode (Naik *et al.*, 2010; Peng and Wu, 2010; Wang *et al.*, 2009; Hongzhang and Liying, 2007; Sain and Panthapulakkal, 2006; Ouajai and Shanks, 2005; Sun *et al.*, 2005; Carrillo *et al.*, 2004). KBr disc preparation is very time-consuming and it requires considerable skill to obtain a good spectrum. Among other FTIR sample preparation methods, reflectance sampling with attenuated total reflectance (ATR) is another option which is considered simpler and more user-friendly. Among the reviewed literature, only Kristensen *et al*. (2008) and Tamaki *et al.* (2011) used reflectance sampling method for lignocellulose biomass study. ATR-FTIR was used in this study for investigating the physicochemical changes taking place during pre-treatment of lignocellulose and compared with previous studies to further verify the method.

The FTIR spectra for the samples are shown in **Figure 4.3**. The spectra of wheat straw with and without pre-treatment are dominated by the peaks at ~3291 and ~1031 cm^{-1} indicate the stretching vibrations of O-H and C-O, respectively.

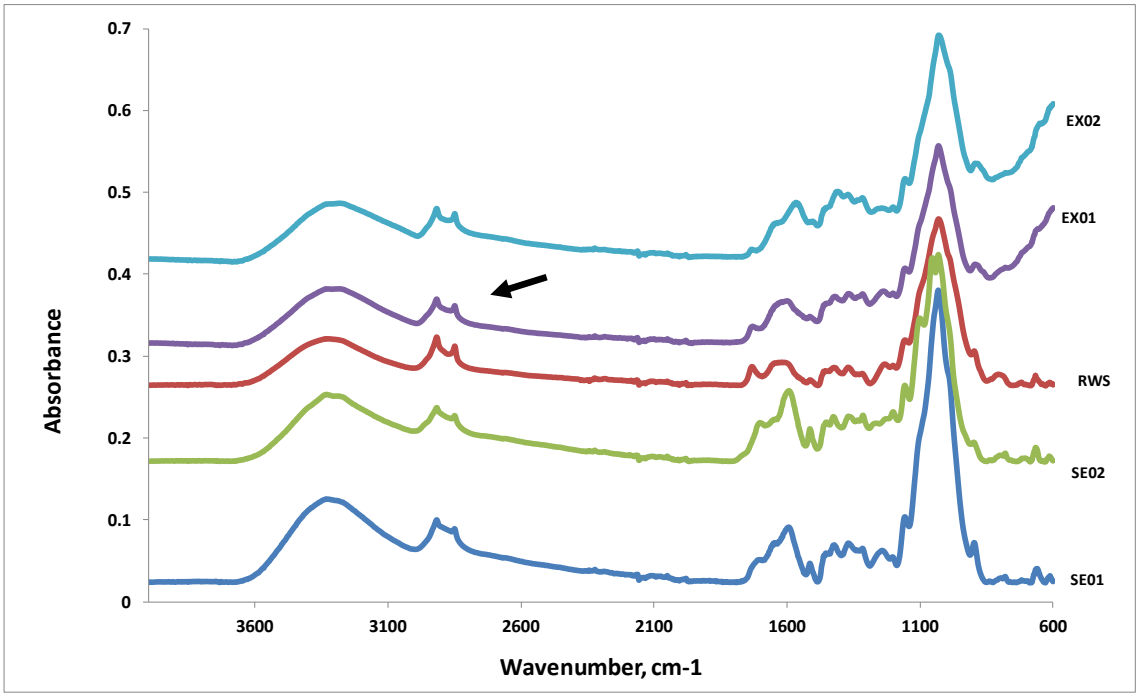

Figure 4.3: Complete spectra of wheat straw from all pre-treatments

The arrow points to the bands at 2850 and 2920cm^{-1} (CH_2- stretching bands ascribed to wax) (Le Troëdec *et al.*, 2009; Kristensen *et al.*, 2008). In the cross section of straw, the epidermis cells are the outmost surface cells, covered by a very thin wax layer (Han *et al.*, 2010). All the pre-treatments partially removed epidermal wax and this was evidenced by the decrease in the 2850cm^{-1} peak intensity. For bio-fuel application, this hydrophobic feature of raw wheat straw has to be altered to hydrophilic in order to enhance the efficiency of enzymatic hydrolysis in aqueous medium. Observation of wax removal is also in line with the reduction of sample brightness in the colour study.

Figure 4.4 shows the excerption of spectra. The dotted vertical lines mark the positions of the bands at 1733 and 1515cm^{-1}, which are associated with hemicellulose and lignin, respectively. The sharp peak at ~1733 cm^{-1} is attributed to acetyl and uronic ester groups of the hemicelluloses or from the ester linkage of carboxylic group of the ferulic and *p*-coumaric acids of lignin and/or hemicelluloses (Le Troëdec *et al.*, 2009; Alemdar and Sain, 2008; Kristensen *et al.*, 2008; Zhang *et al.*, 2008; Sain and Panthapulakkal, 2006). The peak is almost cleaved in the steam exploded samples in particular SE02, this suggests that steam explosion is effectiveness in removing hemicelluloses (Sun *et al.*, 2005) even with no chemical added during the steam explosion. When NaOH

(alkaline) was added to the system, significant reduction of 1733 cm^{-1} peak is observed which indicates that the extrusion combining chemical and thermo-mechanical pre-treatments has reduced further the ester bond from the hemicelluloses and/or lignin.

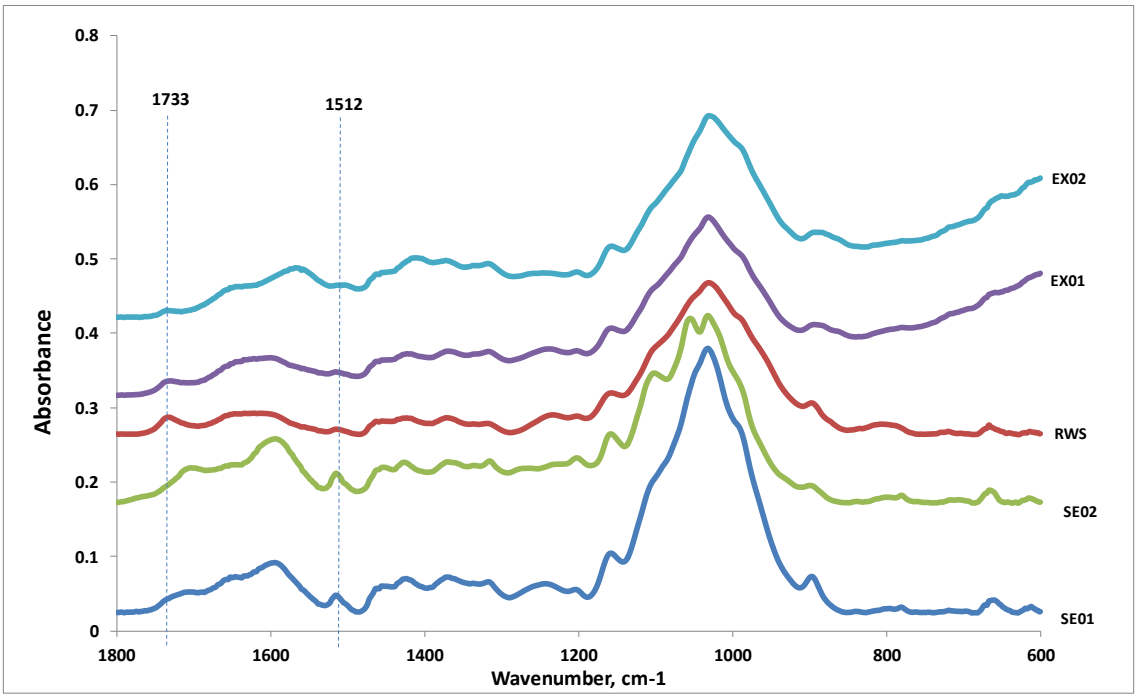

Figure 4.4: The excerption of spectra for various straw sample from wave number range 600 – 1800cm^{-1}

By visual comparison, it is not always easy to tell the changes in certain characteristic peaks. = Peak height (intensity) of the target peaks are normalised by that of a reference key component to give more sensitive & quantitative measure [28]. For instance, peak 1422 cm^{-1} for CH_2 bending of cellulose compound has been used as main component for the peak height ratio calculation here as in [28]. A selection of the peak height ratio indices are shown in **Table 4.2** for the samples Apart from serving as relative semi-quantitative indices to ease the spectra comparison, the peak height ratio is also able to correct the difference of contact area for solid ATR sampling, which improves the consistency of ATR-FTIR analysis.

Table 4.2 : Average Peak Height Ratio for Target Peaks from FTIR Spectra

Indications	Aliphatic compound	Hemicellulose linkage	Water (OH)	Aromatic - Lignin	Polysaccharides
Sample	A2918/A1422	A1733/A1422	A1632/A1422	A1512/A1422	A1371/A1422
RWS	2.04	1.01	1.19	0.63	1.00
EX 01	1.72	0.76	1.17	0.57	0.98
EX 02	1.39	0.39	0.79	0.58	0.91
SE 01	1.43	0.73	1.19	0.68	1.03
SE 02	1.18	0.91	1.28	0.81	1.00

Lignin (Guaicyl C-O)	Polysaccharides (β-glycosidic link)	Crystalinity Information	
A1240/A1422	A897/A1422	A1422/A897	A1371/A2918
1.12	1.33	0.76	0.49
0.82	0.98	1.03	0.57
0.42	0.74	1.36	0.66
0.90	1.01	0.99	0.72
0.72	0.60	1.67	0.85

Peak height ratio index for A1733/A1422 showing the reduction from ~ 1.00 for RWS to ~ 0.39 for straw after alkaline extrusion. A1733/A1422 for SE01 and SE02 were expected to be very low because the IR peak at 1733cm^{-1} was nearly cleaved. However, as shown in **Table 4.2**, the ratio of A1733/A1422 for SE01 and SE02 were 0.73 and 0.91, respectively. This is because a significant peak at ~ 1710 cm^{-1} was picked up within the corrected region during the data collection. The signal at ~ 1710 cm^{-1} was related to stretching carbonyl group from lignin compounds (Alriols *et al.*, 2009; Lammers, Arbuckle-Keil and Dighton, 2009a; Lammers, Arbuckle-Keil and Dighton, 2009b; Hongzhang and Liying, 2007). The peak at ~ 1240 cm^{-1} was contributed by C-O-aryl of lignin (guaiacyl unit) (Lammers, Arbuckle-Keil and Dighton, 2009b; Zhang *et al.*, 2008; Hongzhang and Liying, 2007). Based on the peak ratio index shown in **Table**

4.2, about 60% of guaiacyl lignin removal was recorded for alkaline extrusion pre-treatment. Severe steam explosion caused about 36% removal of guaiacyl lignin. Mild steam explosion and purely extrusion pre-treatment did not cause significant removal of guaiacyl and it can be seen on the spectra in **Figure 4.4** where the peak ~ 1240 remained after pre-treatment. Alkaline is a strong agent in term of lignin guaiacyl removal in the lignocellulose biomass even at the low level of heat and mechanical shearing in this study.

Interestingly, evidence of aromatic lignin bands at ~ 1594 and 1515 cm^{-1} (Kaushik, Singh and Verma, 2010; Naik *et al.*, 2010; Alriols *et al.*, 2009; Lammers, Arbuckle-Keil and Dighton, 2009b; Alemdar and Sain, 2008; Kristensen *et al.*, 2008; Zhang *et al.*, 2008; Sain and Panthapulakkal, 2006) were picked up significantly in the steam exploded samples (SE01 and SE02), as shown in **Table 3.1**, Chapter 3. This finding is in line with the stretching carbonyl group signal detected at ~ 1710 cm^{-1} in both steam exploded samples. Similar trends were found by Kristensen *et al.* (2008) using FTIR analysis and Sun *et al.* (2005) using wet chemical analysis (Klason lignin). According to Sun *et al.* (2005), the reason for this higher lignin content was due to the hydrolysis of substantial amount of hemicelluloses during steam pre-treatment and lignin re-condensation reactions. Another possible reason highlighted by Kristensen *et al.* (2008) was on the sampling technique of ATR-FTIR. ATR is a surface reflectance technique; hence concern of lignin re-deposition on the surface was raised. The similar signals of aromatic bands and stretching carbonyl group were not observed in either extruded samples. It was believed attributable to the lower severity of pre-treatment for extrusion at low temperature.

There was a sharp peak at ~ 897 cm^{-1} in **Figure 4.4** contributed by β-glucosidic linkages between sugars units, indicating β-linked hemicelluloses (Peng and Wu, 2010; Alriols *et al.*, 2009). By looking at the peak height ratio for A897/A1422 in **Table 4.2**, a decreasing trend was observed for all the pre-treated straw. This is an indication to prove the reduction of hemicellulose by decreasing the degree of polymerisation. Again, the highest reduction was recorded on SE02 and follow by EX02 pre-treatment, which is in agreement with the observation of removal of ester carbonyl linkages (~ 1733 cm^{-1}).

Crystallinity information of lignocellulosic biomass can also be obtained based on FTIR spectra analysis and it has widely been used by researchers (El Oudiani *et al.*, 2009; Wang *et al.*, 2009; Kristensen *et al.*, 2008; Hongzhang and Liying, 2007; Oh *et al.*, 2005; Ouajai and Shanks, 2005). Crystallinity information for the sample can be estimated by the peak ratio index of A1422/A897, where peak 1422 cm^{-1} represented crystalline portion while 897 cm^{-1} represented amorphous portion (Kristensen *et al.*, 2008; Hongzhang and Liying, 2007; Ouajai and Shanks, 2005). A trend of increased crystallinity after pre-treatment was observed, which was consistent with Chen et al. (on wheat straw) using FTIR analysis and Wang et al. (on Lespedeza stalks) and Alemdar et al. (on wheat straw) using X-ray diffraction, XRD analysis (Wang *et al.*, 2009; Alemdar and Sain, 2008; Hongzhang and Liying, 2007). The reason for the increase is believed due to the proportion of cellulose being higher as the hemicellulose and lignin decrease. Cellulose is the key crystalline component in lignocellulose biomass. In order to further strengthen the hypothesis, the crystallinity of the same set of sample was determined again by using XRD analysis. The crystallinity index was 35.6%, 35.5%, 37.5%, 23.9% and 32.3% for the sample RWS, EX01, EX02, SE01 and SE02, respectively. Using the method of Segal (Thygesen *et al.*, 2005), the crystallinity was determined by using the height of 200 peak ($2\theta \sim 22^{\circ}$) ratio to the minimum of between the 200 and 110 peaks ($2\theta \sim 18^{\circ}$) as described in sub-section 3.8.7, Chapter 3. However, for all the pre-treated straw sample, a sharp peak at ~ 26.5° was found on the X-ray diffractogram and the intensity is higher in steam exploded sample and followed by alkaline extrusion and lastly pure extrusion sample. This peak was not counted in the crystallinity data for XRD. A recent paper from Kaushik et al. (2010) indicated the need to include this peak in the crystallinity calculation. Hence, the crystallinity data with inclusion of this peak should then higher than the RWS.

4.2.3 Thermal analysis

TG and DTG analysis were used to further investigate the structure and component change of straw sample under different pre-treatment processes. The derivative thermogravimetry (DTG) curves for raw and pre-treated straw samples tested under inert conditions are shown in **Figure 4.5**.

The onset temperature of the degradation, peak at maximum, maximum degradation rate associated with peak of maximum and residue at 650°C of different straw samples are compared in **Table 4.3**. The DTG curve for the entire samples show an initial peak around 40 – 150°C, which corresponds to a mass loss of absorbed moisture of approximately 4 – 5%. The next phase of the thermogram displayed a distinct pyrolysis zone whereas sharp drop in mass of sample occurred, when the threshold temperature for thermal decomposition of the sample material is reached. This zone was termed the active pyrolysis zone (Ghaly and Ergudenler, 1991). A huge DTG peak was observed in the active pyrolysis zone (~ 200 – 400°C) which corresponded to the degradation of hemicelluloses and cellulose (Le Troëdec *et al.*, 2009; Serapiglia *et al.*, 2009; Yang *et al.*, 2007; Ouajai and Shanks, 2005)

.

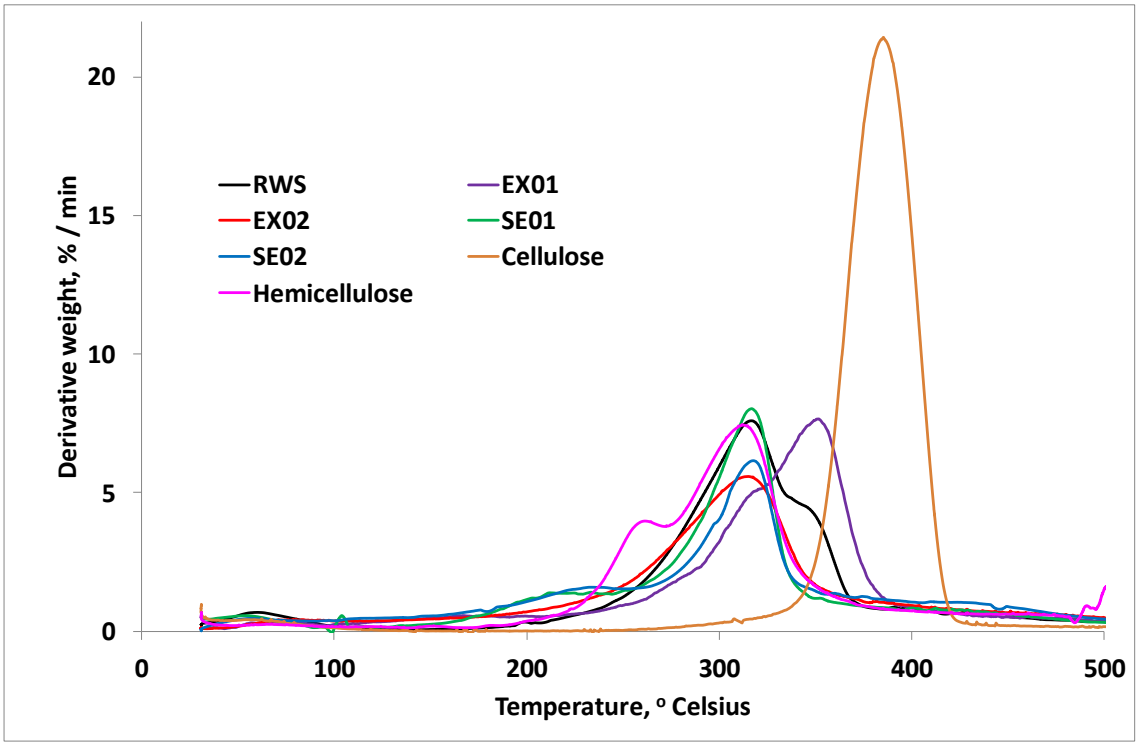

Figure 4.5 : The DTG curves for various straw samples under inert condition

Following the pre-treatments, the shoulder at 340°C for raw wheat straw disappeared in all the pre-treated samples, which might be explained by the reduction of lower molecular mass organic constituents (waxes and extractives) (Mészáros *et al.*, 2009).

This is in agreement with findings from physical colour change (brightness in the sub-section 4.2.1) and FTIR (indication of the aliphatic wax reduction).

For the steam exploded straws (SE01 and SE02), a shoulder was observed at a peak temperature of ~ 220°C beside the main pyrolysis peak. This may indicate a more significant fractionation of hemicelluloses from cellulose which required a higher degradation temperature (Serapiglia *et al.*, 2009; Tsujiyama and Miyamori, 2000). Previous research from Sun *et al.* (2005) and Alemdar *et al.* (2008) on pre-treated wheat straw reported increased thermal stability of pre-treated straw as indicated by a shift in the onset of degradation temperature. This phenomenon is not observed in SE01, SE02 and EX02 because no further separation step such as post washing was applied to these samples. A washing process would be able to remove hemicellulose, soluble lignin and extractives from the substrate and the remaining water insoluble portion would be rich in higher crystalline cellulose. The information of DTG curve shift can thus be used to predict the purity of the pre-treated substrate.

Table 4.3 : Summary Table for Data from Thermal Gravimetric Analysis under Inert Conditions

Sample	Onset Degradation Temperature (^{0}C)	Peak Temperature (^{0}C)	Maximum Degradation Rate (%/min.)
RWS	**276.58**	**317.99**	**7.6**
EX01	**290.96**	**333.48**	**7.9**
EX02	**254.61**	**306.14**	**5.6**
SE 01	**279.39**	**318.62**	**6.2**
SE 02	**279.31**	**314.79**	**8.0**
Cellulose	**337.97**	**362.77**	**21.3**
Hemicellulose (Birchwood)	**246.20**	**293.80**	**7.5**

The onset of degradation temperature for EX02 shifted to 254.61°C after the pre-treatment. A similar observation was reported by Meszaros *et al.* (2009) in their study of corn fibers pre-treated by amylolytic enzymes followed by alkaline treatment. This indicated that straw pre-treated with alkali in combination with extrusion has less thermal stability than the rest of the straw samples under investigation. This DTG curve shifted towards the hemicellulose degradation zone in **Figure 4.5**. However, it does not mean that more hemicelluloses have been degraded but indicates that more low-molecular mass hemicellulose components are present following the pre-treatment process.

EX01 which is purely extruded straw shows a DTG curve shift towards the cellulose degradation zone. It may indicate an increase in cellulose content within the pre-treated straw but it is not consistent with the findings from the physical, microscopic and FTIR analysis and hence more investigation is necessary using additional analyses such as TG-MS and Pyrolysis GC-MS in order to understand the component degraded at this particular zone.

4.2.4 Yield of Glucose Recovery

Pre-treated straw samples were subjected to enzymatic hydrolysis and the yield of glucose is used as an indication of effectiveness of the pre-treatment processes. The percentage of glucose recovery from available glucose in straw is shown in **Figure 4.6**. RWS without pre-treatment gives the lowest glucose recovery showing the importance of necessary pre-treatment for decent sugar yield. After a pre-treatment process, there is at least a more than 35 fold increase in glucose recovery. The trend of glucose recovery is in agreement with the findings obtained from SEM (degree of physical disruption or fractionation), FTIR (reduction in bounded hemicellulose) and TGA(changes on DTG curve). The steam exploded sample, SE02, shows highest glucose recovery followed by EX02 which is extrusion in combination with alkaline treatment. The alkali level in used in EX02 is 4% w/w NaOH based on dry straw. It is relatively low in comparison to alkali-related pre-treatment on lignocellulosic biomass from the literature. For instance, Zeitoun *et al.* (2010) used 1g NaOH / g for wheat bran and Karunanithy *et al.* (2011a) used 0.105g NaOH/ g for prairie cord grass in their pre-treatment. Higher

dosages of NaOH have been used for lignocellulosic biomass pre-treatment for bio-composite application (Alemdar and Sain, 2008; Ouajai and Shanks, 2005).

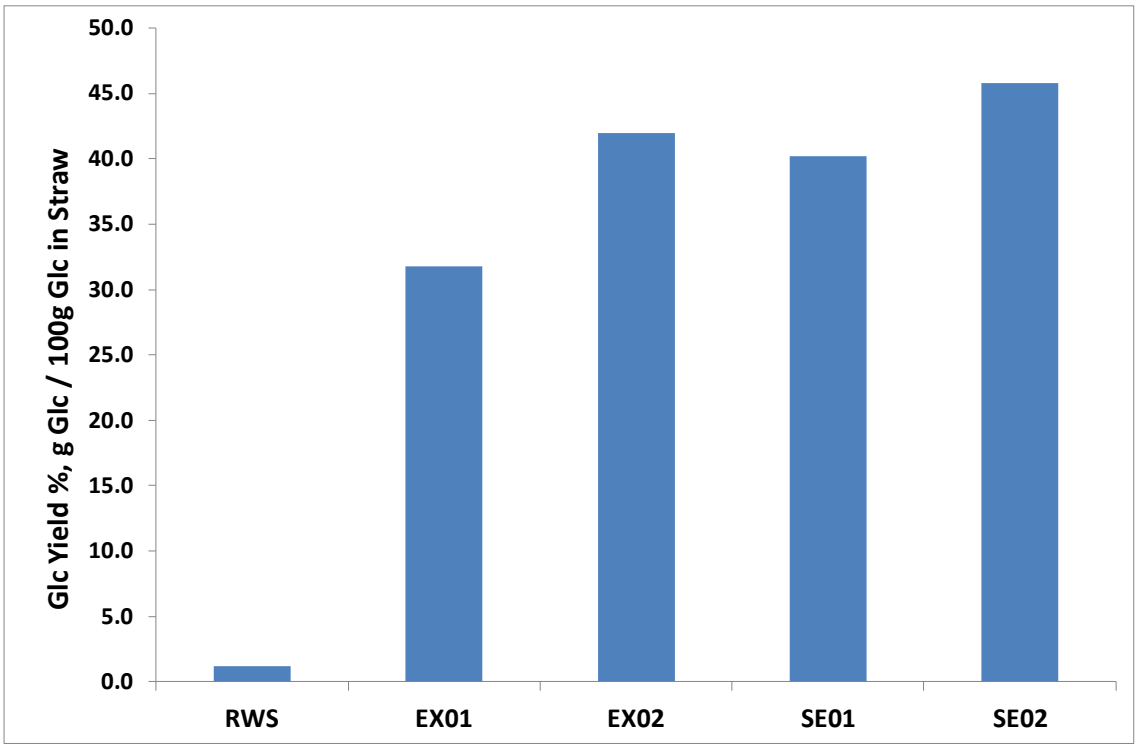

Figure 4.5 : Glucose recovery yield

4.3 Summary

Steam explosion and extrusion pre-treatment of wheat straw are compared. The effectiveness of physical and chemical fractionation is assessed using a portfolio of techniques including characterisation of changes in colour, microstructure (SEM), chemical structure (FTIR), crystallinity (XRD) and thermal degradation behaviour (TGA). Direct correlation is also made to glucose recovery in subsequent enzymatic hydrolysis of the treated straws.

Steam explosion at severe condition (SE02) demonstrated highest yield which evidenced by the more physical disruption and changes in FTIR and TGA. However, signal of lignin deposition picked up by FTIR could be a potential drawbacks in this conventional pre-treatment method which operating in batch system. In comparison, extrusion is relatively milder pre-treatment e.g. low temperature and low shear. Twin

screw extrusion supplemented with chemical treatment (alkaline – NaOH, EX02) has demonstrated promising saccharification yield when compared with steam explosion under severe processing condition. It is a continuous process which can be a practical technology for lignocellulose biomass pre-treatment. However further optimisation is required to maximise the saccharification yield of extrusion pre-treatment.

4.4 References

1. Alemdar, A. and Sain, M. (2008) "Isolation and characterization of nanofibers from agricultural residues – Wheat straw and soy hulls", *Bioresource technology*, vol. 99, no. 6, pp. 1664-1671.
2. Alriols, M.G., Tejado, A., Blanco, M., Mondragon, I. and Labidi, J. (2009) "Agricultural palm oil tree residues as raw material for cellulose, lignin and hemicelluloses production by ethylene glycol pulping process", *Chemical Engineering Journal*, vol. 148, no. 1, pp. 106-114.
3. Alvira, P., Tomás-Pejó, E., Ballesteros, M. and Negro, M.J. (2010) "Pretreatment technologies for an efficient bioethanol production process based on enzymatic hydrolysis: A review", *Bioresource technology*, vol. 101, no. 13, pp. 4851-4861.
4. Bak, J.S., Kim, M.D., Choi, I.-. and Kim, K.H. (2010) "Biological pretreatment of rice straw by fermenting with Dichomitus squalens", *New Biotechnology*, vol. 27, no. 4, pp. 424-434.
5. Carrillo, F., Colom, X., Suñol, J.J. and Saurina, J. (2004) "Structural FTIR analysis and thermal characterisation of lyocell and viscose-type fibres", *European Polymer Journal*, vol. 40, no. 9, pp. 2229-2234.
6. Chen, H. and Qiu, W. (2010) "Key technologies for bioethanol production from lignocellulose", *Biotechnology Advances*, vol. 28, no. 5, pp. 556-562.
7. El Oudiani, A., Chaabouni, Y., Msahli, S. and Sakli, F. (2009) "Physico-chemical characterisation and tensile mechanical properties of Agave americana L. fibres", *Journal of the Textile Institute*, vol. 100, no. 5, pp. 430-439.
8. Ghaly, A.E. and Ergudenler, A. (1991) "Thermal degradation of cereal straws in air and nitrogen", *Applied Biochemistry and Biotechnology*, vol. 28-29, no. 1, pp. 111-126.
9. Gomez, L.D., Steele-King, C. and McQueen-Mason, S. (2008) "Sustainable liquid biofuels from biomass: the writing's on the walls", *New Phytologist*, vol. 178, no. 3, pp. 473-485.

10. Han, G., Deng, J., Zhang, S., Bicho, P. and Wu, Q. (2010) "Effect of steam explosion treatment on characteristics of wheat straw", *Industrial Crops and Products*, vol. 31, no. 1, pp. 28-33.
11. Hongzhang, C. and Liying, L. (2007) "Unpolluted fractionation of wheat straw by steam explosion and ethanol extraction", *Bioresource technology*, vol. 98, no. 3, pp. 666-676.
12. Kang, Y.G., Xia, W., Song, J. and Tarverdi, K. (2009) " Extrusion fractionation of wheat straw for biocomposites utilising the entire straw constituents", *INTERNATIONAL JOURNAL OF MATERIALS & PRODUCT TECHNOLOGY*, vol. 36, no. 1-4, pp. 334-347.
13. Karunanithy, C. and Muthukumarappan, K. (2011a) "Optimization of alkali soaking and extrusion pretreatment of prairie cord grass for maximum sugar recovery by enzymatic hydrolysis", *Biochemical engineering journal*, vol. 54, no. 2, pp. 71-82.
14. Karunanithy, C. and Muthukumarappan, K. (2011b) "Optimization of switchgrass and extruder parameters for enzymatic hydrolysis using response surface methodology", *Industrial Crops and Products*, vol. 33, no. 1, pp. 188-199.
15. Karunanithy, C. and Muthukumarappan, K. (2010a) *Effect of Extruder Parameters and Moisture Content of Switchgrass, Prairie Cord Grass on Sugar Recovery from Enzymatic Hydrolysis*.
16. Karunanithy, C. and Muthukumarappan, K. (2010b) *Influence of extruder temperature and screw speed on pretreatment of corn stover while varying enzymes and their ratios*.
17. Kaushik, A., Singh, M. and Verma, G. (2010) "Green nanocomposites based on thermoplastic starch and steam exploded cellulose nanofibrils from wheat straw", *Carbohydrate Polymers*, vol. 82, no. 2, pp. 337-345.
18. Kootstra, A.M.J., Beeftink, H.H., Scott, E.L. and Sanders, J.P.M. (2009) "Comparison of dilute mineral and organic acid pretreatment for enzymatic hydrolysis of wheat straw", *Biochemical engineering journal*, vol. 46, no. 2, pp. 126-131.

19. Kristensen, J.B., Thygesen, L.G., Felby, C., Jørgensen, H. and Elder, T. (2008) "Cell-wall structural changes in wheat straw pretreated for bioethanol production", *Biotechnology for Biofuels,* vol. 1.
20. Lammers, K., Arbuckle-Keil, G. and Dighton, J. (2009a) "FT-IR study of the changes in carbohydrate chemistry of three New Jersey pine barrens leaf litters during simulated control burning", *Soil Biology and Biochemistry,* vol. 41, no. 2, pp. 340-347.
21. Lammers, K., Arbuckle-Keil, G. and Dighton, J. (2009b) "FT-IR study of the changes in carbohydrate chemistry of three New Jersey pine barrens leaf litters during simulated control burning", *Soil Biology and Biochemistry,* vol. 41, no. 2, pp. 340-347.
22. Lamsal, B., Yoo, J., Brijwani, K. and Alavi, S. (2010) "Extrusion as a thermo-mechanical pre-treatment for lignocellulosic ethanol", *Biomass and Bioenergy,* vol. 34, no. 12, pp. 1703-1710.
23. Le Troëdec, M., Peyratout, C.S., Smith, A. and Chotard, T. (2009) "Influence of various chemical treatments on the interactions between hemp fibres and a lime matrix", *Journal of the European Ceramic Society,* vol. 29, no. 10, pp. 1861-1868.
24. Lee, S.-., Inoue, S., Teramoto, Y. and Endo, T. (2010) "Enzymatic saccharification of woody biomass micro/nanofibrillated by continuous extrusion process II: Effect of hot-compressed water treatment", *Bioresource technology,* vol. 101, no. 24, pp. 9645-9649.
25. Lee, S.-., Teramoto, Y. and Endo, T. (2010) "Enhancement of enzymatic accessibility by fibrillation of woody biomass using batch-type kneader with twin-screw elements", *Bioresource technology,* vol. 101, no. 2, pp. 769-774.
26. Lee, S.-., Teramoto, Y. and Endo, T. (2009) "Enzymatic saccharification of woody biomass micro/nanofibrillated by continuous extrusion process I - Effect of additives with cellulose affinity", *Bioresource technology,* vol. 100, no. 1, pp. 275-279.
27. Li, Q., He, Y.-., Xian, M., Jun, G., Xu, X., Yang, J.-. and Li, L.-. (2009) "Improving enzymatic hydrolysis of wheat straw using ionic liquid 1-ethyl-3-

methyl imidazolium diethyl phosphate pretreatment", *Bioresource technology*, vol. 100, no. 14, pp. 3570-3575.

28. Lu, X., Zhang, Y. and Angelidaki, I. (2009) "Optimization of H2SO4-catalyzed hydrothermal pretreatment of rapeseed straw for bioconversion to ethanol: Focusing on pretreatment at high solids content", *Bioresource technology*, vol. 100, no. 12, pp. 3048-3053.
29. Ma, F., Yang, N., Xu, C., Yu, H., Wu, J. and Zhang, X. (2010) "Combination of biological pretreatment with mild acid pretreatment for enzymatic hydrolysis and ethanol production from water hyacinth", *Bioresource technology*, vol. 101, no. 24, pp. 9600-9604.
30. Mészáros, E., Jakab, E., Gáspár, M., Réczey, K. and Várhegyi, G. (2009) "Thermal behavior of corn fibers and corn fiber gums prepared in fiber processing to ethanol", *Journal of Analytical and Applied Pyrolysis*, vol. 85, no. 1-2, pp. 11-18.
31. Mohammad J. Taherzadeh, Keikhosro Karimi (2007) "Acid-Based Hydrolysis Processes for Ethanol From Lignocellulosic Materials : A Review", vol. 2, no. 3, pp. 472-499.
32. Mosier, N., Hendrickson, R., Ho, N., Sedlak, M. and Ladisch, M.R. (2005) "Optimization of pH controlled liquid hot water pretreatment of corn stover", *Bioresource technology*, vol. 96, no. 18, pp. 1986-1993.
33. Naik, S., Goud, V.V., Rout, P.K., Jacobson, K. and Dalai, A.K. (2010) "Characterization of Canadian biomass for alternative renewable biofuel", *Renewable Energy*, vol. 35, no. 8, pp. 1624-1631.
34. Oh, S.Y., Yoo, D.I., Shin, Y., Kim, H.C., Kim, H.Y., Chung, Y.S., Park, W.H. and Youk, J.H. (2005) "Crystalline structure analysis of cellulose treated with sodium hydroxide and carbon dioxide by means of X-ray diffraction and FTIR spectroscopy", *Carbohydrate research*, vol. 340, no. 15, pp. 2376-2391.
35. Ouajai, S. and Shanks, R.A. (2005) "Composition, structure and thermal degradation of hemp cellulose after chemical treatments", *Polymer Degradation and Stability*, vol. 89, no. 2, pp. 327-335.

36. Peng, Y. and Wu, S. (2010) "The structural and thermal characteristics of wheat straw hemicellulose", *Journal of Analytical and Applied Pyrolysis,* vol. 88, no. 2, pp. 134-139.
37. Pienkos, P.T. and Zhang, M. (2009) "Role of pretreatment and conditioning processes on toxicity of lignocellulosic biomass hydrolysates", *Cellulose,* vol. 16, no. 4, pp. 743-762.
38. Sain, M. and Panthapulakkal, S. (2006) "Bioprocess preparation of wheat straw fibers and their characterization", *Industrial Crops and Products,* vol. 23, no. 1, pp. 1-8.
39. Sánchez, O.J. and Cardona, C.A. (2008) "Trends in biotechnological production of fuel ethanol from different feedstocks", *Bioresource technology,* vol. 99, no. 13, pp. 5270-5295.
40. Serapiglia, M.J., Cameron, K.D., Stipanovic, A.J. and Smart, L.B. (2009) "Analysis of biomass composition using high-resolution thermogravimetric analysis and percent bark content for the selection of shrub willow bioenergy crop varieties", *Bioenergy Research,* vol. 2, no. 1-2, pp. 1-9.
41. Sims, R.E.H., Mabee, W., Saddler, J.N. and Taylor, M. (2010) "An overview of second generation biofuel technologies", *Bioresource technology,* vol. 101, no. 6, pp. 1570-1580.
42. Sun, F. and Chen, H. (2008) "Comparison of atmospheric aqueous glycerol and steam explosion pretreatments of wheat straw for enhanced enzymatic hydrolysis", *Journal of Chemical Technology and Biotechnology,* vol. 83, no. 5, pp. 707-714.
43. Sun, X.F., Xu, F., Sun, R.C., Fowler, P. and Baird, M.S. (2005) "Characteristics of degraded cellulose obtained from steam-exploded wheat straw", *Carbohydrate research,* vol. 340, no. 1, pp. 97-106.
44. Tamaki, Y. and Mazza, G. (2011) "Rapid determination of carbohydrates, ash, and extractives content of straw using attenuated total reflectance fourier transform mid-infrared spectroscopy", *Journal of Agricultural and Food Chemistry*, vol. 59, no. 2, pp. 6356-6352.

45. Thygesen, A., Oddershede, J., Lilholt, H., Thomsen, A.B. and Ståhl, K. (2005) "On the determination of crystallinity and cellulose content in plant fibres", *Cellulose,* vol. 12, no. 6, pp. 563-576.
46. Tsujiyama, S. and Miyamori, A. (2000) "Assignment of DSC thermograms of wood and its components", *Thermochimica Acta,* vol. 351, no. 1-2, pp. 177-181.
47. Wang, K., Jiang, J.X., Xu, F. and Sun, R.C. (2009) "Influence of steaming pressure on steam explosion pretreatment of Lespedeza stalks (Lespedeza crytobotrya): Part 1. Characteristics of degraded cellulose", *Polymer Degradation and Stability,* vol. 94, no. 9, pp. 1379-1388.
48. Yang, H., Yan, R., Chen, H., Lee, D.H. and Zheng, C. (2007) "Characteristics of hemicellulose, cellulose and lignin pyrolysis", *Fuel,* vol. 86, no. 12-13, pp. 1781-1788.
49. Zeitoun, R., Pontalier, P.Y., Marechal, P. and Rigal, L. (2010) "Twin-screw extrusion for hemicellulose recovery: Influence on extract purity and purification performance", *Bioresource technology,* vol. 101, no. 23, pp. 9348-9354.
50. Zhang, L., Li, D., Wang, L., Wang, T., Zhang, L., Chen, X.D. and Mao, Z. (2008) "Effect of steam explosion on biodegradation of lignin in wheat straw", *Bioresource technology,* vol. 99, no. 17, pp. 8512-8515.

Chapter 5

Development of Pre-treatment of Wheat Straw Using Twin Screw Extrusion Technology

5.1 Introduction

In chapter 4, extrusion of wheat straw with and without alkali treatment has been compared with conventional steam explosion in term of changes in physical and chemical structures of straw characterised with FTIR, TGA, colour and electron microscopy analysis. It was demonstrated that glucose yield after enzymatic hydrolysis from extrusion treated straw under relatively mild conditions is comparable with that of steam exploded under intensive treatment condition (220°C and 22.2 Bars) and thus worth more detailed studies so as to identify the optimum processing conditions including effects of the following factors on the effectiveness of the treatment and subsequent yield of glucose so as to develop the technology further for industrial biomass pre-treatment applications;

i. The feed stock conditioning and additives including:
    - Initial size of the straw feedstock;
    - Water content in barrel;
    - NaOH concentration in the straw;
    - The post-extrusion washing;

ii. Processing conditions including
    - Barrel temperature profile;
    - Screw speed;
    - Die pressure / compaction impact;

5.2 Results and Discussion

The detail of the experimental set up has been outlined in sub-section 3.2, Chapter 3. It included the details of

- Materials in used
- Detail of extruder
- Extrusion conditions
- Description of sample ID and sample preparation
- Condition of enzymatic hydrolysis
- Analytical condition for analysis

On top of it, some short description was given in each of the data comparison paragraph to ease the understanding of reader. However, the detail of experiment was still recorded in the above mentioned chapter.

During extrusion of straw, shear stress generated within the material between the rotating screws is a key mechanism to open up the straw structure i.e. as a method of mechanical fractionation. The fractionation process is however much more complex as it is also accompanied by

- heat generated internally from friction as well as external heating from the barrels, which affects materials e.g. thermal softening.
- chemical activity of additive e.g. alkaline concentration
- the total moisture level (in feedstock and water added in the feedstock) which affect e.g. flow behaviour of the material and thus the shear stress and autohydrolysis.
- pressure in the barrels (related to die size, screw and feeding speeds), which affect structural openness of the material and residence time;
- other additives such as alkaline or acids which are known as agent to help on the fractionation (Choi and Oh, 2012; Zhang, Xu and Hanna, 2012).

In the following discussion, we will go through the sets of data for two main categories:

i) wheat straw extrusion without chemical additive and ii) wheat straw extrusion with chemical additive (NaOH). Glucose yield of each trial was determined to serve as an indication of pre-treatment effectiveness. The influence factors being discussed were moisture level of feedstock, barrel temperature, compaction impact, particle size / size of straw feedstock and screw speed. For NaOH combined extrusion, additional factor such as concentration of NaOH and post-washing were also included.

5.2.1 Influence of extrusion conditions for wheat straw feedstock without any chemical treatment

Under this section, various extrusion trials were conducted with incorporation of the trial factor /s. No chemical additive been introduced for trial under this section. All the samples have been prepared as per outlined in sub-section 3.2, Chapter 3. Individual sample ID was captured under Table 3.2 (Chapter 3). The results are going to discussed in following sub-section.

5.2.1.1 Effect of moisture level and combination with barrel temperature change

Moisture level is referred to wheat straw feedstock moisture level. RWS was having moisture ~ 10% and water was added to the wheat straw mixture to increased the moisture of feedstock to defined level (in accordance to the ratio of straw : water or s:w). Barrel temperature was controlled by setting the temperature of each barrel at the temperature control board on Betol twin screw extruder. As per described in Chapter 3, temperature for first barrel is always set at 30°C and the temperature of subsequent of four barrels are per specified in trial detail eg. if only one temperature such as 50°C been mentioned, then the setting of barrel temperature for the rest of four barrel will be set at 50°C. Five samples were compared under this sub-section,

i. RWS – Raw wheat straw as received without extrusion
ii. WCB10004 – RWS extruded at 50°C, dry (low moisture)
iii. WCB10006 – RWS extruded at 100°C, dry (low moisture)
iv. WCB10008 – RWS extruded at 50°C with s:w at 1:2
v. WCB09008 – RWS extruded at 120°C with s:w at 1:2

Figure 5.1 shows effect of moisture level in straw and barrel temperature set-ups on the glucose yield at 10% substrate.

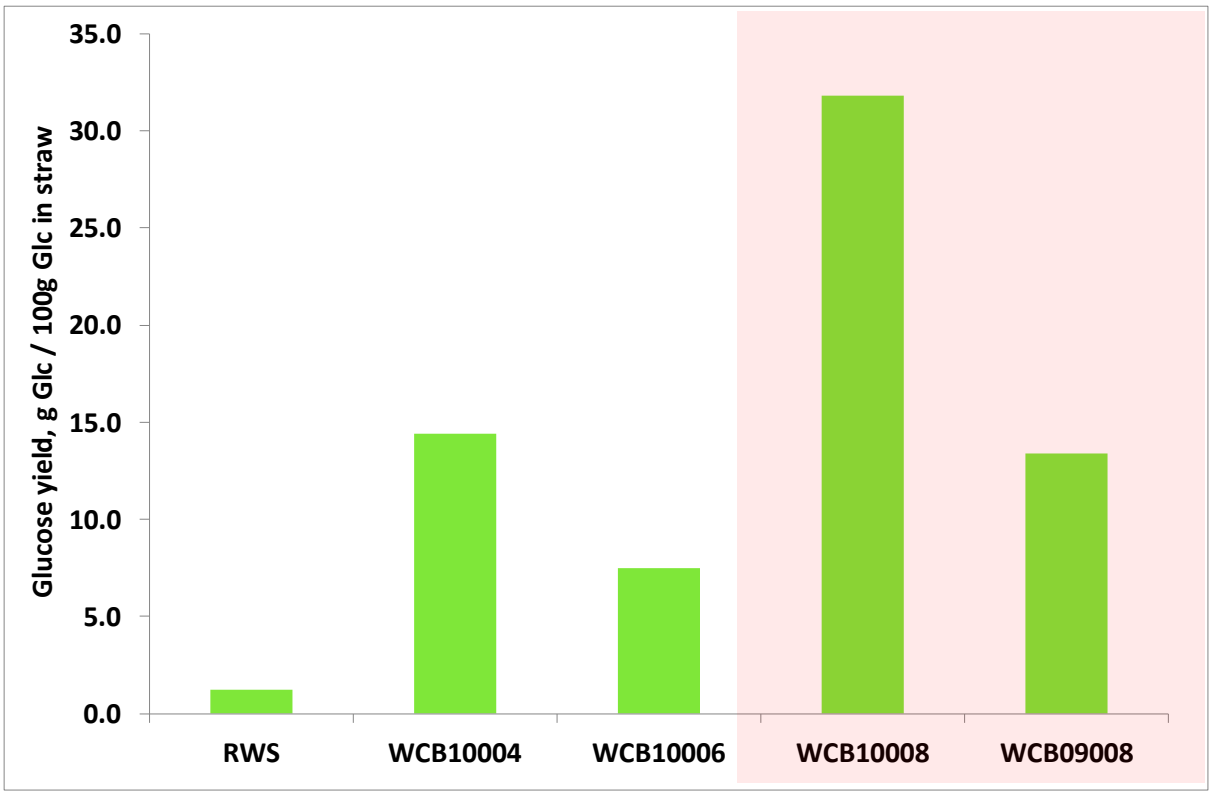

Figure 5.1 : Comparison of glucose yield (at 10% substrate) for extrusion trial with moisture level 10 and 70%, respectively under various barrel temperature.

In comparison with the as-received raw wheat straw, RWS without extrusion, which gave glucose yield of 1.2%. The wheat straw, WCB10004, extruded at the ~ 10% as-received moisture level gave glucose yield of 14.4%, which is 14 folds that of RWS without extrusion. This shows the necessity of the mechanical fractionation even at dry state - mechanical shear and friction between straw particles assist its size reduction and structural breakdown.

Additional of water to 70 % (at straw/water mass ratio of 1:2) in WCB10008 at the same extrusion temperature (50°C) without changing the other extrusion conditions, resulted in further increase of glucose yield to 31.8 %. This is attributable to softening of the biomass under increased moisture level and led to more structural breakdown under mechanical shear. Similar observation was reported by Chen *et al*. (2010) on twin

screw extrusion of soybean, where more deterioration of physical properties and formation of fibrous structure in the extrudate were observed. These are indications of more fractionation on the biomass at high moisture content (up to 60 wt%). Reverse trend was found by Karunanithy *et al*. in extrusion of corn stover, switchgrass, big bluestem, prairie cord grass and pine wood chips using a single-screw extruder (Karunanithy and Muthukumarappan, 2011b; Karunanithy and Muthukumarappan, In press). Reason for the different of moisture impact on pre-treatment effectiveness could be due to the different of physical mechanism between single screw and twin screw extruder.

It should be noted that comparison between WCB10004 and 10008 was for low extrusion temperature (50°C). At elevated extrusion temperatures, while the other parameter remain unchanged, as shown in **Figure 5.1**, (e.g. at 100°C for WCB10006 and 120°C for WCB09008, at initial moisture level ~10% for the former and ~70% for later), the glucose yield of the extruded straw dropped by about half compared to extrusion at 50°C. This could be due to reduction of mechanical shear stress as a result of more thermal softening of biomass in the extruder and reduced the effect of mechanical shear. Also, the possibility of water loss at high temperature due to drying during extrusion at open system.

5.2.1.2 Effect of compaction impact, residence time and barrel temperature change

Extrusion pressure affects the compaction impact of the material being extruded, internal friction and residence time. This can be adjusted, in part, by the nozzle size of the die to increase the resistance to material flow. Compaction impact was introduced by adding a 28mm diameter die cap at the end of extruder discharge point (as per described in Chapter 3). With the die, the residence time of biomass in the extruder become longer and a compaction zone with high pressure inside the barrel generated.

Comparison was made in **Figure 5.2** where, six samples were selected for comparison under this sub-section, those are,

i. Extrusion at 50°C with (WCB10004) and without (WCB10003) die cap at low moisture condition (moisture level ~ 10%).

ii. Extrusion at 100°C with (WCB10006) and without (WCB10005) die cap at low moisture condition (moisture level ~ 10%).

iii. Extrusion at 50°C, low moisture (moisture level ~10%), with die cap, two times extrusion in total (WCB10007). The first round extrudate was put directly back to extruder one more time to evaluate the effect of double extrusions (longer residence time) in comparison with WCB10004.

iv. Extrusion at 50°C, s:w at 1:2 (WCB10008). This sample was included for comparison purpose between WCB10004 to observe the gap of yield different between 1% and 10% substrate at both low and high moisture level condition.

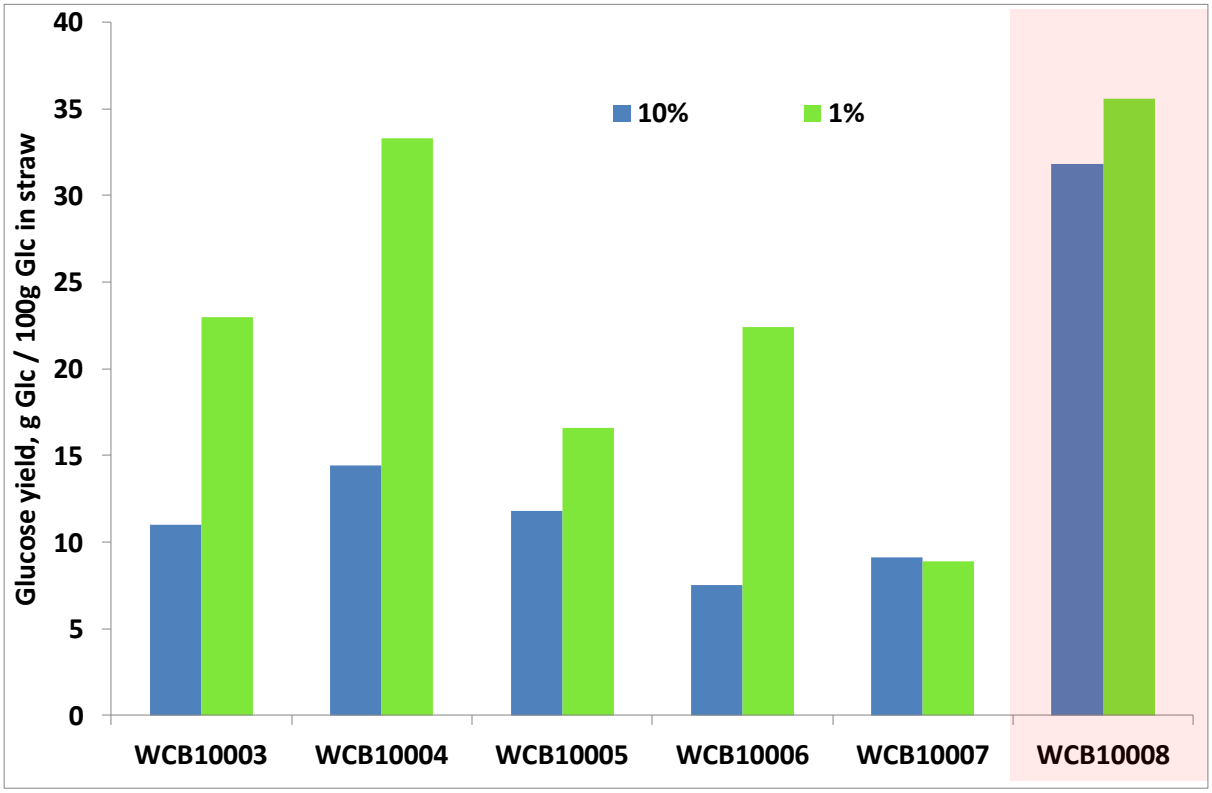

Figure 5.2 : Effect of compaction impact, residence time and barrel temperature on glucose yields at 1% and 10% substrate.

In order to have a more detail observation, glucose yield at 1 wt% substrate for the selected samples was determined to serve as supplemented data to support the trend from yield at 10 wt% substrate. It shows trends of increase glucose yield when the

degree of compaction is increased, by adding the die cap; comparing WCB10003 and WCB10004 at barrel temperature 50°C and comparing WCB10005 and WCB10006 at barrel temperatures 100°C, respectively. This trend was observed clearly for glucose yield at 1% substrate but not for 10%. This could be due to more sensitive glucose yield evaluations at the low substrate level, though it is not an economic practice of hydrolysis.

By comparing the barrel temperature factor on those samples, again higher yields were observed at lower temperature (WCB10003 and WCB10004) in comparison to higher temperature extrusion (WCB10005 and WCB10006). Similar explanation was given in sub-section 5.2.1.1. The gap of yield different at 1% and 10% substrate for higher moisture level sample (WCB10008) was not that huge in comparison to the dry (low moisture level extrusion). We shall observe the trend of this finding in the subsequent discussion. Double extrusion (WCB10007) did not give any increased yield, comparing WCB10007 with WCB10004 and thus increase of residence time alone has limited contribution to the yield.

5.2.1.3 Effect of particle size of straw feedstock

Smaller particle sizes of the straw feedstock give rise to higher specific surface area and hence better accessibility by enzymes (Karunanithy and Muthukumarappan, In press). Samples of different particle size were summarised as below,

i. RWS or raw wheat straw with average length of 10mm;
ii. Ground straw - RWS grinded with cutting mill with 4mm sieve;
iii. Powdered straw - Ground straw milled with grinder with 1mm sieve.

Figure 5.3 showed glucose yield (at 10% substrate level) for different initial size of the wheat straw feedstock without extrusion treatment.

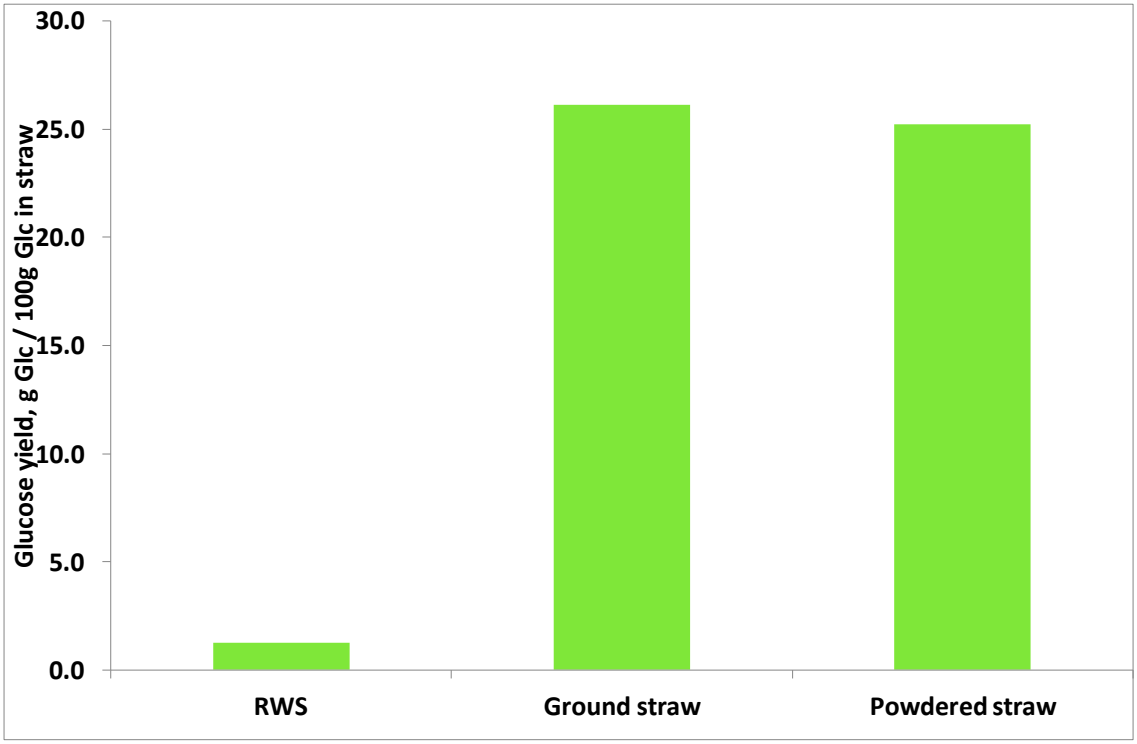

Figure 5.3 Glucose yield at 10% substrate for wheat straw at various particle size. Based on the yields from straws without extrusion showed in **Figure 5.3**, reducing size from the RWS to the ground straw (from average 10mm to ≤ 4mm) resulted in 25 times increase in the glucose yield but only marginal difference in glucose yield was found between the ground straw and powdered straw. This confirms that size does matter in the enhancement of hydrolysis, especially initially from coarse to fine particles but the gain would become marginal for further refined feedstock. For comparison, samples of the ground straw directly hydrolysed without extrusion and extruded ground straw were compared. It included samples,

i. Ground straw - RWS grinded with cutting mill with 4mm sieve. To serve as control purpose;
ii. WCB11002 – Ground straw with s:w at 1:2, extruded at 50°C;
iii. WCB11003 – Ground straw with s:w at 1:2, extruded at 150°C;
iv. WCB11004 – Ground straw with s:w at 1:2, extruded at 250°C;

Glucose yields for above mentioned samples were showed in **Figure 5.4**.

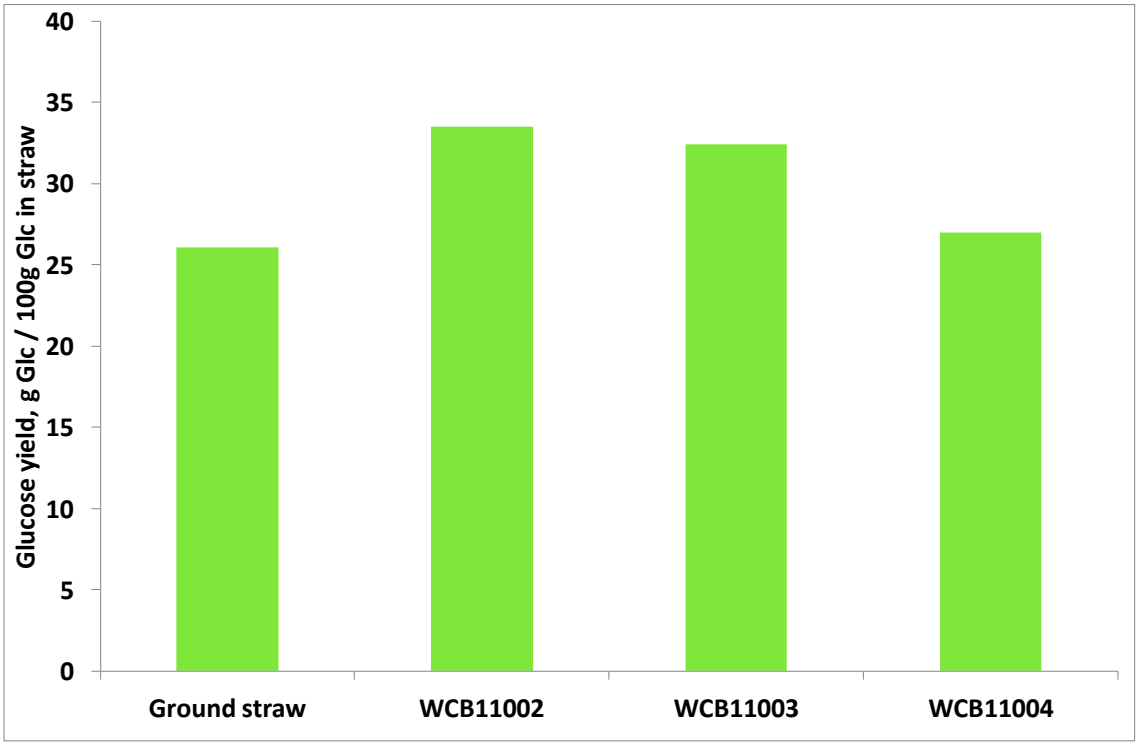

Figure 5.4 : Comparison of glucose yield (10% substrate) for ground straw and extruded ground straw at barrel temperature 50°C (WCB11002), 150°C (WCB11003) and 250°C (WCB11004).

After extrusion, it had resulted in about 28% increased in glucose yield for best case of the post-extruded samples (WCB11002 in comparison with the ground wheat straw, GWS).

Similar to the observations mentioned earlier (sub-section 5.2.1.1 and 5.2.1.2), increase in the extruder barrel temperature from 50 to 125 and 250°C gave rise in some decreased yields, as show in **Figure 5.4**. Several reasons might be attributing to the reduction of glucose yield at high temperature extrusion:

a) In addition to potential influence of increased temperature on softening of biomass and thus reduced shearing (see sub-section 5.2.1.1);

b) It is also possible that the high temperature may have caused thermal degradation of sugars as reported in the Chen *et al*. (2011) study on rice straw extrusion combined with diluted acid.

c) Possible drying / loss of water at elevated temperature in open extrusion system. The moisture level of extrudates were 69%, 52% and 10% for WCB11002 (50°C), WCB11003 (150°C) and WCB11004 (250°C), respectively. It will directly reduce the autohydrolysis phenomenon which is helping on hemicelluloses fractionation. As this most likely the reason, hence further investigation prompted in next sub-section.

5.2.1.4 Effect of temperature profile and die end modification

Auto-hydrolysis is expected in a fractionation process in presence of water (Yang and Wyman, 2008). Modification in temperature profile and extension of die (with an additional temperature chamber) were made, as described in sub-section 3.2, Chapter 3. In order to

- retain the moisture at the front barrels by using relatively lower temperature in the 3 front barrels while high temperature at last two barrels to maximise the "cooking" effect and
- create a higher temperature and pressure zone near the exit – i.e. to mimic the similar state of steam explosion so as to opening up the biomass structure by sudden release of internal vapour pressure at the die.

These were achieved by setting the temperature profiles and use of the extension die. Two samples were selected for this comparison.

i. WCB10008 – extrusion at 50°C which the barrel temperature setting : 30°C, 50°C, 50°C, 50°C and 50°C, respectively from 1st to 5th barrel. Die extender temperature 150°C. s:w at 1:2. This sample was selected because of the best yield among flat temperature profile.
ii. WCB11017 – extrusion with barrel temperature setting : 30°C, 50°C, 70°C, 200°C and 200°C, respectively from 1st to 5th barrel. Die extender temperature 150°C. s:w at 1:2.

The glucose yield comparison was showed in **Figure 5.5**, where the glucose yield in used was gram of glucose / 100 gram of straw. This unit of yield indication was used because of lacking of data for digestible cellulose yield (gram of glucose / 100g of

glucose in straw), which been used for previous sub-sections comparison. Both 1 and 10% substrate yield were quoted for comparison.

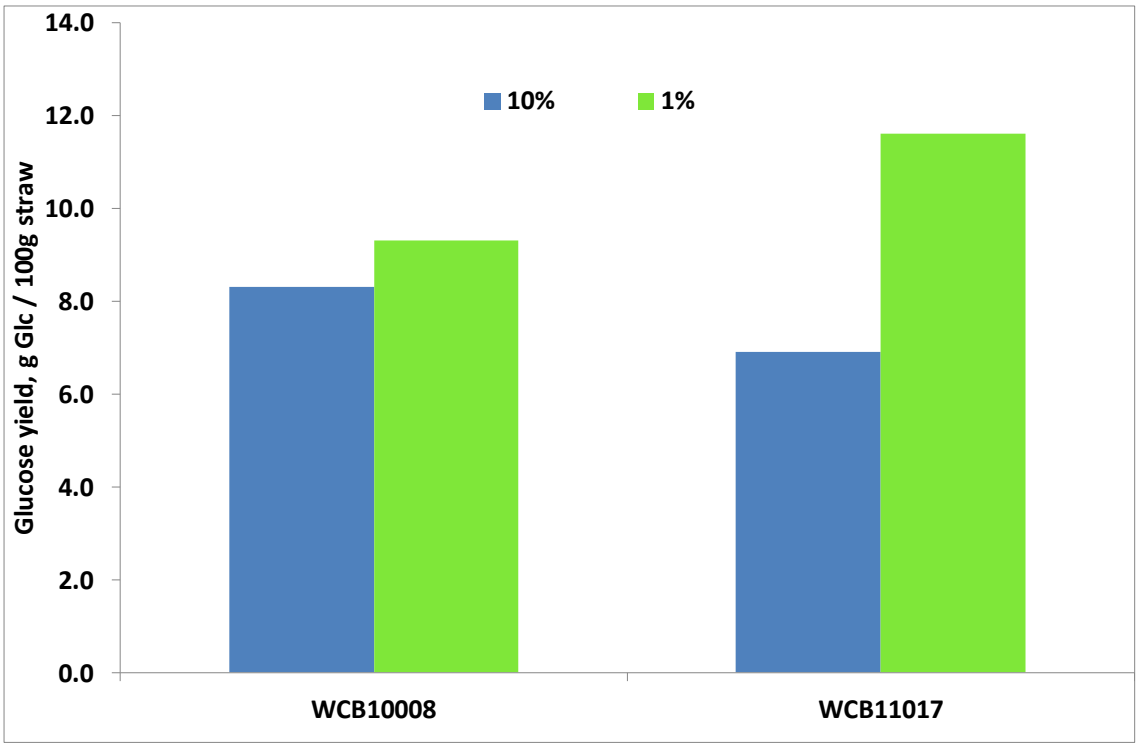

Figure 5.5 : Effect of temperature profile and die end modification on glucose yield at both 1 and 10% substrate.

The impact of improvement only observed at glucose yield at 1% substrate. Under new temperature profile, it was recorded about 25% improvement over the yield. However, the improvement was not observed on yield at 10% substrate. To further support the findings, picture for the pre-treated straw under this category of trial was showed in **Figure 5.6**. In fact, with the high barrel temperature set, extrusion was encountering continuous explosion during the extrusion pre-treatment. More fibrous straw observed after the extrusion.

Figure 5.6 : of wheat straw before and after pre-treatment : a) RWS, b) WCB11017

5.2.1.5 Effect of screw speed

Influence of screw speed on sugar yield was investigated by Lamsal *et al.* (2010) and Zhang *et al.* (2012) for twin screw extruded wheat bran and corn stover by using twin screw extruder at temperature 140 – 150°C. It was found that sugar yield: increased with increase of screw speed. In this study, wheat straw was extruded at 240°C (flat setting across barrels except 1st barrel) with s:w at 1:4 and vary on screw speed,

i. WCB09031 – at screw speed 100 rpm,
ii. WCB09033 – at screw speed 150 rpm,
iii. WCB09032 – at screw speed 200 rpm.

The glucose yield was found increased proportionally with the increase in the screw speed (see **Figure 5.7**). Higher screw speed enhance sheering of the materials and results in better fractionation. It will also give rise to relatively shorter residence time at fixed material feed rate which helps to avoid thermal degradation of the straw at the processing temperature.

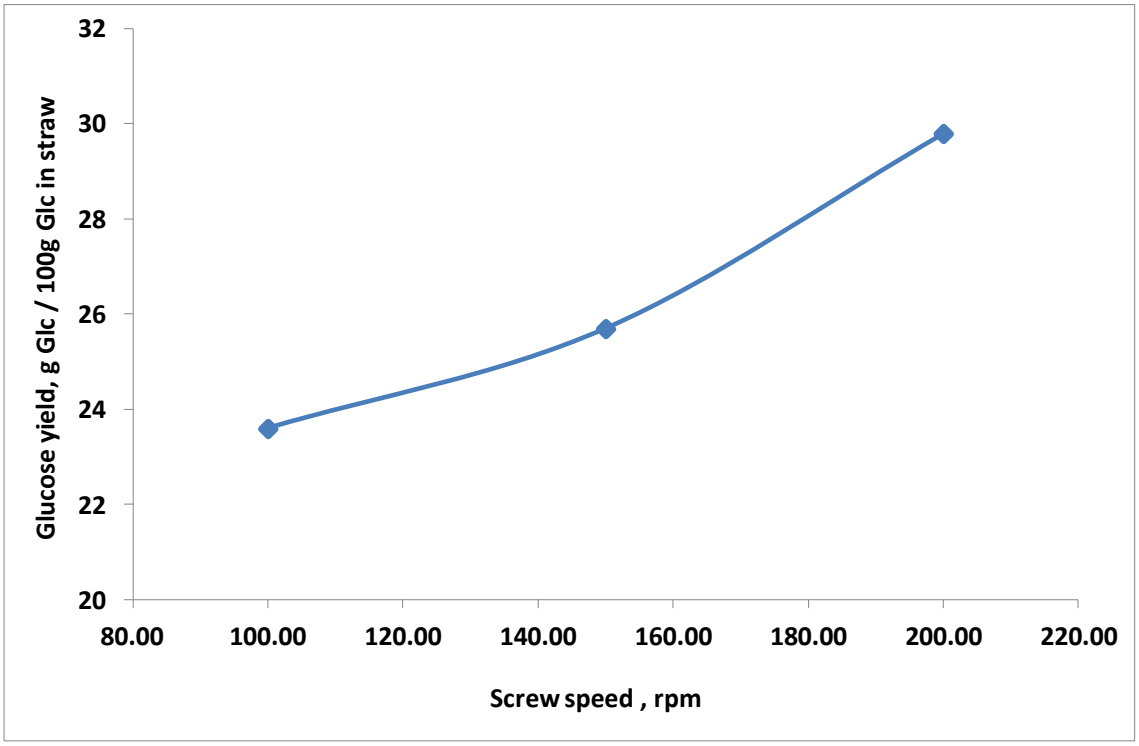

Figure 5.7 : Effect of screw speed on glucose yield for extrusions at 240°C.

5.2.2 Extrusion pre-treatment of wheat straw with alkaline

Flexibility of extruder allows various other on-line pre-treatment methods to be used in combination with extrusion to further improve the effectiveness of the pre-treatment process. The rationale in using on-line chemical addition to the feedstock in extrusion is to combine the physical-mechanical pre-treatment with chemical influence to create a more intensive fractionation condition. Sodium hydroxide, NaOH, calcium hydroxide, maleic acid and ethylene glycol have been used as chemical additives to enhance the extrusion pre-treatment effectiveness (Kang *et al.*, 2009; Karunanithy and Muthukumarappan, 2009; Kootstra *et al.*, 2009; Le Troëdec *et al.*, 2009; Lee, Teramoto and Endo, 2009). In this work, NaOH was selected as it has been shown as an effective delignification agent (Karunanithy and Muthukumarappan, 2011a). Diluted sodium hydroxide causes swelling and therefore, increasing internal pore volume, disrupting lignin structure and decreasing polymerisation and crystallinity (Zhang *et al.*, 2012; Fan, Gharpuray and Lee, 1987). Alkali pre-treatment does not cause as much sugar

degradation and requires much lower pressure and temperature compared to other chemical pre-treatment methods (Mosier *et al.*, 2005). In the following sessions, discussion is breaking down into individual sub-section. Sample details can be traced from sub-section 3.2, Chapter 3.

5.2.2.1 Pre-screening of difference chemical additive

Under this sub-section, sample involved are mainly RWS was extruded at 50°C, 100 rpm screw speed and the following conditions,

i. WCB10009 – s:w at 1:2 with 4% w/w NaOH
ii. WCB10010 – s:w at 1:2 with 1% w/w $Ca(OH)_2$
iii. WCB10011 – s:w at 1:2 with 4.8% w/w Maleic acid
iv. WCB10012 – s:w:ethylene glycol at 1:1:1

The glucose yield in **Figure 5.8** showed that, wheat straw (WCB10009) extruded at 50°C, 100rpm screw speed with 4% w/w NaOH based on dry straw (and resulting in 0.04g/ g straw, added to water to make up ~70% moisture content) gave highest glucose yield in comparison the rest of trials which were extrusion with $Ca(OH)_2$, maleic acid and ethylene glycol. It is about 40 folds of glucose yield compared to RWS as received without additional pre-treatment and a 30% improvement over extrusion trial with the above mentioned chemicals (WCB10010, WCB10011 and WCB10012). NaOH was then selected as alkali chemical for subsequence extrusion trial.

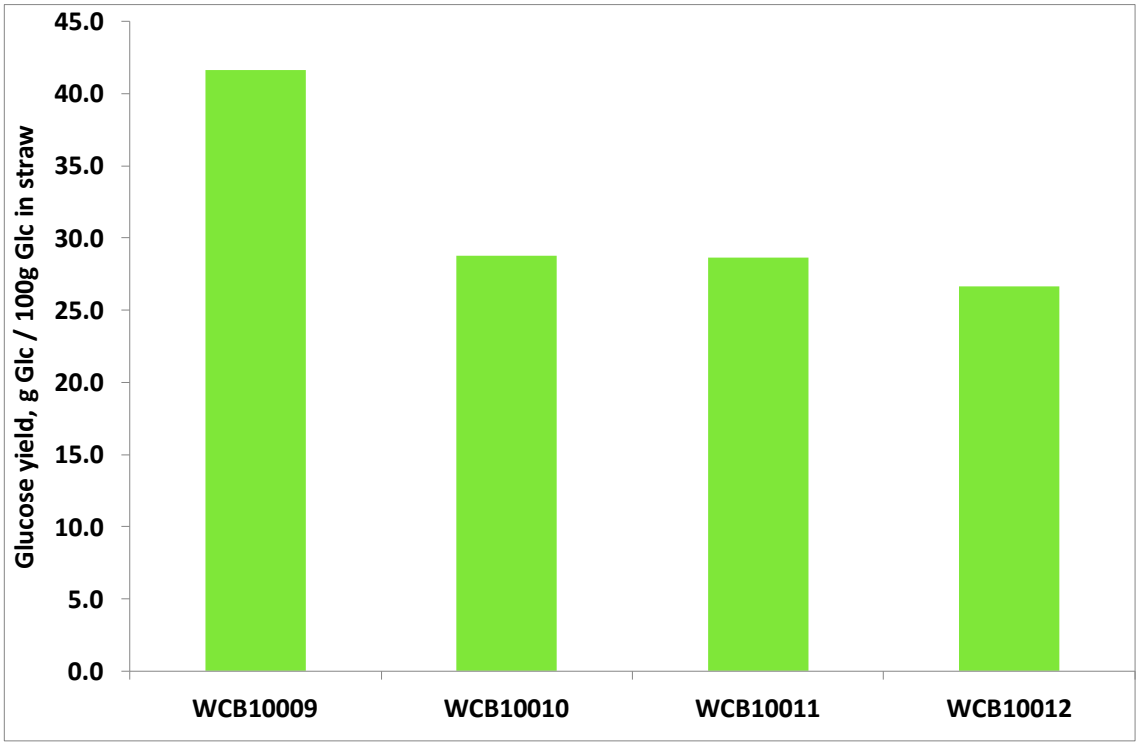

Figure 5.9 : Glucose yield for extrusion with addition of various chemicals : WCB10009 – NaOH, WCB10010 – $Ca(OH)_2$, WCB10011 – maleic acid and WCB10012 – ethylene glycol.

5.2.2.2 Effect of NaOH concentration

Concentration of NaOH was extended at 4 w/w% and 10 w/w%. **Figure 5.9** showed the glucose yield for the straw sample with and without extrusion plus NaOH,

i. WCB10025 – RWS treated only with 10% w/w NaOH , s:w at 1:2. No extrusion was conducted on this sample. This sample was used as Control for this comparison.
ii. WCB10009 – RWS extruded at 50°C, 100rpm screw speed, s:w at 1:2 with 4% w/w NaOH.
iii. WCB10013 – RWS extruded at 50°C, 100rpm screw speed, s:w at 1:2 with 10% w/w NaOH.

Glucose yield for both 10% and 1% substrates were compared. Glucose yield for 1% was included here to show the impact of NaOH concentration in the more sensitive

scale. Based on glucose yield at 10% substrate, increase in NaOH concentration from 4 to 10% only resulted in a 15% increase. However, when comparing the yield at the 1% substrate level, that at 10% NaOH the yield increased almost doubled (from 50.2% to 91.3% g of glucose per 100g glucose in pre-treated straw), which mean at 1% substrate, the 10% NaOH extruded straw having more than 90% glucose converted from cellulose. When comparing with the un-extruded RWS control, the extrusion treatment gave rise to 35% improvement based on 10% substrate glucose yield (WCB10013 vs WCB10025).

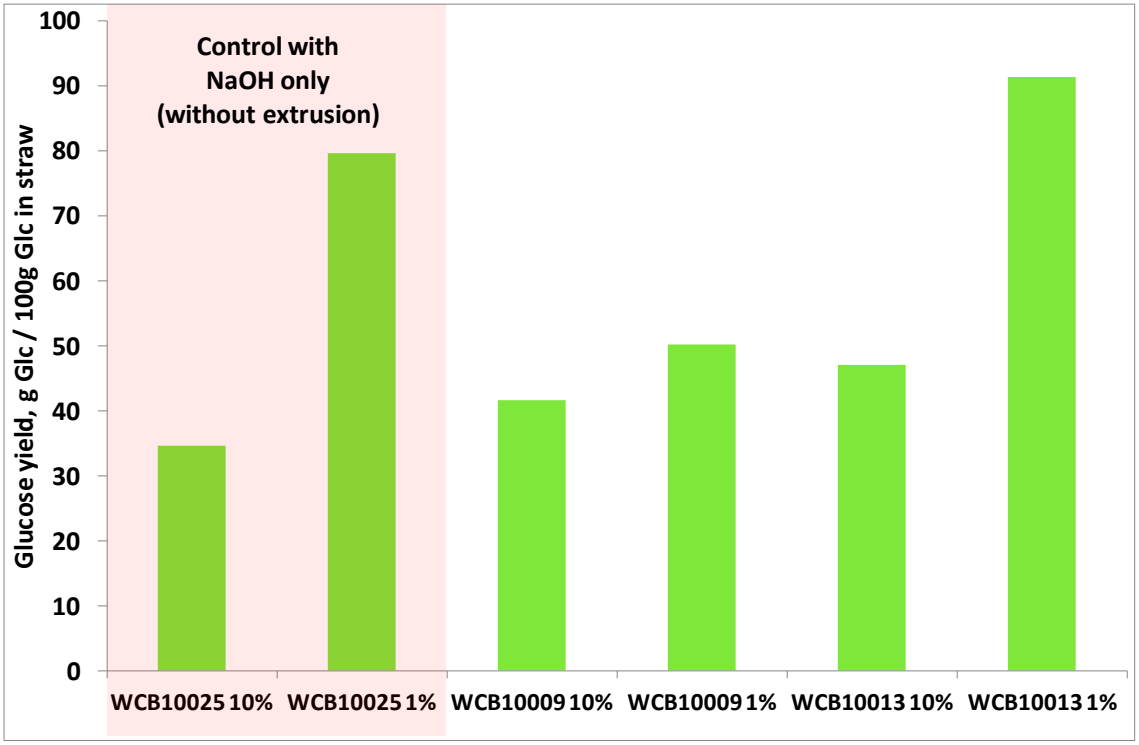

Figure 5.9 : Glucose yield for 4 and 10% NaOH combined extrusion pre-treatment with control.

5.2.2.3 Effect of barrel temperature under influence of NaOH

Impact of barrel temperature on glucose yield at both NaOH concentrations was tested. The tested temperature covered from ambient temperature to 250°C. The comparison of glucose yield for 4 and 10% NaOH combined extrusion trial were showed in **Figure**

5.10 and **5.11**. Sample details again can be referred back to Chapter 3 but some short description are given here for understanding,

Extrusion sample with 4% NaOH concentration, s:w at 1:4, screw speed 100rpm, showed in **Figure 5.10**,

i. WCB09035 – RWS extruded at 140°C,
ii. WCB09036 – RWS extruded at 180°C
iii. WCB09034 – RWS extruded at 200°C
iv. WCB09037 – RWS extruded at 220°C

Extrusion sample with 10% NaOH concentration, s:w at 1:2, screw speed 100rpm, showed in **Figure 5.11**,

i. WCB10024 – RWS extruded at ambient temperature
ii. WCB10013 – RWS extruded at 50°C
iii. WCB10015 – RWS extruded at 150°C
iv. WCB10019 – RWS extruded at 250°C

The effect of barrel temperature is not significant when NaOH was added in the straw extrusion pre-treatment.

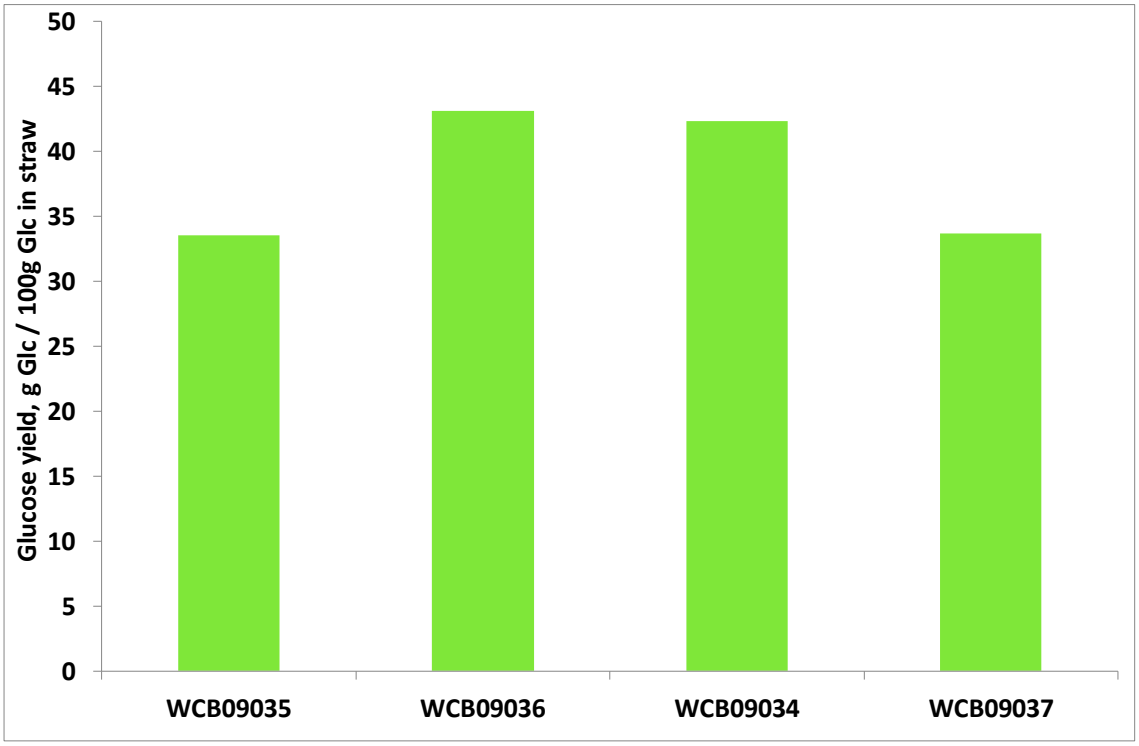

Figure 5.10 : Glucose yield at 10% substrate for 4% NaOH combined extrusion comparison under effect of barrel temperature.

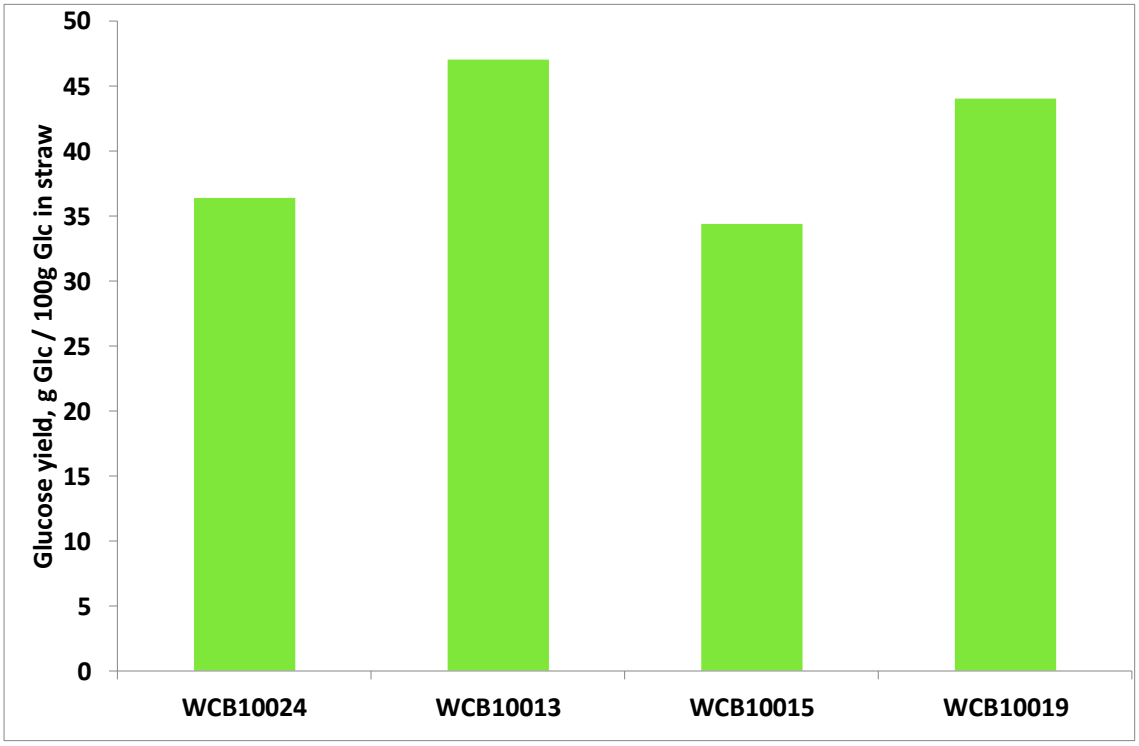

Figure 5.11 : Glucose yield at 10% substrate for 10% NaOH combined extrusion comparison under effect of barrel temperature.

5.2.2.4 Effect of screw speed under influence of NaOH

Same observation with the effect of barrel temperature, screw speed did not have a significant impact on glucose yield under the tested screw speed interval (see **Figure 5.12**). The trend screw speed effect under influence of NaOH is different with the screw speed effect defined in sub-section 5.2.1.5, which the glucose yield was increased in proportional to screw speed.

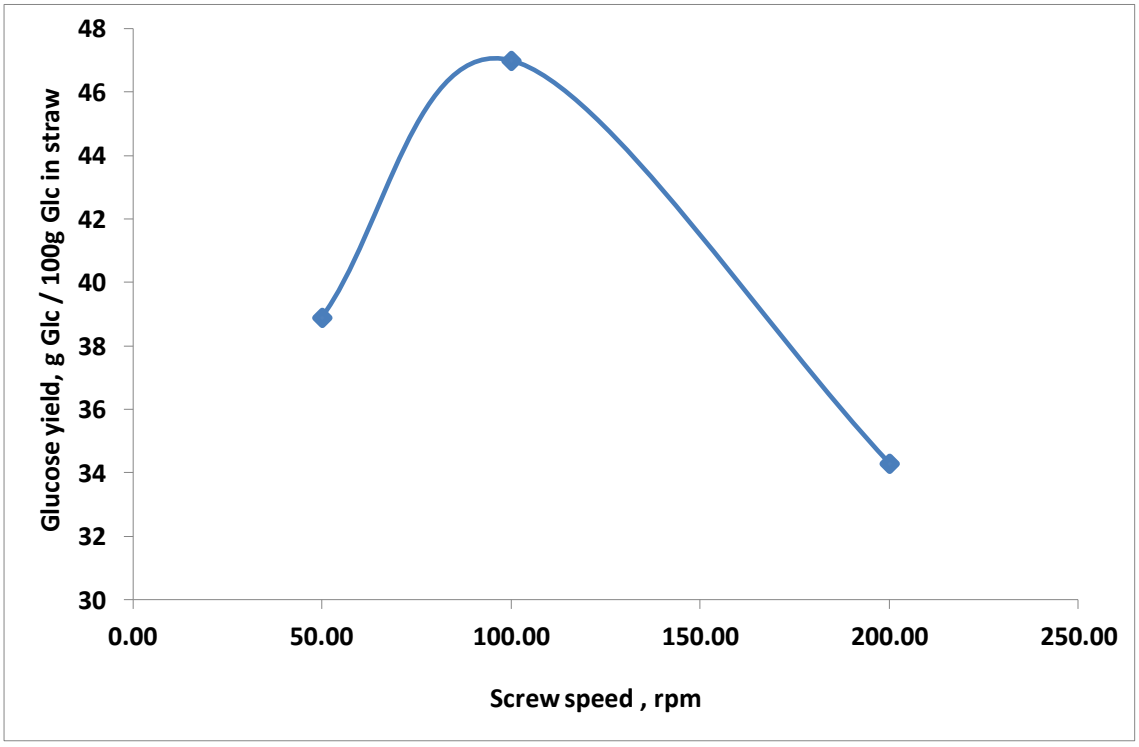

Figure 5.12 : Glucose yield at 10 and 1% substrates for 10% NaOH combined extrusion under screw speed study.

5.2.2.5 Effect of size reduction, temperature profile and die end modification

As continuation from extrusion trial without chemical, size reduction and temperature profile factor were tested in 4% NaOH combined extrusion and the results showed in **Figure 5.13**. The glucose yield showed in **Figure 5.13** was the glucose yield in gram of glucose / 100 gram of straw. Same reason as detailed in sub-section 5.2.1.4, this unit of yield indication was used because of lacking of data for digestible cellulose yield (gram of glucose / 100g of glucose in straw), which been used for previous sub-sections comparison. Both 1 and 10% substrate yield were quoted for comparison. Sample

WCB10009 and WCB11005 were extruded at 50°C, 100 rpm screw speed, s:w at 1:2 with 4% NaOH and were used for comparison under the effect of size reduction in **Figure 5.13**.

i. WCB10009 – RWS at average length of 10mm
ii. WCB11005 – Ground straw passed through 4mm sieve

Under influence of NaOH, effect of size reduction was also not significant. The improvement over yield was only observed on 1% substrate and not on 10% substrate yield.

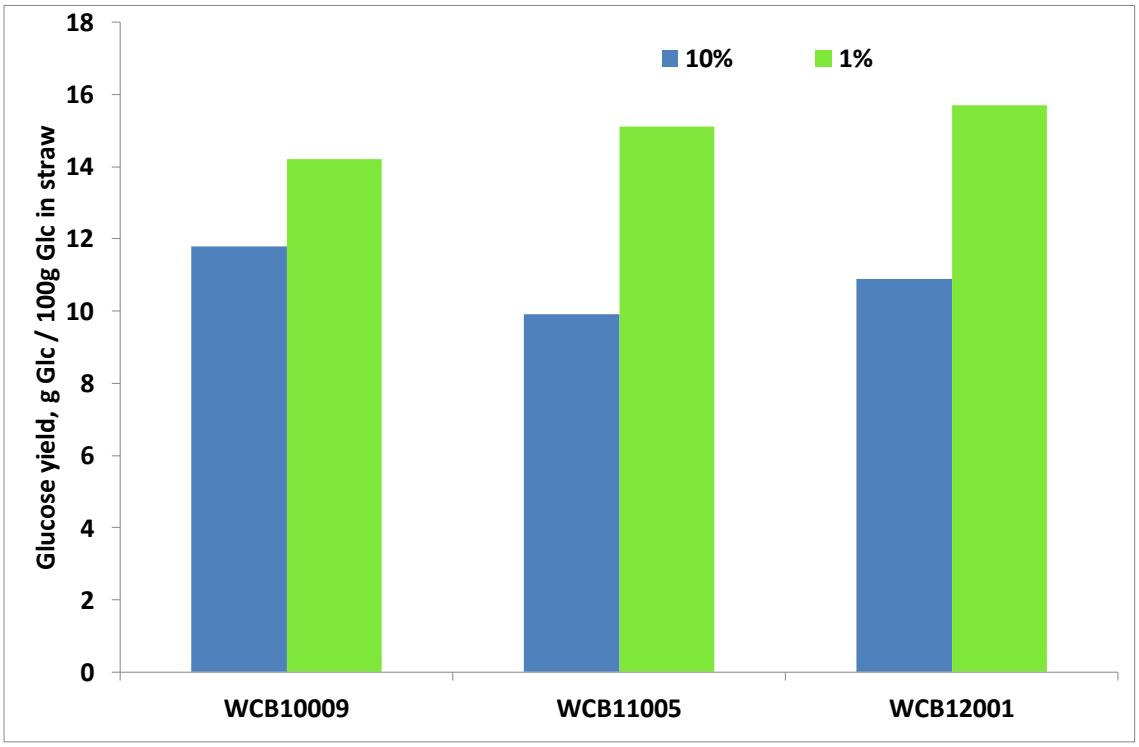

Figure 5.13 : Glucose yield at 10 and 1% substrates for 4% NaOH combined extrusion under effect of size reduction and modified temperature profile.

WCB12001 was RWS extruded with barrel temperature setting : 30°C, 50°C, 70°C, 200°C and 200°C, respectively from 1st to 5th barrel and die extender temperature 150°C. It was used to compare with WCB10009 in **Figure 5.13** too to investigate the effect of temperature profile under influence of NaOH. Again, the improvement wasn't picked up in 10% substrate yield and only picked up 1% substrate yield and not significant too. **5.2.2.6 Effect of post washing on NaOH combined extrusion**

Post washing process can be critical especially for the NaOH combined extrusion. By conducting post washing, it will allow a better control over the pH before enzymatic hydrolysis. With the post washing process as well, an efficient separation of solid and liquid portion after pre-treatment can be achieved. Solid substrate, ideally, should have higher cellulose content and readily for enzymatic hydrolysis. While for the liquid portion, it is basically black liquor contains high soluble hemicelluloses and lignin. With an efficient solid liquid separation step, it can provides a better platform for bio-refinenery of hemicellulose and lignin into other bio-based chemical and can further support the sustainability of bioalcohol production of lignocellulosic biomass. Three categories of post washing trial were conducted :

i. 10% NaOH combined extrusion at 50°C, 100 rpm screw speed, s:w at 1:2,

- WCB10013 – single extruded
- WCB10014 - WCB10113 with double extruded
- WCB10017 – washed WCB10014

ii. 10% NaOH combined extrusion at 250°C, 100 rpm screw speed, s:w at 1:2,

- WCB10019 – single extruded
- WCB10020 – WCB10019 with double extruded
- WCB10021 – washed WCB10020

iii. 4% NaOH combined extrusion at 50°C, 100 rpm screw speed, s:w at 1:2,

- WCB10009 – single extruded
- WCB10009W – WCB10009 washed

Glucose yield for the entire trial samples were illustrated in **Figure 5.14**. A decreasing trend of glucose yield observed at both tested temperature – 50°C and 250°C, for 10% NaOH combined extrusion started from single extrusion, double extrusion and post extrusion washing. Double extrusion doesn't seem to give benefit in term of glucose yield for extrusion with (sub-section 5.2.1.2) and without NaOH. It could be due to further compaction over extrudate will lead to 'close pore' effect. Apart from separating

soluble hemicelluloses and lignin in black liquor, post-washing process may also remove fractionated hexose sugars. This might be another reason of reduce glucose yield due to solid loss during washing process. Glucose yield for post-washed 4% NaOH combined extrusion (WCB10009W) did show a slight drop but not as significant as the yield for post-washed 10% NaOH double extruded straw.

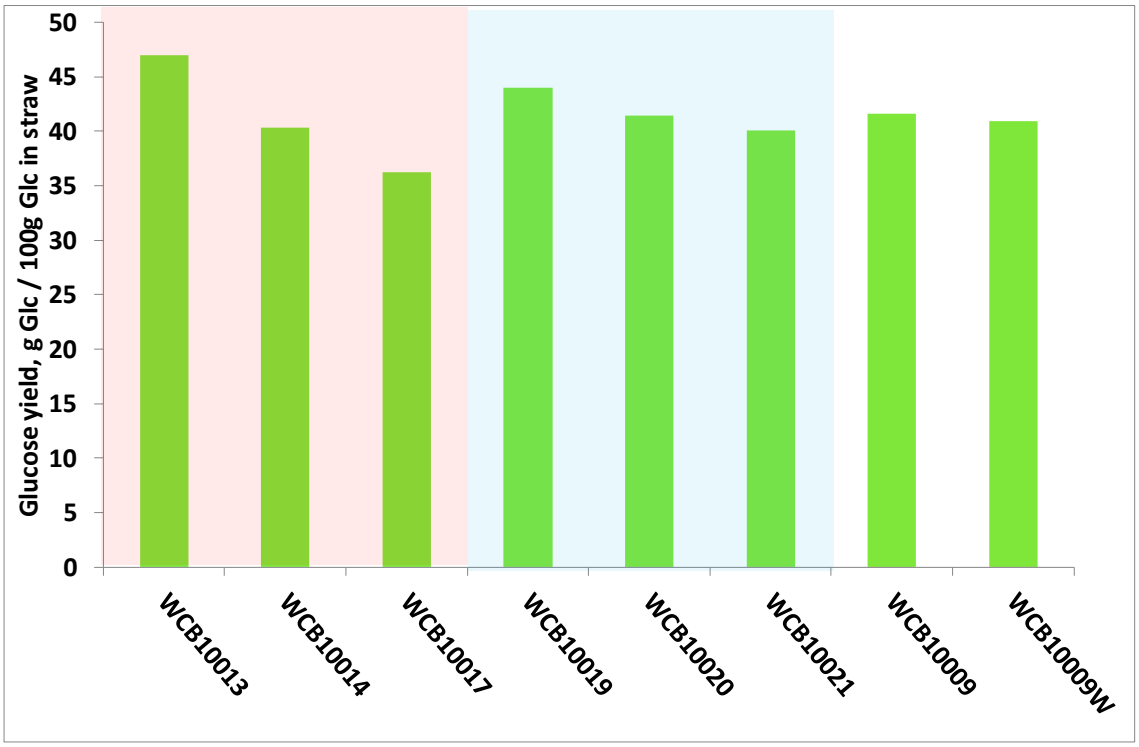

Figure 5.14 : Glucose yield for post-washing NaOH combined extrusion trials.

5.2.3 Analysis of physico-chemical changes during the pre-treatments using FTIR and TGA techniques

Based on the literature (Alemdar and Sain, 2008; Kristensen *et al.*, 2008; Sun *et al.*, 2005) and our previous work in Chapter 4, we know that FTIR and TGA techniques have been demonstrated as valuable tools to reveal the physico-chemical changes in pre-treatment of biomass. The applications in the assessment of the fractionations and understanding of the mechanisms behind change in glucose yield are discussed below.

5.2.3.1 FTIR Analysis

For instance, change in FTIR signals can be used as fingerprint of changes in many functional groups in the straw structure as listed in **Table 5.1**.

Table 5.1 : Key infrared bands, their association to function groups and sources

FTIR bands	Function groups	References
~2917, 2850	CH_3- and CH_2- stretching (wax and cellulose)	(Lamsal *et al.*, 2010; Kristensen *et al.*, 2008)
~1733	C=O ester linkage (hemicelluloses, lignin)	(Le Troëdec *et al.*, 2009; Alemdar and Sain, 2008; Kristensen *et al.*, 2008; Zhang *et al.*, 2008; Sain and Panthapulakkal, 2006)
~1710, 1594, 1515	Stretching carbonyl and aromatic lignin bands	(Kaushik, Singh and Verma, 2010; Naik *et al.*, 2010; Alriols *et al.*, 2009; Lammers, Arbuckle-Keil and Dighton, 2009a; Lammers, Arbuckle-Keil and Dighton, 2009b; Alemdar and Sain, 2008; Kristensen *et al.*, 2008; Zhang *et al.*, 2008; Hongzhang and Liying, 2007; Sain and Panthapulakkal, 2006)
~1420, 1106, 1050	C-O stretching and CH_2 bending (Cellulose)	(Nelson and O'Connor, 1964)
~1560	COO' stretching (cellulose I)	(Klemm, 1998)
~1402, 890	C-H bend (Alkyl) C_1-H bend (β-D-xylose)	(Peng and Wu, 2010)
~1370	In-the-plane C-H bending (polysaccharides)	(Le Troëdec *et al.*, 2009)
~1335	C-O aromatic ring (cellulose)	(Le Troëdec *et al.*, 2009)
~1240	C-O aryl of lignin (guaiacyl unit)	(Lammers, Arbuckle-Keil and Dighton, 2009a; Zhang *et al.*, 2008; Hongzhang and Liying, 2007)
~1130	C-O-C asymmetrical stretching (polysaccharides)	(Le Troëdec *et al.*, 2009)
~897	Glycosidic bond (polysaccharides)	(Le Troëdec *et al.*, 2009)
~670	C-OH out-of-plane bending	(Le Troëdec *et al.*, 2009)

(cellulose)

Figure 5.15 shows that the key bands: ~ 2917 and 2850 cm^{-1} (CH_3- and CH_2 stretching for cellulose and wax) and ~1733 cm^{-1} (C=O ester linkage of hemicelluloses and lignin) can be assessed by spectra overlapping comparison to identify the effects from the representative straw pre-treated using different conditions to gain insight into the effect of moisture content, barrel temperature, size reduction and temperature profile on changes of the bands. The infrared absorbance reduced for the above mentioned peaks and the trend of reduction was indirect proportional to the severity of extrusion pre-treatment condition. With the physical and mechanical disruption on wheat straw cell wall during extrusion pre-treatment, more surface hydrocarbon waxes has also been removed and this was evidenced by the reduction on peak at ~2850 cm^{-1}. The observation was more significant on the high moisture, low temperature extrusion (WCB10008) and temperature profile modified extrusion (WCB11017), as discussed earlier in sub-section 5.2.1.4. With the removal of surface waxes, the pre-treated wheat straw became more hydrophilic in which favours enzymatic hydrolysis as it takes place in an aqueous medium. Similar observation can be found for peak ~1733, which is an indication of more breakdown of ester linkage for hemicellulose and / or lignin .

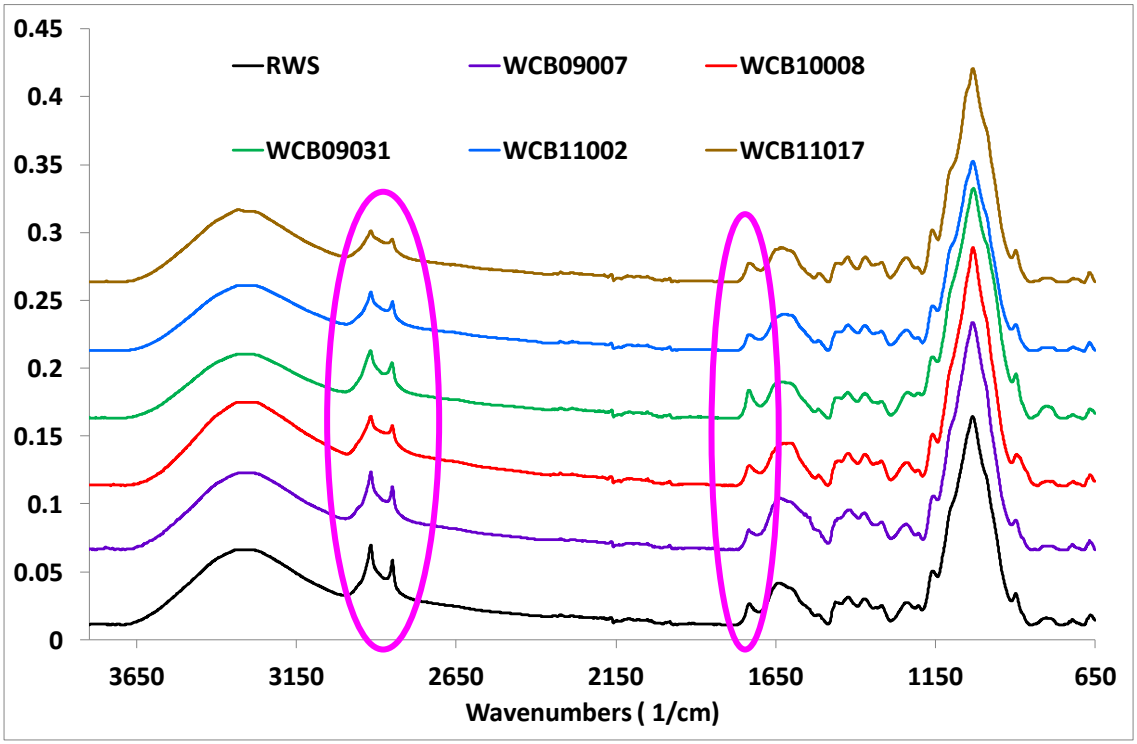

Figure 5. 15: Infrared spectra for RWS and selected representative pre-treated wheat straw: Representation RWS - Control, WCB09007 – low moisture or dry extrusion, WCB10008 – high moisture extrusion, WCB09031 – high temperature extrusion, WCB11002 – reduced size extrusion, WCB11017 – modified temperature profile extrusion.

Principal component analysis (PCA) using e.g. TQ Analyst (Thermo Fisher Scientific) can be employed to identify minor differences, and combination of them, that influences the outcome (sugar yield %) but difficult to notice by visual observation of the spectra. The principal component spectra for the 3 major principle components (PCs) are presented in **Figure 5.16**. PC 1, 2 and 3 contributed a total of 83.6% of percentage variance with individual percentage variance at 42.5, 25.7 and 15.4%, respectively. The key peak areas contributed to the calculated variance were well correlated with the infrared interpretations and finger prints summarised in **Table 5.1** such as signal at ~ 2917, 2850, 1733, 1594, 1560, 1515, 1235 and 897 cm^{-1}.

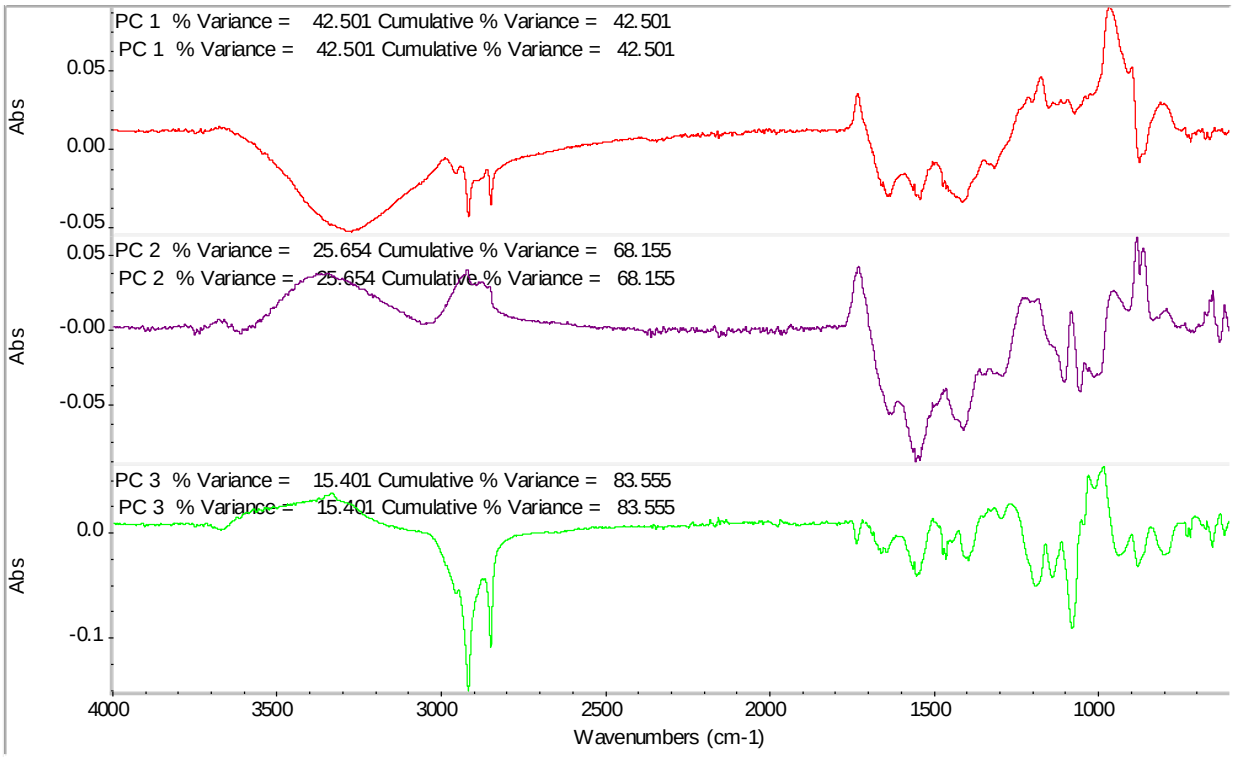

Figure 5.16 : Principle component spectra for extrusion trials without NaOH

Infrared spectra for selected representative NaOH combined extrusion treatments are shown in **Figure 5.17**. It consists of spectra of a control (RWS without extrusion and straws after extrusion treatments:

i. WCB10009 – straw extruded at 50°C, 100rpm screw speed, s:w at 1:2 with 4% w/w NaOH,

ii. WCB10013 – straw extruded at 50°C, 100rpm screw speed, s:w at 1:2 with 10% w/w NaOH and

iii. WCB12001 – straw extruded with barrel temperature setting : 30°C, 50°C, 70°C, 200°C and 200°C, respectively from 1st to 5th barrel and die extender temperature 150°C., 100rpm screw speed, s:w at 1:2 with 4% w/w NaOH

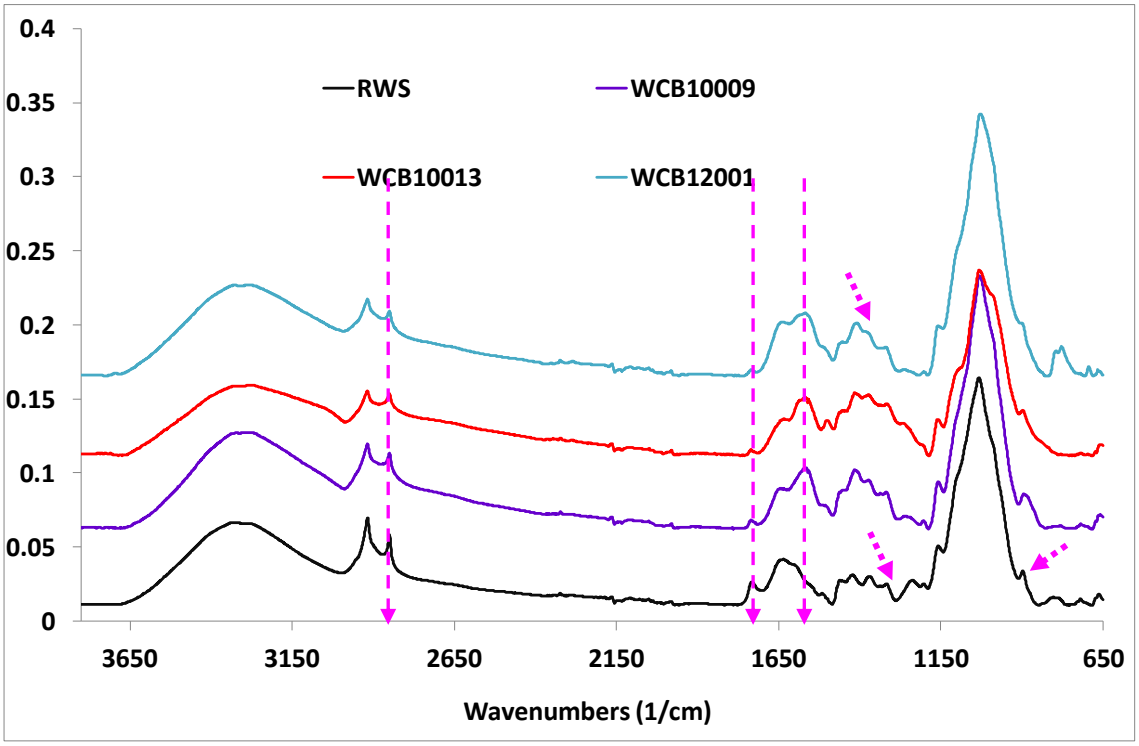

Figure 5.17 : Infrared spectra for selected representative straws extruded with NaOH.

Severity of the pre-treatment is ranked from WCB10013 > WCB12001 > WCB10009 > RWS based on the factor of NaOH concentration and barrel temperature in used in the extrusion. **Figure 5.18** shows that the reduction in infrared absorbance at ~ 2917, 2850 and 1733 cm^{-1} (related to aliphatic waxes and ester linkage as per explained earlier) is proportional to the increase trend of pre-treatment severity. In addition, a few other interesting signals were found, such as more polysaccharides information at ~ 1560, 1420 and 1370 cm^{-1} on the pre-treated straw (see Table 5.1 for detailed information of association to functional groups). Furthermore, the reduction if IR absorption at ~1240 and 897 cm^{-1}, indicates more removal of C-O aryl of lignin (Guaicyl unit) and glycosidic bond from polysaccharides. Similar information was also picked-up by the first 3 Principal Components (PC1, 2 and 3) in the PCA results shown in **Figure 5.18** in which the three principal component account for total cumulative variance of 88.9%.

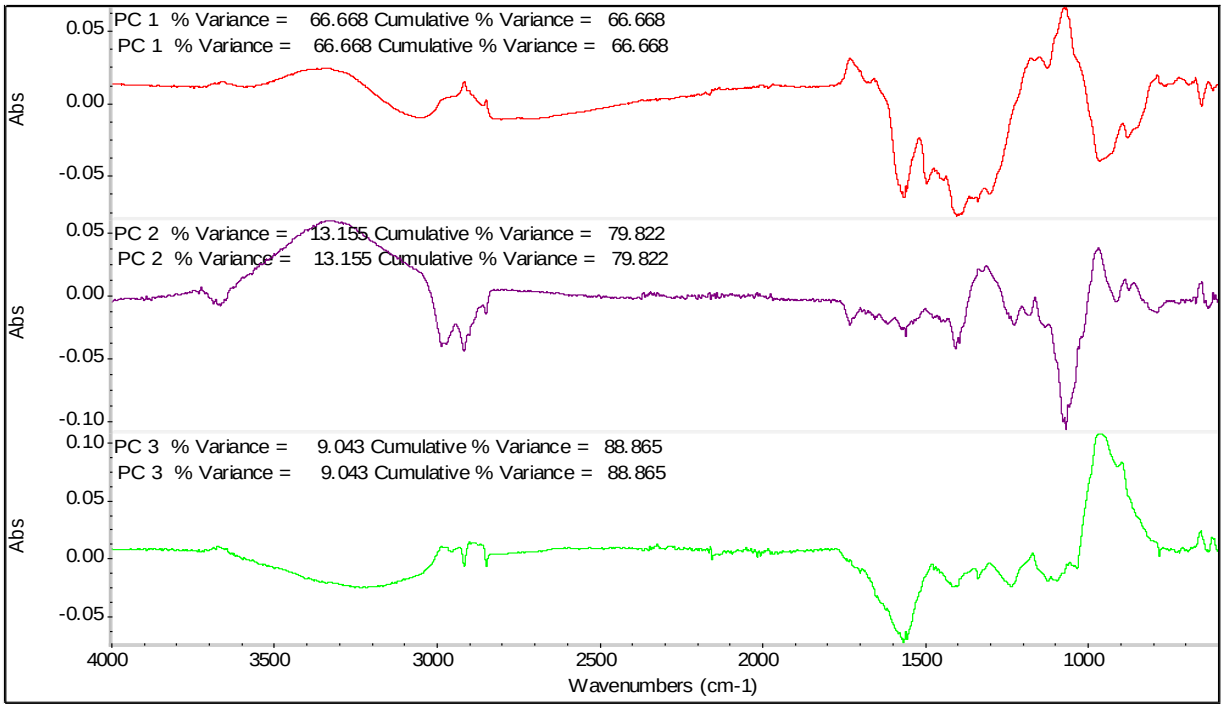

Figure 5.18 : Principle component spectra NaOH combined extrusion trial

Infrared spectra shown in **Figure 5.19** are from the control RWS and straw samples after extrusion with and without washing:

a) WCB10019 (10% NaOH extruded at 250°C, as described in sub-section 5.2.2.6),
b) WCB10021(basically as washed sample of WCB10019 as described in sub-section 5.2.2.6 too),
c) Standard analytical grade cellulose and hemicelluloses from Sigma-alrich.

The spectra obtained are overlapped with that for RWS, standard cellulose and hemicellulose for comparison purpose. It was found that after post extrusion washing, information on polysaccharides at ~ 1560, 1420 and 1370 cm^{-1} reduced significantly. It is thus evident that the fractionated polysaccharides from solid substrate can be removed by the washing process.

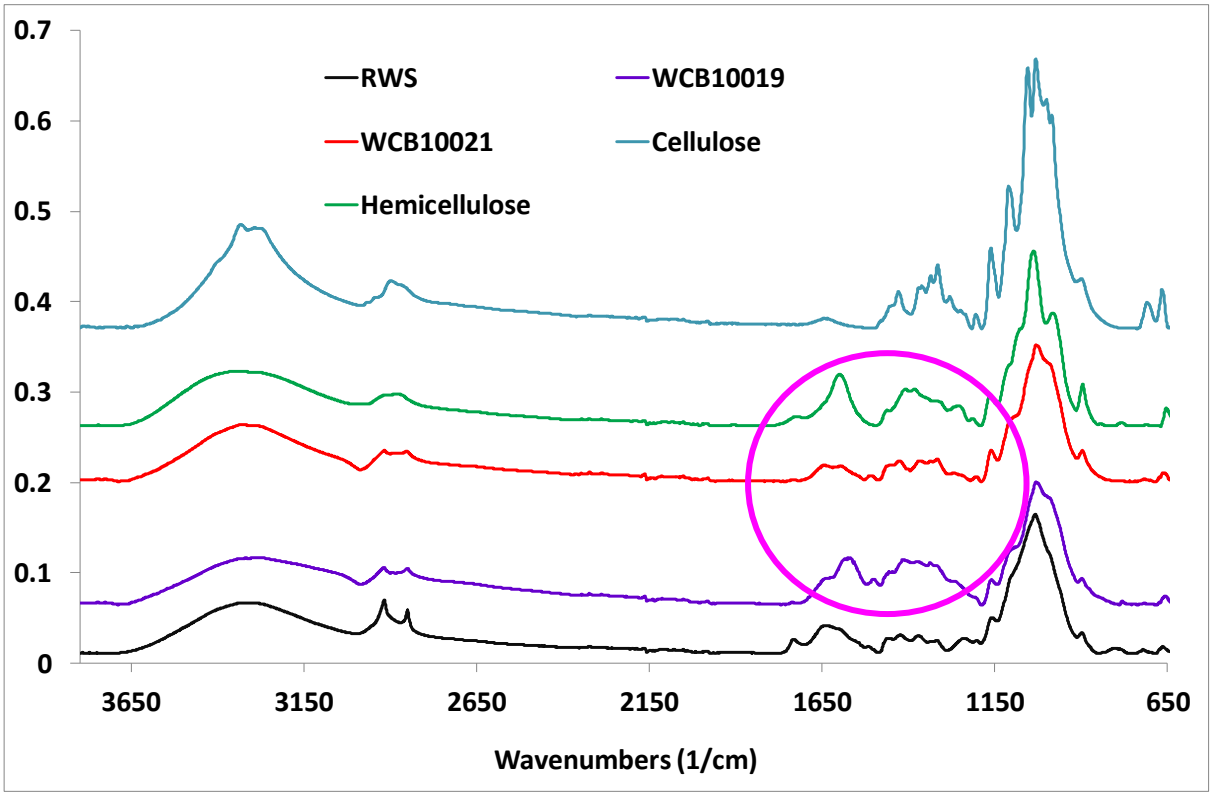

Figure 5.19 : Infrared spectra for selected NaOH combined extrusion compared with that for the RWS control, and standards of cellulose and hemicelluloses showing effect of post-washing on infrared spectra.

5.2.3.2 TGA

TGA was used to further investigate the structure and component change of wheat straw samples under different extrusion pre-treatment conditions. The derivative thermogravimetry, DTG curves for raw and selected representative of the pre-treated straw samples tested under inert conditions are shown in **Figure 5.20**. Theses include:

i. RWS
ii. WCB09031 – RWS extruded at 240°C, s:w at 1:4 and 100 rpm screw speed,
iii. WCB10008 – RWS extruded at 50°C, s:w at 1:2 and 100 rpm screw speed,
iv. WCB11002 – Ground straw extruded at 50°C, s:w at 1:2 and 100 rpm screw speed,
v. WCB11009 – Ground straw extruded with barrel temperature setting : 30°C, 50°C, 70°C, 160°C and 180°C, respectively from 1st to 5th barrel and die extender temperature 150°C, 100rpm screw speed, s:w at 1:2

vi. Standard cellulose and hemicellulose.

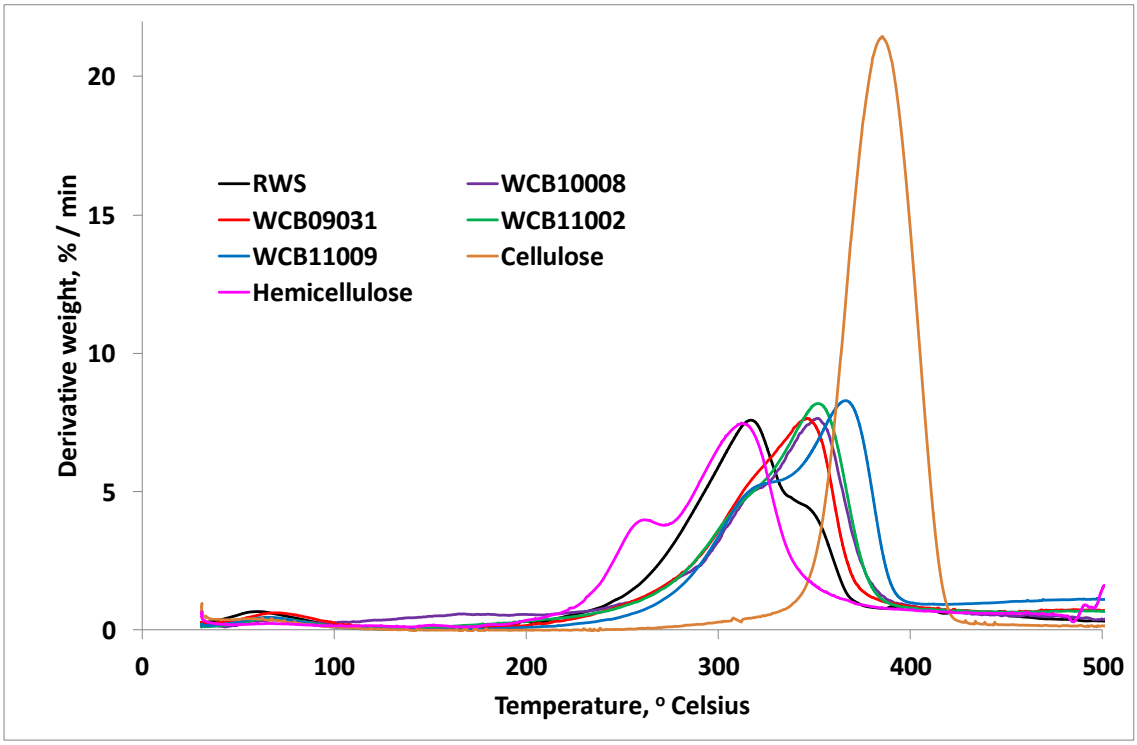

Figure 5.20 : Derivative weight curves for RWS and the representative pre-treated straws.

The key parameters are onset temperature of the thermal degradation, maximum degradation rate and the associated temperature. A huge DTG peaks can be found in **Figure 5.20** in the active pyrolysis zone (~ 200 – 400°C) which correspond to the degradation of hemicellulose (~200 - 315°C) and cellulose (~315 - 400°C) (Le Troëdec *et al.*, 2009; Serapiglia *et al.*, 2009; Yang *et al.*, 2007; Ouajai and Shanks, 2005). Following the pre-treatment, the shoulder at 340°C for raw wheat straw disappeared in all the pre-treated samples thermogram, which might be explained by the reduction of lower molecular mass organic constituents (waxes and extractives) (Mészáros *et al.*, 2009) or perhaps an indication of more cellulose exposed as the DTG peak shifted more to the cellulose degradation zone. The indication of waxes loss is in agreement with findings from FTIR (aliphatic wax indication reduction). DTG Spectra of WCB11009, which experienced severe extrusion conditions and (size reduced and temperature profile changed) resulted in relatively high glucose yield 12.4 gram glucose / 100gram straw (among selected samples at 1% substrate compared under sub-section 5.2.1.4), as

found to have shifted relatively more toward the cellulose degradation zone and a small shoulder appeared at ~ 315°C area. WCB11002, with slightly lesser glucose yield than WCB11009 followed the similar trend with the similar maximum rate of degradation. The trend of curve shift is followed by WCB10008 and WCB09031 and the degree of shifting is well correlated to their glucose yields.

With addition of NaOH in the extrusion, the DTG curves are slightly different than those without NaOH as shown in **Figure 5.21.**

As described in sub-section 5.2.3.1, tt consists of DTG curves of a control (RWS without extrusion and straws after extrusion treatments:

i. WCB10009 – straw extruded at 50°C, 100rpm screw speed, s:w at 1:2 with 4% w/w NaOH,
ii. WCB10013 – straw extruded at 50°C, 100rpm screw speed, s:w at 1:2 with 10% w/w NaOH and
iii. WCB12001 – straw extruded with barrel temperature setting : 30°C, 50°C, 70°C, 200°C and 200°C, respectively from 1st to 5th barrel and die extender temperature 150°C., 100rpm screw speed, s:w at 1:2 with 4% w/w NaOH

The shoulder at 340°C for raw wheat straw disappeared in those for all the straws extruded with NaOH. The active pyrolysis DTG curve shifted to hemicellulose degradation zone at ~ 230 – 330 °C. This could be attributable to the fact that the pre-treated straws contain fractionated polysaccharides with higher water soluble hemicelluloses and fractionated lignin. Compared with extrusion without NaOH, they contain more fractionated hemicelluloses (under effect of chemical) and hence the thermal stability reduced and DTG curves shift to lower temperature zone. The rate of degradation was indirect proportional to severity of pre-treatment, which increase in the order:

$$WCB10013 < WCB12001 < WCB10009$$

based on NaOH concentration and barrel temperature factor.

Comparison of straws extruded with NaOH and their washed counterparts (WCB10021), as shown in **Figure 5.22**, the DTG curve for the washed sample shifted toward high temperature degradation zone (the cellulose degradation zone) and with higher degradation rate. This indicates that once fractionated hemicellulose is removed by washing, the substrate will be higher in cellulose content.

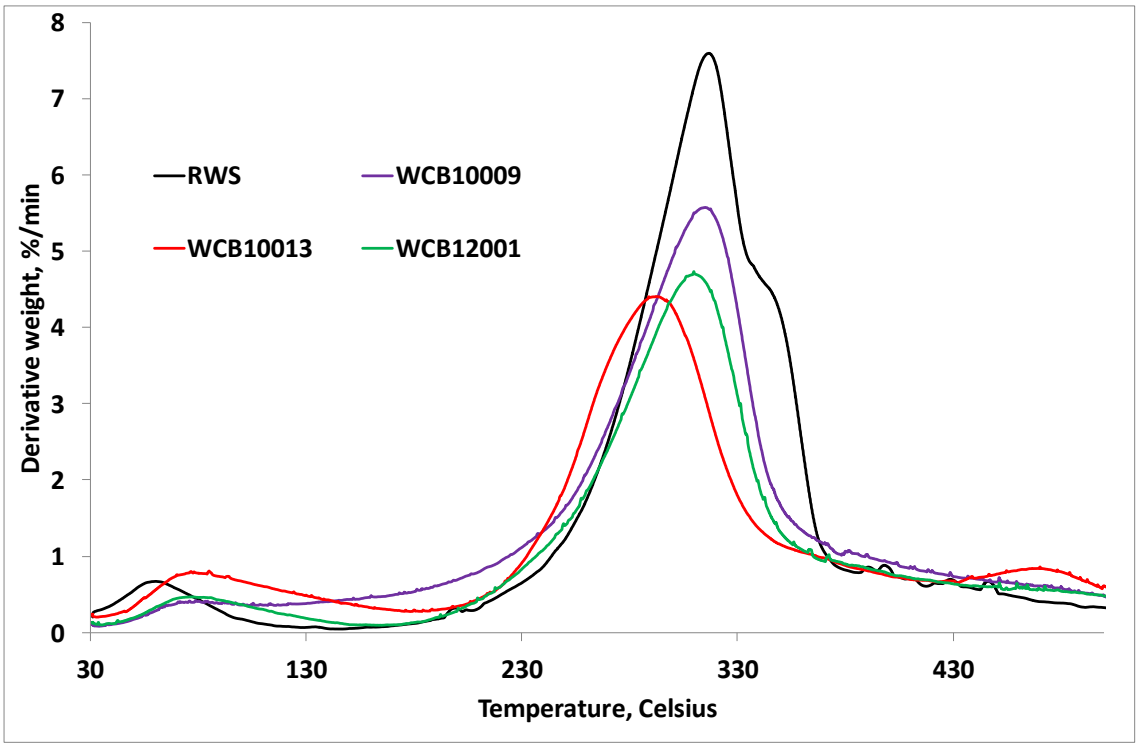

Figure 5.21 : Derivative weight curves for RWS and representative straws extruded with NaOH .

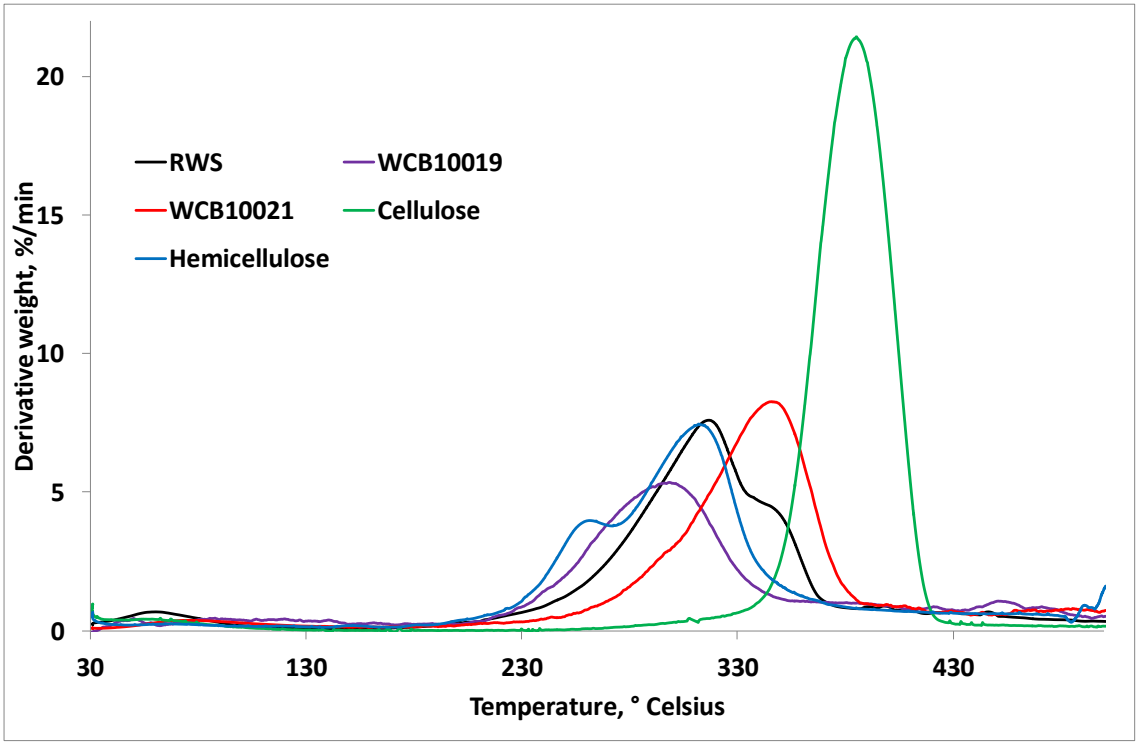

Figure 5.23 : Derivative weight curves for RWS, straw that NaOH combined extruded straw (WCB10019) and its washed counterpart (WCB10021) versus that for the standard cellulose and hemicellulose.

5.3 Summary

This study reveals the impact of physical operating parameter over pre-treatment of wheat straw with Betol twin screw extrusion within two main categories – extrusion with and without NaOH. By purely pre-treated with extrusion, high moisture (~ 70%), low temperature and with die capped are in favour. The yield can be further improved by optimise the temperature profile to include the cooking (auto-hydrolysis) and continuous steam explosion effects. By reducing the size of wheat straw feedstock, it did help to improve the yield of glucose after extrusion. However the cost of mechanical size reduction will burden to the economic of overall pre-treatment cost. Double extrusion is not offering advantage by looking at the yield of glucose after enzymatic hydrolysis.

By addition of NaOH to the extrusion, at least ~ 30% of glucose yield increased (WCB10009 vs WCB10008). All the entire of physical operating parameter were not having significant impact when NaOH added into extrusion. Post washing step is still recommended for the NaOH combined extrusion to provide another platform of bio-refinery while improve the pH control prior enzymatic hydrolysis. Analysis from FTIR and TGA help to support the mechanism of change after the pre-treatment and are well correlated to the glucose yield after enzymatic hydrolysis.

Based on the above findings, extrusion demonstrate a highly potential green pre-treatment tool for wheat straw as it requires only low temperature, simple handling and can be easily improve yield by combine with other pre-treatment technology.

5.4 References

1. Alemdar, A. and Sain, M. (2008) "Isolation and characterization of nanofibers from agricultural residues – Wheat straw and soy hulls", *Bioresource technology*, vol. 99, no. 6, pp. 1664-1671.
2. Alriols, M.G., Tejado, A., Blanco, M., Mondragon, I. and Labidi, J. (2009) "Agricultural palm oil tree residues as raw material for cellulose, lignin and hemicelluloses production by ethylene glycol pulping process", *Chemical Engineering Journal*, vol. 148, no. 1, pp. 106-114.
3. Chen, F.L., Wei, Y.M., Zhang, B. and Ojokoh, A.O. (2010) "System parameters and product properties response of soybean protein extruded at wide moisture range", *Journal of Food Engineering*, vol. 96, no. 2, pp. 208-213.
4. Chen, W., Xu, Y., Hwang, W. and Wang, J. (2011) "Pretreatment of rice straw using an extrusion/extraction process at bench-scale for producing cellulosic ethanol", *Bioresource technology*, vol. 102, no. 22, pp. 10451-10458.
5. Choi, C.H. and Oh, K.K. (2012) "Application of a continuous twin screw-driven process for dilute acid pretreatment of rape straw", *Bioresource technology*, vol. 110, no. 0, pp. 349-354.
6. Fan, L., Gharpuray, M. and Lee, Y. (1987) "Cellulose hydrolysis", *Biotechnology monographs*, vol. 3.
7. Hongzhang, C. and Liying, L. (2007) "Unpolluted fractionation of wheat straw by steam explosion and ethanol extraction", *Bioresource technology*, vol. 98, no. 3, pp. 666-676.
8. Kang, Y.G., Xia, W., Song, J. and Tarverdi, K. (2009) " Extrusion fractionation of wheat straw for biocomposites utilising the entire straw constituents", *INTERNATIONAL JOURNAL OF MATERIALS & PRODUCT TECHNOLOGY*, vol. 36, no. 1-4, pp. 334-347.
9. Karunanithy, C., and Muthukumarappan, K. (In press) "Thermo-Mechanical Pretreatment of Feedstocks" in *Green biomass pretreatment for biofuels production*, 1st edn, SpringerLink, .
10. Karunanithy, C. and Muthukumarappan, K. (2011a) "Optimization of alkali soaking and extrusion pretreatment of prairie cord grass for maximum sugar

recovery by enzymatic hydrolysis", *Biochemical engineering journal*, vol. 54, no. 2, pp. 71-82.

11. Karunanithy, C. and Muthukumarappan, K. (2011b) "Optimization of switchgrass and extruder parameters for enzymatic hydrolysis using response surface methodology", *Industrial Crops and Products*, vol. 33, no. 1, pp. 188-199.
12. Karunanithy, C. and Muthukumarappan, K. (2009) "Combined effect of alkali soaking and extrusion conditions on fermentable sugar yields from switchgrass and prairie cord grass", , pp. 5165.
13. Kaushik, A., Singh, M. and Verma, G. (2010) "Green nanocomposites based on thermoplastic starch and steam exploded cellulose nanofibrils from wheat straw", *Carbohydrate Polymers*, vol. 82, no. 2, pp. 337-345.
14. Klemm, D. (1998) "Application of Instrumental Analysis in Cellulose Chemistry" in *Comprehensive cellulose chemistry Volume 1* Wiley-VCH, Weinheim ; New York, pp. 187 - 190.
15. Kootstra, A.M.J., Beeftink, H.H., Scott, E.L. and Sanders, J.P.M. (2009) "Comparison of dilute mineral and organic acid pretreatment for enzymatic hydrolysis of wheat straw", *Biochemical engineering journal*, vol. 46, no. 2, pp. 126-131.
16. Kristensen, J.B., Thygesen, L.G., Felby, C., Jørgensen, H. and Elder, T. (2008) "Cell-wall structural changes in wheat straw pretreated for bioethanol production", *Biotechnology for Biofuels*, vol. 1.
17. Lammers, K., Arbuckle-Keil, G. and Dighton, J. (2009a) "FT-IR study of the changes in carbohydrate chemistry of three New Jersey pine barrens leaf litters during simulated control burning", *Soil Biology and Biochemistry*, vol. 41, no. 2, pp. 340-347.
18. Lammers, K., Arbuckle-Keil, G. and Dighton, J. (2009b) "FT-IR study of the changes in carbohydrate chemistry of three New Jersey pine barrens leaf litters during simulated control burning", *Soil Biology and Biochemistry*, vol. 41, no. 2, pp. 340-347.

19. Lamsal, B., Yoo, J., Brijwani, K. and Alavi, S. (2010) "Extrusion as a thermo-mechanical pre-treatment for lignocellulosic ethanol", *Biomass and Bioenergy*, vol. 34, no. 12, pp. 1703-1710.
20. Le Troëdec, M., Peyratout, C.S., Smith, A. and Chotard, T. (2009) "Influence of various chemical treatments on the interactions between hemp fibres and a lime matrix", *Journal of the European Ceramic Society*, vol. 29, no. 10, pp. 1861-1868.
21. Lee, S.-., Teramoto, Y. and Endo, T. (2009) "Enzymatic saccharification of woody biomass micro/nanofibrillated by continuous extrusion process I - Effect of additives with cellulose affinity", *Bioresource technology*, vol. 100, no. 1, pp. 275-279.
22. Mészáros, E., Jakab, E., Gáspár, M., Réczey, K. and Várhegyi, G. (2009) "Thermal behavior of corn fibers and corn fiber gums prepared in fiber processing to ethanol", *Journal of Analytical and Applied Pyrolysis*, vol. 85, no. 1-2, pp. 11-18.
23. Mosier, N., Wyman, C., Dale, B., Elander, R., Lee, Y.Y., Holtzapple, M. and Ladisch, M. (2005) "Features of promising technologies for pretreatment of lignocellulosic biomass", *Bioresource technology*, vol. 96, no. 6, pp. 673-686.
24. Naik, S., Goud, V.V., Rout, P.K., Jacobson, K. and Dalai, A.K. (2010) "Characterization of Canadian biomass for alternative renewable biofuel", *Renewable Energy*, vol. 35, no. 8, pp. 1624-1631.
25. Nelson, M.L. and O'Connor, R.T. (1964) "Relation of certain infrared bands to cellulose crystallinity and crystal latticed type. Part I. Spectra of lattice types I, II, III and of amorphous cellulose", *Journal of Applied Polymer Science*, vol. 8, no. 3, pp. 1311-1324.
26. Ouajai, S. and Shanks, R.A. (2005) "Composition, structure and thermal degradation of hemp cellulose after chemical treatments", *Polymer Degradation and Stability*, vol. 89, no. 2, pp. 327-335.
27. Peng, Y. and Wu, S. (2010) "The structural and thermal characteristics of wheat straw hemicellulose", *Journal of Analytical and Applied Pyrolysis*, vol. 88, no. 2, pp. 134-139.

28. Sain, M. and Panthapulakkal, S. (2006) "Bioprocess preparation of wheat straw fibers and their characterization", *Industrial Crops and Products,* vol. 23, no. 1, pp. 1-8.
29. Serapiglia, M.J., Cameron, K.D., Stipanovic, A.J. and Smart, L.B. (2009) "Analysis of biomass composition using high-resolution thermogravimetric analysis and percent bark content for the selection of shrub willow bioenergy crop varieties", *Bioenergy Research,* vol. 2, no. 1-2, pp. 1-9.
30. Sun, X.F., Xu, F., Sun, R.C., Fowler, P. and Baird, M.S. (2005) "Characteristics of degraded cellulose obtained from steam-exploded wheat straw", *Carbohydrate research,* vol. 340, no. 1, pp. 97-106.
31. Yang, B. and Wyman, C.E. (2008) "Characterization of the degree of polymerization of xylooligomers produced by flowthrough hydrolysis of pure xylan and corn stover with water", *Bioresource technology,* vol. 99, no. 13, pp. 5756-5762.
32. Yang, H., Yan, R., Chen, H., Lee, D.H. and Zheng, C. (2007) "Characteristics of hemicellulose, cellulose and lignin pyrolysis", *Fuel,* vol. 86, no. 12-13, pp. 1781-1788.
33. Zhang, L., Li, D., Wang, L., Wang, T., Zhang, L., Chen, X.D. and Mao, Z. (2008) "Effect of steam explosion on biodegradation of lignin in wheat straw", *Bioresource technology,* vol. 99, no. 17, pp. 8512-8515.
34. Zhang, S., Keshwani, D.R., Xu, Y. and Hanna, M.A. (2012) "Alkali combined extrusion pretreatment of corn stover to enhance enzyme saccharification", *Industrial Crops and Products,* vol. 37, no. 1, pp. 352-357.
35. Zhang, S., Xu, Y. and Hanna, M. (2012) "Pretreatment of Corn Stover with Twin-Screw Extrusion Followed by Enzymatic Saccharification", *Applied Biochemistry and Biotechnology,* vol. 166, no. 2, pp. 458-469.

Chapter 6

FT-NIR and FT-MIR characterisation of pre-treated wheat straw and chemometric analysis for prediction of saccharification in enzymatic hydrolysis

6.1 Introduction

Physical and chemical changes during the pre-treatment of lignocellulose biomass needs to be characterised to determine the effectiveness of the fractionation and understand correlations between processing conditions and change in the physical and chemical states of the biomass and the subsequent saccharification. Such characterisations can be used for calculating mass balance, process yields, techno economic analysis, evaluations of process configuration, reactor design and process performance (Pronyk and Mazza, 2011; Tamaki and Mazza, 2011a). Physical/chemical changes in pre-treated biomass can be obtained by a combination of microscopic (e.g. SEM) thermal (e.g. TGA and DSC) and conventional wet chemical analysis with gravimetric, colorimetric and chromatographic techniques. These off-line techniques can be time-consuming, expensive, labour-intensive and difficult to integrate into on-line operation in a commercial setting (Tamaki and Mazza, 2011a; Liu *et al.*, 2010; Philip Ye *et al.*, 2008).

Infrared spectroscopy is a powerful technique for obtaining information about chemical structural changes. It is based on the absorption of infrared radiation by molecules at specific frequencies that are characteristic of vibrations of the bonds or groups in the molecular structure (Tamaki and Mazza, 2011b). Near infrared spectroscopy (NIR) detects absorptions in the region of 14000 - 4000 cm^{-1} based on overtones and combinations of fundamental vibrations, while mid-infrared spectroscopy (MIR or FTIR) detects absorptions in the region 4000 – 400 cm^{-1} based on the fundamental vibrations and associated rotational-vibrational structure (Tamaki and Mazza, 2011b). Both methods are fast in comparison with many of the conventional wet chemical analysis. FTIR is currently an off-line technique which requires sample preparation but

more sensitive to chemical information. NIR is a fast technique which requires minimum sample preparation and has proven capability for on-line analysis e.g. in an extrusion system (Kelly *et al.*, 2012), and hence is a potentially useful tool for rapid analysis of extrusion pre-treatment biomass.

Complex data are obtained from near infrared absorption spectra. It can be difficult to identify the key structural changes and to correlate such changes to processing conditions. Chemometric techniques that are capable of accessing this data include multivariate techniques, e.g., partial least squares (PLS) and principal component analysis (PCA). These can be applied to complex and collinear data and have found applications to extract relevant information from IR spectra (Sills and Gossett, 2012). The use of PCA and PLS reduce large spectral data sets by combining collinear variables (e.g., wavenumber intensities) into a small number of latent variables (LVs), which are then used in place of the full data set to build regression models (Sills and Gossett, 2012). PLS has been used with FTIR spectra to determine lignin, carbohydrates, ash and extractives contents of triticale and wheat straw (Tamaki and Mazza, 2011a; Tamaki and Mazza, 2011b) and saccharification from alkali pre-treated biomasses (Sills and Gossett, 2012; Sills and Gossett, 2011). Similar PLS models, but based on FT-NIR spectra, were also built by (Krongtaew *et al.*, 2010b) on wheat and oat straw and by (Liu *et al.*, 2010) on corn stover and switchgrass. All studies demonstrated the good potential of FTIR and FT-NIR when coupled with chemometric analysis.

To our knowledge, there is no published study on the comparison between FTIR and FT-NIR coupled with chemometric analysis for extrusion pre-treatment of wheat straw. In this study, wheat straws, after various pre-treatment conditions, were analysed with FTIR and FT-NIR using the attenuated total reflectance and diffuse reflectance methods, respectively. Wheat straw was pre-treated using twin screw extrusion, with or without the addition of sodium hydroxide, and compared with straw after conventional steam explosion. Chemical information obtained from both FTIR and FT-NIR methods was correlated to glucose yield after enzymatic hydrolysis using chemometric analysis. A comparison was made between the two IR methods together with a study on necessary pre-processing of the data for optimum regression of the models.

Models built were validated for the glucose yield prediction performance and assessed for robustness.

The detail of methodology is captured in Chapter 3,

i. Sub-section 3.2 mainly for extrusion sample preparation and a summary table for sample ID and description were showed in Table 3.4 (including sample steam explosion).
ii. Detail for steam explosion and enzymatic hydrolysis were outlined in sub-section 3.3 and 3.4.
iii. Experimental work instruction for FTIR and FT-NIR were summarised in sub-section 3.8.1 and 3.8.2.
iv. Chemometric analysis is explained in sub-section 3.8.3.

6.2 Results and Discussion

6.2.1 Infrared spectra and interpretation

Figure 6.1 and **6.2** are selected as representative spectra covering wavenumber ranges 4000 – 600 cm^{-1} (MIR) and 7400 – 4000 cm^{-1} (NIR) respectively. These were spectra selected from those of wheat straws post various pre-treatments including **Figure 6.3** presents NIR spectra for various straw samples from 5400 – 5150 cm^{-1}. A total of 45 samples were included and categorised as below,

a) RWS – Raw wheat straw sample, 1 sample,
b) PWS – Powdered straw, 1 sample,
c) EX – extrusion pre-treated wheat straw (without NaOH), 18 samples,
d) EXC – NaOH combined extrusion pre-treated wheat straw, 21 samples,
e) EXCW – washed sample of NaOH combined extrusion pre-treated wheat straw, 1 sample and
f) SE – steam exploded sample

details of which can be found in **Table 3.4**, Chapter 3.

Table 6.1 : FTIR and NIR wavenumbers and their assignments

FTIR	Assignment	References	NIR	Assignment	References
~2917, 2850	CH_3- and CH_2- stretching (wax and cellulose)	(Lamsal *et al.*, 2010; Kristensen *et al.*, 2008)	~4250	CH_2 bend 2nd overtone (Cellulose)	(Aenugu *et al.*, 2011; Krongtaew *et al.*, 2010a; Shenk, J.S., Workman, J.J., and Westerhaus, M.O., 2008)
~1733	C=O ester linkage (hemicelluloses, lignin)	(Le Troëdec *et al.*, 2009; Alemdar and Sain, 2008; Kristensen *et al.*, 2008; Zhang *et al.*, 2008; Sain and Panthapulakkal, 2006)	~5213	C=O stretch 2nd overtone	(Shenk, J.S., Workman, J.J., and Westerhaus, M.O., 2008)
~1710, 1594, 1515	Stretching carbonyl and aromatic lignin bands	(Kaushik, Singh and Verma, 2010; Naik *et al.*, 2010; Alriols *et al.*, 2009; Lammers, Arbuckle-Keil and Dighton, 2009a; Lammers, Arbuckle-Keil and Dighton, 2009b; Alemdar and Sain, 2008; Kristensen *et al.*, 2008; Zhang *et al.*, 2008; Hongzhang and Liying, 2007; Sain and Panthapulakkal, 2006)	~6913	O-H stretch 1st overtone	(Krongtaew *et al.*, 2010a)
~1240	C-O aryl of lignin (guaiacyl unit)	(Lammers, Arbuckle-Keil and Dighton, 2009a; Zhang *et al.*, 2008; Hongzhang and Liying, 2007)	~5990	CH_3 acetyl lignin 1st overtone of C-H	(Krongtaew *et al.*, 2010a)
~1420, 1106, 1050	C-O stretching and CH_2 bending (Cellulose)	(Nelson and O'Connor, 1964)	~7000, 6722 and 6300	O-H stretch 1st overtone (amorphous and semi-crytalline cellulose) and CH combination and CH 1st overtone of saccharides	(Krongtaew *et al.*, 2010a; Tsuchikawa and Siesler, 2003a; Tsuchikawa and Siesler, 2003b)
~1560	COO' stretching (cellulose I)	(Klemm, 1998)	~5800	CH stretch 1st overtone (CH_2)	(Shenk, J.S., Workman, J.J., and Westerhaus, M.O., 2008)
~1402, 890	C-H bend (Alkyl) C_1-H bend (β-D-xylose)	(Peng and Wu, 2010)			

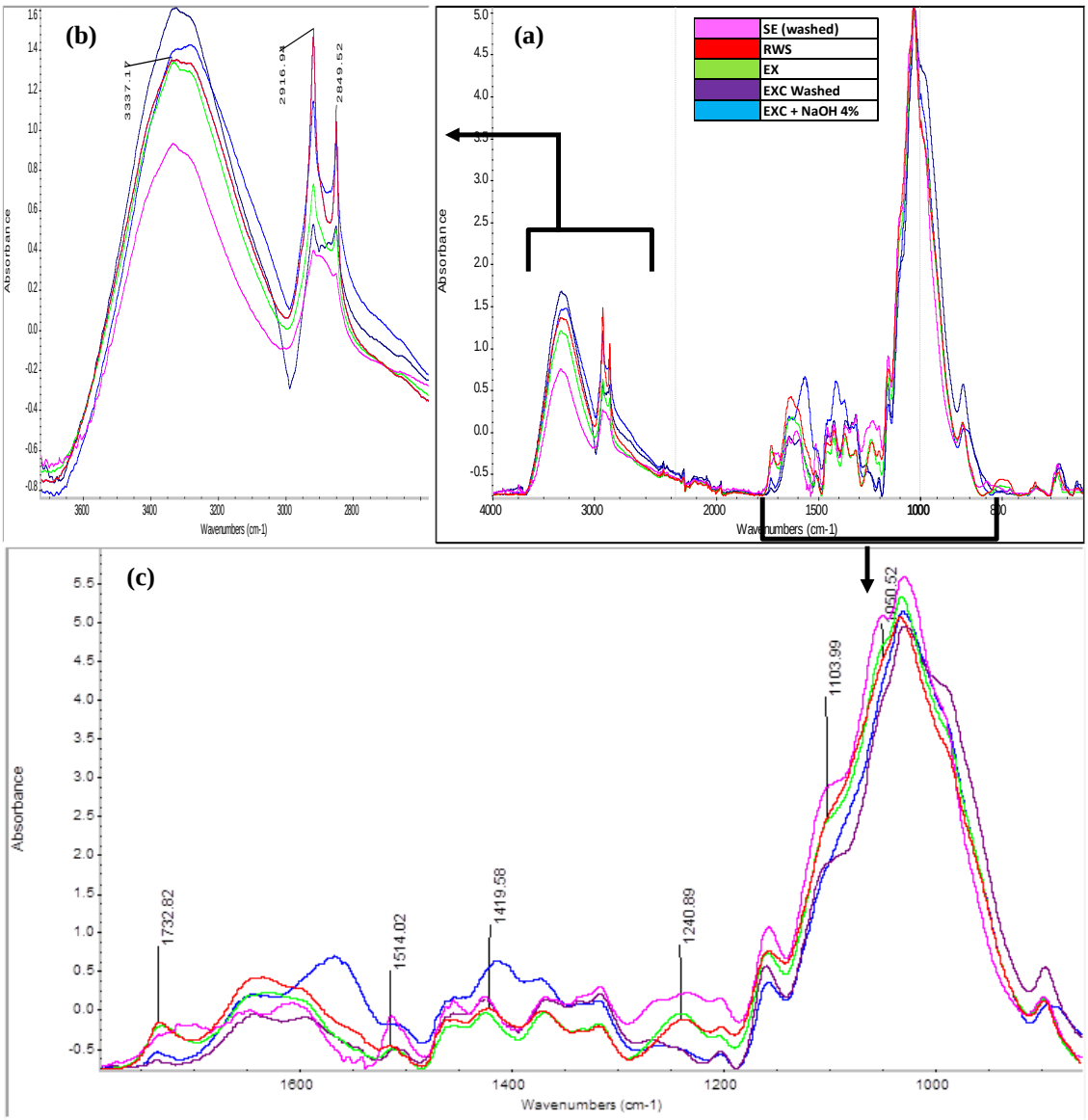

Figure 6.1 : FTIR spectra for various straw samples (a) and the two regions of interests are show as blow-ups (b and c) to show more details.

The assignments of the infrared wavenumbers for the key functional groups are tabulated in **Table 6.1** for identification of them. FTIR spectra (**Figure 6.1a**) were dominated by the peaks at ~3291 and 1031cm^{-1} representing the stretching vibrations of O-H and C-O, respectively. Raw FT-NIR spectra were converted to second derivative format to enhance the NIR signals (**Figure 6.2**). The bands at ~2917 and ~2850 cm^{-1} in **Figure 6.1a** and **6.1b** are contributed to by CH_3- and CH_2- stretching bands ascribed to

hydrocarbon in wax and polysaccharides (Le Troëdec *et al.*, 2009; Kristensen *et al.*, 2008). Epidermis cells are the outmost surface cells of straw, covered by a very thin wax layer (Han *et al.*, 2010). To different extents, all the pre-treatments partially removed the wax content in the epidermis layer and this was evident by the decreased intensity of the ~2850cm^{-1} peak. Similar information was also picked up at ~4250 cm^{-1} in **Figure 6.2**, which is contributed by CH_2 second overtone bending vibration (Krongtaew *et al.*, 2010a). The removal of the hydrophobic surface wax layer is desirable to enhance the access of the enzyme in water-based medium and thus increasing the efficiency of enzymatic hydrolysis. Another interesting observation is the ratio of CH_3 / CH_2 peak height in **Figure 6.1**. It increased from the lowest value (3.33) for the un-treated straw (RWS) to highest value (13.15) for the steam exploded straw (SE). This could be an indication on the reduction of cellulose content in the pre-treated straws.

The sharp peak at ~1733 cm^{-1} (**Fig. 6.1c**) is attributed to the acetyl and uronic ester groups of the hemicelluloses or from the ester linkage of carboxylic group of the ferulic and *p*-coumaric acids of lignin and/or hemicelluloses (Le Troëdec *et al.*, 2009; Alemdar and Sain, 2008; Kristensen *et al.*, 2008; Zhang *et al.*, 2008; Sain and Panthapulakkal, 2006). Significant reduction of the 1733cm^{-1} peak was observed for SE, EXC and EXCW samples. When sodium hydroxide (alkaline) was employed in the pre-treatment, a significant reduction of 1733cm^{-1} peak was observed (**Figure 6.1c**). This indicated that sodium hydroxide played an important catalytic role to reduce the ester bond from the hemicelluloses and/or lignin. This was in-line with the weak NIR band at ~5213 cm^{-1} from C=O stretch 2nd overtone (See **Figure 6.3**).

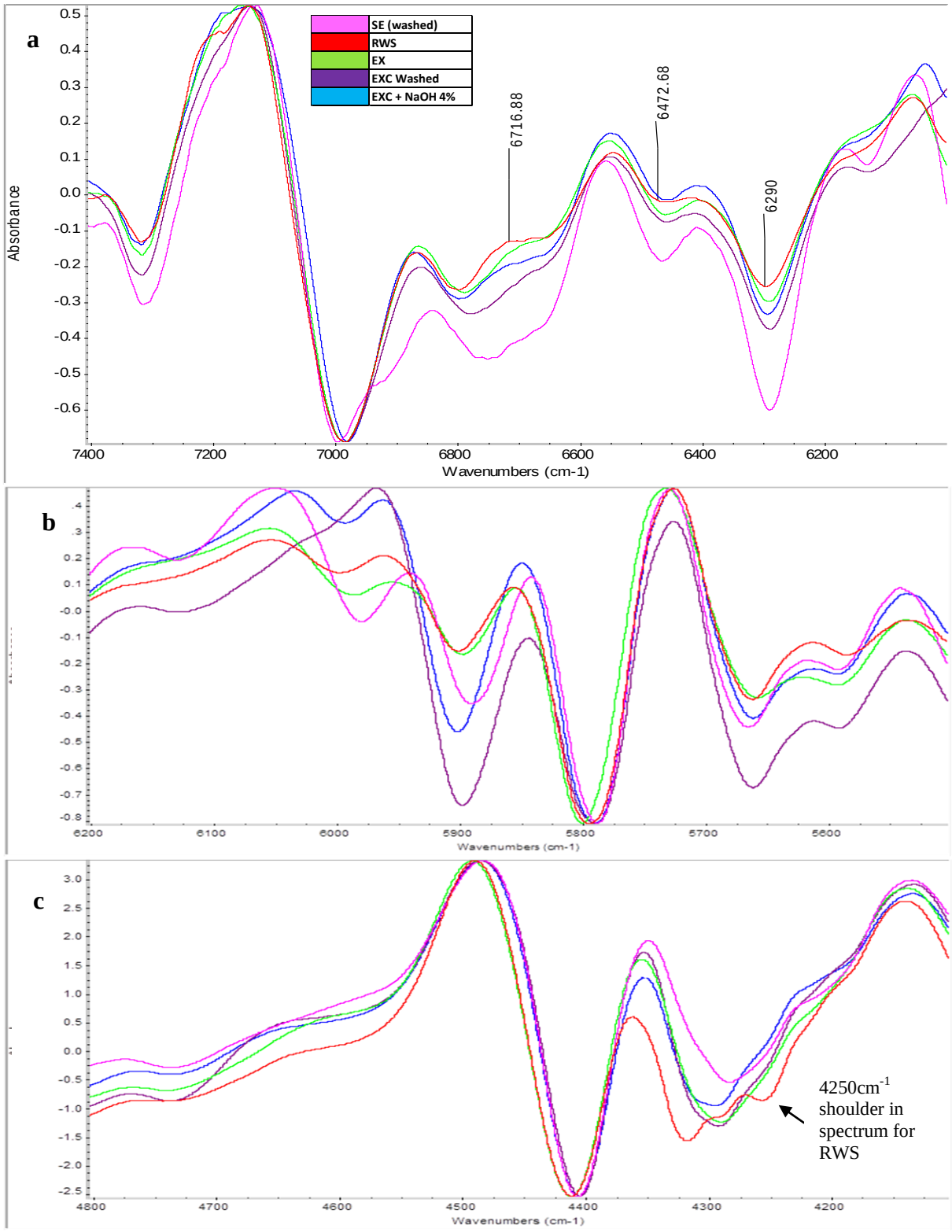

Figure 6.2 : FT-NIR spectra for various straw samples in different wave number regions: a) 7400 – 6000 cm^{-1}, b) 6200 – 5500 cm^{-1} and c) 4800 – 4100 cm^{-1}.

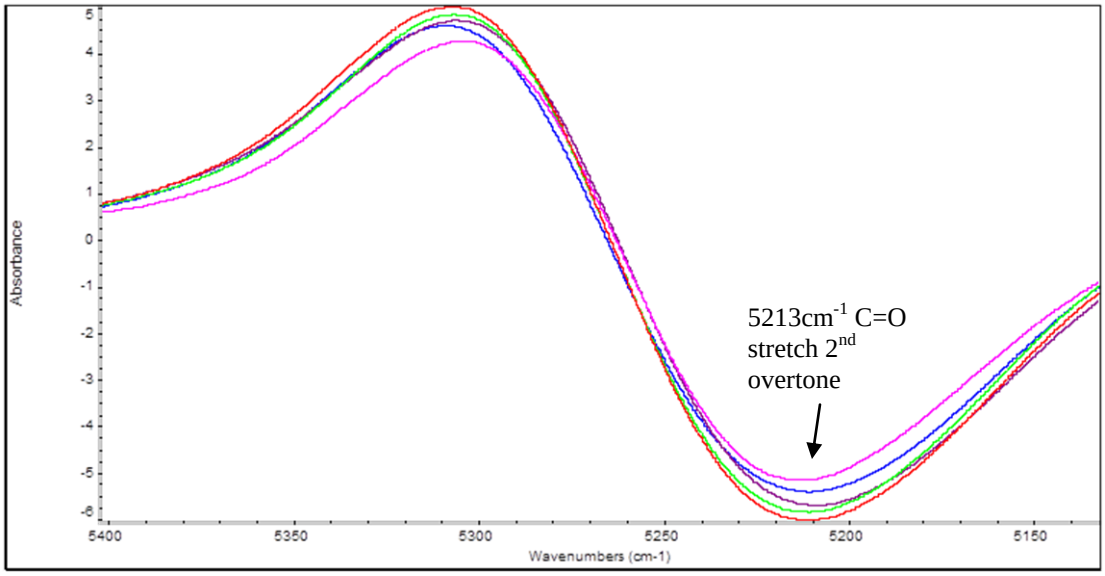

Figure 6.3 : NIR spectra for various straw samples from 5400 – 5150 cm^{-1}.

Significant peaks at ~ 1710 cm^{-1}, ~ 1594 and 1515 cm^{-1} were noticed in the spectrum for the SE sample (**Figure 6.1c**) relating to the stretching carbonyl group and the aromatic lignin bands from lignin compounds (Kaushik, Singh and Verma, 2010; Naik *et al.*, 2010; Alriols *et al.*, 2009; Lammers, Arbuckle-Keil and Dighton, 2009a; Alemdar and Sain, 2008; Kristensen *et al.*, 2008; Zhang *et al.*, 2008; Hongzhang and Liying, 2007; Sain and Panthapulakkal, 2006). The findings from the FTIR spectra were in line with those from the FT-NIR spectra where a shoulder contributed by the O-H stretch first overtone (Krongtaew *et al.*, 2010a) was found in the SE sample at ~6913 cm^{-1}. This has been further supported from the findings reported in Chapter 4 and by Kristensen *et al.* (2008) using FTIR analysis and Sun *et al.* (2005) using wet chemical analysis (Klason lignin). According to Sun *et al*. (2005), the reason for this higher lignin content was due to the hydrolysis of a substantial amount of hemicelluloses during steam pre-treatment and a lignin re-condensation reaction.

The efficiency of lignin fractionation from pre-treatment can be seen in both NIR and FTIR spectra. The peak at ~ 1240cm^{-1} was from C-O-aryl of lignin (guaiacyl unit) (Lammers, Arbuckle-Keil and Dighton, 2009a; Zhang *et al.*, 2008; Hongzhang and Liying, 2007), the peak decreased significantly after sodium hydroxide pre-treatment. Supporting evidence was also found from the NIR spectra (**Figure 6.2b**), where the band at ~ 5990 cm^{-1} showed the same trend. This band is related to the CH_3 acetyl lignin

first overtone of C-H (Krongtaew *et al.*, 2010a). The mechanism of the sodium hydroxide reaction with lignin can be explained as an initial electrophilic reaction by reactive oxygen species, followed by a nucleophilic attack on the phenolic hydroxyl groups and phenolate ions of lignin moieties. This opens the aromatic ring, the main structure of lignin subunits (Krongtaew *et al.*, 2010a).

With regards to the assignment of the polysaccharides content, the peaks at ~1050, 1106 and 1420 cm^{-1} are cellulose signature peaks from C-O stretching and CH_2 bending (Nelson and O'Connor, 1964). The SE sample showed a shoulder at ~ 1050 and 1106 cm^{-1}, which implied it was higher in cellulose content. This was supported by the NIR bands (Figure 6.2a) at ~7000 cm^{-1} (O-H stretch first overtone amorphous) with a more shifted band for the SE sample as well as bands at ~6300 cm^{-1} (CH combination and CH first overtone of saccharides) and ~6722 cm^{-1} (OH stretch first overtone semi-crystalline region of cellulose) (Krongtaew *et al.*, 2010a; Yonenobu, Tsuchikawa and Sato, 2009; Watanabe, Morita and Ozaki, 2006; Tsuchikawa and Siesler, 2003a; Tsuchikawa and Siesler, 2003b). These bands were showing an increasing trend of polysaccharides content with RWS < EX < EXC < EXCW < SE. Sample EXC was found to have more overlapped bands at ~ 1560, 1415 and 890 cm^{-1}. These are believed to be an indication of fractionated polysaccharides after sodium hydroxide pre-treatment as the peaks disappeared after washing (see. spectrum for EXCW).

6.2.2 Qualitative discriminant analysis using Principal Component Analysis (PCA)

PCA projects objects and variables into low dimensional spaces, and it can be used to find patterns, relationships and differences between objects and / or variables (Maltesen *et al.*, 2011). FT-NIR and FTIR spectra (pre-treated) for all 45 samples (1 Control RWS, 1 PWS, 18 EX, 21 EXC, 1 EXCW and 3 SE) were subjected to PCA. The multivariate spectral data space, in which variables are often correlated to each other, was reduced to 10 orthogonal latent factors – the principal components (PCs). Different numbers of factors were used in FTIR and NIR models depending on the explained variance. The contribution of each of the variables to each factor is plotted in the principal component loading spectra (See **Figure 6.4** and **6.5**). These charts show the percentage of variance modelled from the first three PCs. These account for a total of

88.3% and 94.5% of the variance (influence) from the FTIR (**Figure 6.4**) and NIR (**Figure 6.5**) spectra data sets, respectively. PC1 had a cumulative variance of 78% for the NIR data with maxima and minima at ~ 5210 cm^{-1} and 5297 cm^{-1}. These are key regions for C=O stretch second overtone and O-H stretch combined with C-O stretch second overtone. PC1 derived from the FTIR spectra had a cumulative variance of 66% with maxima at ~ 1560 and 1402 cm^{-1} and minima at 1071 cm^{-1}. These are key regions for hemicelluloses absorption.

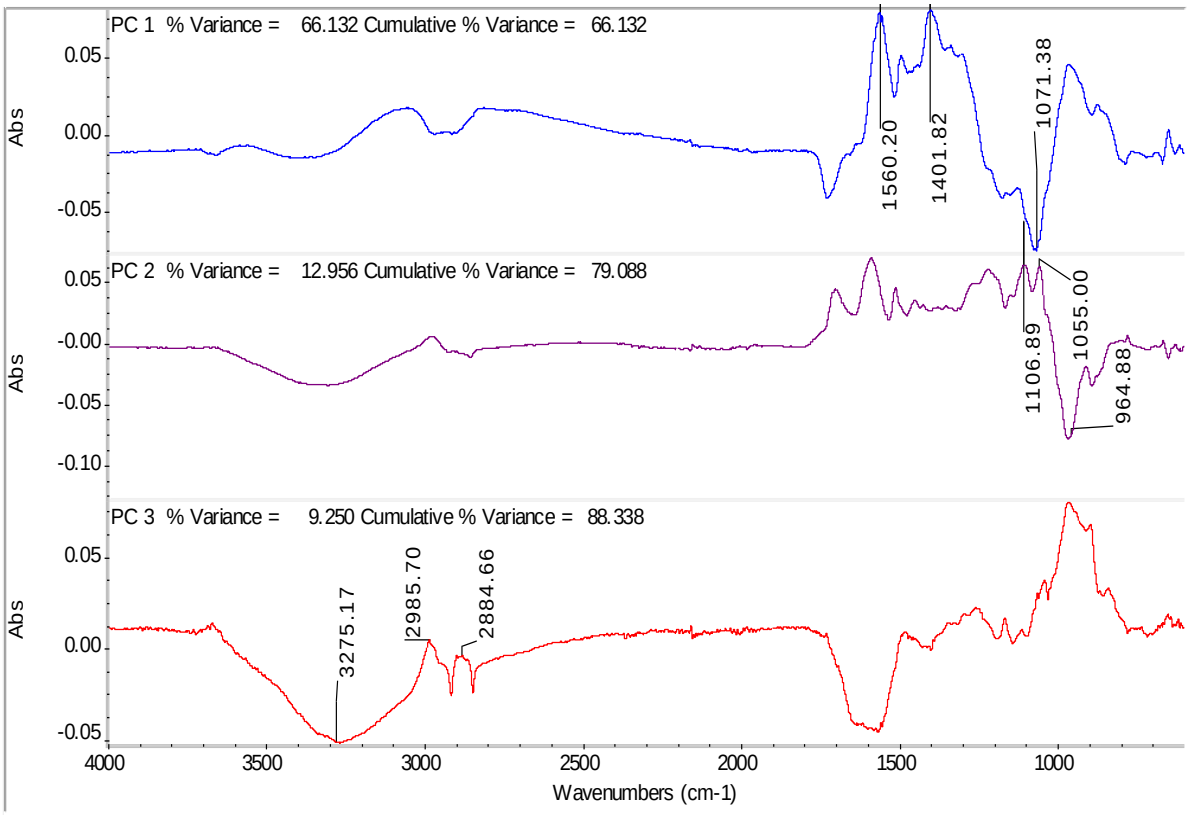

Figure 6.4 : Plot of loading variances of the dominant three principal component (P1-P3) for FTIR spectra.

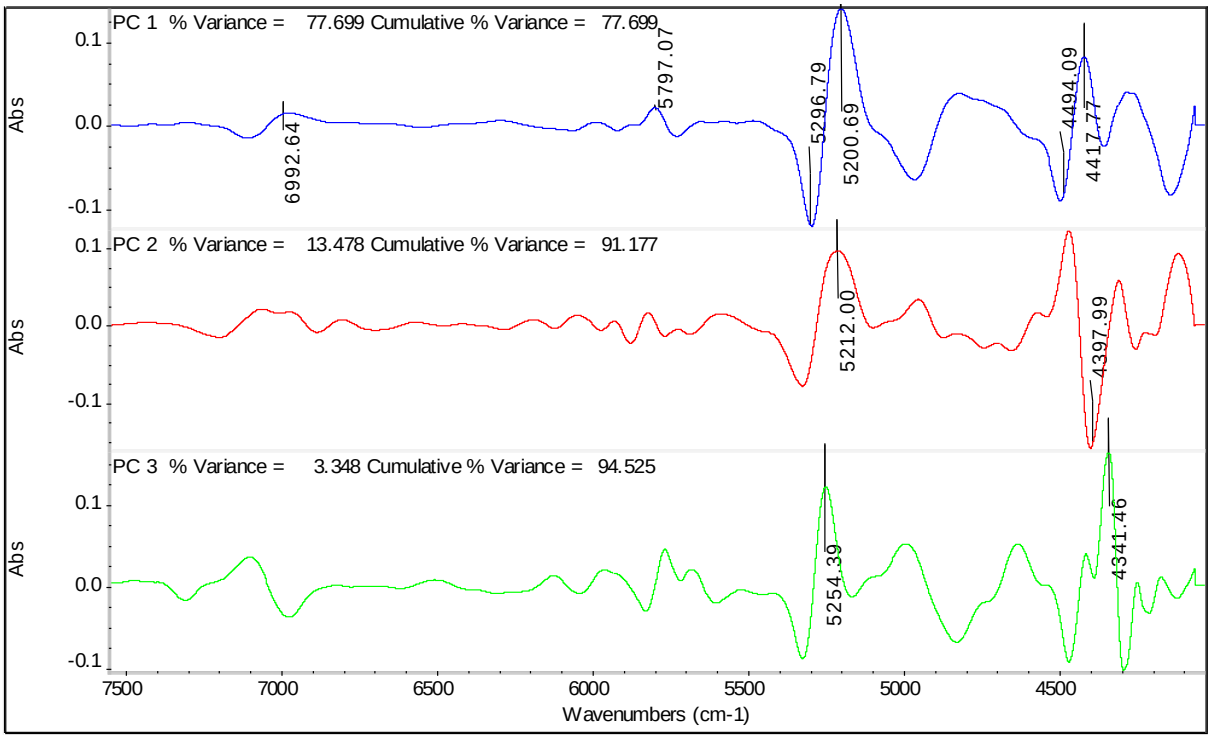

Figure 6.5 : Plot of loading variances of the dominant three principal component (P1-P3) for FT-NIR spectra.

Figures 6.6 and **6.7** show 3-dimensional plots of the first three PC scores which can be used to assess the uniqueness of chemical information extracted from spectra. In order to aid the display, elipses and circles have been drawn around each cluster of samples, but these do not have any statistical significance. The plot illustrates that samples with differing pre-treatments fall into clusters in identifiable envelopes. The charts also enable to differentiate the pre-treatment conditions, e.g. the level of sodium hydroxide used, the severity of extrusion conditions and the subsequent washing.

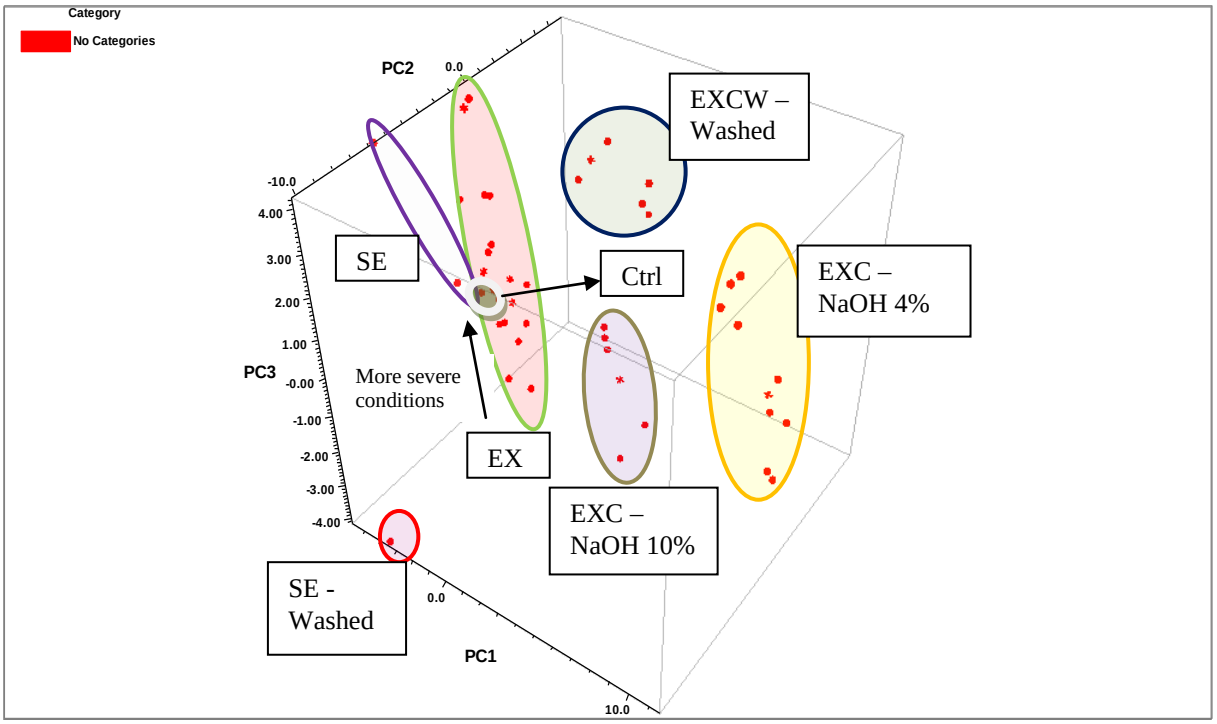

Figure 6.6 : Plot of the three dominant principal components (P1-P3) for FTIR showing the clusters correlated to pre-treatments and conditions

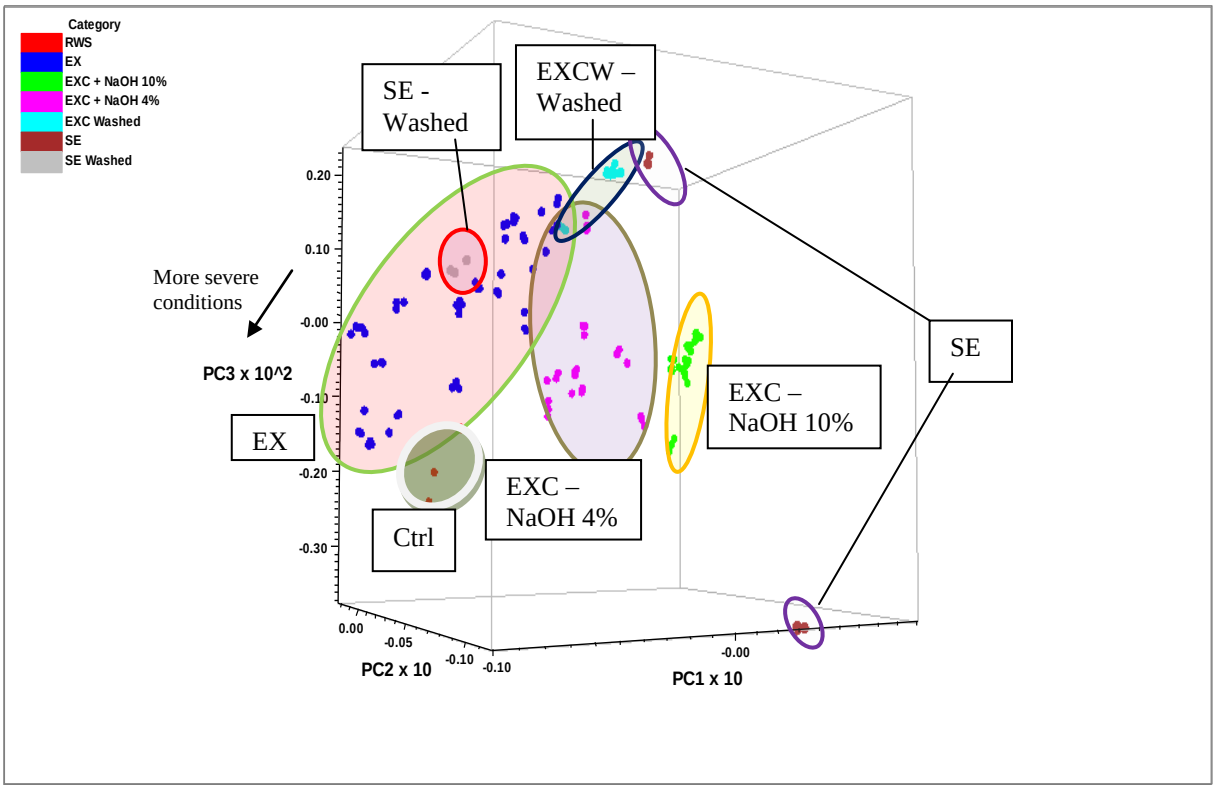

Figure 6.7 : Plot of the three dominant principal components (P1-P3) for FT-NIR showing the clusters correlated to pre-treatments and conditions

6.2.3 Glucose yield from enzymatic hydrolysis

Glucose yield used for this chapter is defined here as the grammes of glucose solubilised per 100 gram of dry pre-treated straw obtained after 72 hours enzymatic hydrolysis process as shown in **Table 6.2**. RWS with no pre-treatment resulted in the lowest glucose yield. The highest glucose yield was recorded from the SE sample. The trend of glucose yield in decreasing order is

SE > EXCW > EXC > EX > RWS

Glucose yield increased with the loading of sodium hydroxide and severity of the extrusion process. Glucose yield was also improved after the washing process as washing removed water soluble fractionated parts and left a cellulose-rich substrate.

Table 6.2 : Summary of glucose yield from enzymatic hydrolysis.

Sample	Glucose Yield (g glucose/ 100g pre-treated straw)	
	Average	Min - Max
RWS	0.4	-
Powdered RWS	7.4	-
EX	6.1	2.28 – 8.97
EXC	10.6	9.40 – 12.80
EXCW	16.5	-
SE	15.8	11.30 – 20.10

6.2.4 PLS regression model evaluation

One of the purposes of this study was to establish a prediction model to correlate spectral changes from different methods of pre-treatment to enzymatic hydrolysis performance (sugar yield). To achieve this, a broad-based model was required and all the sample data, including the two different categories of pre-treatment (steam explosion and extrusion), were included for the model calibration.

PLS regression models were constructed by correlating principal components from the spectra of 45 straw samples (X matrix) to the glucose yield (Y response vectors). Various spectral pre-treatments were explored to optimise the best model calibration outcome. This was carried out using the software package TQ Analyst version 8 (Thermo Fisher Scientific, UK) and pre-processing of the spectra data to reduce noise level and improve correlation coefficient of the regression. To evaluate the performance of the model built, various statistic indicators (R^2_C, RMSEC, R^2_P, RMSEP and RMSECV) and slope of the calibration line were calculated. The optimised spectral pre-treatment combinations and the calibration statistic indicators for FT-NIR and FTIR data are summarised in **Table 6.3** and **Figure 6.8**. A total of 7 factors were used for FTIR model while only 4 were used for the FTNIR model. Past research studies reported that R^2_P, with values between 0.66 and 0.80, indicates approximate quantitative prediction. Whereas a value between 0.81 and 0.90 indicates good prediction and a value of > 0.90 is considered to be excellent (Sills and Gossett, 2012; Sills and Gossett, 2011; Tamaki and Mazza, 2011a; Tamaki and Mazza, 2011b; Krongtaew *et al.*, 2010b; Liu *et al.*, 2010). For the slope term, values of < 0.8 or > 1.2, 0.8 – 1.2, and 0.9 – 1.1 are assessed as less reliable, reliable and very reliable, respectively (Tamaki and Mazza, 2011b). The difference between R^2_P and R^2_C has also been considered for model assessment, with the suggestion that this difference should be < 0.2 for models with good predictive ability (Sills and Gossett, 2012; Chen *et al.*, 2010). The PLS regression models from both FT-NIR and FTIR spectra were good and had excellent predictive performance as judged by the R^2_P value. This was supported by the slope value for the models with a small difference (<0.04 for both models) between R^2_P and R^2_C. RMSECV was recorded at 2.09 and 2.71 respectively both FT-NIR and FTIR models.

Table 6.3 : Summary of optimised spectral pre-treatments and statistical variation indices (with total of 45 samples including SE samples) based on a) FT-NIR and b) FTIR spectra.

a) FT-NIR

Spectral Pre-treatments Combination			Note :
SNV, 2nd Dev., Filter 7,7, process spectrum, 4000 - 7500 cm^{-1}	R^2_c	0.9173	RMSECV = 2.09
	RMSEC	1.60	4 factors

	R^2_P	0.8809	
	RMSEP	1.79	

b) FTIR

Spectral Pre-treatments Combination			Note :
SNV, Spectrum, No smoothing, process spectrum, 700 - 1800 & 2700 - 3700 cm^{-1}	R^2_C	0.9459	RMSECV = 2.71 7 factors
	RMSEC	1.31	
	R^2_P	0.9219	
	RMSEP	1.61	

As the SE sample had a very different spectrum compared with the extrusion pre-treated samples, a trial was conducted by removing the SE sample from the data set to try to improve the performance accuracy. Table 6.5 showed the summary for the model performance after the SE sample removal. The performance for the models from both categories was indeed improved to excellent (R^2_p = 0.9123 and 0.8954 for NIR and FTIR respectively). Only 4 factors were needed to optimise the model from the FTIR spectra and the RMSECV was reduced to 2.11 from 2.71. This suggests that the PLS regression is more accurate when conducted on data from a specific process.

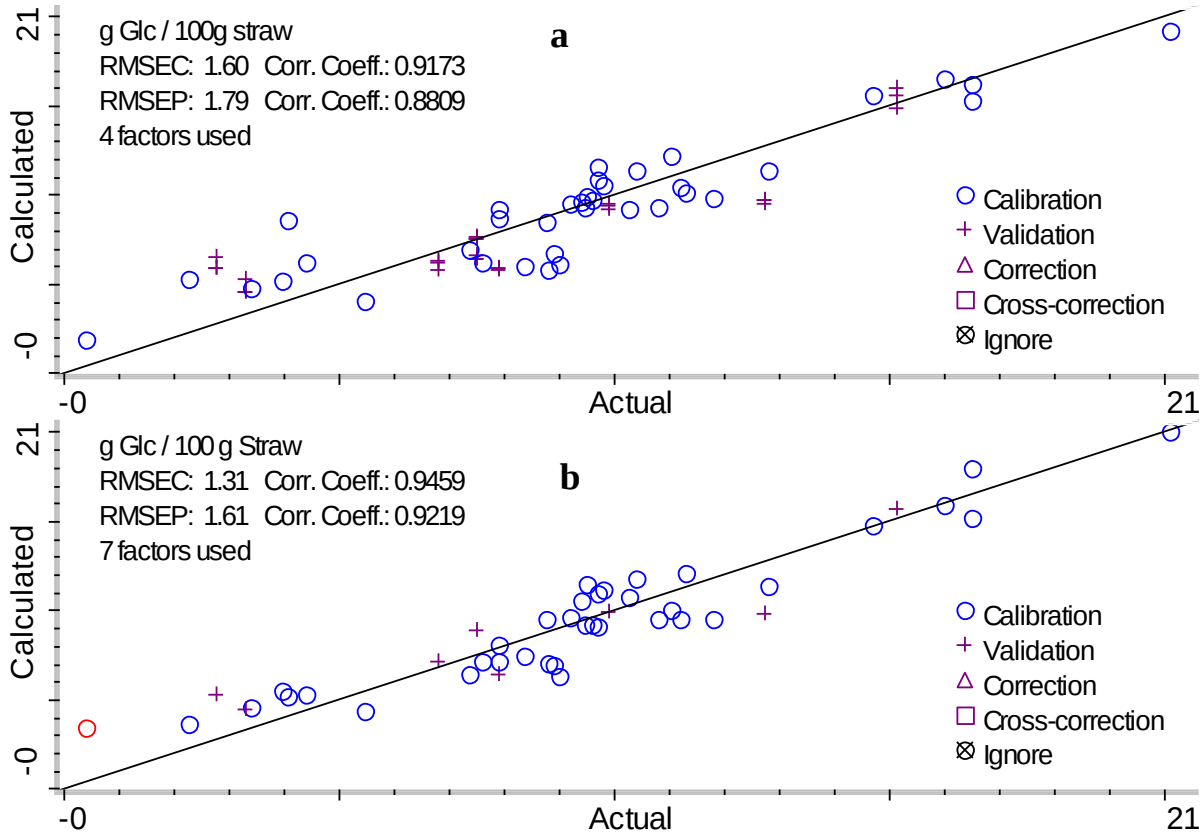

Figure 6.8: Plots of predicted versus actual value of g Glucose / 100g straw in straw samples :
(a) plot with FT-NIR spectra and
(b) plot with FTIR spectra (with SE samples included for both models).

Table 6.4 : Performance of optimised models based on a) FT-NIR and b) FTIR spectra (with exclusion of SE samples)

a) PLS Analysis FT-NIR (without SE samples, N=42)

Spectral Pre-treatments Combination			Note :
SNV, 2nd Dev., Filter 7,7, process spectrum, , 4000 - 7500 cm^{-1}	R^2_C	0.9043	RMSECV = 2.09
	RMSEC	1.6	4 factors
	R^2_P	0.9123	
	RMSEP	1.31	

b) PLS Analysis FTIR (without SE samples, N=42)

Spectral Pre-treatments Combination			Note :
SNV, Spectrum, No smoothing, process spectrum, 700 - 1800 & 2700 - 3700 cm^{-1}	R^2_C	0.9135	RMSECV = 2.11
	RMSEC	1.53	4 factors

R^2_P	0.8954
RMSEP	1.37

To assess the validity of models further, the influence of the chemistry on the spectra and the plot of correlation index vs infrared wavenumbers were examined (see **Figure 6.9** and **6.10** in the correlation index plot at top of both figures). The key correlated areas were matched with the critical FTIR and NIR spectra information as described in the section under infrared spectra interpretation. For example, key correlated areas such as ~ 6722, 6300, 5990 and 5800 cm^{-1} in **Figure 6.9** and ~ 2920, 1732 and 1240 cm^{-1} in **Figure 6.10**, respectively.

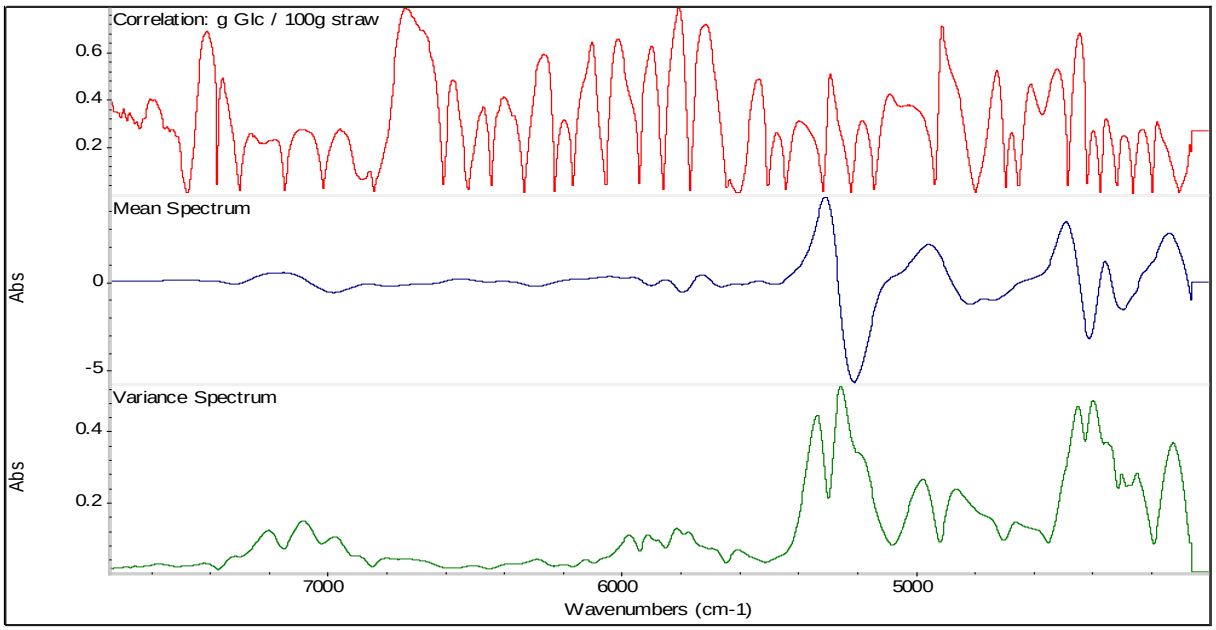

Figure 6.9 : Plot of correlation index plot in the NIR region, the top part of the figure is the actual correlation index and followed by mean and variance spectrum.

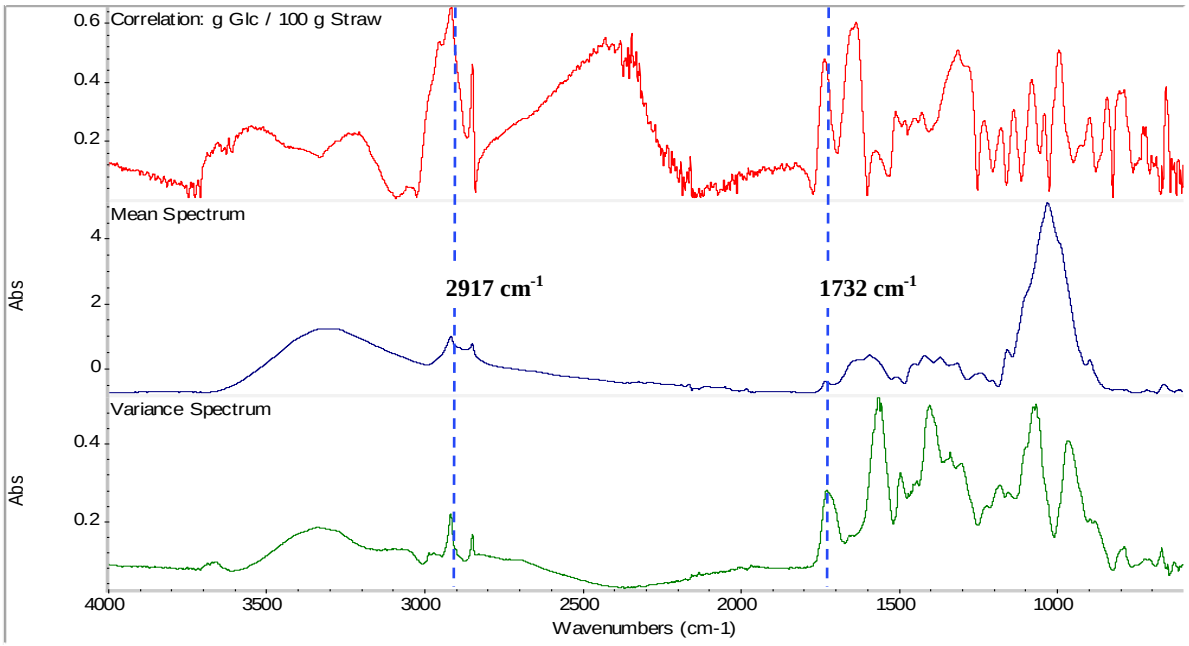

Figure 6.10 : Plot of correlation index plot in the FTIR region, the top part of the figure is the actual correlation index and followed by mean and variance spectrum.

6.3 Summary

In conclusion, FTIR and FT-NIR analysis coupled with chemometrics can be used for qualitative and quantitative analysis of wheat straw pre-treated with extrusion and steam-explosion to correlate chemical changes to effectiveness of fractionation and sugar yield.

A satisfactory evaluation is obtained for the multivariate calibration models. The PCA method is able to distinguish the effect of processing methods and the conditions. The PLS statistical models are well correlated with the chemical information extracted from FTIR and FT-NIR spectra and is capable of predicting sugar yield from FTIR or FT-NIR information.

FT-NIR using diffuse reflectance measurements has an advantage of minimum sample preparation and it is feasible to be use in-line and off-line. The validity of chemical information from FT-NIR spectra is further supported by direct spectral interpretation by FTIR. However, to improve the accuracy more samples are needed to strengthen the

reliability of the model; in particular for the creation of a broad-based model to captured various type of pre-treatment method.

6.4 References

1. Aenugu, H.P.R., Kumar, D.S., Parthiban, N., Srisudharson, Ghosh, S.S. and Banji, D. (2011) "Near Infra Red Spectroscopy- An Overview", *International Journal of ChemTech Research,* vol. 3, no. 2, pp. 825-836.
2. Alemdar, A. and Sain, M. (2008) "Isolation and characterization of nanofibers from agricultural residues – Wheat straw and soy hulls", *Bioresource technology*, vol. 99, no. 6, pp. 1664-1671.
3. Alriols, M.G., Tejado, A., Blanco, M., Mondragon, I. and Labidi, J. (2009) "Agricultural palm oil tree residues as raw material for cellulose, lignin and hemicelluloses production by ethylene glycol pulping process", *Chemical Engineering Journal,* vol. 148, no. 1, pp. 106-114.
4. Chen, H., Ferrari, C., Angiuli, M., Yao, J., Raspi, C. and Bramanti, E. (2010) "Qualitative and quantitative analysis of wood samples by Fourier transform infrared spectroscopy and multivariate analysis", *Carbohydrate Polymers*, vol. 82, no. 3, pp. 772-778.
5. Han, G., Deng, J., Zhang, S., Bicho, P. and Wu, Q. (2010) "Effect of steam explosion treatment on characteristics of wheat straw", *Industrial Crops and Products*, vol. 31, no. 1, pp. 28-33.
6. Hongzhang, C. and Liying, L. (2007) "Unpolluted fractionation of wheat straw by steam explosion and ethanol extraction", *Bioresource technology*, vol. 98, no. 3, pp. 666-676.
7. Kaushik, A., Singh, M. and Verma, G. (2010) "Green nanocomposites based on thermoplastic starch and steam exploded cellulose nanofibrils from wheat straw", *Carbohydrate Polymers*, vol. 82, no. 2, pp. 337-345.
8. Kelly, A.L., Gough, T., Dhumal, R.S., Halsey, S.A. and Paradkar, A. (2012) "Monitoring ibuprofen–nicotinamide cocrystal formation during solvent free continuous cocrystallization (SFCC) using near infrared spectroscopy as a PAT tool", *International journal of pharmaceutics*, vol. 426, no. 1–2, pp. 15-20.
9. Klemm, D. (1998) "Application of Instrumental Analysis in Cellulose Chemistry" in *Comprehensive cellulose chemistry Volume 1* Wiley-VCH, Weinheim ; New York, pp. 187 - 190.

10. Kristensen, J.B., Thygesen, L.G., Felby, C., Jørgensen, H. and Elder, T. (2008) "Cell-wall structural changes in wheat straw pretreated for bioethanol production", *Biotechnology for Biofuels*, vol. 1.
11. Krongtaew, C., Messner, K., Ters, T. and Fackler, K. (2010a) "Characterization of key parameters for biotechnological lignocellulose conversion assessed by FT-NIR spectroscopy. Part I: Qualitative analysis of pretreated straw", *BioResources*, vol. 5, no. 4, pp. 2063-2080.
12. Krongtaew, C., Messner, K., Ters, T. and Fackler, K. (2010b) "Characterization of key parameters for biotechnological lignocellulose conversion assessed by FT-NIR spectroscopy. Part II: Quantitative analysis by partial least squares regression", *BioResources*, vol. 5, no. 4, pp. 2081-2096.
13. Lammers, K., Arbuckle-Keil, G. and Dighton, J. (2009a) "FT-IR study of the changes in carbohydrate chemistry of three New Jersey pine barrens leaf litters during simulated control burning", *Soil Biology and Biochemistry*, vol. 41, no. 2, pp. 340-347.
14. Lammers, K., Arbuckle-Keil, G. and Dighton, J. (2009b) "FT-IR study of the changes in carbohydrate chemistry of three New Jersey pine barrens leaf litters during simulated control burning", *Soil Biology and Biochemistry*, vol. 41, no. 2, pp. 340-347.
15. Lamsal, B., Yoo, J., Brijwani, K. and Alavi, S. (2010) "Extrusion as a thermo-mechanical pre-treatment for lignocellulosic ethanol", *Biomass and Bioenergy*, vol. 34, no. 12, pp. 1703-1710.
16. Le Troëdec, M., Peyratout, C.S., Smith, A. and Chotard, T. (2009) "Influence of various chemical treatments on the interactions between hemp fibres and a lime matrix", *Journal of the European Ceramic Society*, vol. 29, no. 10, pp. 1861-1868.
17. Liu, L., Ye, X.P., Womac, A.R. and Sokhansanj, S. (2010) "Variability of biomass chemical composition and rapid analysis using FT-NIR techniques", *Carbohydrate Polymers*, vol. 81, no. 4, pp. 820-829.
18. Maltesen, M.J., Bjerregaard, S., Hovgaard, L., Havelund, S., van de Weert, M. and Grohganz, H. (2011) "Multivariate Analysis of Phenol in Freeze-Dried and

Spray-Dried Insulin Formulations by NIR and FTIR", *AAPS PharmSciTech*, , pp. 1-10.

19. Naik, S., Goud, V.V., Rout, P.K., Jacobson, K. and Dalai, A.K. (2010) "Characterization of Canadian biomass for alternative renewable biofuel", *Renewable Energy*, vol. 35, no. 8, pp. 1624-1631.
20. Nelson, M.L. and O'Connor, R.T. (1964) "Relation of certain infrared bands to cellulose crystallinity and crystal latticed type. Part I. Spectra of lattice types I, II, III and of amorphous cellulose", *Journal of Applied Polymer Science*, vol. 8, no. 3, pp. 1311-1324.
21. Peng, Y. and Wu, S. (2010) "The structural and thermal characteristics of wheat straw hemicellulose", *Journal of Analytical and Applied Pyrolysis*, vol. 88, no. 2, pp. 134-139.
22. Philip Ye, X., Liu, L., Hayes, D., Womac, A., Hong, K. and Sokhansanj, S. (2008) "Fast classification and compositional analysis of cornstover fractions using Fourier transform near-infrared techniques", *Bioresource technology*, vol. 99, no. 15, pp. 7323-7332.
23. Pronyk, C. and Mazza, G. (2011) "Optimization of processing conditions for the fractionation of triticale straw using pressurized low polarity water", *Bioresource technology*, vol. 102, no. 2, pp. 2016-2025.
24. Sain, M. and Panthapulakkal, S. (2006) "Bioprocess preparation of wheat straw fibers and their characterization", *Industrial Crops and Products*, vol. 23, no. 1, pp. 1-8.
25. Shenk, J.S., Workman, J.J., and Westerhaus, M.O. (2008) "Application of NIR spectroscopy to agricultural products" in *Handbook of near-infrared analysis*, ed. Burns, D.A., and Ciurczak, E.W.(eds.), 3rd edn, CRC, New York, pp. 348 - 382.
26. Sills, D.L. and Gossett, J.M. (2012) "Using FTIR to predict saccharification from enzymatic hydrolysis of alkali-pretreated biomasses", *Biotechnology and bioengineering*, vol. 109, no. 2, pp. 353-362.
27. Sills, D.L. and Gossett, J.M. (2011) "Using FTIR spectroscopy to model alkaline pretreatment and enzymatic saccharification of six lignocellulosic biomasses", *Biotechnology and bioengineering*, , pp. n/a-n/a.

28. Sun, X.F., Xu, F., Sun, R.C., Fowler, P. and Baird, M.S. (2005) "Characteristics of degraded cellulose obtained from steam-exploded wheat straw", *Carbohydrate research,* vol. 340, no. 1, pp. 97-106.
29. Tamaki, Y. and Mazza, G. (2011a) "Rapid determination of carbohydrates, ash, and extractives content of straw using attenuated total reflectance fourier transform mid-infrared spectroscopy", *Journal of Agricultural and Food Chemistry,* vol. 59, no. 2, pp. 6356-6352.
30. Tamaki, Y. and Mazza, G. (2011b) "Rapid determination of lignin content of straw using Fourier transform mid-infrared spectroscopy", *Journal of Agricultural and Food Chemistry,* vol. 59, no. 2, pp. 504-512.
31. Tsuchikawa, S. and Siesler, H.W. (2003a) "Near-infrared spectroscopic monitoring of the diffusion process of deuterium-labeled molecules in wood. Part I: Softwood", *Applied Spectroscopy,* vol. 57, no. 6, pp. 667-674.
32. Tsuchikawa, S. and Siesler, H.W. (2003b) "Near-infrared spectroscopic monitoring of the diffusion process of deuterium-labeled molecules in wood. Part II: Hardwood", *Applied Spectroscopy,* vol. 57, no. 6, pp. 675-681.
33. Watanabe, A., Morita, S. and Ozaki, Y. (2006) "Temperature-dependent structural changes in hydrogen bonds in microcrystalline cellulose studied by infrared and near-infrared spectroscopy with perturbation-correlation moving-window two-dimensional correlation analysis", *Applied Spectroscopy,* vol. 60, no. 6, pp. 611-618.
34. Yonenobu, H., Tsuchikawa, S. and Sato, K. (2009) "Near-infrared spectroscopic analysis of aging degradation in antique washi paper using a deuterium exchange method", *Vibrational Spectroscopy,* vol. 51, no. 1, pp. 100-104.
35. Zhang, L., Li, D., Wang, L., Wang, T., Zhang, L., Chen, X.D. and Mao, Z. (2008) "Effect of steam explosion on biodegradation of lignin in wheat straw", *Bioresource technology,* vol. 99, no. 17, pp. 8512-8515.

Chapter 7

Characterisation of morphology and surface information of pre-treated wheat straw and correlation to saccharification in enzymatic hydrolysis

7.1 Introduction

Change in specific surface of biomass reflects the effectiveness of the pre-treatment to open up the fibrous structure and enhance the accessibility of enzyme in subsequent hydrolysis. Microscopic assessment of pre-treated biomass can give direct observation of the refinement but difficult or time consuming to assess the openness of the structure and obtain representative quantifications. Potentially, simple measurement of specific surface area of biomass can be used as an indication in monitoring and control of pre-treatment process. BET nitrogen gas absorption method has been used to determine the surface area of wheat straw (Chesson, Gardner and Wood, 1997). Water vapour and dye sorption have also been used for surface chemistry characterisation of lignocelluloses (Lee, Teramoto and Endo, 2010; Lee, Teramoto and Endo, 2009; Klemm, 1998) and cellulose type of materials (Ougiya , 1998; Inglesby and Zeronian, 1996). However, it is necessary to compare these methods based on surface absorption of different medium (nitrogen, water vapour and dye) so as to understand the difference in absorption mechanisms, the accuracy of measurements and correlation to the output of enzymatic hydrolysis for selection of them, if necessary.

In this study, samples from different extrusion and steam explosion pre-treatments were included so as to assess the efficiency of the pre-treatments. Surface area measurements from all three sorption methods from these samples were compared with reference to electron microscopic observations of the pre-treated biomass. In addition, crytallinity information for the involved sample was also included to investigate the relationship of crytallinity and the effectiveness of pre-treatment. The characterisations were then correlated to yields of glucose in subsequent enzymatic hydrolysis.

7.2 Results and Discussion

All the samples used in this chapter have been prepared and analysed as per detailed in sub-section 3.2, 3.3 and 3.8.8, Chapter 3. **Table 7.1** summarised the sample IDs with brief descriptions of the pre-treatment conditions (see sub-section 3.2 more details) .

Table 7.1: Summary of samples and pre-treatments

Sample IDs	Pre-treatment Conditions
RWS	Wheat straw as-received without any pre-treatment.
WCB10008	RWS pre-soaked in water (at straw: water =1:2) at ambient temperature for overnight and extruded at screw speed of 100 rpm and temperature 50°C.
WCB11008	Ground straw, GWS pre-soaked in water (at straw: water=1:2 w/w) at ambient temperature overnight and extruded with the extension die, at screw speed range of 100 rpm and temperature profile 30, 50, 70, 150, 150 and 150°C.
WCB10009	RWS pre-soaked in NaOH solution at ambient temperature overnight (straw:water =1:2 resulting in 4% NaOH on dry mass of straw) and extruded at screw speed of 100 rpm and temperature 50°C
WCB10009W	WCB10009 washed and rinsed with water as per sub-section 3.2.
W11	RWS (straw: water = 1:0.7) steam exploded after holding at 220°C and 22.2 bar for 10 minutes holding time .

7.2.1 SEM observations of morphology before and after various treatments

The main purpose of pre-treatment is to liberate cellulose from the surrounding lignocellulosic biomass so as to maximise the exposure of cellulose to subsequent enzymatic hydrolysis. SEM images in **Figure 7.1** reveal change in straw morphology before and after the pre-treatments. **Figure 7.1a** shows an almost intact outer surface of the RWS which has a surface damage (due to the straw cutting process) in the epidermis to allow a view of internal parenchyma and lumens. **Figure 7.1b**, shows steam exploded wheat straw (W11) with severe physical disruption. The twin-screw extrusion pre-treatment with (WCB10009) and without NaOH (WCB10008 and WCB11008) had further modified the structure of the RWS as shown in **Fig. 7.1c – e**, which reveals the effect of size reduction of straw. Evident of removal of fractionated portion seen in the **Figure 7.1f** for washed sample of WCB10009.

The outer surface had been destroyed with exposed epidermal cell by the extrusion treatment as in **Figure 7.1b** and **Figure 7.1c**. Some of the fibers with serrations at the edges were observed. In **Figure 7.1e**, the extrusion pre-treatment with NaOH conditioning had further disrupted the straw vessel with noticeable broken lumen, vascular bundle and annular ring. After washing, some long fibers with diameter approximately 5 μm were observed (**Figure 7.1f**). The conventional steam explosion with a high temperature and pressure combination had effectively opened up the structure of RWS. This pre-treatment had led to more cellulose fibers exposed. As no formal separation stage was imposed on W11, there is a mixture of cellulose fibers with fractionated components (such as fractionated lignin and hemicelluloses) present.

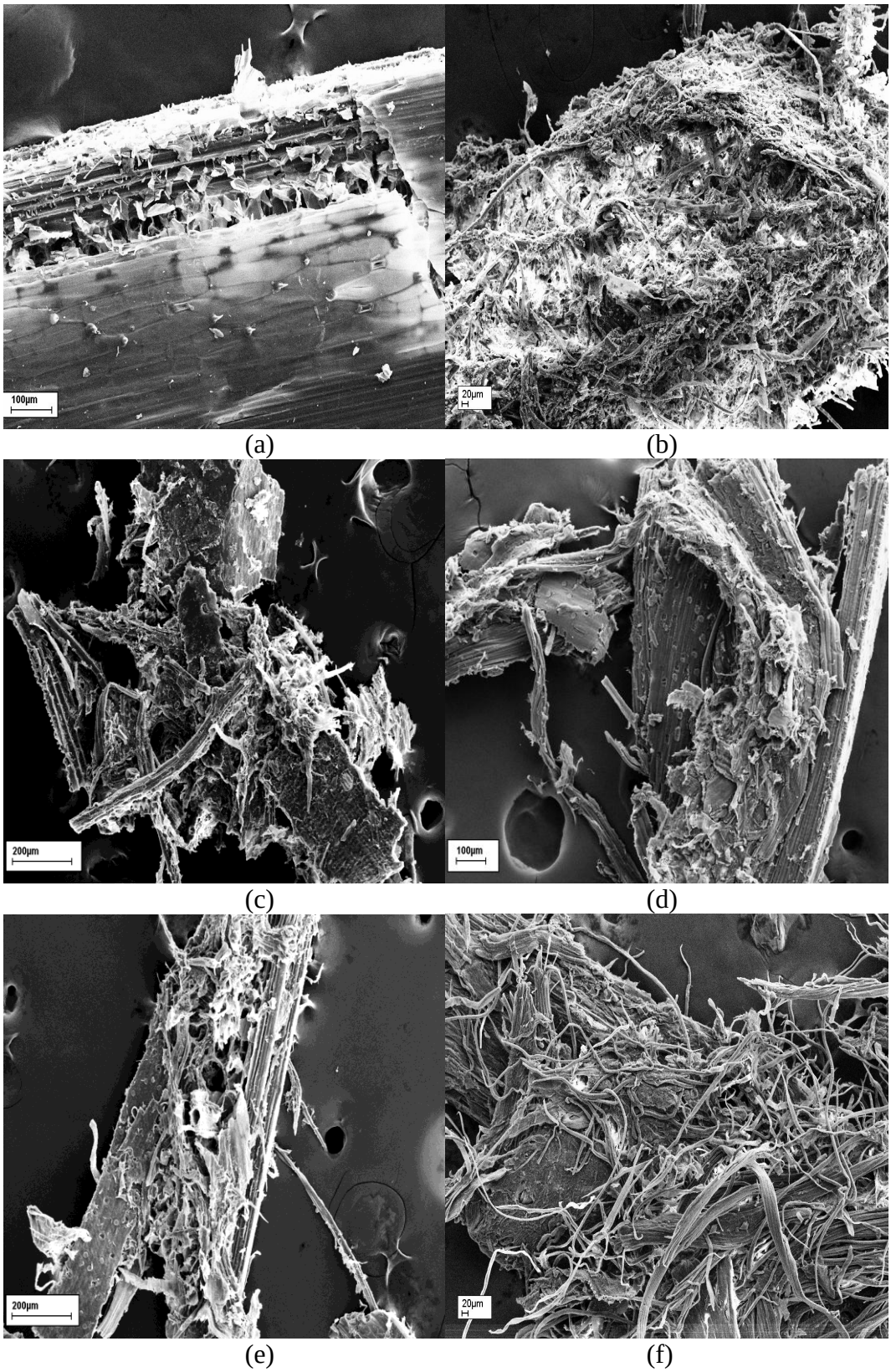

Figure 7.1 : SEM showing morphology of RWS and pre-treated straw samples:
a) RWS,
b) W11 – steam exploded wheat straw at severe pre-treatment condition,

c)WCB10008 – extrusion with no NaOH at low temperature,
d) WCB11008 – extrusion with no NaOH but with modified temperature profile,
e) WCB10009 – extrusion with NaOH at low temperature,
f) WCB10009 – washed WCB10009.

7.2.2 Crystallinity index

The crystalline portion of the cellulose fiber gives rise to coherent x-ray scattering that exhibits a characteristic spectral pattern while the amorphous components of the fiber exhibit a far less coherent scattering whose intensity lies between the background scattering and that of crystalline lattice (El Oudiani , 2009**).** The crystallinity index can be calculated based on the Equation 1 (sub-section 3.8.7, Chapter 3). The diffractogram of RWS and various pre-treated straws were obtained and superimposed for comparison about the impact of the pre-treatments on crystallinity of the substrates (see **Figure 7.2**). The diffraction patterns are showing more on cellulose I allomorph with major diffraction peaks of the (101), (10$\bar{1}$), (002) and (040). The peak intensity at 2θ around 22° usually corresponding to 002 lattice plane for crystalline lattice (Kaushik, Singh and Verma, 2010). For all the pre-treated straw (except WCB10009W), a narrow peak at ~ 26.5° was observed. The intensity of this peak increased with the increase of severity of the pre-treatments:

W11 > WCB10009 > WCB10008

Zhang *et al.* (2012b) reported that this additional peak was due to the new crystal structure caused by recrystallsation. With this observation, the actual crystallinity index for W11 and WCB10009 should be even higher than the reading recorded in **Table 7.2** if the crystalinity calculation included the peak at ~ 26.5°. The crystallinity indices for the samples was summarised in **Table 7.2**. Crystallinity for a majority of the samples are at around 35%. Crystallinity for WCB10009W has been washed to remove those fractionated lignin and hemicellulose. The substrate is expected to be slightly higher in cellulose content, hence resulted a crystallinity index of ~ 50%. Apart from this sample, there is no apparent change in crystalinity among the treatments. Zhang *et al.* (2012a and 2012b) and Lee *et al.* (2010) stated that extrusion improved enzymatic saccharification by inducing fibrillation on biomass at micro or nano scale without

dissipating energy to destroy the crystallinity and thus yield in enzymatic hydrolysis may not be sensitive to crystallinity change.

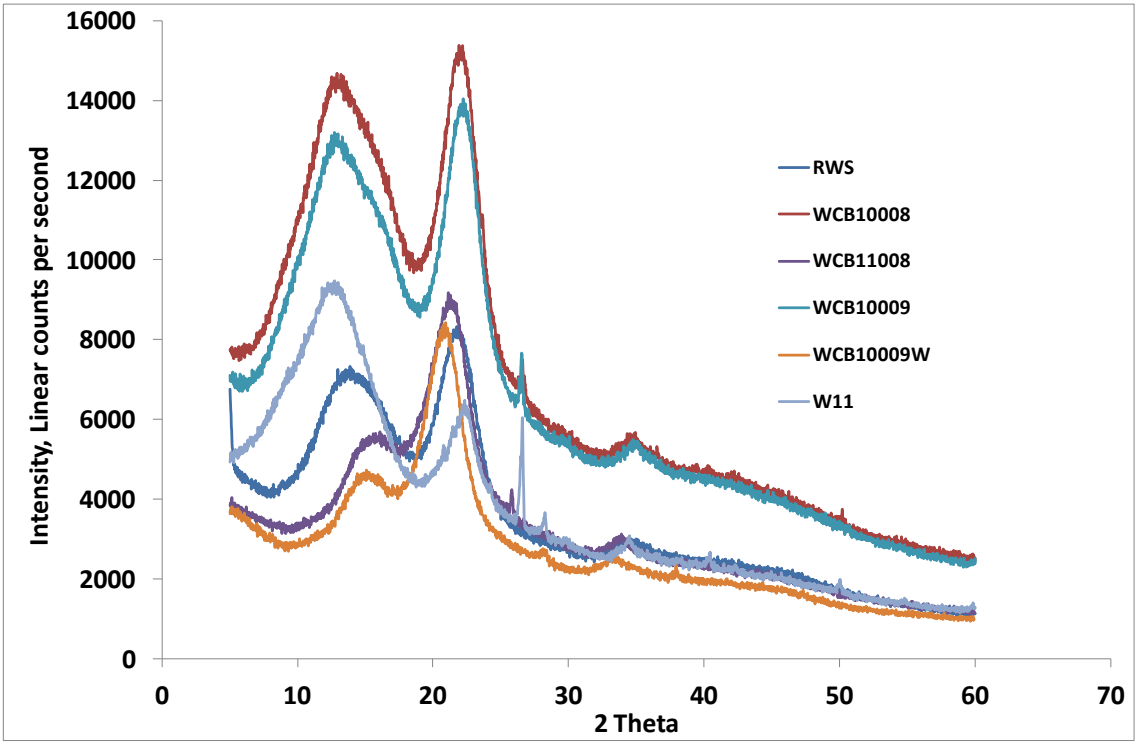

Figure 7.2 : X-ray diffractograms for RWS and straws after various pre-treatments (refer Table 7.1 for sample description).

Table 7.2 : Crystallinity index of cellulose from RWS and various pre-treated straws (Table 7.1).

Sample	Crystallinity, %
RWS	35.60
WCB10008	35.50
WCB11008	42.50
WCB10009	37.50
WCB10009W	50.00
W11	32.30

7.2.3 Specific surface area, SSA

Specific surface area for RWS and various pre-treated straws were examined with BET Nitrogen sorption, DVS and Dye sorption methods as described in sub-section 3.8.7, Chapter 3. **Table 7.3** summarise results of specific surface area readings, water sorption capacity and amount of dye adsorbed at equilibrium.

Table 7.3 : Specific surface area and relevant sorption data obtained from DVS, BET(N_2) and Dye sorption methods.

Sample	Dynamic Vapour Sorption		BET	Dye sorption	
	SSA DVS (m^2/g)	Water Sorption Capability (%)	SSA N_2 (m^2/g)	SSA Dye (m^2/g)	Dye adsorbed (mg/g)
RWS	173.45	23.93	0.71	3.00	1.68
WCB10008	137.70	28.00	1.09	3.33	1.82
WCB11008	161.30	23.96	1.39	3.10	1.72
WCB10009	174.79	59.62	0.78	3.33	1.81
WCB10009W	177.55	24.33	0.97	3.68	1.92
W11	98.63	43.00	3.49	-*	2.47

Note : * SSA can't be calculated owning to that the dye was fully absorbed as explained in sub-section 7.2.3.1.

The BET (N_2) and dye sorption methods suggest a general consistent trend of increase of SSA with the intensity of treatment observed in SEM (sub-section 7.2.1). There is considerable difference in absolute values of SSA from each method for the same sample. However, the absolute value of SSAs is of secondary importance in the case here in comparison with the trend of variation in SSA as it is a crude estimate relying on departure from the assumed single molecular layer absorption and size of single molecules without consideration to their packing configurations or interactions. The trend in SSA from DSV is inconsistent with the other two methods and hence necessary to discuss characteristics in more detail for each method to explain further.

7.2.3.1 SSA using Organic Dye Sorption

Organic dye Congo Red (CR) is known to be able to adsorb specifically to the surface of cellulose molecules according to Langmuir's adsorption theory (Ougiya , 1998; Inglesby and Zeronian, 1996). The area occupied by a CR molecule was calculated on the basic of the adsorption model of Woodcock under the assumption that each CR molecule adsorbs in parallel to the cellulose molecule (Ougiya , 1998). As colour of the supernatant vary with straw sample pre-treatment, background correction was carried out and taken into account in absorbance calculation, despite that the UV reading was read at specified wavelength. The result obtained in **Table 7.3** suggest that all treated samples have higher SSA in good agreement with that in BET (N_2). SSA for the steam exploded straw W11 should be the highest since all the CR in the solution (2.48 mg/g) had been completely absorbed (i.e. no CR left in the supernatant to be detected). However, due to the completely absorbed CR, SSA for W11 is not being able to be determined based on the Equation 2 &3 (sub-section 3.8.8.3, Chapter 3). For WCB10009W (the washed straw from extrusion pre-treatment with NaOH (WCB10009), the washing process is believed to have removed the water soluble fractions (hemicelulose, lignin and amorphous region of cellulose) and left a cellulose-rich straw substrate which allows more dye adsorption. This is also supported by the SEM images (**Figure 7.1e**). In comparison, WCB10009, WCB10008 and WCB11008 have similar levels of SSA.

7.2.3.2 SSA from BET Nitrogen Sorption

The data in **Figure 7.3** show that all of the pre-treatments gave statistically significantly (at p=0.05) higher SSA values compared with the untreated straw. Extrusion pre-treated sample WCB10008 and WCB11008 show increase SSA with increase of the severity level of extrusion pre-treatment. WCB10009 is NaOH combined extrusion which is expected to have higher SSA in comparison to WCB10008 and WCB11008. However, the tested SSA is lower than the compared samples. Reason for this could be due to the influence of the fractionated components which pore has been blocked / binded by fractionated hemicelluloses and lignin. The washed sample of WCB10009 was then tested. It shows an increase on the SSA but still lesser when compared with WCB10008

and WCB11008. The harsh steam pre-treatment (W11), gave rise to the highest SSA, with values significantly (at p=0.05) higher than the other treatments, in contrast to that obtained by DVS where SSA was the lowest, but in good agreement with the that derived from the dye determination.

This suggest that the aggressive steam explosion treatment for W11 had disrupted the plant tissue and opening up the cells more effectively than the other pre-treatments, as suggested by and the SEM observations (in **Figure 7.1b**).

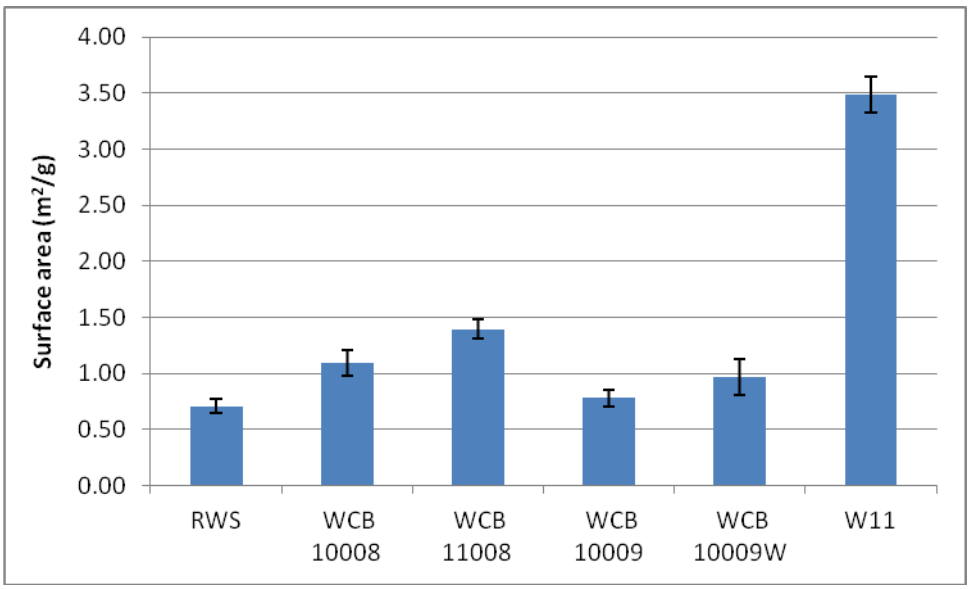

Figure 7.3 : Mean SSA by nitrogen absorbance (error bars show standard deviation)

7.2.3.3 SSA from Dynamic Vapour Sorption, DSV

There exists a considerable discrepancy in the results of SSA (**Table 7.3**) from DSV compared with that for the other two methods and thus deserve more detailed scrutiny. **Figure 7.4** shows the dynamic water sorption behaviour on RWS at 25^{o}C. It can seen that at lower relative humidity (RH < 50%), the uptake is low, but reaches equilibrium fast and at higher RH steps (> 50%), the uptake is relative high, but equilibrium has not

reached. The low uptake at the lower RH is the contribution of suface sorption and the sorption is gradually developing from the surface into the bulk at higher RH, hence high uptake.

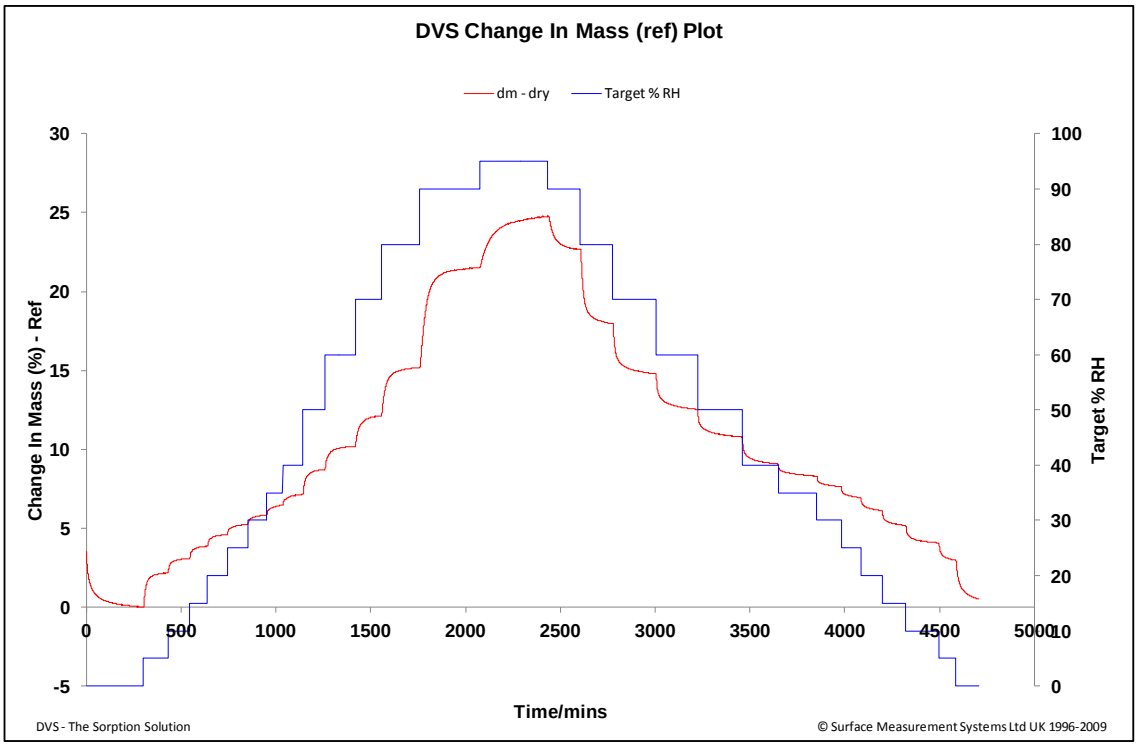

Figure 7.4 : Dynamics water sorption onto the raw wheat straw, RWS at 25^{o}C

The corresponding isotherms in **Figure 7.5** show a mixed Type II/III absorption behaviour, indicated by low initial sorption and substantial uptake at higher RH. The Type II behaviour indicates a more or less surface monolayer sorption mechanism which makes BET surface calculation feasible via the water sorption measurement (organic solvents, e.g. octane, are usually used for BET surface area measurements by DVS). Since biomass pre-treament is, generally speaking, an aqueous thermal process, water sorption is therefore preferable. The hysterisis of the desorption further verifies the bulk sorption. The BET plot is shown in **Figure 7.6**, which indicates a specific surface area of 173.45 m^2/g.

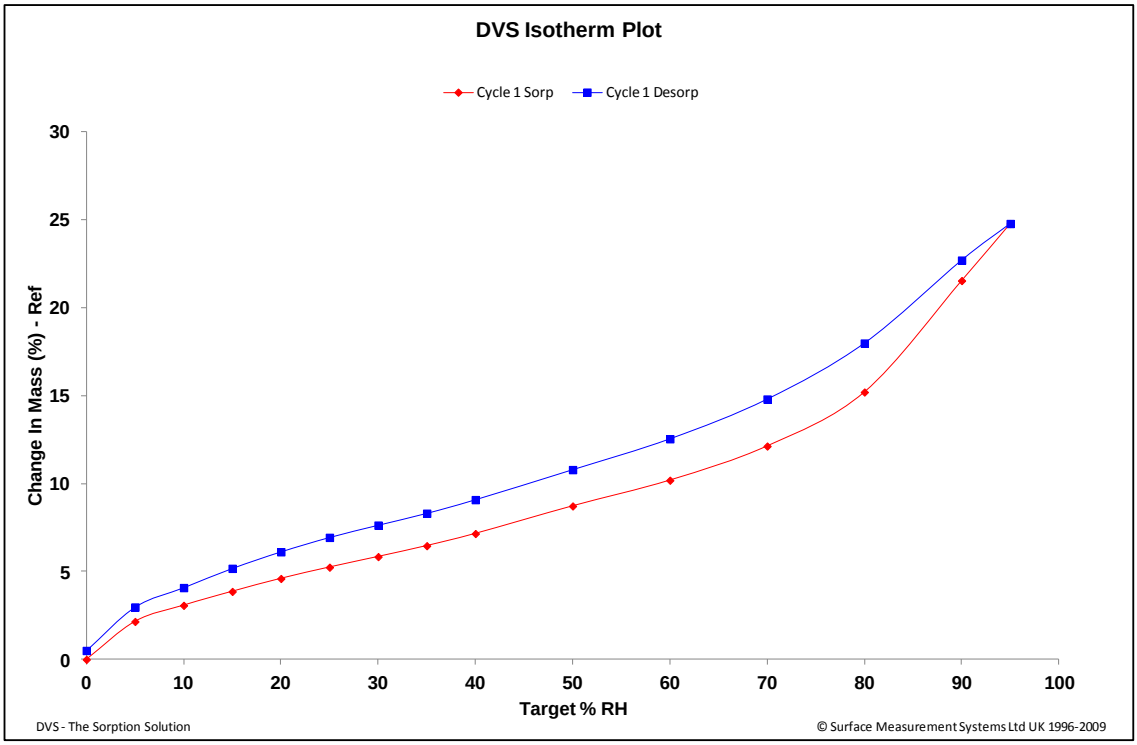

Figure 7.5 : Isotherm of water sorption on raw wheat straw, RWS at 25°C.

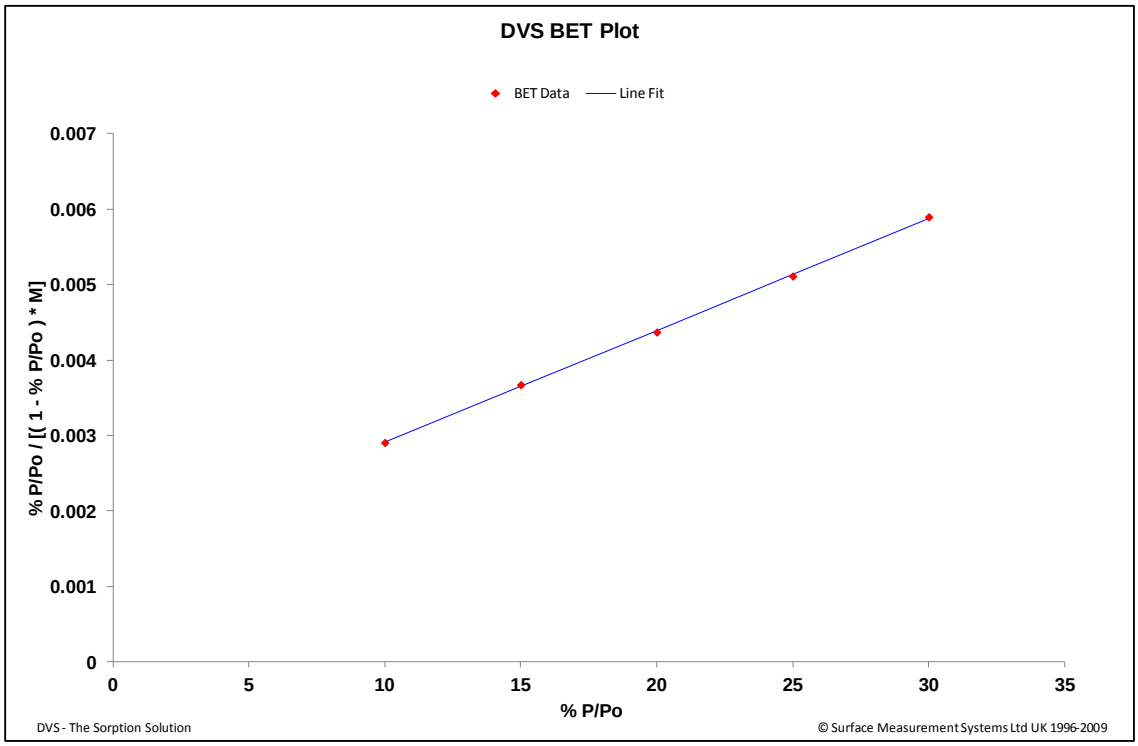

Figure 7.6 : BET plot of water sorption on the raw wheat straw, RWS at 25°C

The water sotption measurements were also performed on other two pre-treated samples (WCB10009 and WCB10009W as detailed in **Table 7.1**) with the same experimental conditions. A superimposed plot of the isotherms for the three samples is shown in **Figure 7.7**. All isotherms show a similar mixed Type II/III absorption behaviour, especially at lower RH (< 40%) where the suface sorption is dominant. This indicates that the surface hydrophilicity of wheat straw does not change significatly before and after the pre-treatment, which is a little bit out of expectation as in general, surface hydrophilicity should be improved due to the removal of the waxes on the straw surface during the pre-treatment and the isotherm shape should be more Type II like. However it cannot be simply concluded that the waxes were not efficiently removed by the pre-treatment as opposed to the proves by the FTIR analysis (in Chapter 4, 5 and 6) and hydrophilicity is also dependent on the fibre type of the biomass. So a further investgation is needed.

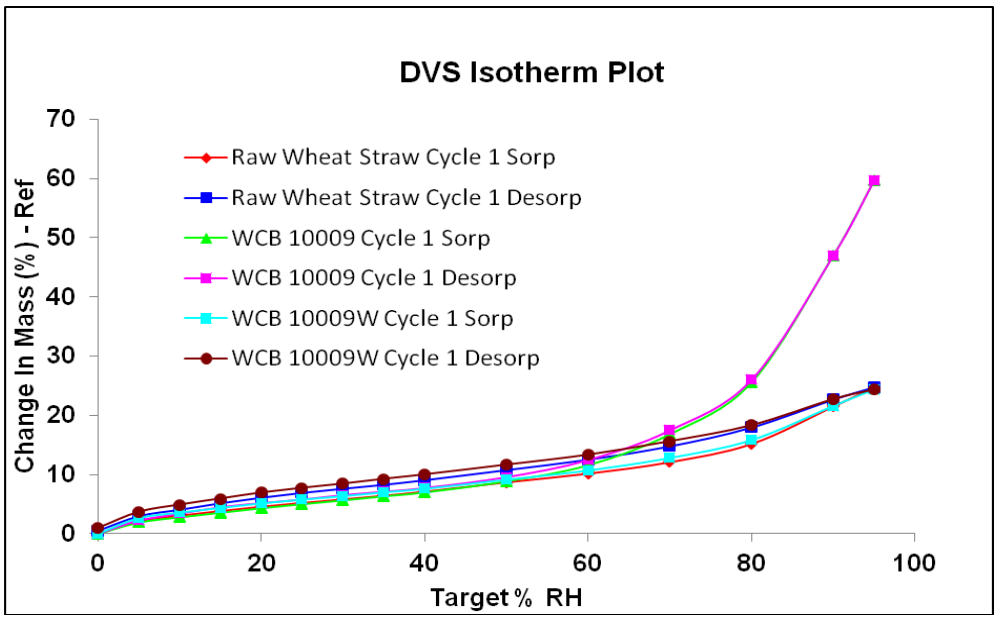

Figure 7.7 A superimposed plot of isotherms of the three samples (RWS, WCB10009 and WCB10009W) showing both absorption and deabsorption.

In terms of total uptake at 95% RH (see **Table 7.3** under water sorption capability), the pre-treated sample of WCB10009 has an uptake of 59.62% which is much higher than 23.93% of the untreated sample (RWS), indicating an open-up of more accessible sites to water molecules, which will be beneficial to subsquent hydrolysis process. Since

most reactants, including water can mainly penetrate amorphous region and the surface of crystalline cellulose, so the uptake of water is also an indication of amorphous content of the biomass, i.e. the higher uptake, the higher amorphous content. Unlike other two samples (RWS and WCB10009W), the water sorption behaviour on the pre-treated sample WCB10009 does not show hysteresis. This is probably due to the swelling of the pores in the material, hence less capillary force.

Comparing the isotherm of the raw wheat straw sample with that of the pre-treated sample WCB10009W, one can see that their isotherms are more or less identical and the total uptake at 95% RH is 24.76% and 24.33%, respectively. The low uptake of the pre-treated and washed sample (WCB10009W) is likely due to the post pre-treatment wash with water, which is expected to remove, in part, amorphous cellulose as it is much more soluble than crystalline cellulose. The similarity in hysteresis of the untreated sample (RWS) and the pre-treated sample (WCB1000W9) implies that the modification to pore size mainly takes place in the amorphous region of the cellulose.

Comparing the isotherm of the sample W11, WCB10008 and WCB11008,(**Figure 7.8, 7.9 and 7.10**) one can see that the isotherms for W11 and WCB10008 are similar and does not show hysteresis compared with WCB11008. The absence of hysteresis is probably due to swelling of the pores in the material, hence less capillary force. This has further impacted on the reading on SSA for both samples.

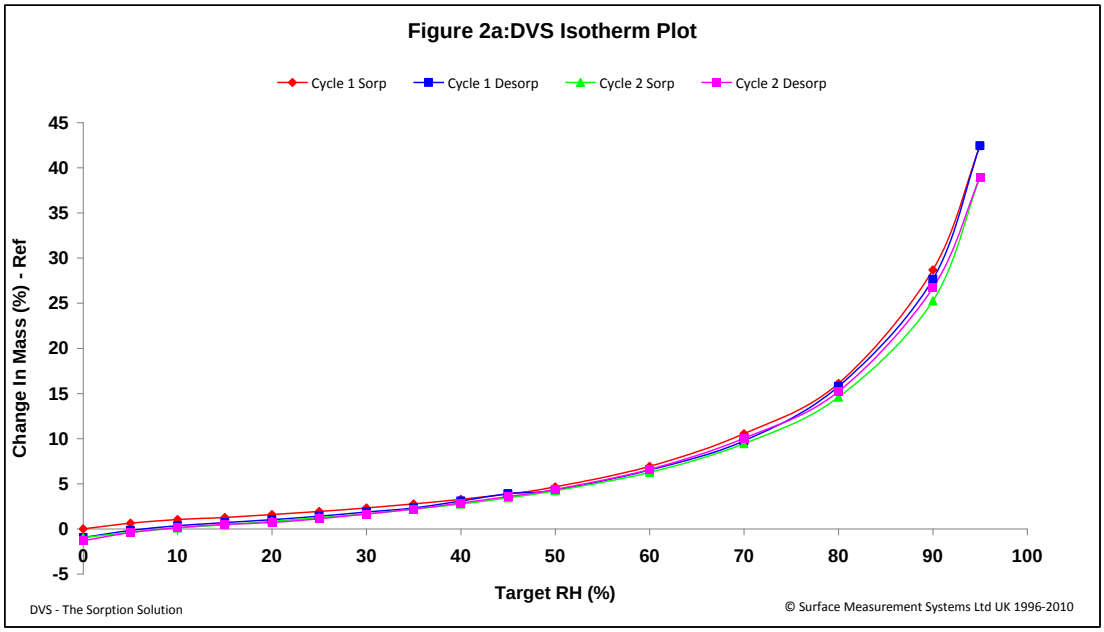

Figure 7.8 : Isotherm of water sorption on steam exploded wheat straw sample W11 at 25 °C

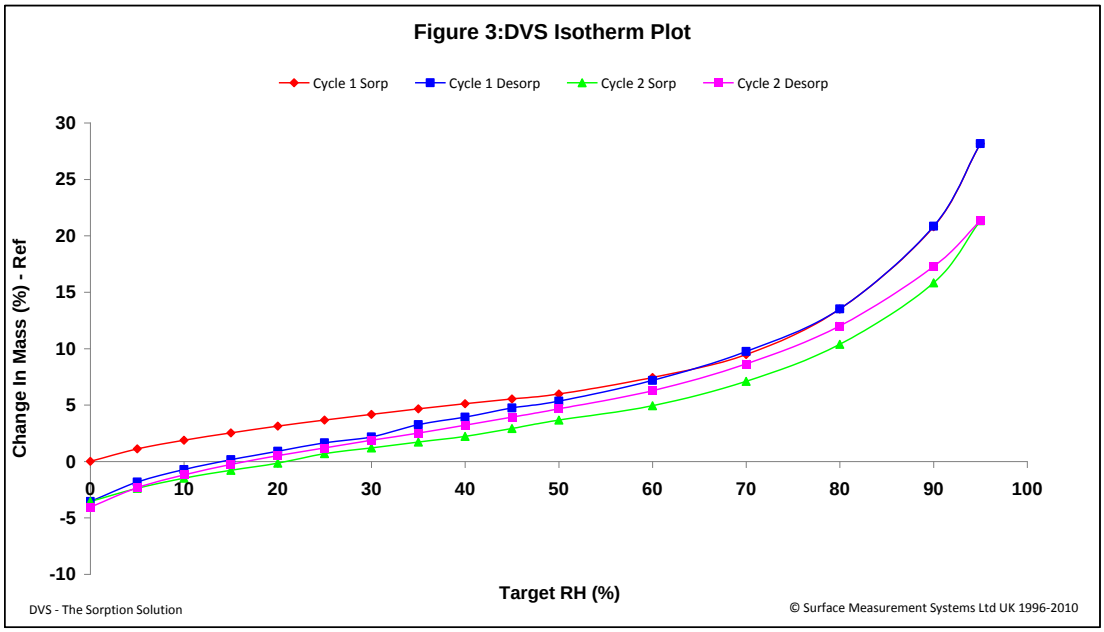

Figure 7.9 : Isotherm of water sorption on extrusion treated wheat straw sample WCB10008 at 25 °C.

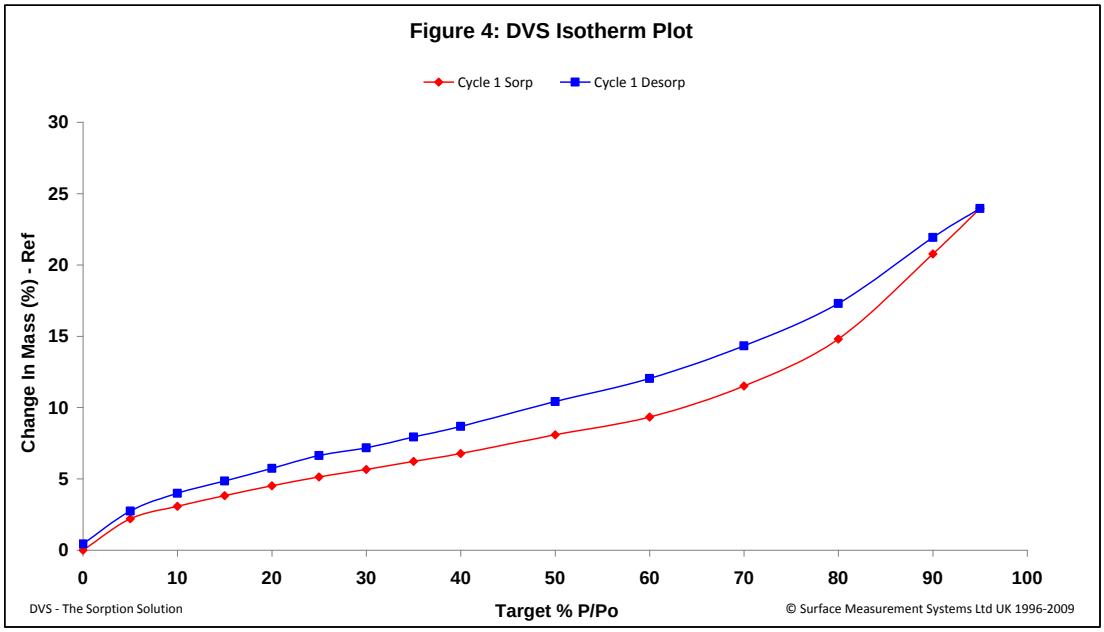

Figure 7.10 Isotherm of water sorption on ground and extrusion treated wheat straw sample WCB11008 at 25 °C.

The results of SSA values for all the above mentioned samples summarised in **Table 7.3.** It suggests that pre-treatment for WB10009 and WBC10009W increases the specific surface area hence presents more accessible sites to hydrolytic reaction which is expected to directly help sugar yield. However, SSA for W11, WCB10008 and WCB11008 are unexpectedly lower than the RWS although the SEM observation showed otherwise. This is discussed further below.

Although the BET equation can be applied to any adsorption system where there is no adsorbate – adsorbate interactions, highly polar adsorbates such as water tend to have very strong adsorbate-adsorbate interactions and may adsorb preferentially at specific adsorption sites. In order to further support the surface area data on the straw samples, the isotherms have been fitted to the Young and Nelson isotherm model using the Surface Measurement System's Isotherm Suite, which contains a wide range of theoretical and semi-empirical equations to fit sorption isotherms. By deconvoluting the isotherms to monolayer and multilayer, the Young and Nelson model produces a term related to the strength of vapour interaction with the surface (*E* term), amount of vapour on the surface (*A* term) and amount of vapour in the bulk (*B* term).

Figures 7.11 and **7.12** show plots of the Young and Nelson components (given in **Table 7.4**) for samples RWS and WCB10009, respectively. The Young and Nelson parameters show that the surface interactions between the treated sample WCB 10009 and water molecules are significantly higher than the interactions of water and the untreated RWS sample. As a result of the enzymatic pre-treatment of sample WCB 10009 the water adsorption is considered to take place on the surface of the inner pores/cracks rather than on the exterior surface of the material. Therefore, increase in the accessible site of straw to enzymatic activity will be resulted from the increase in substrate-water interaction (the higher constant *E*) and the specific surface area.

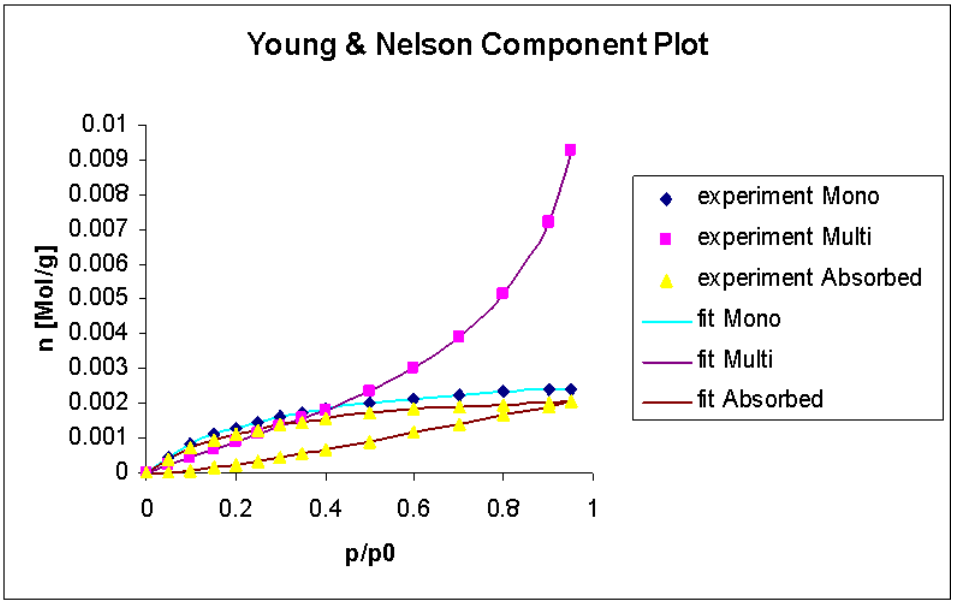

Figure 7.11 : The Young and Nelson component plots for the untreated RWS sample

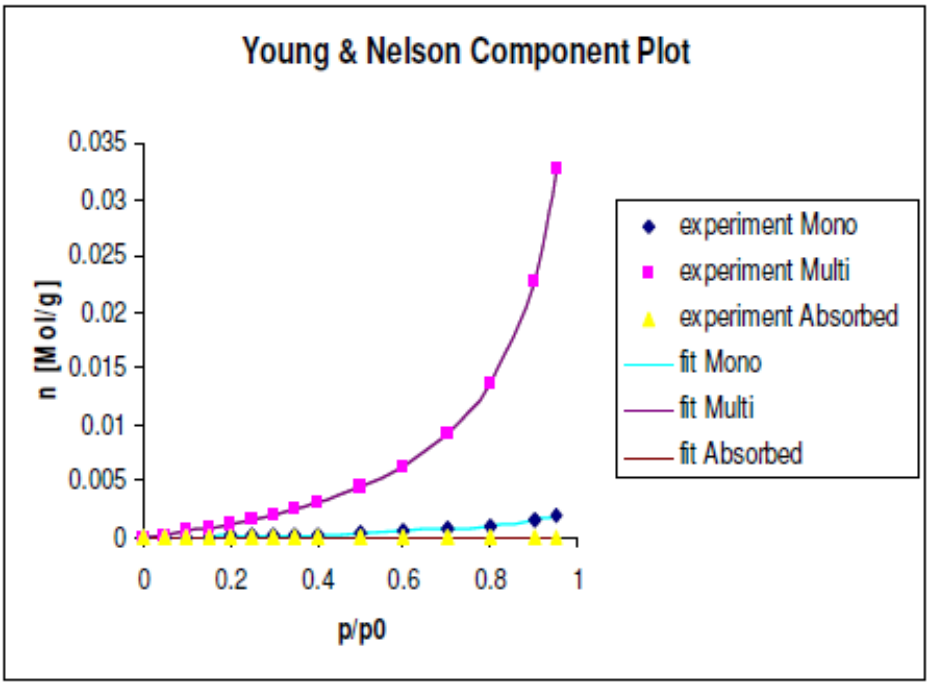

Figure 7.12 : The Young and Nelson component plots for the treated straw sample WCB 10009.

Table 7.4 : BET specific surface area and the Young and Nelson parameters obtained for Samples RWS and WCB10009.

Sample ID	BET specific surface area (m^2/g)	Young & Nelson Parameter Constant E	Young & Nelson Parameter A (mol/g)	Young & Nelson Parameter B (mol/g)
RWS	173.45	0.22	0.00246	0.002
WCB10009	174.79	5.25	0.00247	3.18×10^{-10}

The Young and Nelson parameters for the W11, WCB10008, WCB11008 were also determined following the approaches and as given in **Table 7.5**. The intensity of substrate-water interactions was found to follow the trend:

W11 > WCB10008 > WCB11008

based on the Young and Nelson sorption constant *E*. It is likely that the exceptional high *E* for sample W11 has introduced significant error in application of BET equation for SSA calculation.

Table 7.5 : BET specific surface area and Young and Nelson parameters for Samples: W11, WCB10008 and WCB11008

Sample ID	BET specific surface area (m^2/g)	Young & Nelson Parameter Constant E	Young & Nelson Parameter A (mol/g)	Young & Nelson Parameter B (mol/g)
W11	98.63	8.81	0.001	1.61×10^{-8}
WCB10008	137.70	2.40	0.001	0.004
WCB 11008	161.30	0.23	0.002	0.002

7.2.4 Correlation between SSAs determined by the three methods : DVS, BET (N_2) and dye sorption.

Both sets of SSA data determined by water vapour and dye sorption were compared to the SSA data obtained from BET (N_2) sorption as the later was a conventional method for SSA determination. **Figure 7.13** shows the correlation trend between the methods. It was found that the SSA by BET N_2 having the best correlation with SSA by dye sorption at coefficient correlation at 0.9206. When correlated with water vapour sorption, the correlation index recorded at 0.8277. Whilst compare between water vapour sorption and dye sorption, the correlation index was 0.7692. Even though the correlation index is not yet excellent but it is a positive trending showing the good potential correlation between three different analytical methods for SSA determination. Validity of DVS with water vapour medium as absorbent will need to be investigate further. More sampling point will be able to improve the trending accuracy.

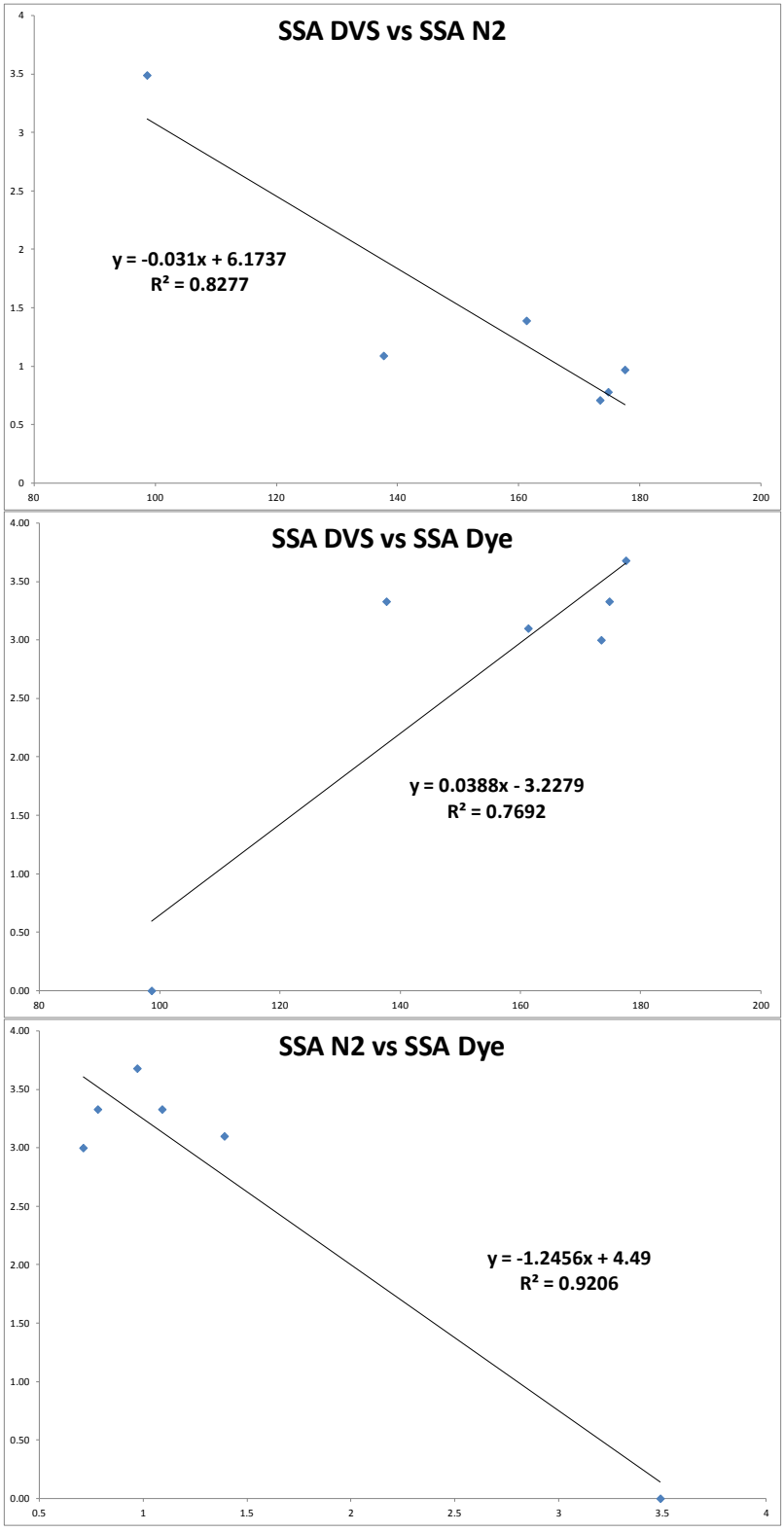

Figure 7.13 : Correlation curve in between SSA N_2, SSA DVS vs SSA Dye

7.2.5 Correlation of SSAs to glucose yield from enzymatic hydrolysis

Table 7.6 showed the summary glucose yield for various involved samples. In comparison with SSAs in **Table 7.3**, it can be seen clearly that :

i. Trend of SSA with pre-treatments from BET (N_2) and dye sorption is in good agreement. DSV as exception owing to discussed reasons in sub-section 7.2.3.3.
ii. Trend of sugar yield with SSA where it has showing a trend where higher SSA the higher the yield. As mentioned in section 7.2.4, more sampling point needed to improve the correlation finding.

Table 7.6 : Glucose yield of selected sample at 10% substrate

No	Sample	g Glc / 100g Glc in Straw %
1	RWS	1.20
2	WCB10008	31.80
3	WCB11008	26.50
4	WCB10009	41.90
5	WCB10009 Washed	39.90
6	W11	45.80

7.3 Summary

Based on the above findings,

i. Morphology information from electron microscope images is well correlated to the SSA findings.
ii. Crystallinity index obtained is not conclusive enough when relates to physical changes and yield of glucose after enzymatic hydrolysis. It is matched with findings from other recent studies (Zhang, Xu and Hanna, 2012; Zhang , 2012; Lee, Teramoto and Endo, 2010).
iii. SSA measurement obtained from the organic dye sorption and BET (N_2) are having similar trend in correlation. However, few SSA readings in DVS measurement were not in range. The data has been further explained with Young & Nelson parameter constant E. Further investigation would be good to understand validity of water vapour as absorbent in DVS for lignocellulosic SSA determination.
iv. More sampling points would help to improve the accuracy of correlation in future work.

7.4 References

1. Chesson, A., Gardner, P.T. and Wood, T.J. (1997) "Cell wall porosity and available surface area of wheat straw and wheat grain fractions", *Journal of the science of food and agriculture,* vol. 75, no. 3, pp. 289-295.
2. El Oudiani, A., Chaabouni, Y., Msahli, S. and Sakli, F. (2009) "Physico-chemical characterisation and tensile mechanical properties of Agave americana L. fibres", *Journal of the Textile Institute,* vol. 100, no. 5, pp. 430-439.
3. Inglesby, M.K. and Zeronian, S.H. (1996) "The accessibility of cellulose as determined by dye adsorption", *Cellulose,* vol. 3, no. 1, pp. 165-181.
4. Kaushik, A., Singh, M. and Verma, G. (2010) "Green nanocomposites based on thermoplastic starch and steam exploded cellulose nanofibrils from wheat straw", *Carbohydrate Polymers,* vol. 82, no. 2, pp. 337-345.
5. Klemm, D. (1998) "Application of Instrumental Analysis in Cellulose Chemistry" in *Comprehensive cellulose chemistry Volume 1* Wiley-VCH, Weinheim ; New York, pp. 187 - 190.
6. Lee, S.-., Teramoto, Y. and Endo, T. (2010) "Enhancement of enzymatic accessibility by fibrillation of woody biomass using batch-type kneader with twin-screw elements", *Bioresource technology,* vol. 101, no. 2, pp. 769-774.
7. Lee, S.-., Teramoto, Y. and Endo, T. (2009) "Enzymatic saccharification of woody biomass micro/nanofibrillated by continuous extrusion process I - Effect of additives with cellulose affinity", *Bioresource technology,* vol. 100, no. 1, pp. 275-279.
8. Ougiya, H., Hioki, N., Watanabe, K., Morinaga, Y., Yoshinaga, F. and Samejima, M. (1998) "Relationship between the physical properties and surface area of cellulose derived from adsorbates of various molecular sizes.", *Bioscience Biotechnology and Biochemistry,* vol. 62, no. 10, pp. 1880-1884.
9. Zhang, S., Keshwani, D.R., Xu, Y. and Hanna, M.A. (2012a) "Alkali combined extrusion pretreatment of corn stover to enhance enzyme saccharification", *Industrial Crops and Products,* vol. 37, no. 1, pp. 352-357.

10. Zhang, S., Xu, Y. and Hanna, M. (2012b) "Pretreatment of Corn Stover with Twin-Screw Extrusion Followed by Enzymatic Saccharification", *Applied Biochemistry and Biotechnology,* vol. 166, no. 2, pp. 458-469.

Chapter 8

Potential utilisation of lignin from biorefinery of lignocelluloses biomass for antioxidant application I : Extraction and evaluation of antioxidant properties

8.1 Introduction

There has been increasing demands for renewable fuels in the global energy sector. Biofuels are expected to meet considerable share of needs of fuels, particularly liquid fuels in road transport and aviation sectors. Lignocellulosic bio-fuel has been intensively researched for the past decades for production of the 2nd generation of bio alcohols (Eisentraut, Brown and Fulton, 2011). However, there exist a significant challenge in economic production of such fuels (de Jong *et al.*, 2012). Currently the relative high cost of biofuels is mitigated by government subsidies and sustainability of biofuels rely on critically co-production of value-added bio-based products such as fine chemicals and biomaterials using the non-cellulose components namely hemicelluloses and lignin. It is estimated that the co-production of bio-based products could generate US$ 10 – 15 bilion per annum of revenue for the global chemical industry (de Jong *et al.*, 2012).

Black liquor generated during paper pulping or the post pre-treatments washing process of lignocelluloses are lignin-rich sources. They would become very valuable resource for conversion to building blocks or fine chemicals instead of being treated as waste effluent during pulp or bioalcohol production.

Lignin from Kraft pulping and bioalcohol pre-treatment processes are good platform of lignin for value added bio-based chemical production. Lignin contains polyphenols and is a three-dimensional amorphous natural polymer composed of phenyl propane units with carbonyl, hydroxyl and methoxyl substitutions (Gregorová, Košíková and Moravčík, 2006; Dizhbite *et al.*, 2004). Lignin was reported to possess high potential

as raw material for sustainable production of chemicals and materials, such as binders, resins, epoxies, adhesives, polyolefins (Ropponen *et al.*, 2011; Mohamad Ibrahim *et al.*, 2010; Stewart, 2008), surfactant (Košíková, Ďuriš and Demianová, 2000) and carbon fibre (Brodin *et al.*, 2012). With the polyphenols in its chemical structure, lignin was also reported for its radical scavenging and antioxidant properties (Dong *et al.*, 2011; Faustino *et al.*, 2010; Dizhbite *et al.*, 2004; Pan X FAU - Kadla, John,F. *et al.*, 0921) and thus explored for application in dietary (Lu, Chu and Gau, 1998) and as additives in polypropylene (Pouteau *et al.*, 2003). For evaluation of antioxidant activity, a method using 2,2-diphenyl-1-picrylhydrazyl (DPPH) as described by Scherer *et al.* (2009) and Faustino *et al.* (2010) is adapted. This method has also been used widely for natural compounds antioxidant activity studies (Maizura, Aminah and Wan Aida, 2011; El Hajaji *et al.*, 2010).

In the present study, both Kraft lignin and wheat straw lignin from the extrusion and steam explosion pre-treatment were fractionated using a range of organic solvents based on the selection with Hildebrand solubility parameter, as described in sub-section 3.6, Chapter 3. The crude lignin and solvent fraction were further characterised with Size Exclusion Chromatography (SEC), UV, FT-IR, ^{13}C NMR, ^{1}H NMR to understand the molecular chemistry of fractionated lignin portion as detailed in sub-section 3.8, Chapter 3. Total phenolic, total lignin (both Klason and acid insoluble) and carbohydrates contents in selected fraction was determined as described in sub-section 3.8 too before evaluation of the antioxidant activity.

Gallic acid, GA was used as a standard reference for the DPPH testing verification. Wingstay L (4-Methylphenol, reaction products with dicyclopentadiene and isobutylene in see **Figure 8.1** (Eliokem, 2012) – is a commercial specialty chemical produced from fossil fuel and commonly in used in rubber and polymer industry as antioxidant. Wingstay L was included in the DPPH testing to serve as a benchmark of industrial reference for the evaluation of the intended application in synthetic rubber gloves.

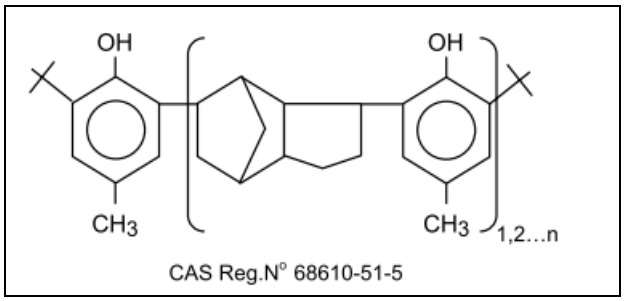

Figure 8.1 : Chemical structure of antioxidant Wingstay L (Eliokem, 2012).

Work for this chapter is divided into two parts,

i. Crude lignin recovery and solvent fractionation

ii. Characterisation analysis and antioxidant application screening

8.2 Results and Discussion

All the experimental details are summarised in Chapter 3. Sample detail and ID were showed in **Table 3.5** and experimental work for crude lignin and solvent fractionation are captured under sub-section 3.5 and 3.6.

In the following sections, discussion is focus on crude lignin and solvent fraction characterisation outcome (see sub-section 8.2.1 to 8.2.4). Findings from the characterisation analysis are correlated to antioxidant screening toward the end of discussion (sub-section 8.2.5).

8.2.1 Solvent fractionation of lignin and molecular weight distribution

Organic solvent fractionation was used to separate various fractions of lignin to have a better understanding about the antioxidant performance of Kraft and wheat straw lignin. The selection of solvents was based on the Hildebrand solubility index and the consideration of stabilizer system in used in the solvent. This is to prevent any potential positive error from the stabilizer (e.g. buthylated hydroxytoluene, BHT) in the antioxidant activity evaluation. Four crude lignins (two Kraft lignins – RH and RF and two wheat straw lignins – REX (wheat lignin via extrusion) and RSE (wheat lignin via steam explosion), as described in **Table 3.5** were subjected to sequential solvent

extraction using a moderately hydrogen bonded (e.g. ethyl acetate, EA) and strongly hydrogen bonded solvent (e.g. methanol, MeOH).

The solvent extraction technique did affecting the yield of fractionation. A comparison example of EA extraction for crude Kraft lignin under this study with both Soxhlet and Soxtec extraction techniques. By using Soxhlet, 5 – 7 wt% of EA fraction can be obtained, but the yield can be ramp up to approximately 20 – 22 wt% of EA fraction when Soxtec being used. This can be attributable to the more aggressive extraction condition in the later with higher cooking temperature. However Soxtec extraction is not considered appropriate for this study as it needs elevated temperature to dry the the extract after each session of extraction. This has to be avoided in this study because high temperature drying might lead to the risk of thermal degradation for phenolic content. Problem of the cellulose thimble tends to weaken under sequential extraction (as explained in sub-section 3.6).

Soxhlet was eventually selected as extraction technique for this study. Yield fraction recovered from the sequential fractionation was presented in **Table 8.1** and illustrated in **Figure 8.2**. One EA and one MeOH fraction were obtained for each of the crude lignin e.g. for crude Kraft lignin H (RH), fraction under EA (named as EH) and fraction under MeOH (named as MH) obtained after sequential fractionation. The fractionation yield depends also on solvent systems used. The extraction with dioxane was aborted due to the observed increase in peroxide content from the use of un-stabilised dioxane. Molecular weight calculation of the lignin fractions was based on derivative lignin against that of the mono-dispersed polystyrene.

Table 8.1 : Fractionation yield, molecular weight averages and polydispersity

Fraction	Yield (wt% over crude lignin)	Mn, g/mol	Mw, g/mol	Polydispersity
EH	7.16	277	834	3.0
EF	5.24	271	858	3.2
EEX	20.2	444	3737	8.4
ESE	21.92	195	596	3.1
MH	11.59	628	2601	4.1
MF	10.28	552	2190	4.0

MEX	**28.66**	**350**	**1662**	**4.8**
MSE	**64.16**	**353**	**1439**	**4.1**

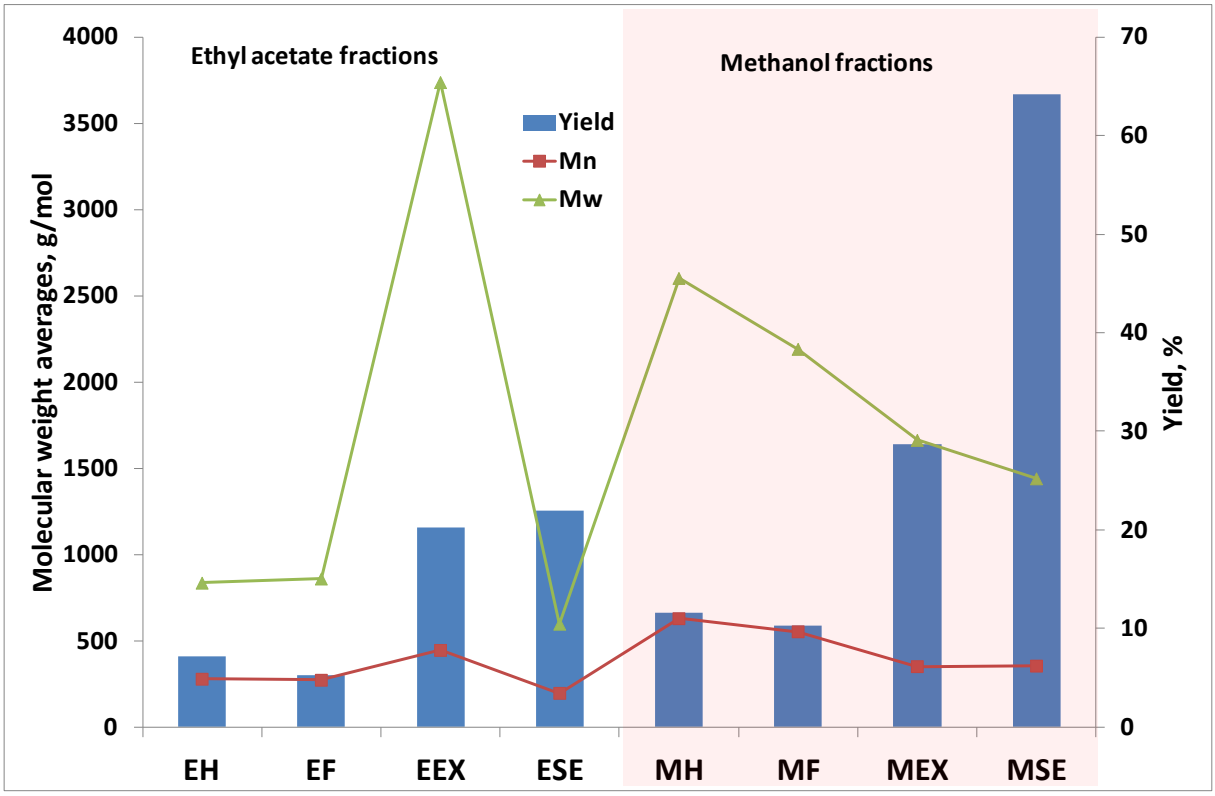

Figure 8.2 : Fractionation yield, molecular weight averages and polydispersity

In general, yield of the soluble fractions is higher from the crude wheat straw lignins in both the solvent categories in comparison with that from the crude Kraft lignins. Unlike the crude Kraft lignins, the crude wheat straw lignins were not purified by acidic water to remove the impurities during the lignin recovery process. Hence, it is known to contain more impurities such as carbohydrates, organic waxes and inorganic salt. Based on the results obtained, lower molecular weight lignin fractions (with Mn = 195 – 277 or Mw = 599 – 858) were found soluble more in organic solvents with moderate hydrogen bonding capacity, e.g. in ethyl acetate with δ_{EA} = 9.1 $(cal/cm)^{1/2}$ while the higher molecular weight lignin fractions (with Mn= 350 – 628 or Mw =1439 – 2601) were found more soluble in solvent with higher hydrogen bonding capacity e.g. in MeOH with δ_{MeOH} = 14.5 $(cal/cm)^{1/2}$. This is in agreement with the findings reported with previous research (Wang, Xu and Sun, 2010; Yuan *et al.*, 2009; Mörck, Yoshida and Kringstad, 1986). Molecular weight reading of EEX was way too high from the

pool of result. Precipitation was observed in the EEX fraction and obvious whitish and brownish portion can be seen. Relatively higher molecular weight (Mn and Mw) was observed for fractions from the solvent fraction of crude Kraft lignins than those from the crude wheat straw lignin. This may be attributable by the higher severity of lignocelluloses treatment condition and thus higher lignin condensation for the crude Kraft lignins (Yuan *et al.*, 2009). The polydispersity for all the fractions measured were wide but a trend of increased from range of 3 to 4 can be observed with increased of molecular weight. This came along with increased yield of lignin fraction too. Similar observation reported by Wang *et al.* (2010), Yuan *et al.* (2009) and Mörck *et al.* (1986). A spike in the MSE fraction yield is believed to be associated with more carbohydrate content in the crude SE wheat straw lignin and was extracted into MeOH. The steam explosion pre-treatment is more severe in comparison to the extrusion pre-treatment as found in Chapter 4 and hence more fractionated carbohydrate is expected in the crude lignin.

8.2.2 UV characterisation, total phenolic and lignin contents

UV spectroscopy has been used to semi-quantitatively determine the purity of lignin or monitor the lignin distribution among various tissues of gymnosperm and dicotyledonous angiosperm with respect to the concentration (Wang, Xu and Sun, 2010; Yuan *et al.*, 2009). The crude lignins and the fraction from EA and MeOH were dissolved in MeOH and UV spectra were obtained in between wavelength 260 – 420 nm. The UV spectra are showed in **Figure 8.3**. The entire spectra exhibit the basic UV spectra for lignin where the maximum absorption coefficient at ~ 280nm. According Yuan *et al.* (2009) and Wang *et al.* (2010), the maximum UV absorption recorded in their work was at ~ 270nm representing non-condensed phenolic groups in the lignin. Yuen *et al.* (2009) commented that shifting of the maximum absorption wavelength could be considered as an indication of syringyl unit content. This explanation is acceptable for wheat straw lignin but not for Kraft lignin. Dence C.W. (Lin and Dence, 1992) used actual absorptivity at 280 nm for quantification of lignin content. Based on this, lignin content in the crude wheat straw lignins and the fractions in the solvents, are estimated to be much lower than that of crude Kraft lignins (**Figure 8.3a**). Same for the lignin content in the fractions of EA (**Figure 8.3b**) and MeOH (**Figure 8.3c**).

The total phenolic and lignin contents in the crude lignin quantified as described in sub-section 3.8.11 and 3.8.12 are shown in **Table 8.2**. Total lignin reported here was a summation of Klason lignin (acid insoluble lignin) and acid soluble lignin while total phenolic content was measure as Gallic acid equivalents, GAE with the Folin-Ciocalteu method. The gap between relative absorption coefficient between the crude Kraft lignins (RH and RF) and wheat straw lignins (REX and RSE) correlate well to total lignin (**Figure 8.3a**) and total phenolic content of the samples (**Table 8.2**). This finding supports further the report from Dence C.W. (Lin and Dence, 1992) as mentioned in above paragraph.

The total phenolic content for the lignin fractions were also measured as described in sub-section 3.8.11 and showed in **Table 8.3**. Based on UV spectra for EA extracted fractions (**Figure 8.3b**), the higher absorption coefficient indicate higher phenolic contents in both EH and EF, respectively while EEX was found to have the lowest phenolic content (**Table 8.3**). This is quite in agreement with the finding in sub-section 8.2.1 which EEX was tested with high molecular weight and high polydispersity index. Total carbohydrate content in crude lignin (RH, RF, REX and RSE) was also reported in **Table 8.2**. Crude wheat straw lignin (REX and RSE) were found with high contents of carbohydrate, this again showed interrelated information on phenolic content and lower absorption coefficient in its UV spectrum (**Figure 8.3a** and **Table 8.2**) and also proven the importance of purification step during lignin recovery (sub-section 8.2.1). The shoulder observed in MEX's UV spectrum at 320nm was believed to associate with hydroxycinnamic acids (p-coumaric and ferulic acids) (Wang, Xu and Sun, 2010). High lignin in crude Kraft lignin was accompanied with low carbohydrate levels.

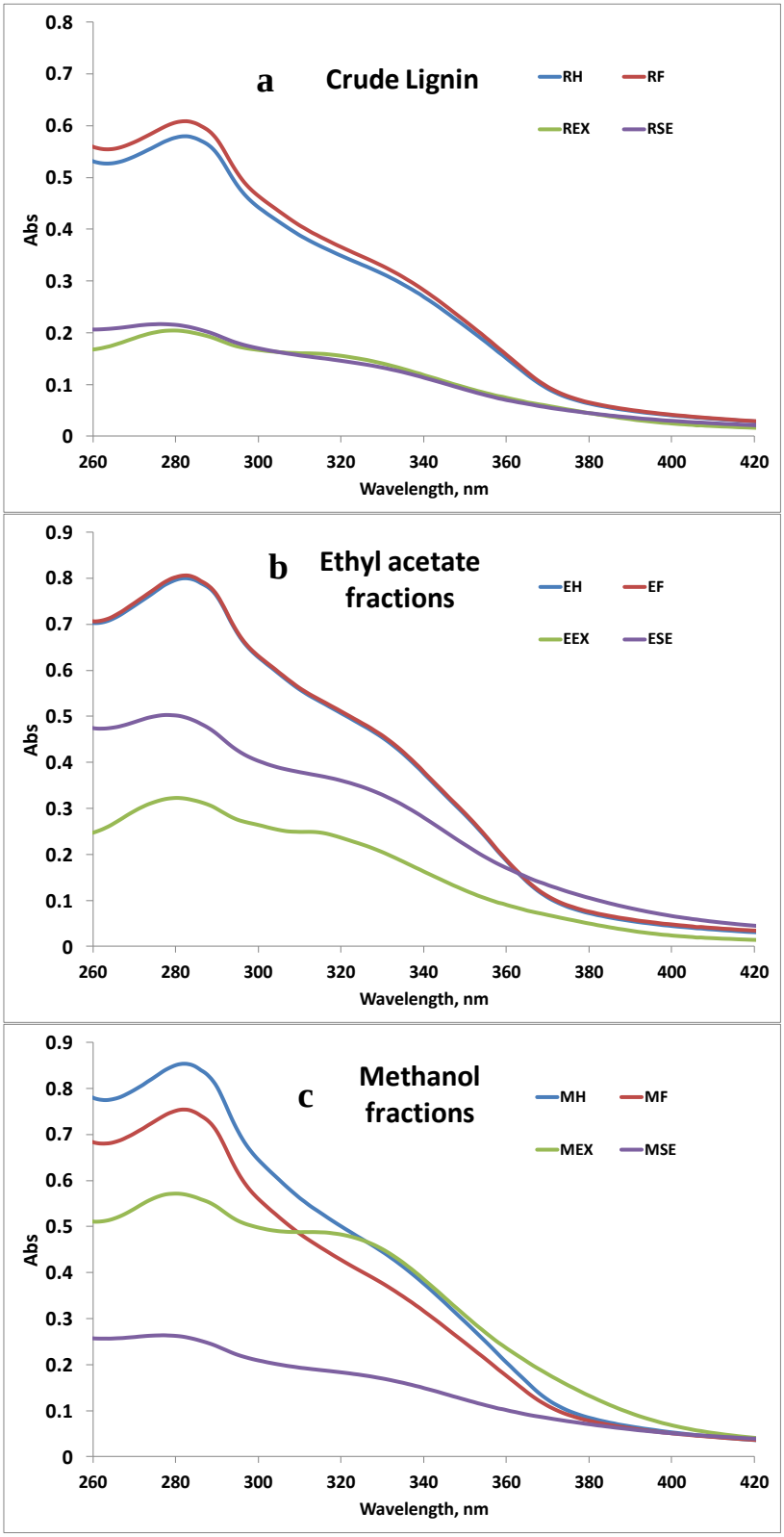

Figure 8.3 : UV spectra for crude lignins and the lignin fractions extracted / dissolved in ethyl acetate and methanol.

Table 8.2 : Total lignin, phenolic and carbohydrate content in the crude lignins

Crude lignin	Klason lignin, ppm	Acid soluble lignin, ppm	Total Lignin, ppm	Total carbohydrate content*, ppm	Total phenolic content, ppm
RH	940	60	1000	9	405
RF	922	59	981	9	374
REX	621	57	678	106	159
RSE	328	89	417	214	159

Note : * Total carbohydrate is a summation of total arabinose, galaktose, glucose, xylose and mannose.

Table 8.3 : Total phenolic content in the lignin fractions

Lignin fraction	Total phenolic content, ppm
EH	383
EF	351
EEX	136
ESE	249
MH	365
MF	395
MEX	218
MSE	115

8.2.3 FTIR analysis

FTIR technique was used to further investigate the structural chemical information on the crude lignins as well as their fractions extracted by solvent. **Figure 8.4** shows the IR spectra for the crude lignins, and those of fractions using EA and MeOH extraction. Kraft lignin RH and RF have almost identical spectra at ~ 1597, 1510 and 1424 cm^{-1} where finger prints of aromatic skeleton vibrations are found (Wang, Xu and Sun, 2010; Yuan *et al.*, 2009) in comparison with the relatively weaker signals from REX and RSE in those regions. This observation was also found in the fractions in EA and MeOH

extraction IR spectra (**Figure 8.4b** and **8.4c**). The bands at ~ 2931 and 2850 cm^{-1} (**Figure 8.4**) arise from the C-H stretching of methyl and methylene groups (Wang, Xu and Sun, 2010). The strong absorption at these two regions for REX indicates existence of high fraction of alkyl methyl and methylene in its structure. Wheat straw lignin from steam explosion (RSE) shows a very significant peak at ~ 1705 cm^{-1} (**Figure 8.4a**) attributable to carbonyl from a formation of keto groups, most likely at C β positions (Li, Gellerstedt and Toven, 2009). Similar signal ~ 1690 – 1712 cm^{-1} is actually significant at wheat straw lignin and slightly lesser in Kraft lignin. In addition, peak signal at ~ 875 cm^{-1} indicates penta-substitution in aromatic rings following lignin condensation caused by the severe steam pre-treatment conditions (Li, Gellerstedt and Toven, 2009).

In spectra obtained from fractions of EA extraction (**Figure 8.4b**), EH and EF are found to contain guaiacyl units associated IR bands at 1270, 1217, 1151 and 1031 cm^{-1} (Yuan *et al.*, 2009). IR bands at 1324 and 1113 cm^{-1} in the spectra from ESE are associated with syringyl structures in the lignin fractions (Yuan *et al.*, 2009).

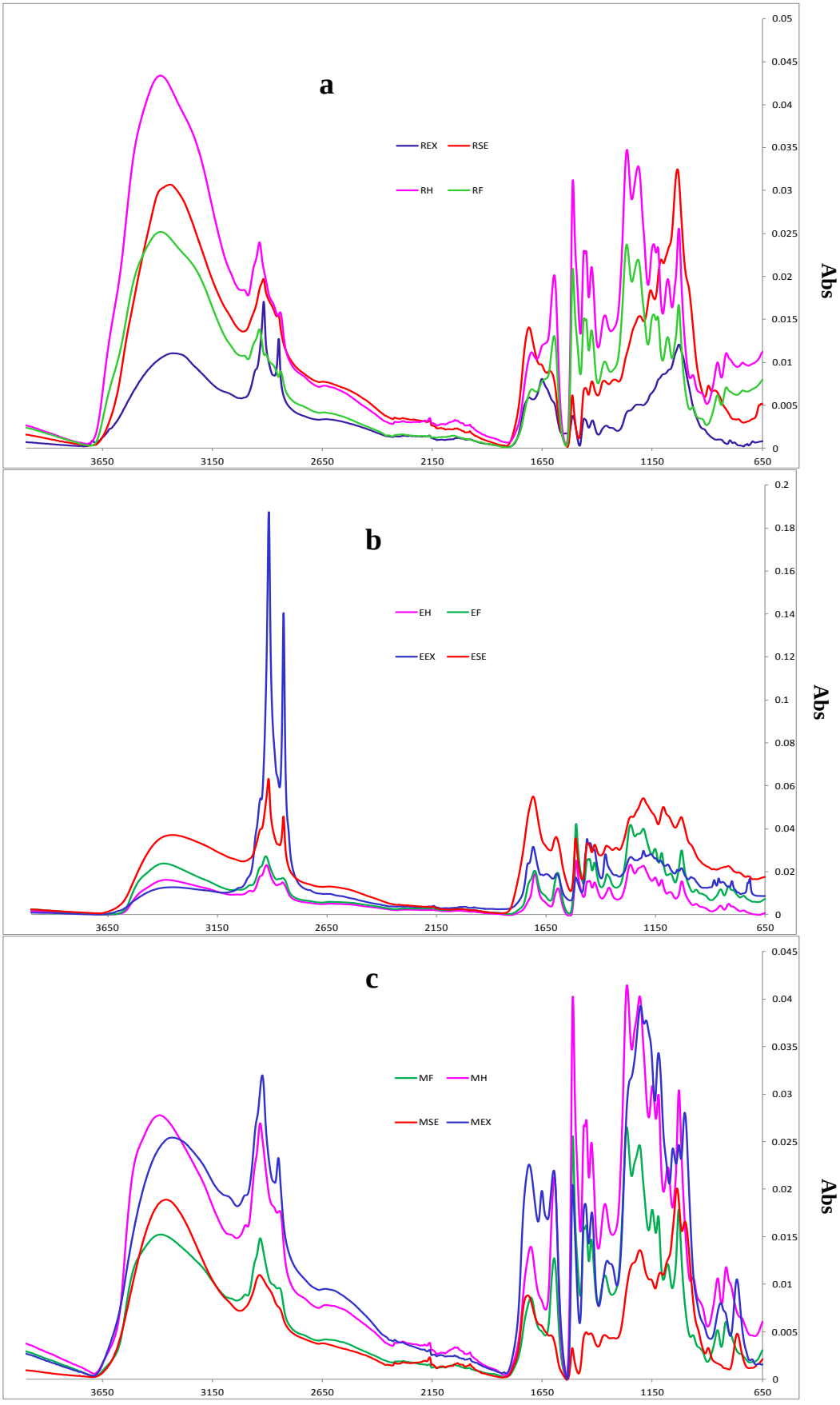
a
REX
RSE
RH
RF
Abs
b
EH
EF
EEX
ESE
Abs
c
MF
MH
MSE
MEX
Abs
3650
3150
2650
2150
1650
1150
650

Figure 8.4 : IR spectra for
- **a) The crude lignins;**
- **b) Fractions from EA extraction;**
- **c) Fractions from MeOH extraction.**

Based on the spectra interpretation as above paragraph, indication of finger prints for lignin aromatic skeleton vibration is in agreement with findings from UV analysis (in sub-section 8.2.2) which more lignin content in RH and RF samples. Lignin signal of guiacyl unit was found on EH and EF fractions. Similar explanation is applied on the spectra for MH, MF and MEX. Those are indications of more lignin in the crude Kraft lignin and the solvent fractions. Lignin signals in MEX are in line with the total phenolic content reported in **Table 8.3**. More carbonyl signal in RSE and REX could be due to the carbohydrates impurities as defined in Table 8.4. Information of alkyl methyl and methylene found in REX could be the indication of more organic hydrocarbon / waxes carried over in the lignin recovery stage.

8.2.4 ^{1}H and ^{13}C NMR spectra

EH and MEX lignin fractions were selected to represent the Kraft and wheat straw lignin for NMR analysis. Both ^{1}H and ^{13}C NMR spectra for each fraction were obtained with the method as described in sub-section 3.8.15 as shown in **Figure 8.5** and **8.6**, respectively. In common (**Figure 8.5**), both fractions show signal at 0.8 to 1.5 ppm, 3.4 to 3.8 ppm and 6.8 to 7.0 ppm, from aliphatic moiety in the lignin, methoxyl protons OCH_3 and aromatic proton for guaiacyl and syringyl units, respectively (Yuan *et al.*, 2009). In addition, EH shows an additional strong signal at 2.0 ppm and 4.0 to 4.1 (in **Figure 8.5a**) from the methyl protons adjacent to double bonds or carbonyl groups and proton γ of β-O-4 (Yuan *et al.*, 2009).

In **Figure 8.6a** and **8.6b**, the peaks at 14.4 to 29.6 are associated with the saturated hydrocarbon structures in the aliphatic side-chains (Wang, Xu and Sun, 2010). It follows by the OCH_3 signal for syringyl and guaiacyl units at ~ 55 – 56 ppm. C-3 / C-5 in *p*-coumaric acid esterified and C-3, C-4 in guaiacyl etherified signals were also picked up for both fractions at ~ 115 – 116 ppm and ~ 148 ppm, respectively. Apart from the above mentioned signals, EH also shows additional signals at ~ 112, ~118 –

121 and ~ 129 ppm which indicated the C-2 in Guaiacyl etherified and C-6 in Guaiacyl and p-hydroxylphenyl present in the structure.

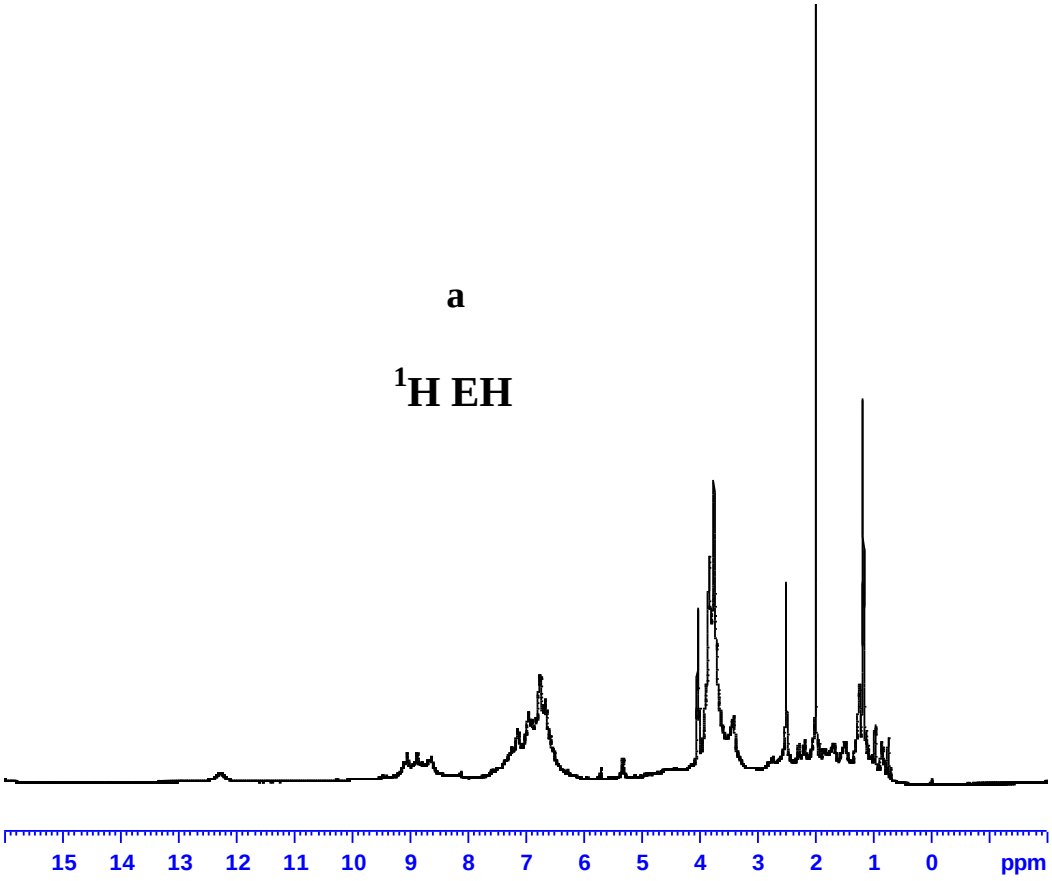

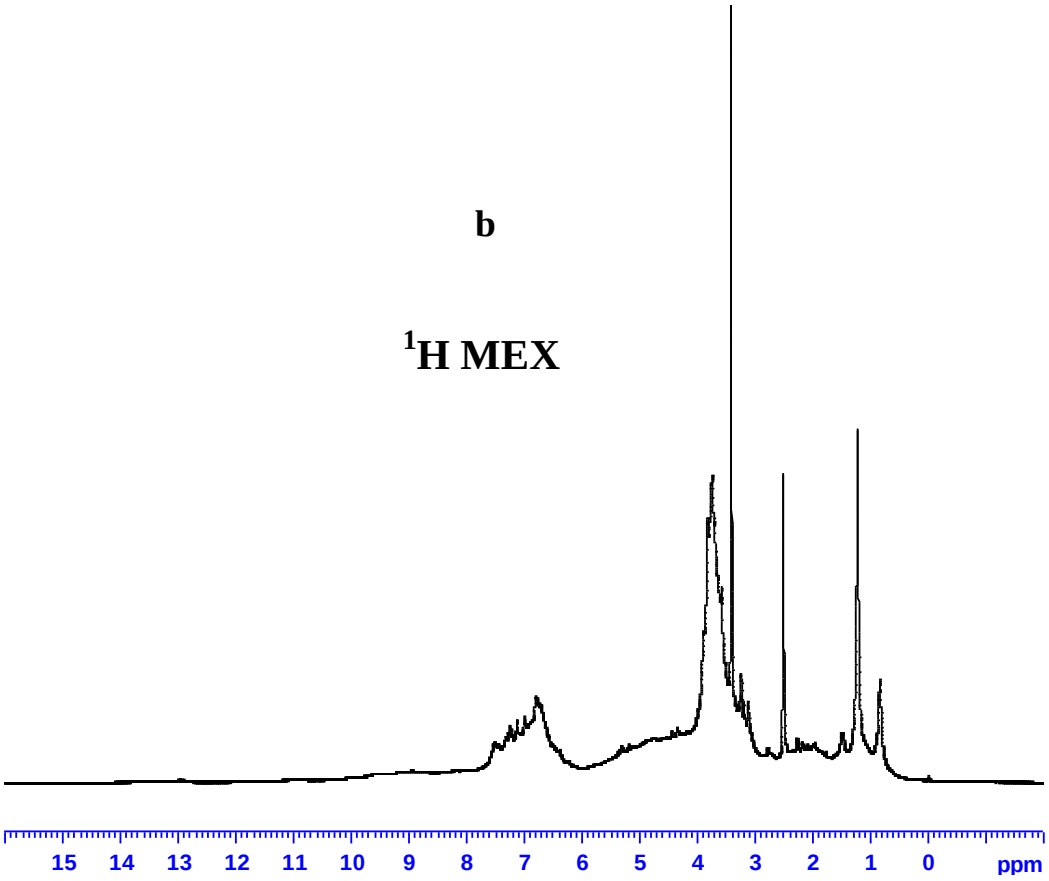

Figure 8.5 : The ^{1}H NMR spectra for a) EH and b) MEX

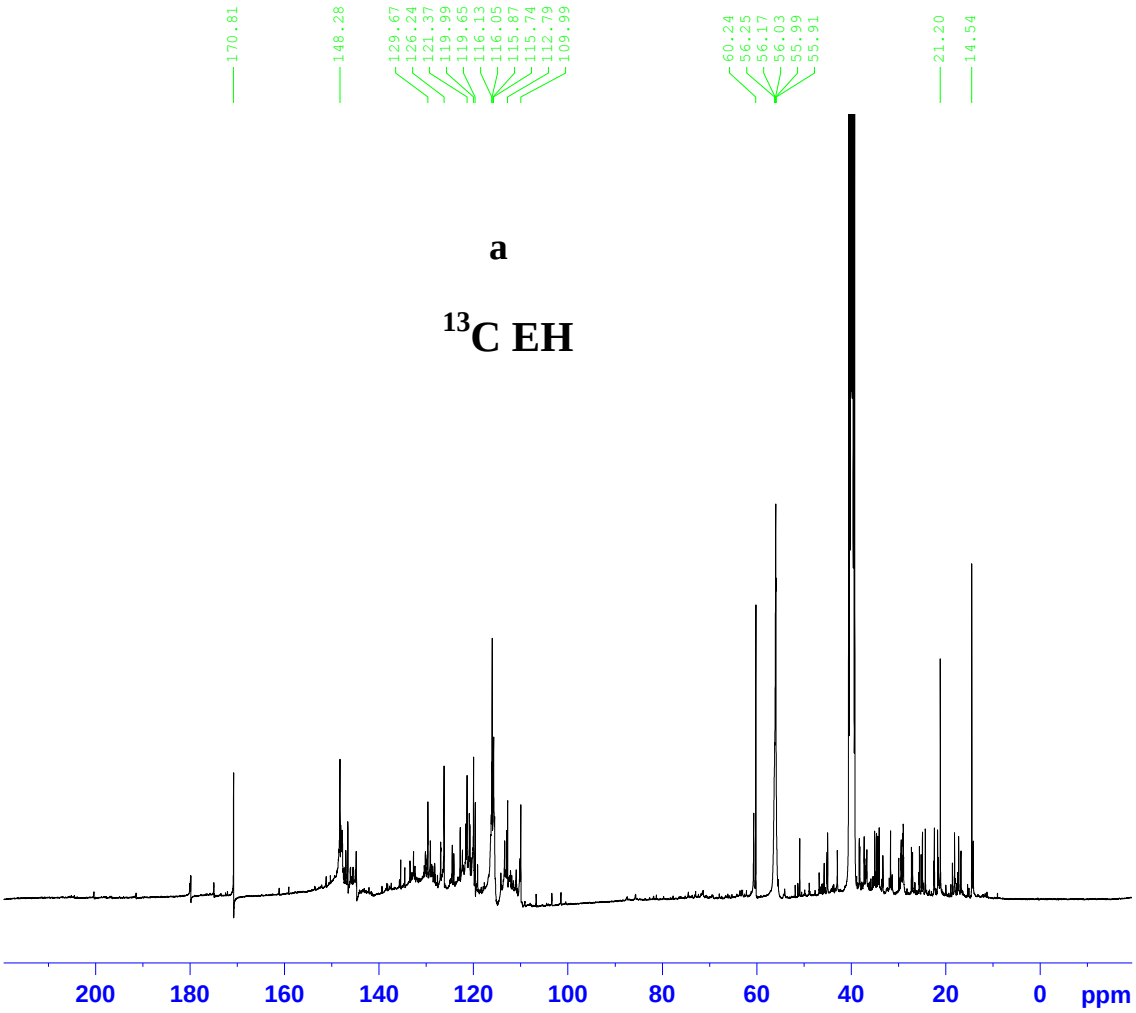
170.81
148.28
129.67
126.24
121.37
119.99
119.65
116.13
116.05
115.87
115.74
112.79
109.99
60.24
56.25
56.17
56.03
55.99
55.91
21.20
14.54
a
13C EH
200
180
160
140
120
100
80
60
40
20
0
ppm

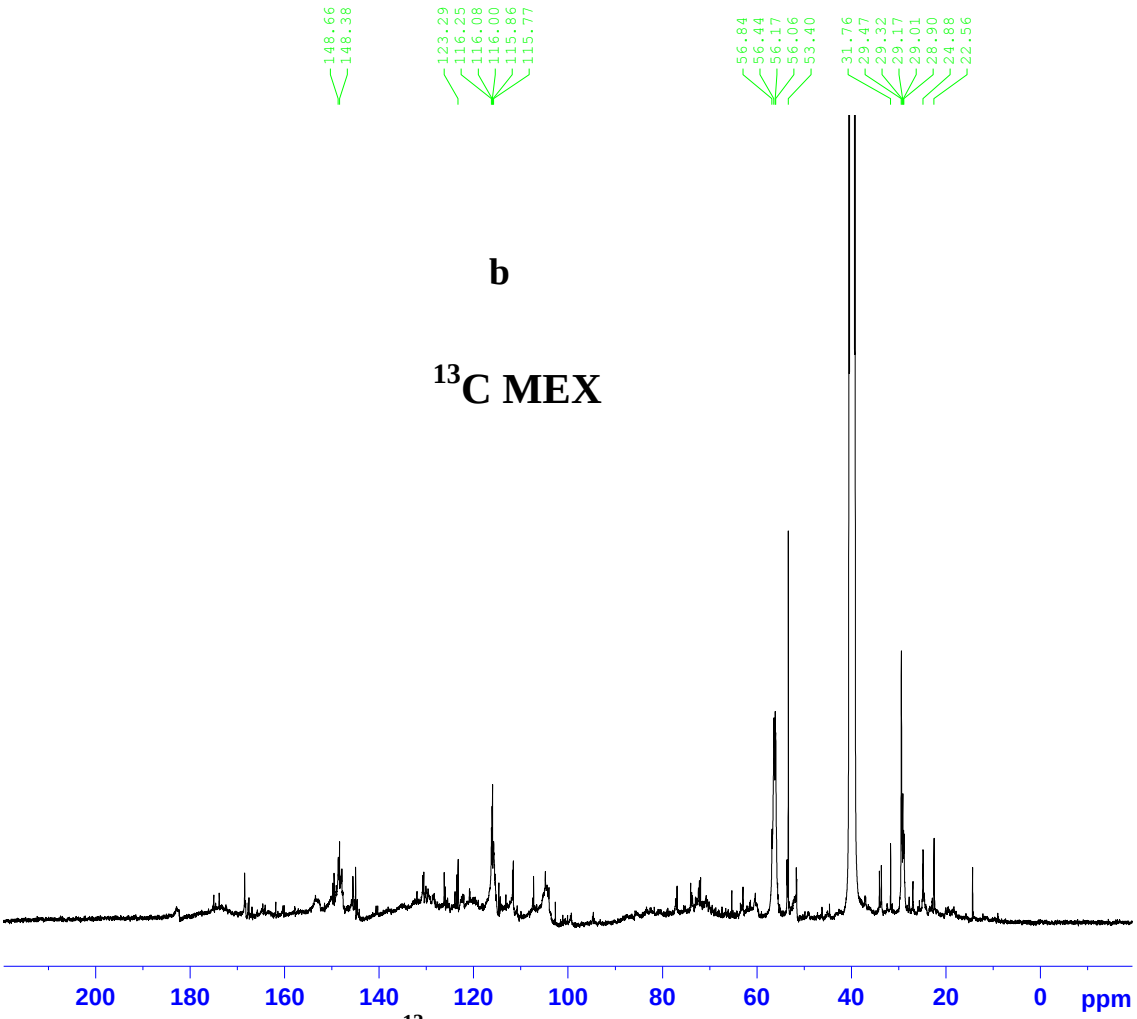

Figure 8.6 : The ^{13}C NMR spectra for a) EH and b) MEX

The limited sample under this section is mainly due to the limited resources on the analysis. The samples are selected based on the best antioxidant performance (to be discussed in following sub-section 8.2.5) from both type of lignin under this study. Information obtained for this sub-section is mainly for lignin structural reference to help on the characterisation analysis.

8.2.5 Screening of antioxidant activity

The above analysis in sub-section 8.2.1 to 8.2.4 obtained necessary information on the key chemical contents in the crude lignins and their solvent fractions. DPPH method as described in sub-section 3.8.16 was then used to determine the antioxidant activity of each sample. Radical scavenging activity in percentage of inhibition (I%), as described in sub-section 3.8.16 is used to compare the activity in radical scavenging. The

antioxidant activity index (AAI) can be calculated with consideration of the mass of DPPH and the mass of the tested compound in the reaction, resulting in a value for each compound, independent of the concentration of DPPH and sample used (Scherer and Godoy, 2009) and described in more details in sub-section 3.8.16. A scale/criteria for screening of antioxidant activity is adapted as follows from previous studies (Faustino *et al.*, 2010; Scherer and Godoy, 2009):

- Poor antioxidant activity when AAI < 0.5
- Moderate antioxidant activity when 0.5 < AAI < 1.0
- Strong antioxidant activity: when 1.0 < AAI < 2.0
- Very strong antioxidant activity when AAI > 2.0

Gallic acid, GA was also tested alongside AAI for method verification purpose. The AAI for GA was tested as 34 in our study, the AAI value for GA was reported as ~ 27 and 30 by Scherer & Godoy (2009) and Faustino et al (2010). As the intended application of the lignin is to provide alternative and bio-based antioxidant for rubber and polymer industry, the commonly used industrial antioxidant – Wingstay L was used as a control for benchmarking and comparison purposes.

Figure 8.7 shows the percentage of inhibition (I%) of the various lignin samples along with the control (Wingstay L) which reaches 83%. Higher I% was recorded in the Kraft lignins and their fractions obtained from EA and MeOH extractions while the crude wheat straw lignin and their fractions show relatively low I% due to high impurities as discussed earlier in 8.2.2.

AAI was calculated with consideration of the mass of DPPH and the mass of the tested compound in the reaction, resulting in a constant for each compound, independent of the concentration of DPPH and sample used (Scherer and Godoy, 2009). Based on the AAI values shown in **Figure 8.8**, all the crude Kraft lignin and their fractions show at least strong antioxidant activity. Among them, fractions obtained from EA extraction (EH and EF) gave very strong antioxidant activity. Similar finding was reported on study of Carob tree leaves (El Hajaji *et al.*, 2010). On the wheat straw lignin, ESE and MEX show moderate antioxidant activity from the wheat straw lignin fractions. The rest were

all under performed. Impurities present in the wheat straw lignin and its fractions was believed to be the main reason for the low performance (García *et al.*, 2012) as the crude wheat straw lignin had not been purified during the lignin recovery stage and thus contain considerable amount of impurities and low content of the active phenol groups, as quantified earlier in 8.2.2. The Low performance of EEX and MSE was related to carry over of impurities from crude lignin during solvent extraction stage as already discussed in sub-section 8.2.1 and 8.2.2. The antioxidant performance could have improved with the inclusion of purification stage during crude lignin recovery process.

Figure 8.7 : The percentage of inhibition, I % for the crude lignins (RH, RF, RSE and REX), fractions by EA extraction (EH, EF, EEX and ESE) and MeOH extractions (MH, MF, MEX and MSE) in comparison with the control (Wingstay L or WL).

The I% and AAI were also further correlated with the total phenolic content (TPC) obtained as described in sub-section 8.2.2 (see **Figure 8.9** and **8.10**). Good linear regression was found (with coefficient correlation, r^2 being 0.9928 and 0.9328, respectively) for relationships between I% and AAI versus TPC. It confirms that the

antioxidant performance is very much dependant on the phenolic content in the lignin or fractions.

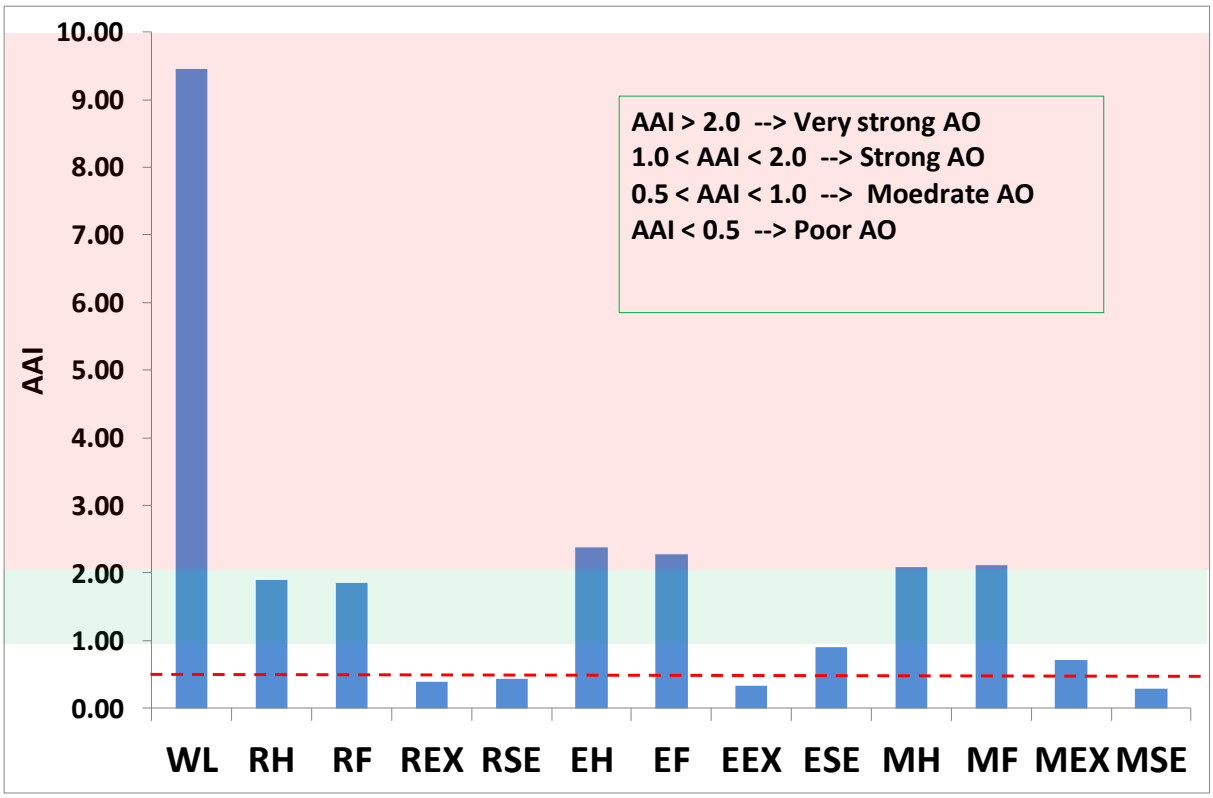

Figure 8.8 : AAI for the crude lignins (RH, RF, REX and RSE), fractions by EA extraction (EH, EF, EEX and ESE) and MeOH extractions (RH, MF, MEX, MSE) in comparison with the control (Wingstay L or WL).

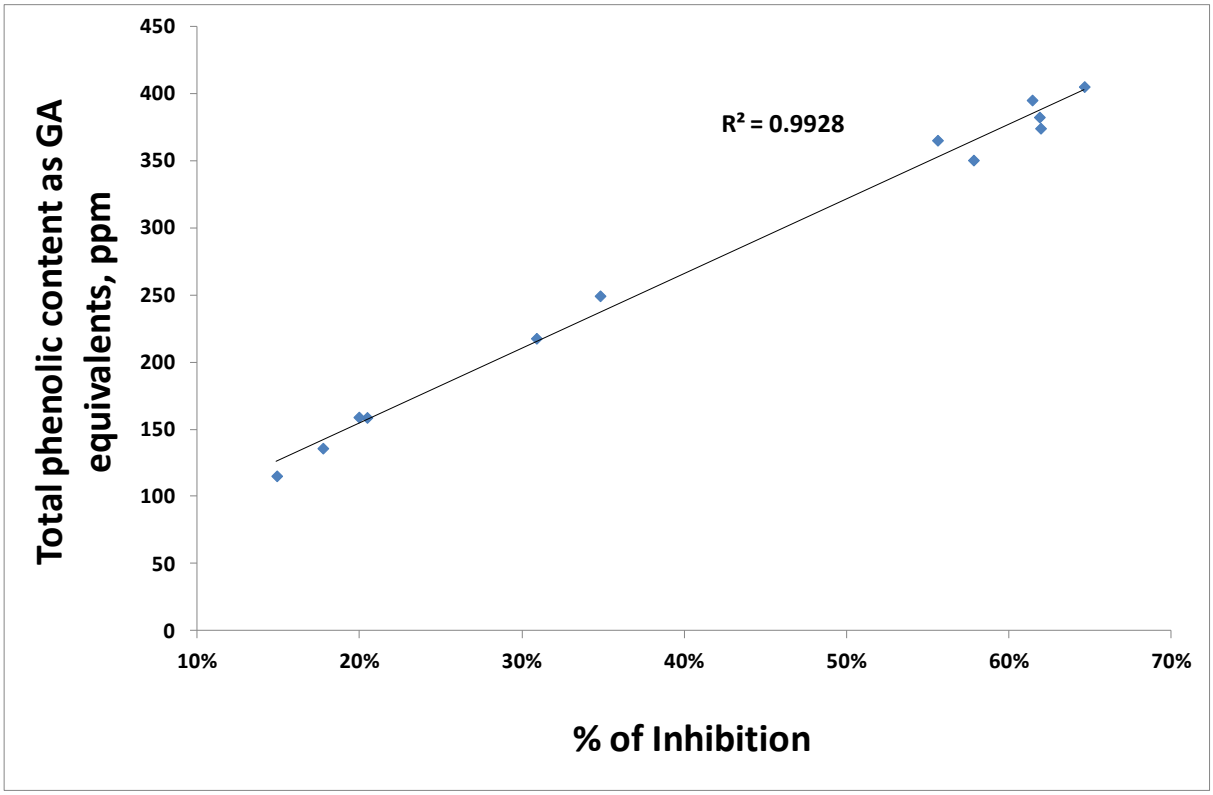

Figure 8.9 : Correlation between I% and TPC

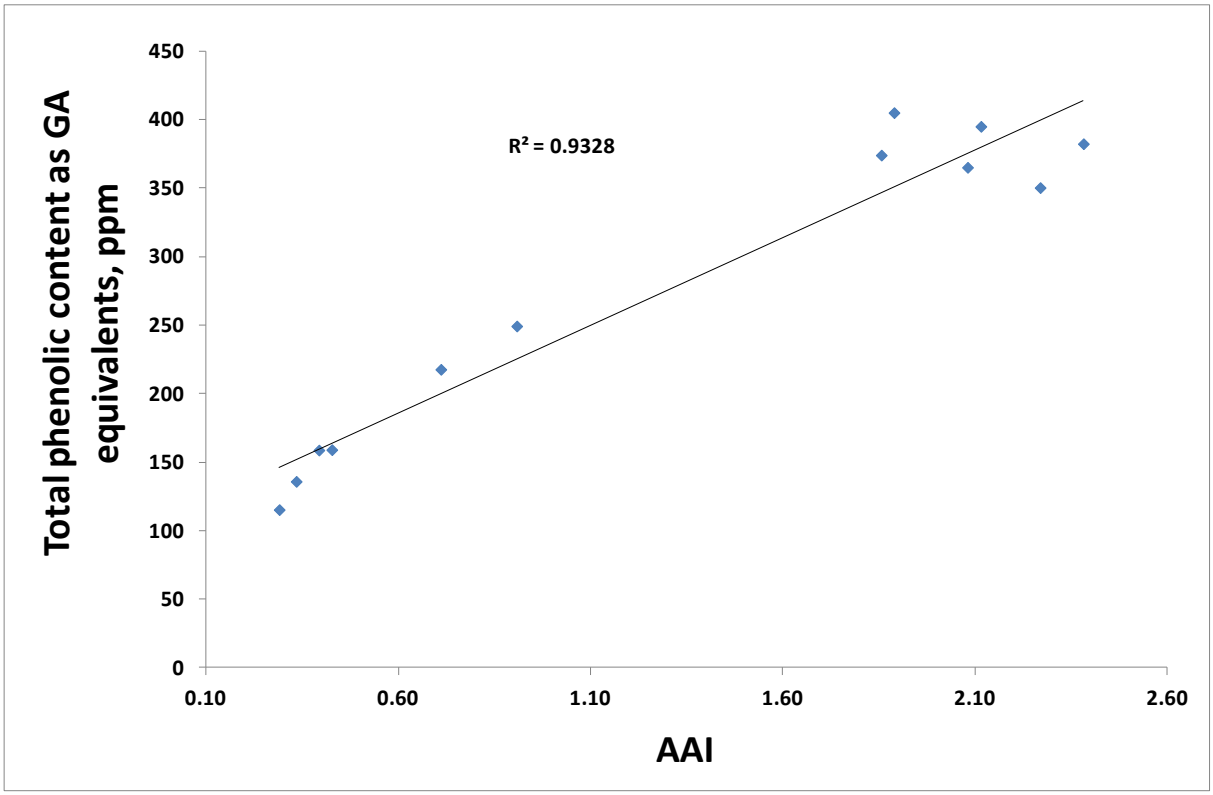

Figure 8.10 : Correlation between AAI and TPC

8.3 Summary

All the crude lignin and their solvent fractions are tested with antioxidant activity ranging from AAI 0.3 – 2.4. The findings from this study reveal the potential of Kraft lignin and wheat straw lignin to be used in the antioxidant application. In this context, refers to rubber and polymer industries. The application findings are also supported further by the characterisation information from

i. solvent solubility – indicated by yield and the observation from solvent fractionation stage,
ii. molecular weight – in compliment with the information from solvent solubility and indication of impurities,
iii. UV, total lignin content, total phenolic content – qualitative and quantitative confirmation on crude lignin and fractions obtained from EA and MeOH extraction,
iv. FTIR – chemical information revealed from IR spectra with regards to the lignin purity in the sample and to some extend of impurity information and
v. NMR – chemical structure information for the selected representative sample from Kraft and wheat straw lignin.

For the Kraft lignin, there is not a huge difference in terms of antioxidant performance for crude and fractionated lignin based on the AAI finding as all fall into category of strong antioxidant and above. While for wheat straw lignin, the problem of impurities is the key reason for under performance. The antioxidant performance is very much dependant on the phenolic content in the lignin or fractions. The utilisation of crude lignin can be a more favourable alternative from an economic point of view in biorefinery project scale up. It would be also interesting to assess the gap in AAI between lignin and Wingstay L when come to actual intended application.

8.4 References

1. Brodin, I., Ernstsson, M., Gellerstedt, G. and Sjöholm, E. (2012) "Oxidative stabilisation of kraft lignin for carbon fibre production", *Holzforschung: International Journal of the Biology, Chemistry, Physics, & Technology of Wood*, vol. 66, no. 2, pp. 141-147.
2. de Jong, E., Higson, A., Walsh, P. and Wellish, M. (2012) *Bio-based Chemicals : Value Added Products from Biorefineries*, IEA Bioenergy, Task 42 Biorefinery.
3. Dizhbite, T., Telysheva, G., Jurkjane, V. and Viesturs, U. (2004) "Characterization of the radical scavenging activity of lignins—natural antioxidants", *Bioresource technology*, vol. 95, no. 3, pp. 309-317.
4. Dong, X., Dong, M., Lu, Y., Turley, A., Jin, T. and Wu, C. (2011) "Antimicrobial and antioxidant activities of lignin from residue of corn stover to ethanol production", *Industrial Crops and Products*, vol. 34, no. 3, pp. 1629-1634.
5. Eisentraut, A., Brown, A. and Fulton, L. (2011) *Technology Roadmap - Biofuels for Transport*, IEA, France.
6. El Hajaji, H., Lachkar, N., Alaoui, K., Cherrah, Y., Farah, A., Ennabili, A., El Bali, B. and Lachkar, M. (2010) "Antioxidant Properties and Total Phenolic Content of Three Varieties of Carob Tree Leaves from Morocco", *Records of Natural products*, vol. 4.
7. Eliokem (2012) *Product data sheet - Wingstay L*. Available at: http://www.eliokem.com/pdf/WSL.pdf (Accessed: August 2012).
8. Faustino, H., Gil, N., Baptista, C. and Duarte, A.P. (2010) "Antioxidant Activity of Lignin Phenolic Compounds Extracted from Kraft and Sulphite Black Liquors", *Molecules*, vol. 15, no. 12, pp. 9308-9322.
9. García, A., González Alriols, M., Spigno, G. and Labidi, J. (2012) "Lignin as natural radical scavenger. Effect of the obtaining and purification processes on the antioxidant behaviour of lignin", *Biochemical engineering journal*, vol. 67, no. 0, pp. 173-185.

10. Gregorová, A., Košíková, B. and Moravčík, R. (2006) "Stabilization effect of lignin in natural rubber", *Polymer Degradation and Stability*, vol. 91, no. 2, pp. 229-233.
11. Košíková, B., Ďuriš, M. and Demianová, V. (2000) "Conversion of lignin biopolymer into surface-active derivatives", *European Polymer Journal*, vol. 36, no. 6, pp. 1209-1212.
12. Li, J., Gellerstedt, G. and Toven, K. (2009) "Steam explosion lignins; their extraction, structure and potential as feedstock for biodiesel and chemicals", *Bioresource technology*, vol. 100, no. 9, pp. 2556-2561.
13. Lin, S.Y. and Dence, C.W. (1992) *Methods in Liginin Chemistry*, Spriner-Verlag Berlin Heidelberg, Germany.
14. Lu, F.-., Chu, L.-. and Gau, R.-. (1998) "Free radical-scavenging properties of lignin", *Nutrition and cancer*, vol. 30, no. 1, pp. 31-38.
15. Maizura, M., Aminah, A. and Wan Aida, W. (2011) "Total phenolic content and antioxidant activity of kesum (Polygonum minus), ginger (Zingiber officinale) and turmeric (Curcuma longa) extract", *International Food Research Journal*, vol. 18, pp. 526-531.
16. Mohamad Ibrahim, M.N., Ahmed-Haras, M.R., Sipaut, C.S., Aboul-Enein, H.Y. and Mohamed, A.A. (2010) "Preparation and characterization of a newly water soluble lignin graft copolymer from oil palm lignocellulosic waste", *Carbohydrate Polymers*, vol. 80, no. 4, pp. 1102-1110.
17. Mörck, R., Yoshida, H. and Kringstad, K. (1986) "Fractionation of Kraft Lignin by Successive Extraction with Organic Solvents I : Functional Groups, 13C-NMR-Spectra and Molecular Weight Distributions", *Supplement*, vol. 40, pp. 51-60.
18. Pan X FAU - Kadla, John,F., FAU, K.J., Ehara, K.F., Gilkes N FAU - Saddler, Jack,N. and Saddler, J.N. (0921) *Organosolv ethanol lignin from hybrid poplar as a radical scavenger: relationship between lignin structure, extraction conditions, and antioxidant activity*.
19. Pouteau, C., Dole, P., Cathala, B., Averous, L. and Boquillon, N. (2003) "Antioxidant properties of lignin in polypropylene", *Polymer Degradation and Stability*, vol. 81, no. 1, pp. 9-18.

20. Ropponen, J., Räsänen, L., Rovio, S., Ohra-aho, T., Liitiä, T., Mikkonen, H., van, d.P. and Tamminen, T. (2011) "Solvent extraction as a means of preparing homogeneous lignin fractions", *Holzforschung: International Journal of the Biology, Chemistry, Physics, & Technology of Wood*, vol. 65, no. 4, pp. 543-549.
21. Scherer, R. and Godoy, H.T. (2009) "Antioxidant activity index (AAI) by the 2,2-diphenyl-1-picrylhydrazyl method", *Food Chemistry*, vol. 112, no. 3, pp. 654-658.
22. Stewart, D. (2008) "Lignin as a base material for materials applications: Chemistry, application and economics", *Industrial Crops and Products*, vol. 27, no. 2, pp. 202-207.
23. Wang, K., Xu, F. and Sun, R. (2010) "Molecular Characteristics of Kraft-AQ Pulping Lignin Fractionated by Sequential Organic Solvent Extraction", *International Journal of Molecular Sciences*, vol. 11, no. 8, pp. 2988-3001.
24. Yuan, T., He, J., Xu, F. and Sun, R. (2009) "Fractionation and physico-chemical analysis of degraded lignins from the black liquor of Eucalyptus pellita KP-AQ pulping", *Polymer Degradation and Stability*, vol. 94, no. 7, pp. 1142-1150.

Chapter 9

Utilisation of lignin from wood Kraft pulping and pre-treatments of wheat straw for antioxidant application II: Assessment of antioxidant performance in acrylonitrile-butadiene rubber gloves

9.1 Introduction

Lignin is a three-dimensional amorphous natural polymer composed of the vinyl propane unit with carbonyl, hydroxyl and methoxyl substitutions (Gregorová, Košíková and Moravčík, 2006). With the unique polyphenol structure, lignin is one of the key biorefinery platforms for bio-based chemicals production. Currently, the vast majority of industrial applications has been developed for lignosulfonates and around 67.5% of world consumption in 2008 was for dispersant applications followed by 32.5% for binder and adhesive applications (de Jong *et al.*, 2012). In addition, the increasingly stringent environmental waste regulations, both at national and European level, mean that all wastes must be dealt with and the diverse chemical moieties inherent in lignins from diverse plant sources and processing/ extraction methods mean that it should profit from this via purification, processing and integration into new and established chemical industry subsectors (Stewart, 2008). Sources of lignin generated from Kraft pulping and bioalcohol production has been explained in details in sub-section 3.5 and 3.6, Chapter 3 and Chapter 8.

For the past decade, researches are on going to study the effect of lignin in polymer and rubber application. The effect of lignin addition in natural rubber and styrene-butadiene rubber (SBR) composites as a reinforcing and / or stabilizing agent is reported (Kramárová *et al.*, 2007; Gregorová, Košíková and Moravčík, 2006; Košíková and Gregorová, 2005). Liao *et al.* (2012) and Setua *et al.* (2000) worked on research of lignin and modified lignin in acrylonitrile-butadiene rubber (NBR) as reinforcing agent too. Pouteau *et al.* (2003)studied on the lignin effect for antioxidant in polypropylene and the solubility issue was underlined.

Following the price issue of natural rubber and the market demand of high chemical resistance disposable thin gloves, carboxylated acrylonitrile-butadiene rubber, XNBR become an good option for the production of thin disposable synthetic rubber. XNBR glove is also another alternative candidate for natural rubber in response to requirements dealing with Type I allergy issue. XNBR is supplied to glove manufacturer in water based emulsion form with antioxidant to protect the latex and subsequently, dipped rubber articles from thermal-oxidation. A synthetic antioxidant – Wingstay L (a buthylated reaction product of p-cresol and dicyclopentadiene, CAS 68610-51-5 is commercially available and commonly used in the rubber glove industry e.g. in natural rubber and XNBR (Eliokem, 2012).

There is a lack of publication on lignin as antioxidant in carboxylated acrylonitrile-butadiene rubber, XNBR thin gloves and thus it is intended in the present work is to study the feasibility of Kraft and wheat straw lignins as bio-based antioxidant in XNBR glove in comparison with Wingstay L as a control. This is also a continuation work from Chapter 8. In this study, lignin was prepared into a dispersion form in the same way as the Wingstay L control and dosed into NBR emulsion latex. Gloves were then dipped from the compounded latex and subjected to a series of physico-mechanical testing. More details can be found in sub-section 3.7.1, 3.7.2 and 3.7.3 under Chapter 3.

9.2 Results and Discussion

A crude Kraft lignin (RH) and a MeOH fraction of wheat straw lignin from extrusion pre-treatment (MEX) are used as lignin sources for this study. Explanation on the selection of lignin sample is detailed in sub-section 3.6 and the sample ID descriptions as well as compounded latex ID are tabulated in **Table 3.5** and **3.6**.

9.2.1 Physical observation.

The WL dispersion was in milky yellowish colour and that of the lignin (RH and MEX) dispersions were in different shades of brown (see **Figure 9.1**). As in low total solid content (TSC) in the MEX dispersion (~ 4.6 wt%), the dispersed lignin was found to be

dissolved fully and after the pH adjustment to pH 13. The low TSC was resulted from the low lignin yield in the lab scale extraction. That is why the dispersion formulation was adjusted to produce lower solid content dispersion. Same issue on the RH too but the amount of RH lignin is slightly higher than EL hence the final TSC (~17%) can be higher than MEX dispersion but still lower than WL dispersion which is at ~ 50%. The RH dispersion has a higher tendency of sedimentation compared with the WL dispersion. Particle size for RH and WL dispersion is tested at 2.6 and 4.0 μm (see sub-section 3.7.1 for detail). More sedimentation observation was believed due to particle size for KL dispersion is smaller and the dispersion was prepared based on standard package of dispersants dosage as WL. Smaller particle size is expected to have bigger surface area and implicated to an increase for total dispersant level demand.

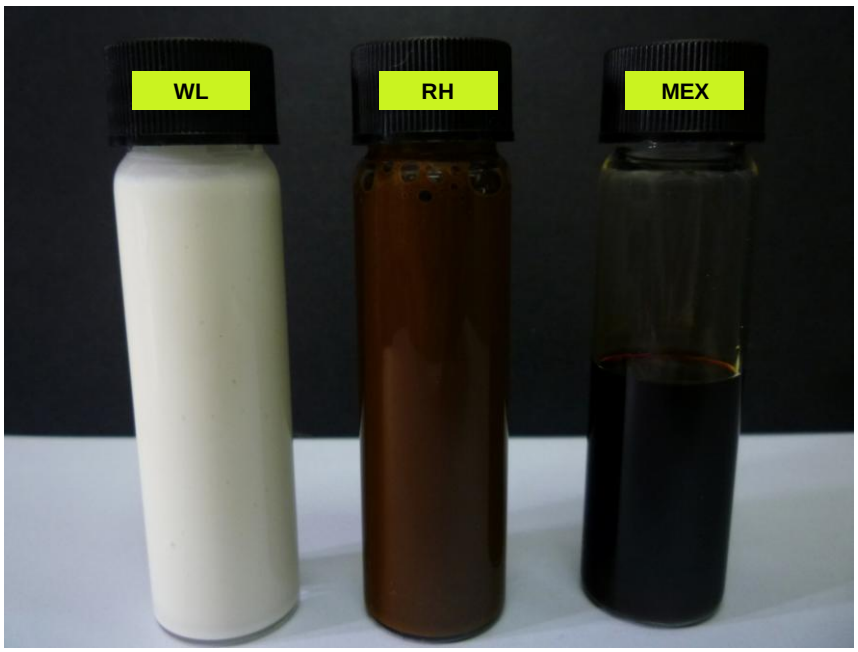

Figure 9.1 : visual observation of the dispersions of the control, WL and the two lignins RH and MEX showing difference in colours/shade.

Colour of XNBR latex compounded was darkening slightly when lignin dispersion being added in to the compound. Based on the colour indication, lignin dispersion seen like mixed well inside the emulsion latex.

Five compounds with same base XNBR latex were prepared with the antioxidant dosage in according to **Table 3.6,** Chapter 3. The compounds are labelled as below,

i. Blank – a Blank sample with no antioxidant,
ii. Control WL – a control sample with WL at 0.6 phr,
iii. KL 0.6 – a compound with RH dispersion at 0.6 phr
iv. KL 1.2 – a compound with RH dispersion at 1.2 phr,
v. EL 0.6 – a compound with MEX dispersion at 0.6 phr.

The use of double dosage in KL 1.2 is attempted to close the gap found, as discussed in sub-section 8.2.5, Chapter 8, between antioxidant performance of the RH and the control. XNBR latex with antioxidant was then further compound with standard glove dipping compounding formulation according to **Table 3.7**.

Glove sample was dipped from the compounded latex and the picture of various glove samples were shown in **Figure 9.2**. Dipped film sample for Compound EL 0.6 was obtained with ceramic dip spade instead of ceramic glove former. Reason for this change is detailed in sub-section 3.7.2. **Figure 9.2** clearly show the colour variation from different latex compound. The glove reflected the sample identity where the opaque white for Blank and Control WL compound. Lignin dosed gloves were found in yellow to golden colour depending on the dosage of lignins. Again, the evenness of the glove colour is an indication that lignin is well dispersed in the dipped rubber article. Homogeneity of lignin in XNBR latex should not be a problem as long as the dispersion well dispersed and stabilised in the emulsion. No advert effect was observed during dipping process.

Figure 9.2 : Glove samples dipped from various compounds

9.2.2 Mechanical properties

Mechanical properties of the dipped film before and after aging process (aged for 22 and 48 hours) were assessed by tensile strength, modulus at 100, 300 and 500% and elongation a break as described in sub-section 3.7.3. The percentage of retention for tensile strength, modulus and elongation at break is defined as percentage of the reading of aged over reading of unaged. Thermal-oxidation aging of glove film was conducted in air ventilated oven to simulate the accelerated aging process as part of the evaluation scope for lignin antioxidant performance.

Mechanical properties of are summarised in **Table 9.1** and illustrated in **Figure 9.3**. Tensile retention for the Blank sample showed an increased trend accompanied by a significant drop in its elongation at break was also observed as in **Figure 9.3**. This may be due to continuous cross-linking that took place in both ionic and covalent cross-linked system in the XNBR film. For the WL and lignin dosed XNBR films, the tensile retention shows a decreasing trend accompanied with improved elongation at break retention (see **Table 9.1**, **Figure 9.3** and **9.4**).

Table 9.1 : Mechanical properties of dipped XNBR films before and after themal-oxidation aging

Compound	M100, MPa	M300, MPa	M500, MPa	Tensile, MPa	Elongation, %
Unaged					
Control Blank	**1.6**	**3.0**	**6.3**	**21.4**	**676**
WL	**1.9**	**3.7**	**8.9**	**24.5**	**639**
KL 0.6	**1.9**	**3.8**	**9.2**	**23.7**	**635**
KL 1.2	**1.7**	**3.6**	**8.1**	**23.4**	**650**
EL 0.6	**2.0**	**4.3**	**10.7**	**23.8**	**608**
Aged 22 hours					
Control Blank	**2.0**	**4.6**	**17.2**	**22.6**	**536**
WL	**2.3**	**5.4**	**18.7**	**24.7**	**521**
KL 0.6	**2.4**	**5.6**	**18.9**	**23.5**	**516**
KL 1.2	**2.2**	**4.8**	**13.9**	**29.3**	**582**
EL 0.6	**2.4**	**5.7**	**19.0**	**23.1**	**516**
Aged 48 hours					
Control Blank	**1.9**	**4.2**	**14.1**	**23.2**	**545**
WL	**1.8**	**3.8**	**13.0**	**21.9**	**552**
KL 0.6	**1.9**	**4.0**	**12.4**	**23.1**	**572**
KL 1.2	**1.6**	**3.1**	**7.5**	**22.2**	**635**
EL 0.6	**2.1**	**4.8**	**16.1**	**22.5**	**540**

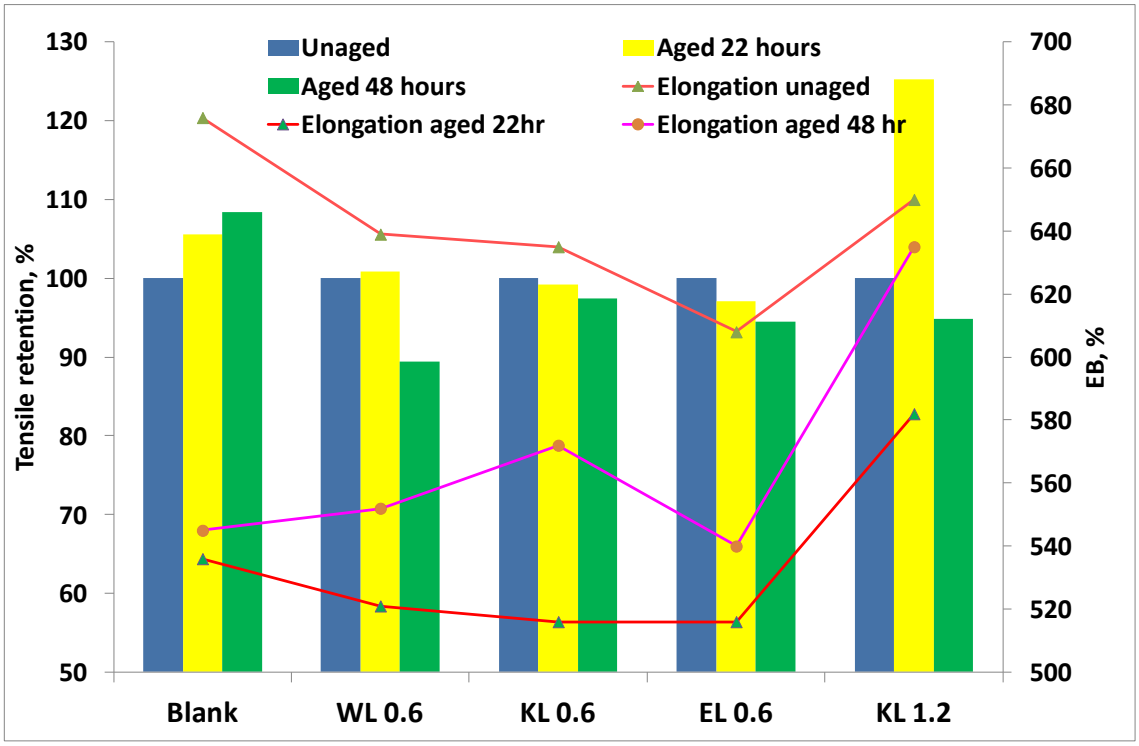

Figure 9.3 : Percent retention of tensile strength and elongation at break for various film samples before and after thermal-oxidation aging.

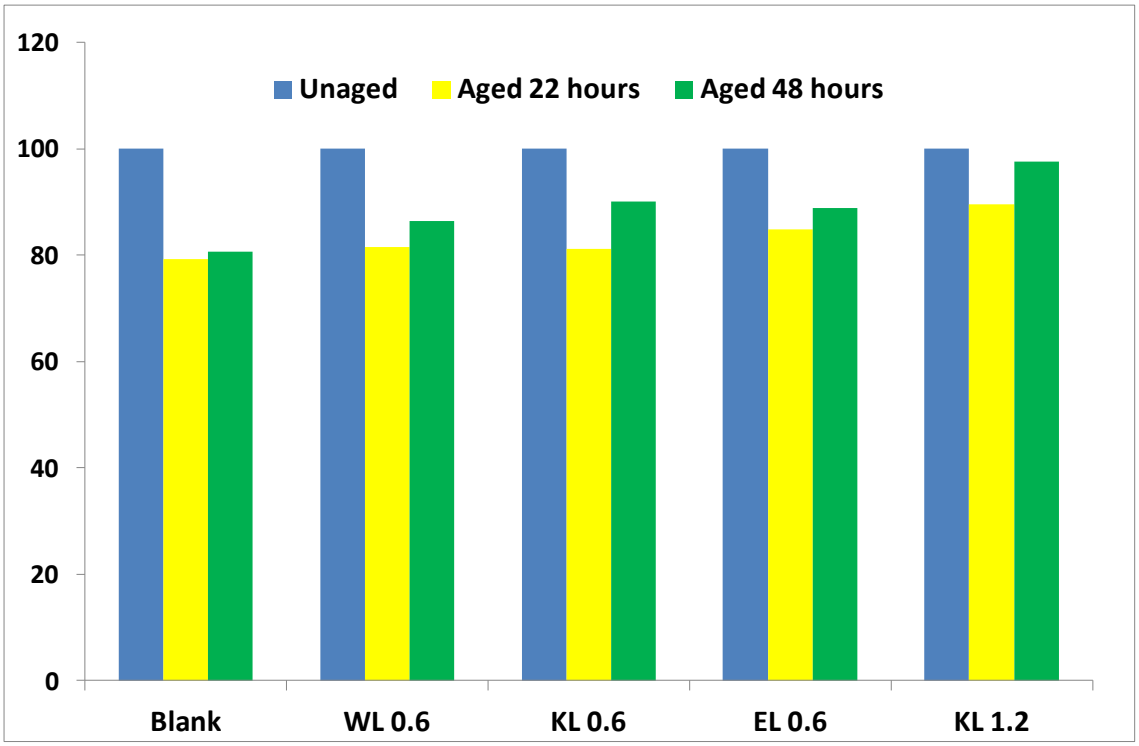

Figure 9.4 : Plot of percent retention of elongation at break for sample films before and after the themal-oxidation aging.

Rubbery indication from the dipped film can be pick up from elongation at break and moduli readings. **Figure 9.5** and **9.6** show the percentage of retention for modulus at 300 and 500% strain, respectively. Based on **Figure 9.5** and **9.6**, almost all the sample showed an increase in modulus at either 300 or 500% strains which with the percentage of modulus retention more than 100%. The increased in modulus reading is rather drastic for Blank sample (without antioxidant) and the rubbery feel for rubber film from Blank sample deteriorated when compared the sample dosed with WL and lignins (RH and MEX). Films produced from WL0.6, KL0.6 and EL0.6 have similar trend. Interesting finding found on the film produced from compound KL1.2 which the compound with double dosage of lignin compared to Control WL. The film was initially tested with highest tensile retention after 22 hr thermal-oxidation aging but then dropped after 48 hour aging. However, the film softness (combination of low modulus and high elongation at break as shown in **Table 9.1**) was the best at all time in comparison to the rest of sample tested in line. Similar trend of findings for lignin dosed compound was reported in NBR (Liao *et al.*, 2012) and SBR composite (Košíková and Gregorová, 2005) but those were with much higher lignin loading. Lignin is believed participate in the cross-linking system in XNBR film. But, we cannot be sure the cross-linking took part in ionic (zinc carboxylate) or covalent (sulphuric) cross-linking system. Nevertheless, the significant increased in elongation at break in coupled with drop in tensile retention for film from KL1.2, implies the hypothesis of lignin took part more in ionic cross-linking system.

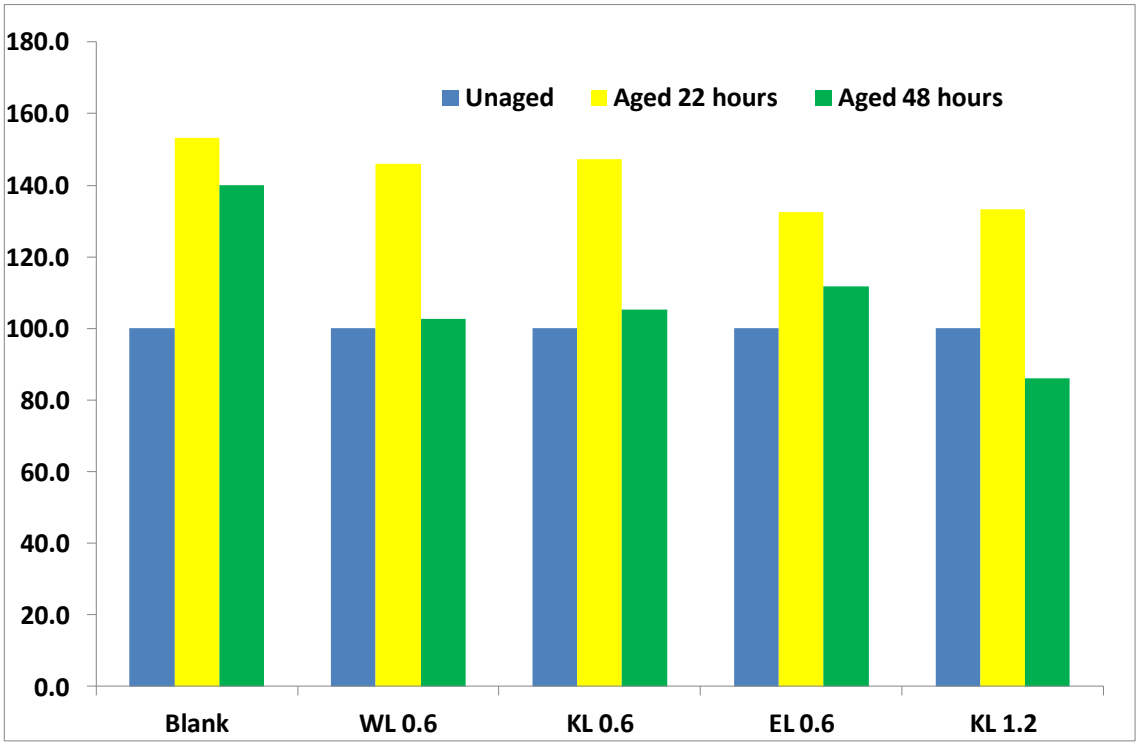

Figure 9.5 : Plot of percent retention of modulus at 300% strain for sample films before and after themal-oxidation.

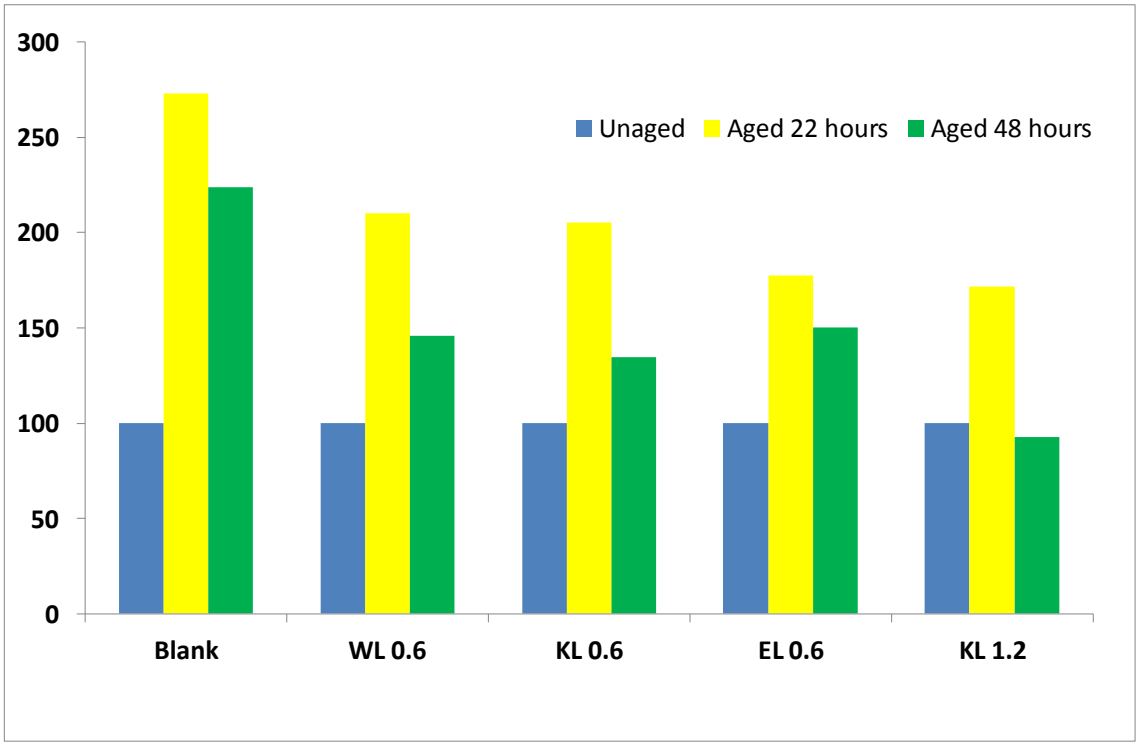

Figure 9.6 : Plot of percent retention of modulus at 500% strain for sample films before and after themal-oxidation.

9.2.3 Differential scanning calorimetry for the oxidation induction time (DSC-OIT)

The mechanical properties alone are insufficient to differentiate antioxidant performance of lignins and provide limited insight. DSC-OIT which has been widely used for antioxidant related study (Nawaz *et al.*, 2012; Karlsson *et al.*, 1993), provides more detail information on thermal oxidation behaviour of polymer. **Figure 9.7** showed the DSC curve for the film sample under studied. The unaged film sample was thermally-oxidised at 175°C and the change in the OIT is a direct measure of antioxidant performance of the samples. Experitmental detail can be found in sub-section 3.8.17, Chapter 3. Comparison of the OIT curves enables ranking of the antioxidant performance in the following order

Blank < EL0.6 < KL0.6 < KL1.2 < WL Control

based on the OIT of 0, 22.8, 26.2, 27.3 and 33.6 min, respectively. This trend is in agreement with the previous findings in DPPH (Chapter 8). The WL control is a specialty chemical tailored for antioxidant application, hence it is not surprising to have performed well. The EL and KL lignin dispersions show significant improvement of antioxidant performance compared with the Blank films. KL1.2 with double dose of the Kraft lignin RH does not give significant boost compared with KL0.6 but resulted interesting enhancement on the mechanical properties.

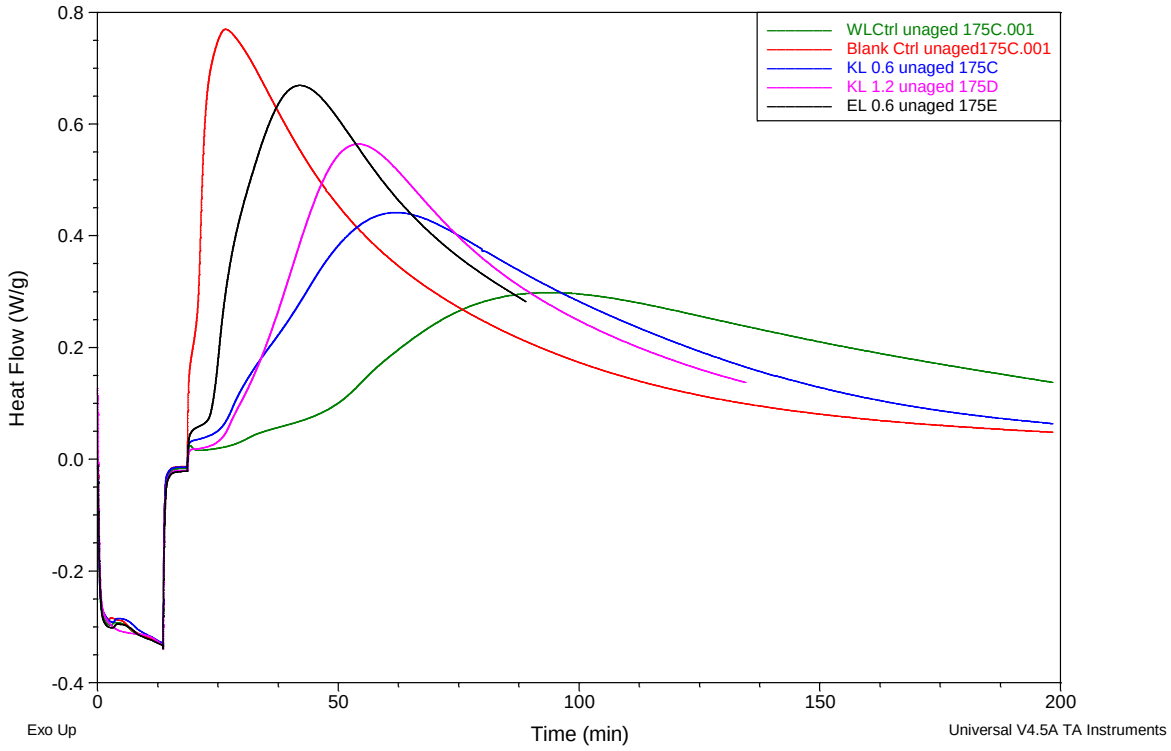

Figure 9.7 : DSC-OIT curves for various sample films showing different induction time under full oxidative condition.

9.3 Summary

The inclusion of lignin gave rise in expected colour change in dipped XNBR films. No adverse effect such as homogeneity, stability and film formation problem observed when lignin dispersion being added into XNBR emulsion system. The mechanical properties testing with inclusion of thermal oxidation aging is not sufficient enough to assess the effect of antioxidant performance of lignin embedded dipped film. DSC-OIT gave firm assessment on lignin antioxidant evaluation in dipped XNBR film and confirmed both RH and MEX lignin contributes to rubber antioxidant protection. The evaluation outcome from DSC-OIT can also be correlated to the findings of antioxidant evaluation under DPPH analysis (Chapter 8). With the finding from mechanical properties evaluation also, lignin is believed took part in XNBR cross-linking system and helps to improve the softness of rubber film. This had been evidenced by low

modulus retention and high elongation at break readings. This could be counted as part of the antioxidant behaviour of lignin as retaining rubbery feel is a benchmark properties for XNBR rubber glove product or simply a good reinforcement agent in rubber compounding system. Further work on effect of lignin in XNBR cross-linking system will be interested.

9.4 References

1. de Jong, E., Higson, A., Walsh, P. and Wellish, M. (2012) *Bio-based Chemicals : Value Added Products from Biorefineries*, IEA Bioenergy, Task 42 Biorefinery.
2. Eliokem (2012) *Product data sheet - Wingstay L*. Available at: http://www.eliokem.com/pdf/WSL.pdf (Accessed: August 2012).
3. Gregorová, A., Košíková, B. and Moravčík, R. (2006) "Stabilization effect of lignin in natural rubber", *Polymer Degradation and Stability*, vol. 91, no. 2, pp. 229-233.
4. Karlsson, K., Eriksson, P., Hedenqvist, M., Ifwarson, M., Smith, G.D. and Gedde, U.W. (1993) "Molecular structure, morphology, and antioxidant-consumption in polybutene-1 pipes in hot-water applications", *Polymer Engineering & Science*, vol. 33, no. 5, pp. 303-310.
5. Košíková, B. and Gregorová, A. (2005) "Sulfur-free lignin as reinforcing component of styrene-butadiene rubber", *Journal of Applied Polymer Science*, vol. 97, no. 3, pp. 924-929.
6. Kramárová, Z., Alexy, P., Chodák, I., Spirk, E., Hudec, I., Kosikova, B., Gregorova, A., Suri, P., Feranc, J. and Bugaj, P. (2007) "Biopolymers as fillers for rubber blends", *Polymers for Advanced Technologies*, vol. 18, no. 2, pp. 135-140.
7. Liao, Z., Wang, X., Xu, Y., Feng, J., Zhu, J. and Su, S. (2012) "Cure characteristics and properties of NBR composites filled with co-precipitates of black liquor and montmorillonite", *Polymers for Advanced Technologies*, vol. 23, no. 7, pp. 1051-1056.
8. Nawaz, S., Nordell, P., Hillborg, H. and Gedde, U.W. (2012) "Antioxidant activity in aluminium oxide – poly(ethylene-co-butyl acrylate) nanocomposites", *Polymer Degradation and Stability*, vol. 97, no. 6, pp. 1017-1025.
9. Pouteau, C., Dole, P., Cathala, B., Averous, L. and Boquillon, N. (2003) "Antioxidant properties of lignin in polypropylene", *Polymer Degradation and Stability*, vol. 81, no. 1, pp. 9-18.

10. Setua, D.K., Shukla, M.K., Nigam, V., Singh, H. and Mathur, G.N. (2000) "Lignin reinforced rubber composites", *Polymer Composites,* vol. 21, no. 6, pp. 988-995.
11. Stewart, D. (2008) "Lignin as a base material for materials applications: Chemistry, application and economics", *Industrial Crops and Products,* vol. 27, no. 2, pp. 202-207.

Chapter 10

Conclusion and suggestion for future work

10.1 Conclusion

This work demonstrated the twin screw extruder is a good potential pre-treatment tool for wheat straw for biofuel production. Operating factor which influencing the pre-treatment efficiency has been studied. Later part of work also demonstrated a way of lignin utilisation started from waste black liquor to a potential bio-based chemical in chemical industry. **Figure 10.1** illustrated the contribution of each chapter in this thesis to the research objectives defined at early of the research.

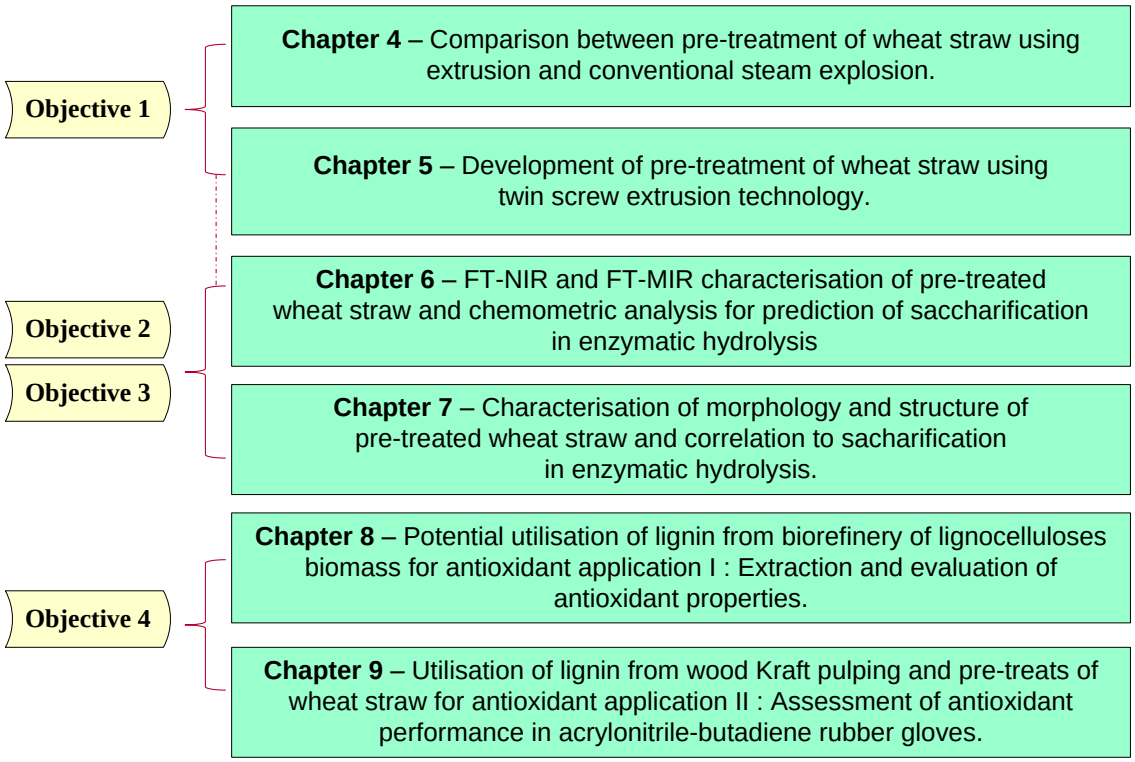

Figure 10.1 : Summary of contribution of each chapter to the research objectives for this PhD work.

10.1.1 Conclusion 1

At the preliminary stage of this research, steam explosion and extrusion pre-treatment of wheat straw are compared and the effectiveness of pre-treatment has been assessed using a portfolio of techniques including characterisation of changes in colour, microstructure (SEM), chemical structure (FTIR), crystallinity (XRD) and thermal degradation behaviour (TGA). Direct correlation is also made to glucose recovery in subsequent enzymatic hydrolysis of the treated straws.

Steam explosion at severe condition (SE02) demonstrated highest yield which evidenced by more physical disruption and changes in FTIR and TGA. However, signal of lignin deposition picked up by FTIR could be a potential drawbacks in this conventional pre-treatment method which operating in batch system. In comparison, extrusion is relatively milder pre-treatment e.g. low temperature and low shear. Twin screw extrusion supplemented with chemical treatment (alkaline – NaOH, EX02) has demonstrated promising saccharification yield when compared with steam explosion under severe processing condition. It is a continuous process which can be a practical technology for lignocellulose biomass pre-treatment.

Study has been extended to further develop and optimise extrusion pre-treatment. Further study reveals the impact of physical operating parameter over pre-treatment of wheat straw with Betol twin screw extruder within two main categories – extrusion with and without NaOH. By purely pre-treated with extrusion, high moisture (~ 70%), low temperature and with die capped are in favour. The yield can be further improved by optimise the temperature profile to include the cooking (auto-hydrolysis) and continuous steam explosion effects. By reducing the size of wheat straw feedstock, it did help to improve the yield of glucose after extrusion. However the cost of mechanical size reduction will burden the economics of overall pre-treatment cost. Double extrusion is not in favour.

By addition of NaOH to the extrusion, at least ~ 30% of glucose yield increased (WCB10009 vs WCB10008). All the entire of physical operating parameter are not having significant impact when NaOH added into extrusion. Post washing step is still

recommended for the NaOH combined extrusion to provide another platform of biorefinery while improve the pH control prior enzymatic hydrolysis. Analysis from FTIR and TGA help to support the mechanism of change after the pre-treatment and are well correlated to the glucose yield after enzymatic hydrolysis.

Based on the above findings, extrusion demonstrated a highly potential green pre-treatment tool for wheat straw as it requires only low temperature, simple handling and can be easily improve yield by combine with other pre-treatment technology. Findings from Chapter 4 and 5 have also form a good base for the subsequent work on understanding of mechanism of change in wheat straw before and after pre-treatment as well as the impact to the downstream process output.

10.1.2 Conclusion 2

Work in Chapter 6 and 7 has further moved on to the characterisation of wheat straw before and after pre-treatment. The FTIR and FT-NIR analysis coupled with chemometrics can be used for qualitative and quantitative analysis of wheat straw pre-treated with extrusion and steam-explosion to correlate chemical changes to effectiveness of fractionation and sugar yield.

A satisfactory evaluation is obtained for the multivariate calibration models. The PCA method was able to distinguish the effect of processing methods and the conditions. The PLS statistical models were well correlated with the chemical information extracted from FTIR and FT-NIR spectra and is capable of predicting sugar yield from FTIR or FT-NIR information.

FT-NIR using diffuse reflectance measurements has an advantage of minimum sample preparation and it is feasible to be use in-line and off-line. The validity of chemical information from FT-NIR spectra was further supported by direct spectral interpretation by FTIR. However, to improve the accuracy more samples are needed to strengthen the reliability of the model; in particular for the creation of a broad-based model to captured various type of pre-treatment method.

Morphology and surface analysis are included to provide further information on the pre-

treated wheat straw. SSA measurement obtained from the organic dye sorption and BET (N_2) are having similar trend in correlation. The findings are well correlated to the physical morphology change observed from the electron microscope and form a trend which can be correlated to yield of glucose. However, few SSA readings in DVS measurement were not in range. The data has been further explained with Young & Nelson parameter constant E. Further investigation would be good to understand validity of water vapour as absorbent in DVS for lignocellulosic SSA determination. Crystallinity index obtained is not conclusive enough when relates to physical changes and yield of glucose after enzymatic hydrolysis. It is in agreement with the recent reported researches as cited in Chapter 7.

10.1.3 Conclusion 3

Lignin is a by-product generated during pre-treatment under biofuel application. The utilisation of lignin has been studied in the work reported in Chapter 8 and 9. Sample Kraft lignin was included for this feasibility study.

All the crude lignin and their solvent fractions were tested with antioxidant activity ranging from AAI 0.3 – 2.4. The findings from this study reveal the potential of Kraft lignin and wheat straw lignin to be used in the antioxidant application. In this context, refers to rubber and polymer industries. The application findings were also supported further by the characterisation information from

i. solvent solubility – indicated by yield and the observation from solvent fractionation stage,
ii. molecular weight – in compliment with the information from solvent solubility and indication of impurities,
iii. UV, total lignin content, total phenolic content – qualitative and quantitative confirmation on crude lignin and fractions obtained from EA and MeOH extraction,
iv. FTIR – chemical information revealed from IR spectra with regards to the lignin purity in the sample and to some extend of impurity information and

v. NMR – chemical structure information for the selected representative sample from Kraft and wheat straw lignin.

For the Kraft lignin, there is not a huge difference in terms of antioxidant performance for crude and fractionated lignin based on the AAI finding as all fall into category of strong antioxidant and above. While for wheat straw lignin, the problem of impurities is the key reason for under performance. The antioxidant performance is very much dependant on the phenolic content in the lignin or fractions. The utilisation of crude lignin can be a more favourable alternative from an economic point of view in biorefinery project scale up.

Work is extended to the intended application screening in industry. Lignin has been assessed as an antioxidant in XNBR rubber glove application. The inclusion of lignin gave rise in expected colour change in dipped XNBR films. No adverse effect such as homogeneity, stability and film formation problem observed when lignin dispersion being added into XNBR emulsion system. The mechanical properties testing with impact of thermal-oxidation aging is not sufficient enough to assess the effect of antioxidant performance of lignin embedded dipped film. DSC-OIT did give firm assessment on lignin antioxidant evaluation in dipped XNBR film and confirmed both RH (crude Kraft lignin) and MEX lignin (wheat straw lignin extracted by MeOH extraction) contributes to rubber antioxidant protection. The evaluation outcome from DSC-OIT can also be correlated to the findings of antioxidant evaluation under DPPH analysis (Chapter 8). With the finding from mechanical properties, lignin is believed took part in XNBR cross-linking system and helps to improve the softness of rubber film. This had been evident by low modulus retention and high elongation at break readings. This could be counted as part of the antioxidant behaviour of lignin as retaining rubbery feel is a benchmark properties for XNBR rubber glove product or simply a good reinforcement agent in rubber compounding system.

10.2 Suggestions for future work

Suggestions for the future work included,

- Include energy consumption information in for extrusion pre-treatment study to provide more input on the energy usage and cost of pre-treatment.
- Further study on the extrusion pre-treatment by changing the screw profile to optimise the physical fractionation.
- Mass balance analysis on extrusion pre-treatment.
- Process optimisation study with multivariate analysis tool.
- Extension of application evaluation after enzymatic hydrolysis.
- Increase the sampling amount of characterisation analysis to improve the data representation.
- Improve the yield of lignin recovery in extrusion pre-treatment by improving the waste black liquor recovery during the extrusion process.
- Further study on effect of lignin in XNBR cross-linking system and other type of rubber article.
- Hemicellulose biorefinery either for biofuel or as platform for other bio-based chemical.